The RESEARCH LABORATORY
of
ELECTRONICS
at the
MASSACHUSETTS INSTITUTE OF TECHNOLOGY
CAMBRIDGE, MASSACHUSETTS 02139

Touch Lab Report 7

Human Haptic Interaction with Soft Objects: Discriminability, Force Control, and Contact Visualization

Jhy-shing Chen and Mandayam A. Srinivasan

RLE Technical Report No. 619

January 1998

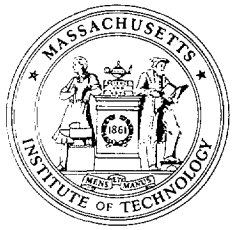

Touch Lab Report 7

Human Haptic Interaction with Soft Objects: Discriminability, Force Control, and Contact Visualization

Jhy-shing Chen and Mandayam A. Srinivasan

RLE Technical Report No. 619

January 1998

Sponsored by the Office of Naval Research
N00014-91-J-1454
N00014-92-J-1814

The Research Laboratory of Electronics
MASSACHUSETTS INSTITUTE OF TECHNOLOGY
CAMBRIDGE, MASSACHUSETTS 02139-4307

Human Haptic Interaction with Soft Objects: Discriminability, Force Control, and Contact Visualization

by

Jyh-shing Chen

Submitted to the Department of Mechanical Engineering
on May 13, 1996, in partial fulfillment of the
requirements for the degree of
Doctor of Philosophy in Mechanical Engineering

Abstract

The haptic interaction of humans with soft objects was studied from three perspectives: softness discrimination, force control, and contact visualization. The abilities of humans in actively discriminating softness was measured by using a specimen presenter system which was built to randomly present the specimens. Two experimental paradigms (1- and 2-finger) and three finger conditions (normal, finger cot, and rigid thimble) were used to examine the importance of various sources of information. When using 1 finger, the Just Noticeable Difference (JND) was about 5% for normal and finger cot conditions and increased to about 50% with the thimble. The JND results from 2-finger discrimination were lower than the 1-finger results for both normal and finger cot conditions, but were higher with the thimble. Examination of the forces exerted on the specimens during 2-finger discriminations revealed possible underlying discrimination strategies. In the force control experiments, subjects were asked to exert several levels of constant forces under various finger conditions. The results indicated that the errors from tracking with visual feedback was significantly lower than that without visual feedback. No significant differences in force control were found with either different softnesses or under the three finger conditions. The absolute errors were higher when controlling higher target forces. Significant difference in force control was found between the two hands of the subject who showed handedness in the softness discrimination experiments. For contact visualization, a real-time imaging setup was built which consisted of a videomicroscopy system and a tactile stimulator system. By using this setup, real-time images from the contact region as well as the contact forces were digitized. Various image processing techniques were developed and applied in order to analyze and improve the contact images to distinguish between the contact and non-contact regions. Contact variables such as force, nominal contact area, actual contact area, nominal pressure and actual pressure were analyzed. Based on the visualization of the active slip phenomenon, a hypothesis on the contact pressure distribution was proposed. The developed hardware can be used for evaluating human haptic abilities and providing biomechanical visualizations. The results obtained have implications on the mechanisms of contact and find applications in dextrous robot finger and haptic interface designs as well as in various steps involved in the automatic fingerprint identification systems.

Thesis Supervisor: Dr. Mandayam A. Srinivasan
Title: Principal Research Scientist

Contents

List of Figures

List of Tables

Chapter 1

Introduction

1.1 Human haptic interaction with soft objects

Our hands are a part of the human haptic system which is comprised of the biomechanical, sensoimotor and cognitive subsystems. Complete understanding of the human haptic system requires an analysis of the mechanics of contact together with other aspects of the system such as physiology, neuroscience and psychophysics. When we interact with objects in an environment, useful information is gathered from information sources involving visual, auditory, and haptic systems. Exploration or manipulation of objects generally involves multimodal perception and intersensory integration [15][46][48]. Even though the interaction is multimodal, we rely heavily on our hands to perceive object properties and control the interaction. This is because the tactile information originates directly from the finger-object contact interface as a result of contact forces imposed on the fingerpads. The mechanoreceptors underneath the skin respond to the imposed loading and the generated neural signals are transmitted to the brain through pathways of the central nervous system. To understand what information is available to the sensors underneath the skin, visualizing the contact process is an important step. In this study, therefore, a videomicroscopy system was built to visualize the contact region of the fingerpad with transparent objects. The image sequences obtained from fingerpad contact with rigid Plexiglas and transparent objects of different softnesses were observed and analyzed by applying various image processing techniques to extract contact information.

At a behavioral level, human perception of the object properties related to the human haptic system have been studied in terms of the detection, discrimination, and recognition (see Sherrick & Cholewiak [37] and Loomis & Lederman [38] for a review). The stimuli that

have been used cover a wide variety such as point loads, surface irregularities, vibrotactile threshold, patterns, roughness, and texture. However, not much is known about the human discriminability of rubber-like soft objects. Early studies on softness perception existed in forms of stimuli ranking, scaling, and psychophysical laws: for example, studies on the skills of test bakers[27], cheese maker and grader craftsmanship, and on scaling, matching and cross-modal comparisons of softness perception[20]. One severe problem that hinders quantitative understanding in such studies is the lack of of high quality stimuli which differ only in softness [28]. In this study, human softness discrimination ability was examined by performing discrimination experiments with visually identical, smooth, compliant objects that had no perceivable surface features and differed only in softness which could be controlled and characterized to a high level of precision.

Two sources of information are available during haptic interaction with objects. Tactile information is gathered from the sensors embedded in the skin during contact; kinesthetic information is generated by the sensory receptors around joints, tendons and muscles [11][21]. In order to determine the relative importance of tactile information at both gross and detailed level as well as that of kinesthetic information during softness discrimination, three different finger conditions were examined: normal finger, finger covered with a finger cot and with a rigid thimble. With normal finger and finger covered with a thin glove-like latex finger cot, both tactile information and kinesthetic information are available. The presence of finger cot can, however, be thought of as a thin layer on top of the finger ridges which would remove some of the fine details that the finger would otherwise perceive with normal fingers. The rigid thimble replaces the fingerpad-object interface with thimble-object and thimble-finger interfaces. Thus, when discriminating softness with the thimble on, useful tactile information which would otherwise be obtained from the contact region are removed. Therefore, the subjects would need to rely on the unperturbed kinesthetic information.

In an attempt to address multifinger interaction with objects, an experimental paradigm that used the two index fingers from both hands was also tested in addition to one-finger softness discrimination experiments. Aside from analyzing the Just Noticeable Difference (JND) results, the forces applied for discrimination were also examined to reveal the strategies adopted by the subjects. To further understand the underlying limitations in the ability to achieve fine discriminations of softness, force control experiments were conducted to examine the subjects' abilities in controlling normal forces of contact with objects of different soft-

nesses. Both left and right index fingers under normal, finger cot, and thimble conditions were examined in following and controlling three different constant target force magnitudes with and without visual force feedback available.

1.2 Specific aims of the thesis

The specific aims of this thesis are (1) to develop a videomicroscopy system for visualization of the contact region of the human fingerpad during contact with transparent objects, (2) to develop a single degree of freedom tactile stimulator capable of transporting stimulus objects to indent the fingerpad at a controlled velocity, (3) to develop a specimen presenter to perform psychophysical experiments on the human haptic discrimination of object softness, (4) to characterize the human ability in controlling normal finger forces with specimens of various softnesses under several contact interface conditions, (5) to perform passive and active touch experiments involving the human finger and transparent soft specimens to characterize how the contact region is affected by the parameters such as contact force and specimen compliance, and (6) to gain a deeper understanding of how contact information and force control affect the ability to discriminate softness. It is hoped that the results of this study on the human haptic performance and the underlying mechanisms will also provide useful data and insights for the design of haptic interfaces and dextrous robot fingers.

1.3 Organization of the thesis

This thesis is organized as three parts: softness discrimination, force control, and contact visualization. Background, devices, experiments, and results related to each topic are provided in the corresponding chapters.

Chapter 2 describes the measurement of the human ability in softness discrimination. Background information on the human haptic system and previous work on softness discrimination are provided. A device for specimen presentation was designed and built to measure the human ability in softness discrimination under various finger conditions and experimental paradigms. The results are discussed and the forces used by subjects are examined.

In Chapter 3, the measurement of the human ability in normal force control with soft objects is presented. Background information on the related human sensory abilities are examined. Experiments to determine the human abilities in controlling normal forces of

contact with objects of various softnesses and under various experimental conditions were conducted. The performance of the subjects on force control under various conditions were measured and compared.

The efforts on contact visualization is presented in Chapter 4. A videomicroscopy system was built to enable visualization of the contact region of the human finger with transparent objects. A tactile stimulator system was built to conduct controlled contact experiments. With the integration of the two systems, real-time experiments to observe both contact region and contact forces are now possible. The device was used to acquire images under both active and passive touch experiments to analyze contact information. Various image processing techniques were applied to facilitate phenomenological description and to quantify the image data for overall (nominal) and actual contact areas.

Chapter 5 concludes the main results from the three aspects of softness discrimination detailed in the previous chapters. Implications of the results on human haptic interactions with soft objects, possible pressure distribution, and slip detection are described. In addition, the applicability of the systems and results from this study to dexterous robot finger design, biomechanical visualization, and automated fingerprint identification systems is discussed.

Chapter 2

Softness Discrimination

2.1 Abstract

The human ability to actively discriminate softness was measured. Pairs of silicon rubber specimens with compliances from 0.293mm/N to 0.635mm/N were randomly presented to estimate the Just Noticeable Difference(JND) of the subjects in softness discrimination. Two experimental paradigms with three different finger conditions were used to evaluate the mechanisms that were used during discrimination. Three finger conditions (normal, finger covered with a finger cot, and finger covered with a rigid thimble) were chosen to affect the sources of information available to the subjects for making the discrimination. With finger cot, the detailed ridge level mechanics of contact was filtered by the thin (0.06mm) latex finger cot. With thimble on, the subject had to rely mostly on the kinesthetic information. Two forced-choice discrimination paradigms were the use of the index finger from the dominant hand sequentially (1I-2AFC) and the use of both index fingers from both hands simultaneously (S-2AFC). In the S-2AFC experiments, the two specimens were available during the whole process of discrimination; thus the effect of memory was expected to be less than that in the 1I-2AFC experiments. With the 1I-2AFC paradigm, the mean JND values for the three subjects were 6%, 7%, and 17% under normal condition, 4%, 5%, and 14% under finger cot condition, and 43%, 50%, and 70% under thimble conditions. Analysis of variance showed that results from normal and finger cot conditions were not significantly different. With S-2AFC paradigm, the mean JND values dropped for both normal and finger cot conditions as expected (less memory effect) and the difference was significant at 1% level: the JND values were 3% to 5% for two subjects and were 8% to 10% for the third. On the other

hand, the resulting JND under the thimble condition increased. Analysis of force profiles used during both 1I-2AFC and S-2AFC paradigms indicated that typical contact duration was 0.5 sec to 1.0 sec. The peak force used ranged from about 10N to 40N. Comparing the peak forces used on the two specimens in the S-2AFC experiments suggested three strategies that might have been used by the subjects: (1) to achieve the same amount of deformation of the two specimens by exerting higher forces on the harder specimen, (2) to compare the contact information obtained by applying the same amount of pressure on both specimens (thus higher peak forces on the softer specimen), and (3) to apply the same amount of peak forces on both specimens and compare the deformations.

2.2 Introduction

Humans use their hands to explore and manipulate objects. In both exploration and manipulation, the contact forces as well as the finger positions must be controlled. In addition, properties of the object such as compliance, shape, and texture are sensed and used to avoid dropping or crushing the objects.

Softness is a subjective measure of the compliance of an object. To assess the softness of an object, the object is squeezed with the hand or indented with the finger. During such a process, two sources of information are available: Tactile information is gathered from the sensors embedded in the skin near the contact region; kinesthetic information is generated by the sensory receptors around joints, tendons and muscles (Srinivasan and LaMotte [42][40][41]).

Researchers have conducted various experiments in measuring human sensory and motor performance. Early studies on softness perception existed in the form of stimuli ranking, scaling, and determination of psychophysical laws. For example, studies have been carried out on the skills of test bakers[27], cheese maker and grader craftsmanship, and on scaling, matching and cross-modal comparisons of softness perception[20]. Roland and Ladegaard-Pedersen[35] found that the discriminability of spring strength was unaffected by local anesthesia of skin and joints when the springs were held between thumb and index finger. However, not much is known about the human resolution and the discrimination mechanisms with rubber-like soft objects. Just Noticeable Difference (JND) is a common measure of human sensory resolution and has been measured for a variety of physical quantities. The JND values for length (Dur-

lach *et al* [13]), force (Pang *et al* [34]), compliance and work have been measured by various researchers. Tan *et al* [45] have measured the JND in compliance between two rigid plates, controlled by linear motors, grasped between the thumb and index finger. They found that the JNDs ranged from about 8% to 99% depending on whether or not the subjects had cues such as terminal grasp force or total work done. Jones and Hunter [26] performed experiments where subjects actively moved the forearm about the elbow joint to sense the compliance of a preprogrammed linear motor attached to one of the wrists, and to match its compliance by modifying that of an identical linear motor attached to the other wrist. They estimated the compliance JND to be about 23% under those conditions. Srinivasan and Chen [39] measured the human ability to control the normal forces of contact with a rigid plate under a variety of experimental conditions and found that performance degraded in the absence of tactile information and visual feedback. Srinivasan and LaMotte [42] investigated the ability of humans to tactually discriminate the softness of elastic objects with deformable (rubber specimens) and rigid surfaces (spring cells). They performed three types of experiments: active touch with normal finger, active touch with local cutaneous anesthesia, and passive touch, to measure the human discriminability and to isolate the associated information-processing mechanisms. They found that tactile information was sufficient for discriminating the rubber specimens used in their study. In some of their experiments, the peak forces were constrained to 50, 75, and 90 gwt in order to study the effect of force on discrimination.

The work reported here was designed to look at the softness discrimination from a different perspective. The subjects, with their eyes closed, were allowed to use any force to discriminate the specimens. Two experimental paradigms together with three different finger conditions were used to study the subjects' JND performance on softness discrimination for rubber specimens.

2.3 Methods

2.3.1 Softness specimen preparation

The specimen casting procedure was similar to what Srinivasan and LaMotte [42] used in their experiments, but the mounting method used here was improved to enable high volume production of the specimens. A series of compliant specimens were cast by mixing different proportions of General Electric (GE) SF96-50 silicon rubber diluent to fixed proportions of

GE RTV615A and RTV615B components. The diluent GE SF96-50 is a replacement for the discontinued GE RTV910 used by Srinivasan and LaMotte.

The component proportions were determined by weight using a digital scale and dispensed via pipet. The mixtures were thoroughly mixed by hand and then poured into 30 mm diameter petri dishes to form transparent specimens. Depending on the proportions of the mixture, it took as long as 24 hours for some of the specimens to cure completely. At least 5 specimens of the same diluent proportion were cast to allow for wear and tear from the experiments and for force control and contact visualization studies. The specimens were visually identical and were mainly distinguished by the label on the side which indicated their batch and sequence code.

Several batches of specimens were made for the pilot experiments on ranking softness in order to determine how close the compliance of the specimens should be. It turned out that specimens with much finer differences than those that Srinivasan and LaMotte used had to be prepared for the JND experiments. The standard specimen chosen for the experiment had an objective compliance (see next section) of 0.30 mm/N.

2.3.2 Specimen objective compliance

An objective measure of the specimen compliance was obtained by the characteristic force-displacement relationship of each specimen. A linear stepper motor system with a micro-stepping drive was used to indent the specimens at a constant velocity of 0.5 mm/sec with the flat end of a 1/4 inch diameter circular probe. As the probe indented the specimen, a force sensor mounted between the probe and the motor was used to measure the indentation force at 1000 samples per second data rate. Since the stepper motor movement was completely determined by the number of digital pulses received, its relative position can be determined to better than 1μm accuracy. The indentations were repeated three times, and the depth of indentation was 3 mm for the soft specimens and smaller for the harder specimens. The resulting force-displacement curves were then used to compute the specimen objective compliance by measuring the slope of a fitted straight line with least square error.

The objective compliance value computed from the characteristic line using least square line fitting is significant to the third decimal place or 0.3% of the compliance value for the specimen with the lowest objective compliance. The resulting values from the three repetitions were averaged and used as the specimen compliance. Figure 2-1 shows the characteristic

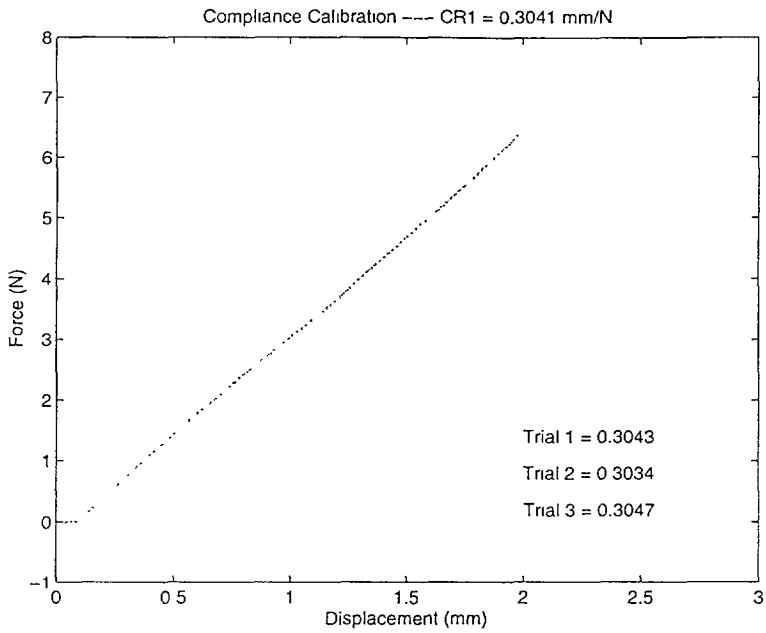

Figure 2-1: Objective compliance data from three repetitions of the probe indenting the standard specimen CR1. The numbers shown are the computed objective compliances in the three trials.

curves for the standard specimen CR1 which shows that the force-displacement data are very repeatable and linear to a high precision. The specimens used in all the discrimination experiments had compliances that ranged from 0.293mm/N to 0.635mm/N. Table 2.1 lists the objective compliance of the batches of specimens used in the discrimination experiments. Serial number shown indicates specimens with identical diluent proportions.

2.3.3 Specimen presenter

The measurement of abilities of human subjects requires experiments with a large number of trials. For conducting such experiments efficiently, a specimen presenter was designed. In essence, the specimen presenter is a stepper motor based system controlled by a computer. It is capable of recording the forces used by subjects during trials and switching specimens between trials. The computer determined randomly how specimens were presented to the subject with a pre-determined probability.

A block diagram of the specimen presenter system is shown in Figure 2-2. The specimens were mounted vertically inside two specimen holders. The holder is slightly tapered to match the shape of the petri dishes. Its bottom has a circular opening but does not allow the specimen to fall through. The specimens fit nicely tight and can also be taken out without

Batch Code	Serial Number					
	1	2	3	4	5	6
CR	0.304	0.298	0.300	0.294	0.293	0.290
DR	0.312	0.309	0.320	0.323	0.326	0.324
ER	0.345	0.347	0.348	0.337	0.341	0.340
FR	0.400	0.382	0.384	0.373	0.375	0.380
HT	0.455	0.450	0.416	0.420	0.442	0.450
IT	0.523	0.514	0.518	0.528	0.531	0.529
JT	0.635	0.611	0.608	0.598	0.610	0.587

Table 2.1: Specimen Objective Compliance (mm/N). Serial number shown refers to specimens with identical diluent proportions.

too much effort. [1]

An Eastern Air Devices model LA23BCK-01 stepper motor was used to rotate the specimens. The motion of the motor was controlled from the parallel input/output interface of the computer. The motor control signals were fed to a model 7006-DB motor driver from American Scientific Instruments Corp. (AMSI) which drove the motor. Two custom made strain gage based force sensors were designed and fabricated to measure the forces exerted by the subjects on the specimens. A finite element analysis was conducted, by using ADINA software, to compare the responses to a point load and a distributed load from three different force sensor designs: simple cantilever beam, cantilever beam with a hole, and cantilever beam with two holes and a slot (binocular). Binocular spring element was chosen to construct the sensors because it is more rigid and less sensitive to location of force application. Four strain gages, made by Measurements Group, were mounted on the top and bottom surfaces of each force sensor near the center of the two holes of the binocular to form a full bridge. The force signals were amplified by a signal conditioner which consisted of an analog module rack from AMSI and two Analog Device model 5B38-05 strain gage input modules. These amplified force sensor signals were then digitized at 1000 samples per second rate by a RTD-ADA3100 data acquisition board made by Real Time Devices Inc. under the control of custom developed C programs.

The choice of having the specimens mounted vertically on the motor has two advantages.

[1] The machining of the force sensors and the specimen holder as well as other attachments for the experiments was carried out at MIT ME student shop under the supervision of Norman Berube. The author wishes to thank him for his patient guidance and advice on machining.

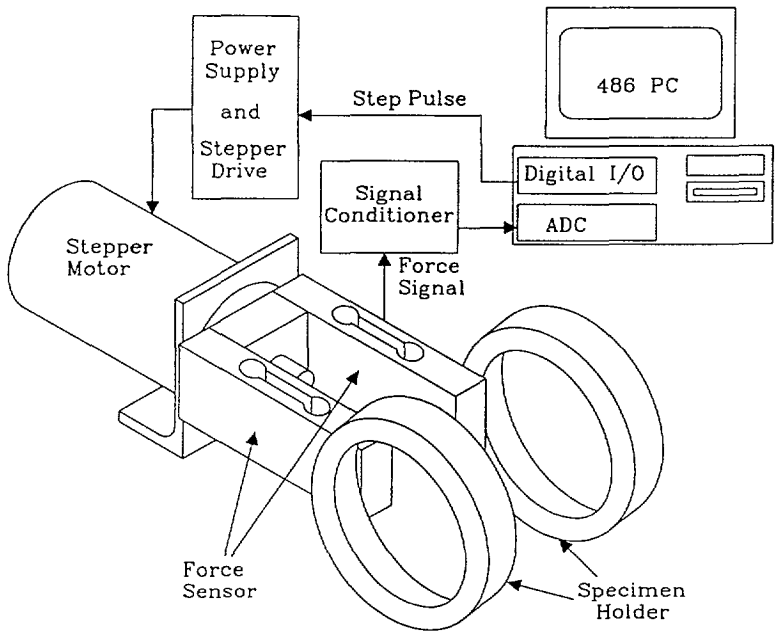

Figure 2-2: The softness specimen presenter system.

First, since the motion of the finger during perception will be horizontal, the gravity effect will be the same for the chosen experimental paradigms. Second, the force sensor offset value need only be measured once and can be applied to the two possible specimen positions used in the experiments.

2.3.4 Finger conditions

To further our understanding of the underlying mechanics of the softness discrimination task, three finger conditions were used: normal finger, finger covered with a 0.06mm thick latex finger cot, and finger covered with a rigid thimble.

With normal finger, subjects have both tactile and kinesthetic information and possibly the surface texture information if there is any. When the finger is covered with a thin latex finger cot, one can still feel the surface easily. It is similar to the glove worn by surgeons, except that the finger cot here was just for a single finger. The compliance characteristics of the finger with and without finger cot is similar as shown in Figure 2-3. However, the finger ridge level contact information is degraded. When the finger wears a rigid thimble, the deformation of the finger and the deformation of the specimen depends on the contact force alone. The interactions between the finger and the specimen is replaced by the interactions between thimble with the specimen and with the finger.

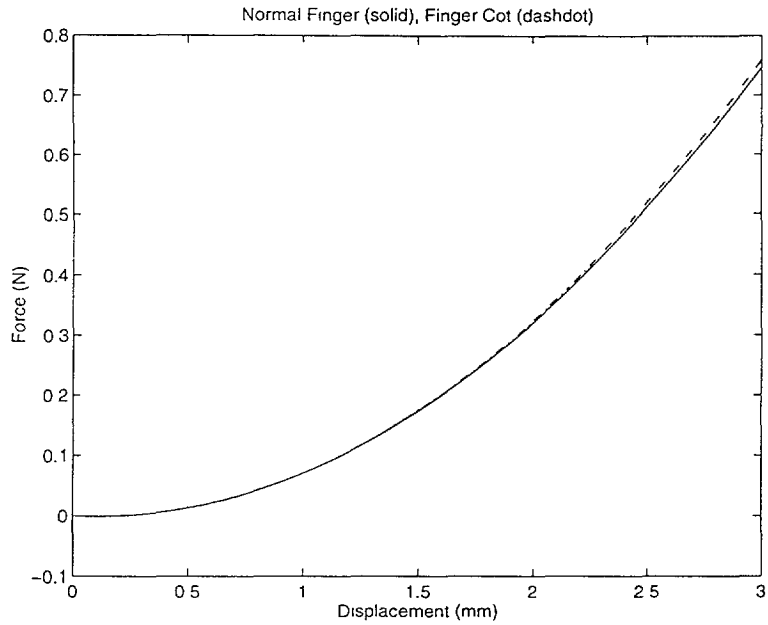

Figure 2-3: The force displacement curves for finger with and without finger cot.

By comparing the results from the three different conditions, we can infer how softness discrimination is affected by the presence of information from the three different information sources: detailed finger ridge contact information, degraded tactile information, and the kinesthetic information.

2.3.5 Experimental paradigms

Since humans interact with objects with multiple fingers most of the time, it is interesting to look into how humans discriminate softness using either a single finger or two fingers. Therefore, two paradigms were used: single finger from the dominant hand and one finger from each hand.

In the single-finger case, the experiment consisted of a one-interval, two-alternative forced choice (1I-2AFC) paradigm with correct answer feedback. The subject moved the index finger to indent the specimen mounted on the specimen presenter while the rest of the fingers grasped a fix rod for achieving a standard posture. The subject had to decide whether the specimen presented was the softer or the harder one of the two. In the two-finger case, the experiment consisted of a two finger simultaneous, two-alternative forced-choice (S-2AFC) paradigm with correct answer feedback. The two index fingers indented the two specimens mounted on the specimen presenter and the subject had to decide whether the left or the

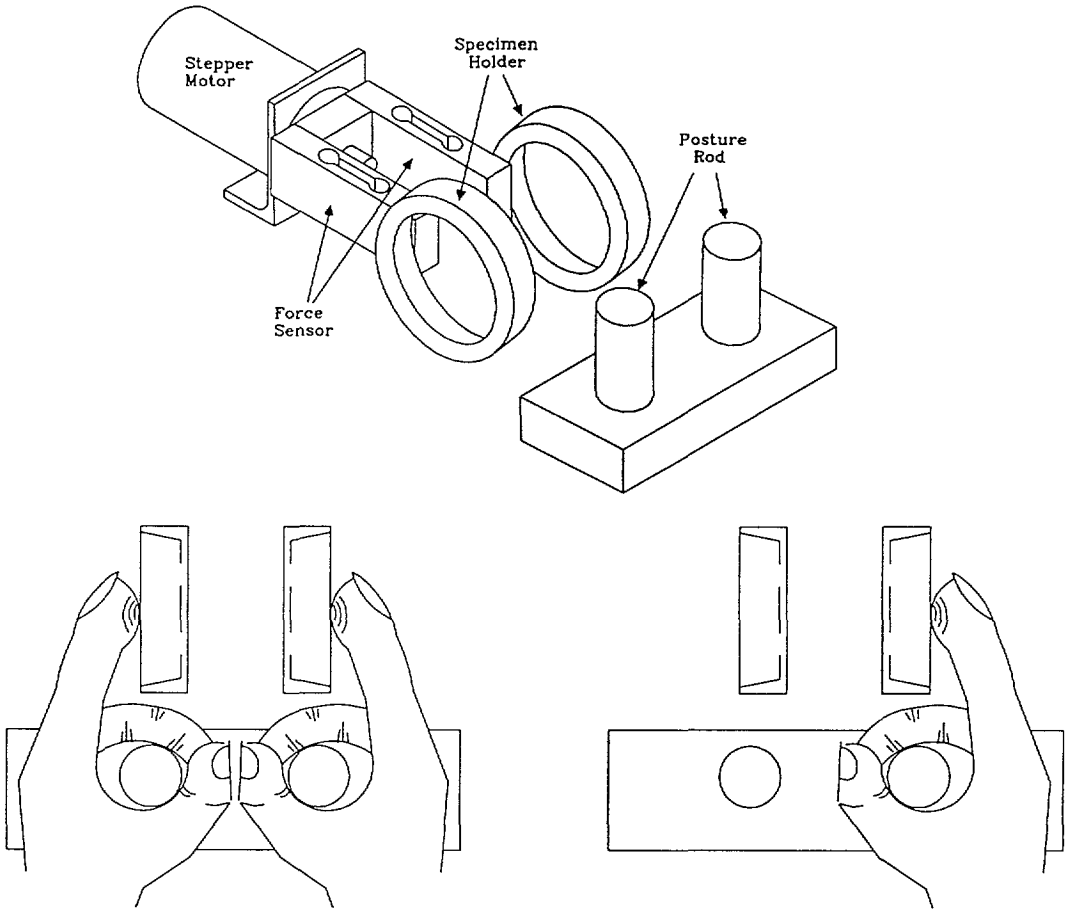

Figure 2-4: Relative positions of the fingers and the specimens for the two experimental paradigms.

right one was the softer specimen of the two. Figure 2-4 shows the relative position of the specimens and the fingers in the two experimental paradigms.

One of the significant differences between the two paradigms is the information available to the subject. In the 1I-2AFC case, subjects must remember how specimens felt like in order to come up with a correct response. In the S-2AFC case, however, both specimens were available to the subject during the discrimination. Therefore, the subject can compare both specimens during the indentation. This will be an easier task if the ability to control and sense at each hand is not reduced by the fact that both hands are involved at the same time. One might expect that since humans use multiple fingers on a daily basis, that should not be too bad an assumption. Clearly, we can squeeze two different rubber balls and distinguish them. But, can we squeeze a rubber ball composed of two semi-spheres with different material properties using fingers from two different hands and distinguish their relative softness ?

2.3.6 Experimental procedures

To obtain statistically significant results, the discrimination experiments require a substantial number of trials for each subject. One standard and four comparison specimens were used for each experimental condition. The comparisons were selected depending on the subject's performance and the finger conditions. Each subject was tested for only one hour per day to avoid boredom or possible injuries from repeated motions. Also, finger exercises were provided in between the four repeated runs of 64 trials. The first run was used as the training run and the data were not used in the final JND calculations. However, it was conducted just like a normal run.

Before each run started, the subject was given an opportunity to touch the two specimens when they were laying on the bench. Afterwards, the specimens were mounted horizontally on the specimen presenter. The subject rested their elbow on a flat surface and the palm grabbed onto a roughly 3/4 inch diameter wooden rod for posture reference and kept their eyes closed. An offset value of the force sensor was taken while the specimens were horizontal. Afterwards, the motor moved to its vertical home position with the hard specimen located on the top and the soft specimen at the bottom. Depending on the random number generated, the motor rotated either clockwise or counterclockwise with an equal probability. Thus either the soft or the hard specimen was located at the right after the motor stopped. During the 64 trials, the program controlled the motor to go to the two possible test configurations 32 times each. After the motor reached its destination for a particular trial, a delay of 0.5 second was in effect to avoid any vibration which might cause incorrect force sensor reading. Afterwards, the computer speaker beeped to prompt the subject to move the finger for indenting the specimen.

A circular buffer was used in the force data collection program which had a threshold force of 0.5N. A total of two seconds of force data was collected for each trial, which consisted of 0.5 seconds before 0.5N force was reached and 1.5 seconds after. This data collection scheme allowed force data from most of the trials to be recorded appropriately. Occasionally, however, the subject would make multiple contacts using forces above the threshold; the data collection was triggered on the first significant contact which might not have all the appropriate data. Or, the subject might start indenting the specimen after the motor stopped but a little before the computer beeped. In that case (less than 1% of the trials), the force

trace showed a sudden jump from zero at time equal to 0.5 second.

2.3.7 Data analysis

In the discrimination experiments, there were two stimuli S_1, S_2 and two possible responses R_1, R_2. If f_{ij} represents the number of trials the subject responded with R_i to a stimulus S_j, the results can be arranged in the following 2 by 2 confusion matrix format:

	R_1	R_2
S_1	f_{11}	f_{12}
S_2	f_{21}	f_{22}

The sum of the elements f_{ij} should add up to 64 for one run. If the subject was 100% correct, then $f_{11} = f_{22} = 32$ and $f_{12} = f_{21} = 0$. If the subject made mistakes, the off-diagonal elements would be higher. By applying the decision model that is used extensively in psychophysics [12] based on signal detection theory [44], the sensitivity index d' and bias β of the subject can be quantified. To get more reliable estimates, the data from the three runs (excluding the training run) were pooled together for such calculations. The JND of softness is the difference in the stimuli (percentage difference of the objective compliance) that corresponds to a d' value of 1 and is estimated by dividing the percentage difference by the calculated sensitivity index d'. To combine the data from different comparison softness, the JND was obtained by employing the standard procedure of averaging the four individual JND estimates.

The analysis of variance (ANOVA) method was used to find out whether the results were influenced by factors such as finger conditions and experimental paradigms. The individual JND estimates from each comparison specimen run was used for the calculations of the ANOVA table. To compare any two JND results obtained under different circumstances, the *Student's t* test [31][24][36] was used. The statistical analysis was performed by using MATLAB statistics toolbox. The results from different subjects were not averaged in order to observe their differences and to analyze why such differences existed.

Specimen	DR1	DR5	ER1	FR1
Difference	2.6%	7.1%	13.5%	31.7%
Confusion Matrix	55 41 29 67	74 22 20 76	74 22 17 79	92 4 1 95
d'	0.70	1.55	1.67	4.04
β	-0.17	-0.04	-0.09	-0.29
JND (%)	3.8	4.6	8.1	7.8
$MeanJND = 6.1\%$				

Table 2.2: 1I-2AFC discrimination results for subject CH under normal condition (Standard: CR1 [0.304mm/N])

2.4 Results

2.4.1 1I-2AFC discrimination

In the 1I-2AFC discrimination, the subjects used the index finger from their dominant hand to indent the specimen. Three subjects participated in the experiments: CH(male), CT(female), and JK (female). Three finger conditions were tested to see how different contact interface conditions affect the performance of the subjects. The batches of trials for different conditions and paradigms were randomized to minimize training effects.

JND results

The discrimination results from an experimental run was represented by a confusion matrix. The calculation of the sensitivity index, d', response bias β, and JND for a given comparison specimen was performed by using the procedure outlined in the Methods section.

For example, table 2.2 shows the discrimination data and the calculated JND value for subject CH under normal condition. Specimen CR1 was used as the standard and the four comparison specimens and the differences in objective compliance from the standard are listed. The confusion matrix was pooled from the three runs. The sensitivity index as well as the response bias was calculated according to the decision theory. The d' value obtained was then used to estimate a JND value by dividing the percentage difference in specimen compliance by d'. Finally, the JND under normal condition for subject CH was obtained by taking the mean of the JND estimates. Figure 2-5 shows how the sensitivity index d' varies with the difference in objective compliance of the comparison specimen. A least square line

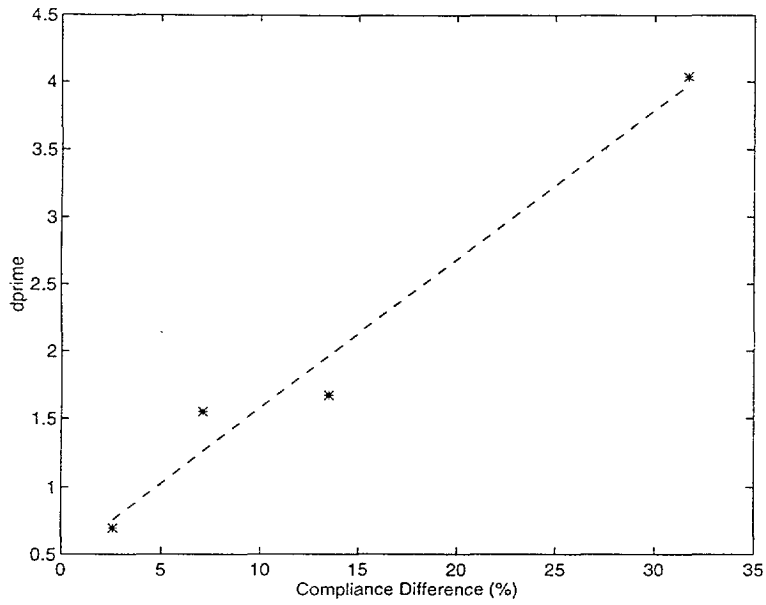

Figure 2-5: A plot of sensitivity index (d') and the specimen objective compliance difference for subject CH under normal condition.

was drawn to show that the relationship was approximately linear.

A summary table for the JND values calculated using this method under various conditions for all subjects are listed in Table 2.3 (Data used for these calculations are presented in Appendix B). With a thimble on the finger, the subjects' performance was a lot worse than the normal and finger cot conditions. For subject CH, the JND increased from 6.1% under normal condition to 43.3% under thimble condition. Keeping in mind the spread of the JND estimates in Table 2.2, we can observe that subjects CH and JK had similar performance under normal and finger cot conditions . The JND values for subject CT were higher than the other two subjects in all three conditions. The JND increased from 17.4% for normal and 14% for finger cot to 70.2% with thimble on. Clearly, with thimble on, none of the subjects were able to perform anywhere close to what they could under either normal or finger cot conditions.

Analysis of variance (ANOVA) was used to test for the effects of subjects and finger conditions and *Student's t* tests were used to compare the performances from different subjects under normal and finger cot conditions. There was a significant difference between the subjects at 1% significance level (the significance is the probability of observing the given result by chance given that the hypothesis is true). However, the differences between normal and finger cot conditions and the interaction between subject and condition factors were small.

Condition	Subject			Mean value
	CH	CT	JK	
Normal	6.1	17.4	7.0	10.2
Finger cot	4.3	14.0	5.0	7.8
Thimble	43.3	70.2	49.8	54.4

Table 2.3: 11-2AFC softness discrimination mean JND (%)

Significant differences of the mean JND, at 5% significance level, were found between subjects (CH,CT) under normal condition and between subjects (CH,CT) and (JK,CT) under finger cot condition. The complete analysis is presented in Appendix C.

Force profiles

A few raw data graphs are shown here to illustrate how the applied forces varied during a trial and how they varied across trials, conditions, and subjects. Figure 2-6 shows the force traces during a discrimination run that consisted of 64 trials. In that particular run, the specimens used were ER1 (comparison) and CR1 (standard) and the finger condition was normal. Even though the subject got 80% correct calls in the discrimination, the force traces varied from trial to trial with a peak force ranging from 10N to 16N. The force traces intersect at 0.5 sec time mark with a force magnitude of 0.5N because of the force data collection mechanism explained in the experimental procedure. The duration of contact was about 500 msec to 800 msec during that run and the indentation phase seems to take a little longer than the releasing phase.

Figure 2-7 shows the same force traces from the 64 trials separated according to the stimuli and responses (the confusion matrix format). The title for each panel indicates which stimulus (S) and response (R) group the force traces came from. The upper left and the lower right graphs show the forces from the correct responses while the upper right and the lower left graphs show the forces from the incorrect responses. The numbers on the upper left corner of each panel indicates the number of force traces in that panel. Those numbers together would make up a confusion matrix. The top row shows the forces used for the softer specimen and the bottom row shows those used for the harder specimen. For the same specimen (panels in the same row), the subject used forces which varied from trial to trial. The force traces from the incorrect responses were similar to the ones from correct responses.

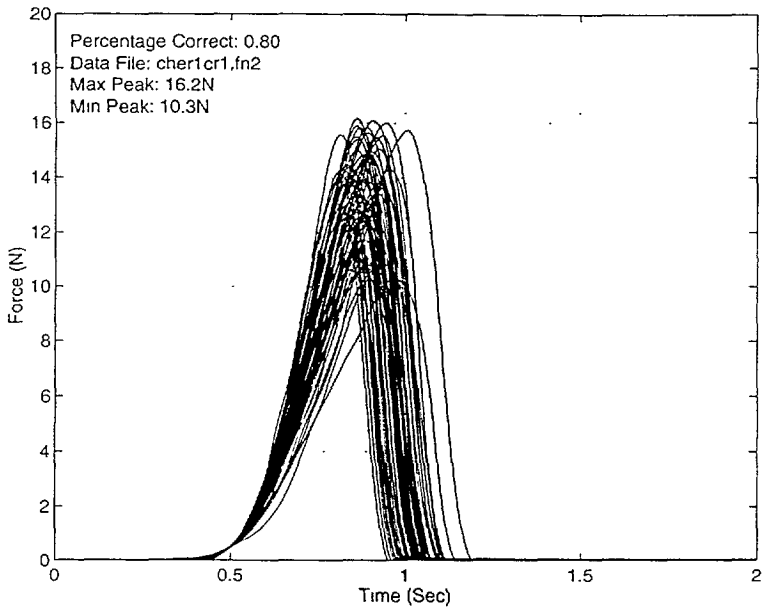

Figure 2-6: Force traces from subject CH during a 1I-2AFC discrimination run under normal condition.

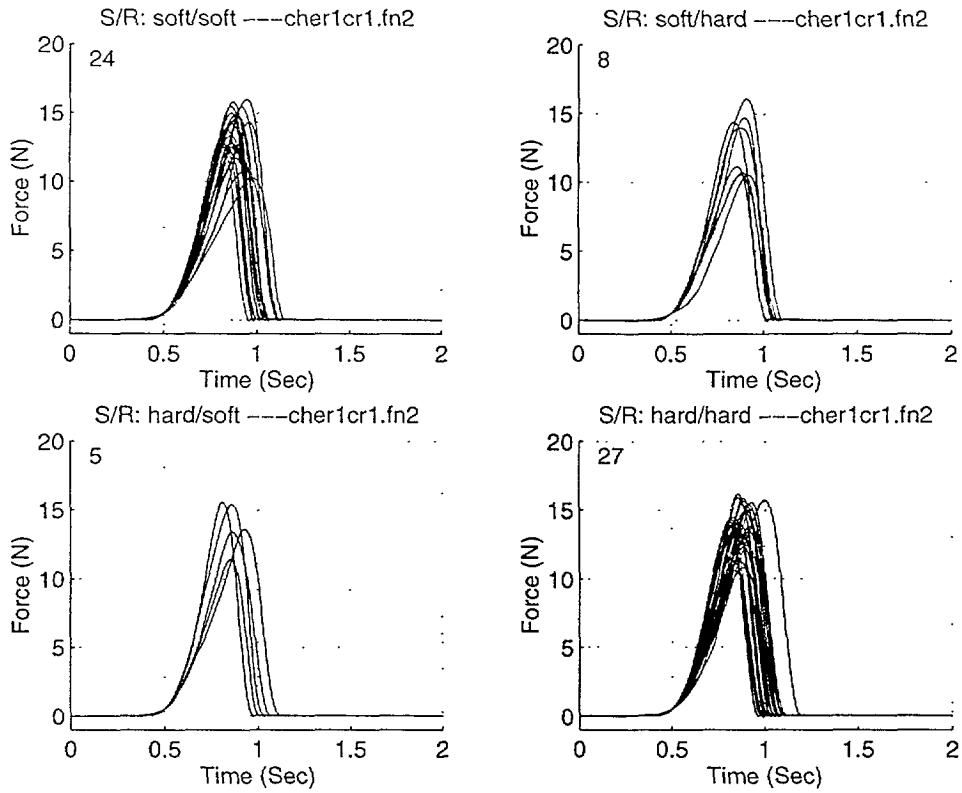

Figure 2-7: Force traces from subject CH during a 1I-2AFC discrimination run under normal condition plotted in the confusion matrix format.

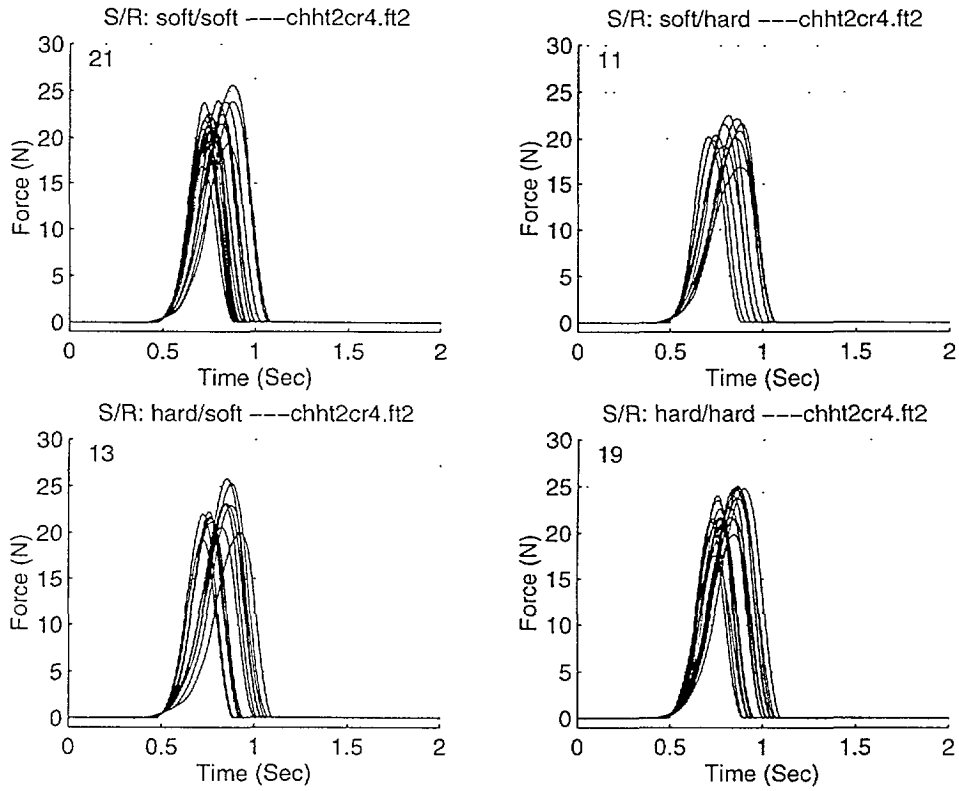

Figure 2-8: Force traces from subject CH during a 1I-2AFC discrimination run under thimble condition.

We cannot conclude that the subject responded incorrectly due to the force profiles applied.

The presence of finger cot and thimble did not seem to have much effect on the general shape of the force profiles for subject CH. Figure 2-8 shows the force profiles from an experimental run with the thimble condition during discrimination of the easiest specimen pair for that condition. Comparing with Figure 2-7 for normal finger, the general shape of the traces looked about the same. However, the forces used were somewhat higher than those used in the normal condition.

Different subjects showed quite different force profiles in terms of peak forces used, duration of contact, and consistency. Figure 2-9 and Figure 2-10 show typical force traces from subject CT and JK under normal, finger cot, and thimble conditions. For subject CT, the shape of the forces was not as consistent as those of subjects CH and JK. Also, the duration of contact, about 0.8 sec to 1 sec, was longer than what CH and JK used (about 0.5 to 0.8 seconds). The force profiles exerted on the specimens by subject JK was quite consistent and the peak forces during each trial were generally higher than that used by the other two

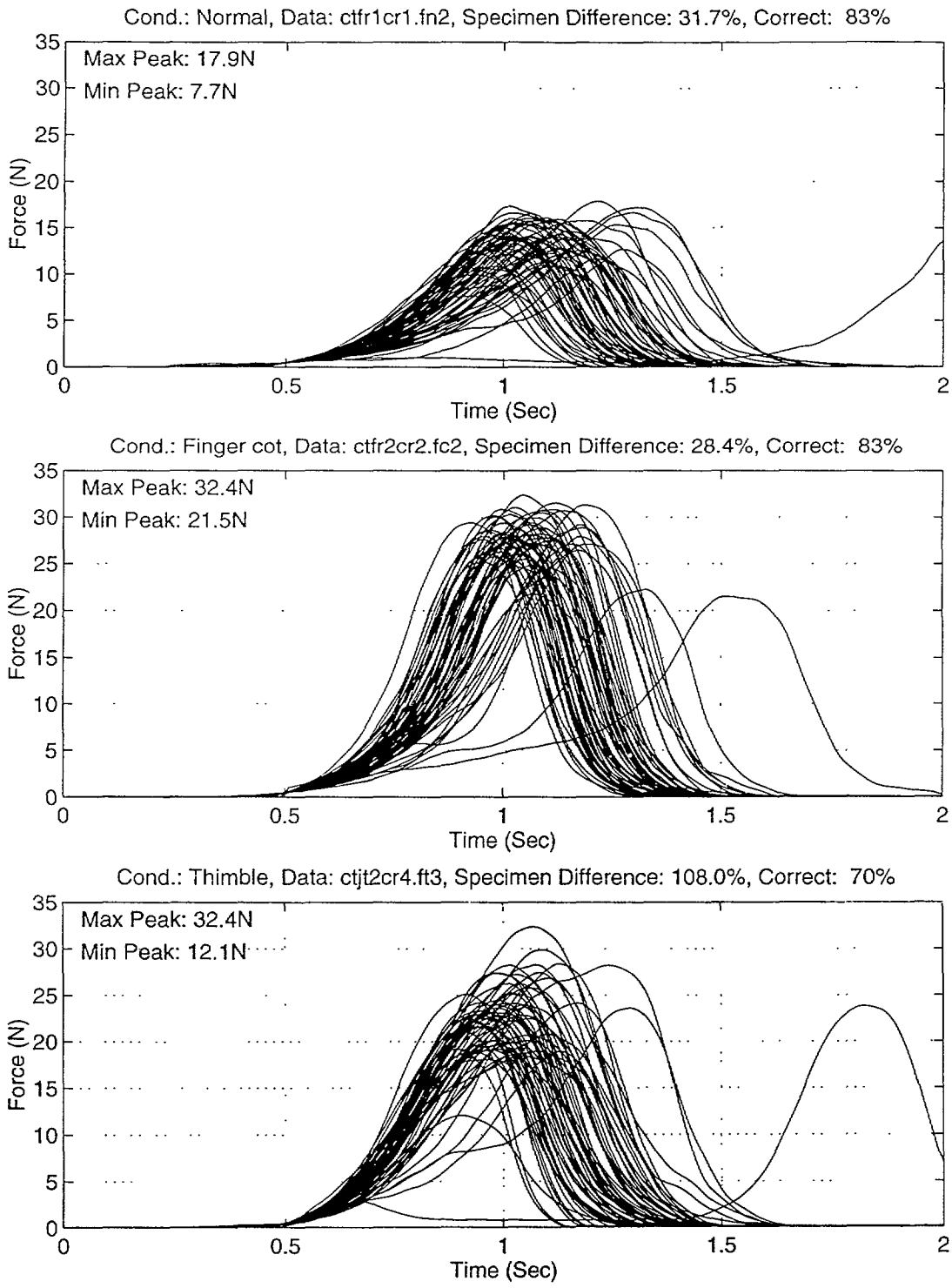

Figure 2-9: Force traces from subject CT during 1I-2AFC discrimination runs under normal(top graph), finger cot(middle graph), and thimble (bottom graph) conditions.

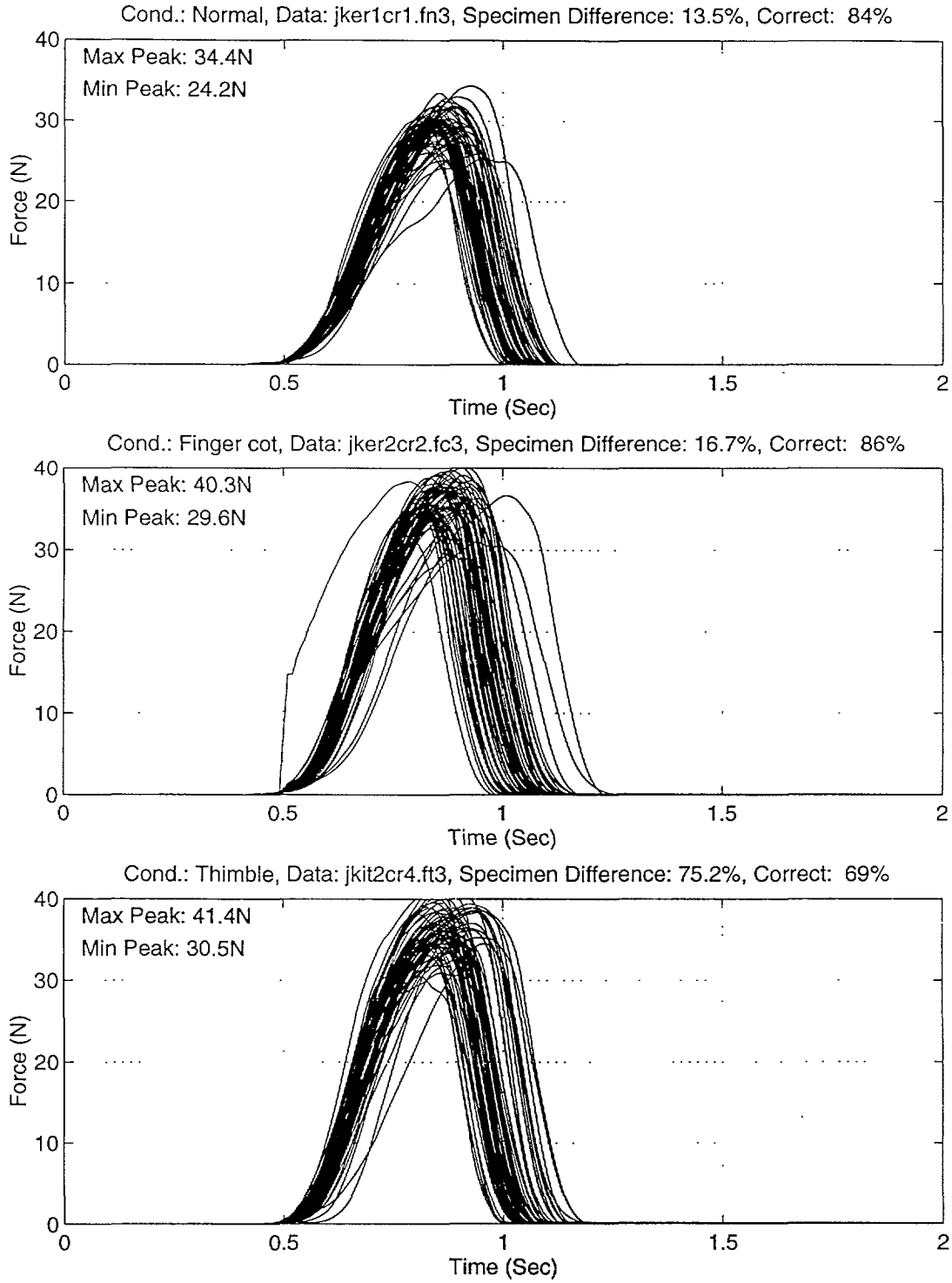

Figure 2-10: Force traces from subject JK during 1I-2AFC discrimination runs under normal(top graph), finger cot(middle graph), and thimble (bottom graph) conditions.

subjects.

2.4.2 S-2AFC discrimination

In the S-2AFC discrimination, the subjects simultaneously used the index fingers from both hands to perform the discrimination. The same three subjects and finger conditions were used. Again, the purpose of using three finger conditions were to see how different contact interface conditions affect the performance of the subjects. The purpose of the simultaneous contact was to reduce the role memory plays, since both specimens were available during the discrimination. The experiments were conducted in parallel with the 1I-2AFC discrimination experiments to reduce possible training effects. Since subjects applied forces on both specimens, the analysis on the force profiles could possibly reveal the underlying strategies used by the subjects for discrimination.

JND results

The JND values for the S-2AFC experiments listed in Table 2.4 were obtained by using the same pooled data method used for calculating the JNDs for the 1I-2AFC experiments. The JND values obtained were lower than the 1I-2AFC case under both normal and finger cot conditions for all three subjects. However, the JND value for the thimble condition was higher than the 1I-2AFC case for each of the three subjects.

Analysis of variance (ANOVA) was performed to determine the effects of subjects and finger conditions and *Student's t* tests were used to compare the performances from different subjects under normal and finger cot conditions. There was significant difference between the subjects at 1% significance level as indicated by the high F ratio from the ANOVA table. However, the differences between normal and finger cot conditions and the interactions of subjects and conditions were small. T-test at 5% significance level revealed significant differences of the mean JND between subjects (CH,CT),(JK,CT) under both normal and finger cot conditions. The complete analysis is presented in Appendix C.

Force profiles

The shape of the force profiles used by the subjects as well as the magnitude of the peak forces are of interest. Figure 2-11 shows the force traces from subject CH during a discrimination run under normal condition. The upper graph shows the forces exerted on the standard specimen

Condition	Subject			Mean value
	CH	CT	JK	
Normal	4.9	8.3	3.1	5.4
Finger cot	3.2	10.4	2.9	5.5
Thimble	57.9	78.4	56.1	64.1

Table 2.4: S-2AFC softness discrimination mean JND (%)

(CR3) whereas the lower graph shows the forces applied on the comparison specimen. Like the 1I-2AFC experiments, the shapes of force profiles vary from trial to trial. The first 9 trials of that run is shown separately in Figure 2-12 with the trial number labeled in the bottom row of upper left corner. Also shown in the upper left corner of each panel are the softer stimulus location (labeled S) and the response of the subject (labeled R). The solid line represents forces on the comparison specimen (the softer one) and the dashed line represents the forces on the standard. In the first trial, the softer specimen was located on the left hand side and the subject correctly responded. The moment of contact on the standard specimen was earlier than for the comparison (softer) specimen for trial 1. Some of the peak forces were about the same for both specimens (trials 2 and 3) while some were higher on the softer specimen (solid line, trials 1,4,7,8,9) and others higher on the harder specimen (dashed line, trials 5,6). The moment of contact was sometimes earlier for the softer specimen and other times earlier for the harder specimen.

To see whether or not the magnitudes of the peak forces exerted by the two fingers on specimens were related to the correctness of discrimination, a plot of the peak forces on the soft specimen versus that on the hard specimen for subject CH under normal condition was shown in Figure 2-13. Symbols 'o' and 'x' were used for correct and incorrect responses, respectively. The four panels are for the four different comparison specimens. The differences in objective compliances for the specimen pairs are shown on top of each graph. The percentage correct (pooled from 3 runs) and the confusion matrix (labeled CM) of the subject are shown in the upper left corner. The numbers labeled FsM are the elements of the following force-specimen-correctness matrix that arranges the correct and incorrect responses according to whether or not the peak force on the hard (standard) specimen is higher than that on the soft (comparison) specimen.

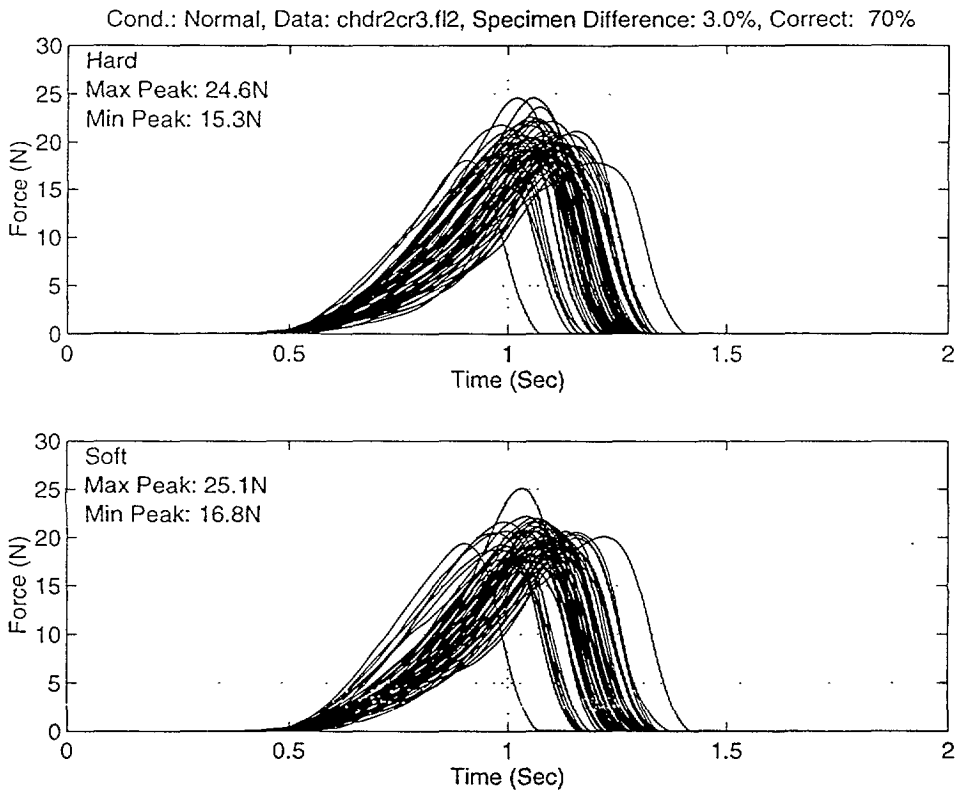

Figure 2-11: Forces on hard and soft specimens from subject CH during a S-2AFC discrimination run under normal condition.

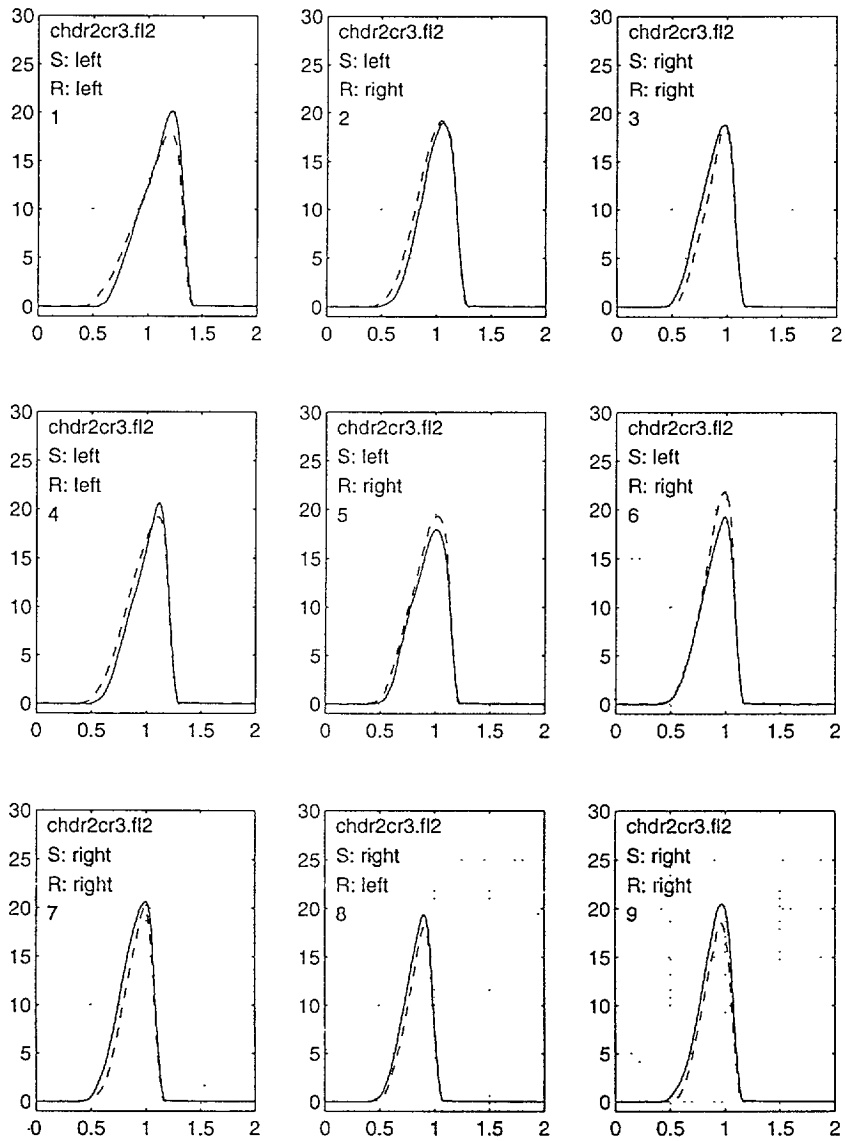

Figure 2-12: Forces exerted on soft (solid line) and hard (dashed line) from the first 9 trials of subject CH during a S-2AFC discrimination run under normal condition.

	Correct	Incorrect
$F_{hard} > F_{soft}$	s_{11}	s_{12}
$F_{hard} \leq F_{soft}$	s_{21}	s_{22}

If the objective of the subject was to obtain the same amount of deformation from both specimens to enable a discrimination based on the peak force applied to achieve the deformation, then the subject had to exert higher forces on the harder specimen pairs and higher force on the hard specimen than on the soft specimen for a given pair. Such hypothesis can be tested by looking at the FsM matrix and comparing the occurrence of higher forces on the hard specimen to that of higher forces on the soft specimen. So, we can sum the first two numbers of the FsM matrix which were the number of trials that had higher peak forces on the hard specimens and compare it to the sum of the last two numbers which were the number of trials that had higher peak forces on the soft specimens. From the matrices shown in Figure 2-13 for subject CH, the numbers from the easiest pair to the most difficult pair were: (97,95), (94,98), (106,86), and (111,81).

For subject CT, plot shown in Figure 2-14, the opposite was observed. The numbers were (75,117), (81,111), (84,108), and (98,94) from the easiest to the most difficult pairs. These numbers indicate that the subject used higher forces for the softer specimens than for the harder specimens in a given pair. This would be consistent with a different hypothesis, namely that the subject was trying to obtain the same amount of pressure from the two specimens. As will be shown in contact visualization, for a given force, the percentage contact area inside the contact region is lower for harder specimens. Thus, the actual pressures for the harder specimens are higher than those for the softer specimens. To obtain the same amount of pressure, therefore, the force on the softer specimen should be higher than that on the harder specimen. As the difference between the two specimens got smaller, the applied peak forces also got closer for this subject.

For subject JK, it is completely different from the other two subjects. Unlike the plots from subjects CH and CT which had data points clustered around the 45 degree line (the two forces did not differ much), the data points separated into two clusters as shown in Figure 2-15. When the difference between the specimen pair was large (16.2% difference), the degree of separation of the two clusters was small. For the most difficult pair (3.0% difference), the degree of separation was largest. Also, subject JK used peak forces that were much higher than the other pairs and saturated the input of the data acquisition system

near 42N. If we look at the upper cluster of the 3% difference specimen pair, most of the peak forces exerted on the harder specimen were within the range of 22N to 33N while most of the peak forces on the softer specimen were more than 40N. The numbers from the FsM matrix from easier to difficult specimen pairs were: (95,97), (96,96), (96,96), and (96,96). It was very consistent, but did not fit either of the two hypothesis so far. This suggests a third hypothesis, namely that the subject was trying to exert the same amount of force and compare the contact information obtained in order to discriminate. If the subject was indeed trying to exert the same force on the two specimens, the fact that Figure 2-15 showed data points in two clusters could mean the subject had a different sensation of force on the two fingers. So, if we plot the peak forces according to hands instead of according to specimens, the data points should be clustered near the hand which used higher forces. Figure 2-16 shows that subject JK used higher forces from the right hand for the three specimen pairs that are more difficult. The definition of the FhM matrix is similar to FsM matrix as shown below:

	Correct	Incorrect
$F_{right} > F_{left}$	h_{11}	h_{12}
$F_{right} \leq F_{left}$	h_{21}	h_{22}

For this subject, summing of the rows of the FhM matrix in a manner similar to that done for FsM above gives (192,0), (192,0), (192,0), and (191,1). These results clearly show that this subject almost always applied higher forces with the right hand.

2.5 Discussion

2.5.1 Effects of finger conditions

The information available to the subjects for softness discrimination under the three different finger conditions was not the same. With normal finger, the subject had detailed tactile as well as kinesthetic information. When the finger were covered with a thin rubber finger cot, the subject could still feel the surface of the specimen but the minute finger ridge level details were degraded. The presence of finger cot acted just like another low-pass filter for the mechanoreceptors underneath the skin which originally receive information already filtered by the skin. When the finger had a rigid thimble on, the deformation of the fingerpads depend only on the interaction force with thimble, and not on the specimen compliance. Thus, the

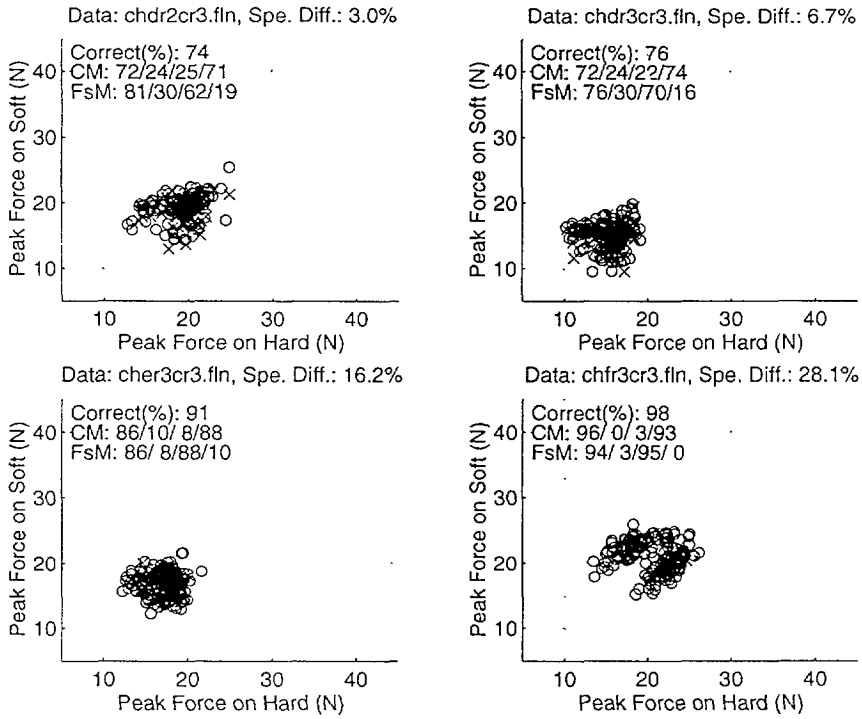

Figure 2-13: Peak forces on soft versus hard specimens for subject CH under normal condition.

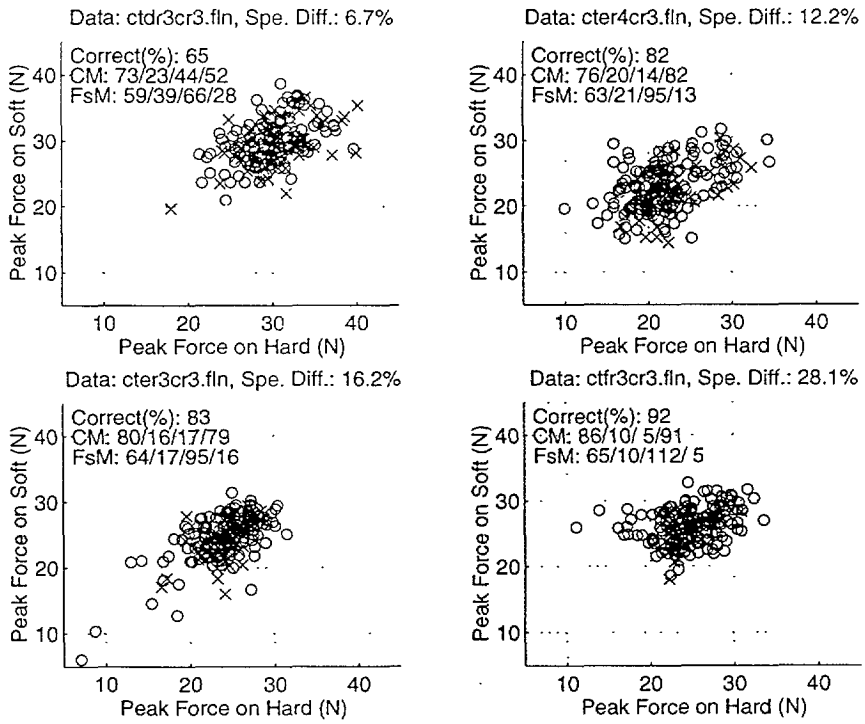

Figure 2-14: Peak forces on soft versus hard specimens for subject CT under normal condition.

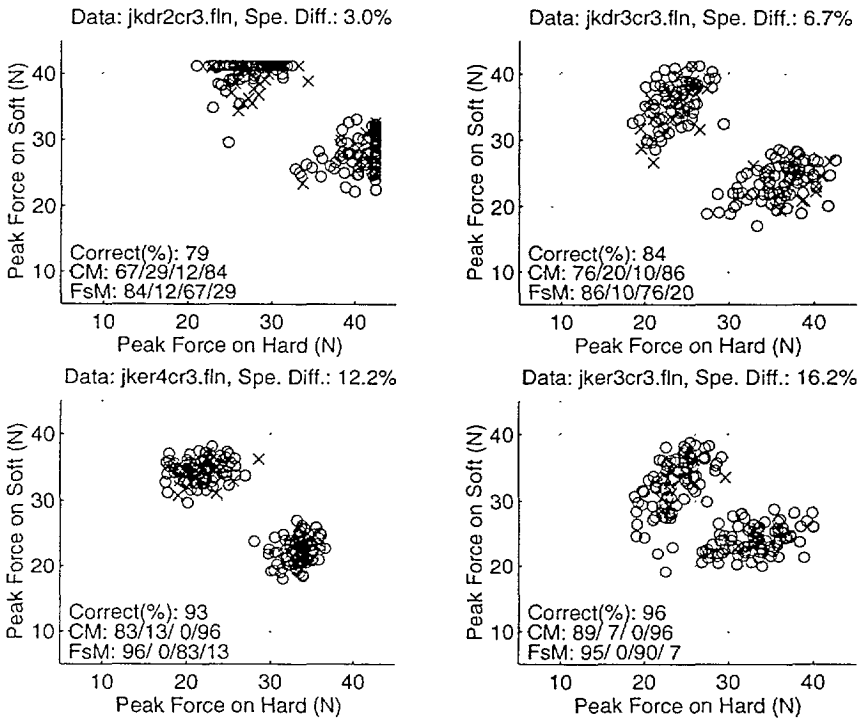

Figure 2-15: Peak forces on soft versus hard specimens for subject JK under normal condition.

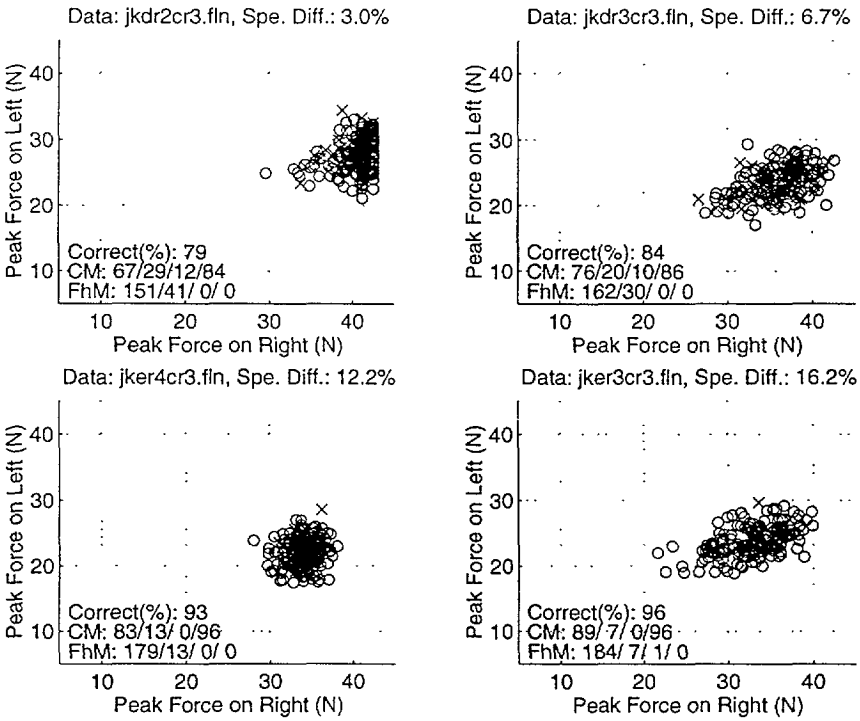

Figure 2-16: Peak forces on left versus right specimens for subject JK under normal condition.

subjects' sense of object softness will have to come mainly from the kinesthetic information. Because all the experiments involved active touch, the motor commands used during the discrimination were also available to the subjects in all conditions.

In both 1I-2AFC and S-2AFC experiments, the presence of the thimble degraded the performance of all three subjects dramatically. The general shape of the force profiles looked similar to the ones from other conditions. However, the subjects were not able to discriminate the specimen pairs at the level they had achieved under normal or finger cot conditions. Therefore, even though the subjects were able to control their forces successfully to produce similar force profiles, the absence of useful tactile information from lack of direct contact with the specimens radically degraded their ability to discriminate.

Analysis of variance, detailed in Appendix C, did not show significant difference between the JND results obtained under normal and finger cot conditions. This implies that missing the detailed information from the ridge level mechanics of contact was not severe enough to degrade the softness discrimination performance as indicated by the JND results.

In summary, by comparing the softness discrimination results from the three different conditions, we see that tactile information was crucial for the softness discrimination based on the poor performance with the thimble. The fact that the presence of finger cot did not significantly affect the result of discrimination suggests that the information from the fine finger ridge level mechanics of contact was not crucial for these experiments.

2.5.2 Effect of experimental paradigms

The main difference between the two experimental paradigms is the information available to the subject. In the S-2AFC case, both specimens were available to the subject during the discrimination. In the 1I-2AFC case, however, subjects had to remember how the other specimen felt like in order to come up with a correct response.

The JND values obtained from S-2AFC paradigm under both normal and finger cot conditions were smaller for all three subjects. This is consistent with our expectation since the subjects had information from both specimens during a trial and thus it was an easier task. The ANOVA analysis in Appendix C indicated that the JND data obtained from the two paradigms are significantly different at 1% significance level.

From the box plots of the JND data from the two paradigms for all three subjects under both normal and finger cot conditions given in Appendix C, the variations of the data from

the S-2AFC experiments were smaller than those from the 1I-2AFC experiments. We cannot treat the results from the one-interval S-2AFC experiments just like a traditional 2I-2AFC experiment. The improvement in performance from these experiments under both normal and finger cot conditions most likely should be attributed to the elimination of the role memory played in the discrimination.

For the thimble condition, the S-2AFC performance was worse than the 1I-2AFC case. This result was not surprising since the subjects had no direct contact with the specimens (no useful tactile information) and the remaining information is from the kinesthetic sense and the knowledge of motor commands executed. Any tactile information received could potentially be misleading since the fingers were contacting the thimble, not the specimens. To control two fingers carefully and at the same time to ignore the misleading tactile information would seem like a tougher job for subjects and it showed up as degraded performance.

2.5.3 Force profiles

The force profiles used by subjects during the discrimination varied across subjects and trials. They were in general bell shaped curves with typical contact durations between 0.5 sec to 0.8 sec for subjects CH and JK. For subject CT, the contact was longer and ranging from 0.8 sec to 1 sec. The profiles did not seem that different under finger cot and thimble conditions. The peak forces exerted on the specimens by the subjects had a wide range, generally between 10N and 40N. Higher forces were used by subject JK during the discrimination.

The force profiles exerted on the two specimens looked similar in the S-2AFC experiments with two fingers. If they were identical, the subject might be able to discriminate based on the resulting deformation of the fingers. However, if the force profiles from the two fingers differed such that the resulting deformation of the two fingers were the same, then the subject would have a hard time discriminating. For example, if higher force rate was exerted on the harder specimen and lower force rate exerted on the softer specimen, the deformation of the hard specimen may be similar or more than that of the softer specimen. In that case, the subject might make mistakes.

A longer contact duration would mean lower force rates and if that information was used during the discrimination then it would explain why the performance of subject CT was not as good as the other two subjects.

2.5.4 Possible softness discrimination mechanisms

If we were to design methodologies for a robot to use its fingers to determine the compliance of an object, we can have strategies that utilize force and displacement information. In the force based strategy, the displacement can be held constant by pushing against an object to a certain deformation. The force developed during the contact can be used to calculate the compliance of the object. On the other hand, the robot can push against the object until a certain maximum force is reached. In that case, the robot finger position profile together with the forces at every instant can be used to determine the object compliance.

In humans, investigating the underlining mechanisms is more complicated. If we just look at the force profiles from the 1I-2AFC discrimination experiments, we would be lost even if we break down the trials according to the stimuli presented and the responses given by the subject (see Figure 2-6). Although the shape of the force profiles was very consistent, the peak forces exerted on the specimens by the subjects varied from trial to trial and had a wide range, generally between 10N and 40N. Also, the duration of contact varied from trial to trial but generally ranged from 0.5 sec to 1.0 sec. It would not be easy, if at all possible, to see the underlying softness discrimination strategies used by the subjects from the 1I-2AFC force profiles. However, it did confirm that tactile information, degraded(finger cot condition) or not(normal condition), was important for the tasks and that each subject's ability can be significantly different from the others.

By looking closely into the peak forces in the force profiles used by the subjects during S-2AFC experiments, it seems quite likely that the subjects were using different strategies (see S-2AFC results). For subject CH, the trend was to exert higher forces on the harder specimens. This would be consistent with trying to obtain the same amount of contact information (through deforming the specimens) from both fingers and thus harder specimen requires higher peak forces. For subject CT, the trend was to use higher forces on the softer specimen. The strategy might be trying to apply the same amount of pressure on the specimen. For softer specimen, higher peak forces were needed because the percentage contact area inside the contact region was higher (see Contact Visualization chapter). Subject JK used a strategy based on exerting equal amount of force on both specimens. However, subject JK exerted very different forces from the two fingers which suggested that the brain also needs to compensate for such differences to make correct discrimination.

The lowest JND values obtained from these experiments were about 3% by subject JK during S-2AFC discrimination under both normal and finger cot conditions. If force, displacement, or their combination were the only cues used, such small JND number would not be possible since the available literature report higher JND values for those physical properties (see Introduction). However, the JND values reported by other researchers might have inevitable memory effects depending on the paradigms used. On the other hand, the subject could also be using other types of information to achieve the discrimination. Even though the forces and strategies used were very different for all subjects, the percentage contact area inside the contact region were higher for softer specimens (see Contact Visualization chapter). The subjects could be using the spatio-temporal pressure distribution to discriminate the specimens. In that case, the finger ridge level details under the finger cot condition might not be very important and the absence of useful tactile information in thimble condition would have a big impact on the JND results.

2.5.5 Important factors in discrimination

In a general discrimination task, our ability to discriminate relies on sensing, control, and cognition. It is only by conducting experiments under carefully designed conditions that the relative role played by each component could be understood.

In the softness discrimination tasks reported here, the finger condition was a key factor that had significant effect on the performance. Without the presence of useful tactile information, the task was difficult as shown by the poor thimble performance. The finger ridge level details of mechanics of contact, however, did not seem to be important in the softness discrimination tasks examined here as shown by the excellent performance of subjects under finger cot condition. A reasonable explanation lies in the fact that the mechanoreceptors are underneath the skin and receive only low-pass filtered signals. The presence of the thin (0.06mm) finger cot did not seem to change the input to the receptors much.

By conducting S-2AFC experiments, we had an opportunity to examine the underlying strategies used by subjects and also effectively reduced the role memory played in the discrimination. The peak force data suggested three different strategies used by three different subjects: to obtain the same amount of deformation, to apply the same amount of pressure, and to apply the same amount of force. No matter which strategies were used by the subjects, the coordination between sensing, control, and cognition seems to be important for successful

discrimination.

Chapter 3

Force Control

3.1 Abstract

To study the ability of humans in controlling the forces of contact applied by the fingerpads, constant normal force control experiments were conducted under several experimental conditions. The experimental parameters were finger contact interface conditions, specimen softness, target normal force magnitude, availability of visual feedback, and the fingers from the left or right hand of the subjects. Three finger contact interface conditions were tested: normal finger, finger covered with a finger cot, and finger covered with a rigid thimble. Four different specimens were used: a rigid Plexiglas and three transparent silicon rubber specimens with different compliance values. Target normal force magnitudes of 2N, 4N, and 8N were used. The experiments consisted of controlling forces during three stages, 5 seconds each, of force feedback: tracking with numerical force display, tracking with graphical force display, and maintaining target force without visual feedback. The numerical feedback stage was used to help the subjects to exert forces close to the target, and therefore the performance was not analyzed; only the data from graphical feedback stage and the maintaining stage were analyzed. Index fingers from both the left hand and right hands were tested. The statistical tests on the data collected indicate that the finger contact condition as well as the specimen softness did not have significant effects on the results. Not surprisingly, when there was visual force feedback, the error was smaller than without feedback for all the subjects. For two subjects, the percentage error increased from less than 2% at 8N target with visual force feedback to about 4% and 6% without visual force feedback, respectively. For the other subject, the increase, from 2% to 11% at 8N, was more dramatic. The subject who had the

highest error without visual feedback was the same one who had higher JND values (less able to discriminate) in the softness discrimination experiments. In both stages analyzed, the tests on the handedness showed that there was a significant difference between the results obtained for the two hands of one of the subjects who also consistently showed handedness during softness discrimination experiments.

3.2 Introduction

The interaction of human hands with objects involves both sensing and control of the contact interface. The human abilities of tactual perception and manipulation are dependent on the haptic system, consisting of the mechanical, sensory, motor, and cognitive subsystems. Tactual sensory information concerning contact with an object can be divided into three classes: (1) tactile information, referring to the sense of the type of contact with the object as well as some of the physical properties of the object, mediated by the responses of receptors innervating the skin within and around the contact region; (2) kinesthetic information, referring to the sense of position and motion of body segments along with the associated forces, conveyed by the sensory receptors in the skin around the joints, joint capsules, tendons, and muscles; (3) neural signals derived from motor commands. The motor subsystem complements the sensory system by enabling control of body postures and motions together with the forces of contact with objects.

In performing manual tasks in real or virtual environments, contact force is perhaps the most important variable that affects both tactual sensory information and motor performance. When the hand is actively pressed against an object, the contact forces are sensed by both the tactile and kinesthetic sensory systems. The Just Noticeable Difference (JND) in contact force is about 7% over a wide range of conditions involving variations in force magnitude, muscle system and experimental method, provided that the kinesthetic sense is involved in the discrimination task (Pang et al[33]). In closely related experiments consisting of distinguishing among different weights of objects, a slightly higher JND of about 10% has been observed (see reviews by Clark and Horch [8] and Jones [25]). In experiments involving grasping and lifting of objects using a two-finger pinch grasp, Johansson and Westling [22] have shown that subjects have exquisite control over maintaining the proper ratio between grasping and lifting forces (i.e., the orientation of the contact force vector), so that the objects

do not slip. However, when tactile information was blocked using local anesthesia, this ability deteriorated significantly because the subjects could not sense contact conditions such as the occurrence of slip, and hence did not apply appropriate compensating grasp forces. Thus, performance in tasks involving contact require sensing of appropriate forces as well as using them to control contact conditions. Srinivasan and Chen [39] measured the human abilities to control the normal forces of contact exerted by the fingerpad on rigid objects under a variety of experimental conditions and found that performance degraded significantly in the absence of tactile information (by using local anesthetized fingertips) and visual feedback (by using an eye mask).

The goal in this study was to measure the human abilities in controlling normal force of contact applied by the fingerpad on objects of various softnesses under several experimental conditions. Three contact interface conditions were used to study the effect of altered tactile information on force control performance. The results of control with visual feedback was compared with those without visually feeding back the applied forces to the subjects. The same experiments were performed on index fingers from both hands of three subjects. The absolute error between the target force and the forces exerted by the subjects were averaged over three trials as a measure of human performance. In addition, the effect of performances under various conditions were compared using analysis of variance (ANOVA).

3.3 Methods

3.3.1 Experimental setup

The same setup used for the softness discrimination experiments was used for the force control experiments in order to study the abilities of humans in controlling normal forces of contact with specimens of different softness. An illustrative diagram of the experimental setup is shown in Figure 3-1.

The soft specimens(see Softness Discrimination Methods) were mounted vertically inside one of the specimen holders depending on the finger being tested. The rigid specimen was mounted on top of the specimen holder. The soft specimens fitted nicely tight in the specimen holder and could also be taken out without too much effort. To record the forces exerted on the specimens, a pair of custom made binocular force sensors, sufficiently stiff (see Softness Discrimination Methods) and not sensitive to the location of load application were interfaced

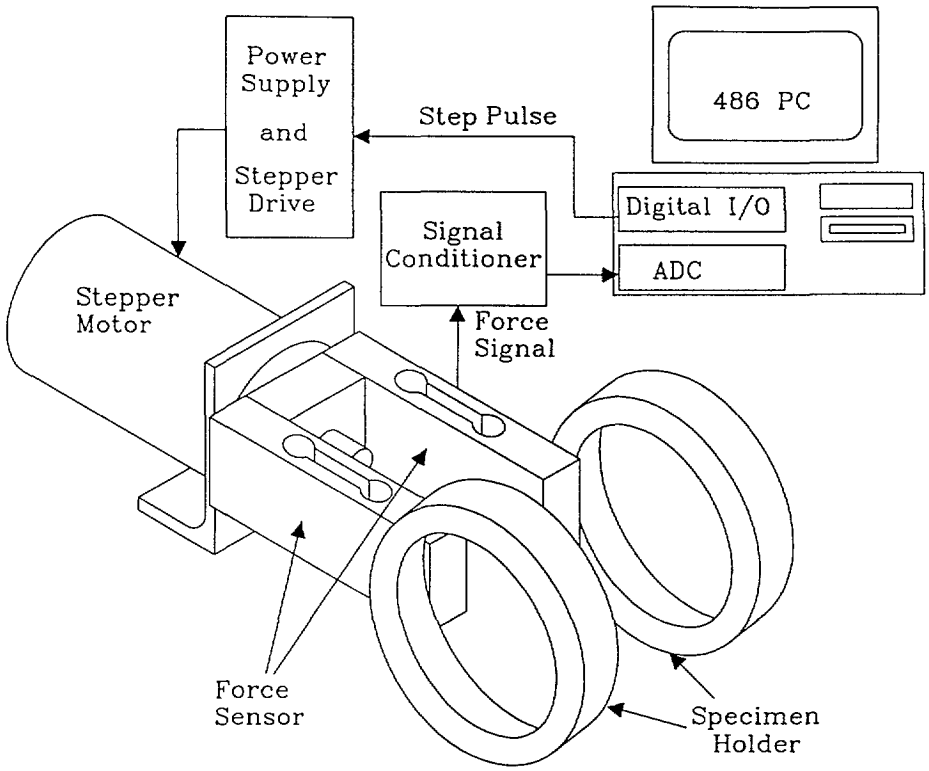

Figure 3-1: The force control experimental setup.

to an analog to digital (A/D) conversion board in a 80486 personal computer. The forces exerted on the specimens were displayed differently in each of the three 5-second experimental stages during each run. The force data as well as the force display were updated at a rate of 200 samples per second. The stepper motor was controlled through digital input/output (I/O) port and was energized to hold the specimen at a vertical configuration during the experiments. The subjects were sitting comfortably in front of the computer monitor with their elbow rested and hands grasping the fixed rods provided for controlling hand posture during the experiments, as shown in Figure 3-2 for left and right hands.

3.3.2 Experimental parameters

The five experimental parameters used were contact interface conditions, specimen softness, target normal force magnitude, visual feedback availability, and the fingers used for experiments. The same three subjects who participated in the softness discrimination experiments were used for tests on all parameter combinations.

In order to determine the relative importance of tactile feedback in controlling the contact

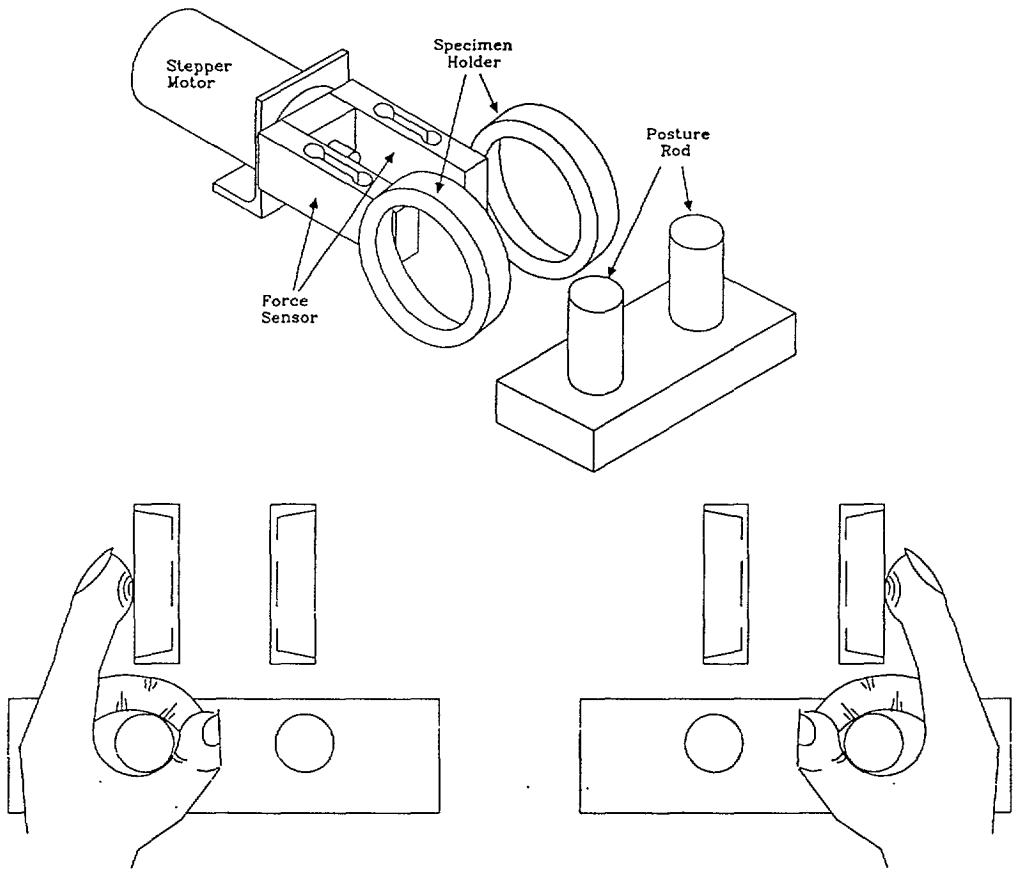

Figure 3-2: Relative positions of the finger and the specimen for experiments on left and right index fingers.

force on the fingerpad, the tracking experiments were conducted with the subject's finger under normal condition (both tactile and kinesthetic information available to the subject), finger cot condition (fine finger ridge contact information is degraded by the thin rubber finger cot), and thimble condition (the tactile information is derived from fingerpad contact with a rigid thimble instead of direct fingerpad contact with the specimens).

Four different specimens were used: a rigid Plexiglas plate and three transparent silicon rubber specimens with different softnesses. The soft specimens were cast by mixing different proportions of General Electric (GE) SF96-50 silicon rubber diluent to fixed proportions of GE RTV615A and RTV615B components. An objective measure of the specimen softness was measured by using a linear stepper motor system with micro-stepping drive to indent the specimen at a constant velocity of 0.5 mm/sec with the flat circular end of a 1/4 inch diameter cylindrical probe. The characteristic force-displacement relationship of the specimens was linear(Figure 2-1). The three specimens chosen had objective compliance of 0.304mm/N (hard), 0.455mm/N (medium), and 0.608mm/N (soft). The variability in these compliance measurement was only $\pm$0.001mm/N.

Target normal force magnitudes of 2N, 4N, and 8N were used as one of the experimental parameters. Although 8N was not as high as the peak forces generally applied by the subjects during tasks such as softness discrimination, it was close to the maximum constant force that subjects could apply and still be comfortable after repeated experiments of 15 seconds each for an hour. The other two reference force magnitudes were used in order to determine how the performance varied with target force magnitude.

The experiments consisted of applying and controlling forces with the fingerpad for 15 seconds under three stages of force feedback: tracking with a numerical force display, tracking with graphical force display, and maintaining target force without visual force feedback. Subjects began the force application in each trial without any external triggering signal. During the first 5 seconds, the force used by the subjects was displayed on the screen as a number(unit:N). During the next 5 seconds, the display changed to a graphical display. A horizontal bar extended out from the right(left) edge of the screen was shown in the middle of the monitor and ended at a distance from the center which was proportional to the force error for trials using right(left) hand. The subjects were instructed to try and maintain the end of the force display bar to be as close as possible to the fixed target line drawn vertically in the middle of the monitor. During the last 5 seconds, the graphical display of the contact

force was deactivated and the bar displayed did not change according to the force applied. Subjects had to maintain the target force based on their manual feel of it. The display of the forces during these three stages are illustrated in Figure 3-3 for both fingers.

In the real world, we manipulate objects with fingers from both hands. To investigate whether or not there is a significant difference in the control of forces for fingers from the two hands, the same tests were conducted for the index fingers from both the dominant and non-dominant hands.

3.3.3 Experimental procedures

Since there are too many parameters for the experiment to be randomized between parameters, the experiments were conducted with a fixed parameter sequence. The experiments on the two different fingers were conducted in two different sessions. The parameter of force feedback method was varied during the stages of each experimental run. The other three parameters were varied in the following way. For each specimen tested, the finger contact interface conditions were varied first. Under each finger condition, the target force was varied from 2N to 4N and finally 8N. The same three subjects tested for softness discrimination repeated the force control trials at each target force level three times.

Before a session started, the subjects were given practice runs with both hard and soft specimens until the procedure was familiar. Each subject was seated so as to comfortably press his/her index finger on specimens attached to the force sensor. The posture rod in front of the specimen provided a good reference position for the subject's hand and finger during the experiments. At the beginning of each trial a target force was shown as a number in Newtons on the monitor and the subject was also informed by the experimenter about the target force magnitude. The subject started the indentation on his/her own without any external triggering signals. The control program written in C language had a circular buffer that waited for the moment of contact to happen before it started logging the force data. After the subject exerted significant amount of force (0.5N) on the specimen, the trial began. During the first stage, the applied force was displayed in numerical format near the left or right side of the screen depending on whether the finger from the left or right hand was involved in the experiment. The first stage, which lasted 5 seconds, was needed to help the subject get to the target force level. During the second 5 seconds, the force was fed back to the subject through graphical force display as described before. A bar started from the sides

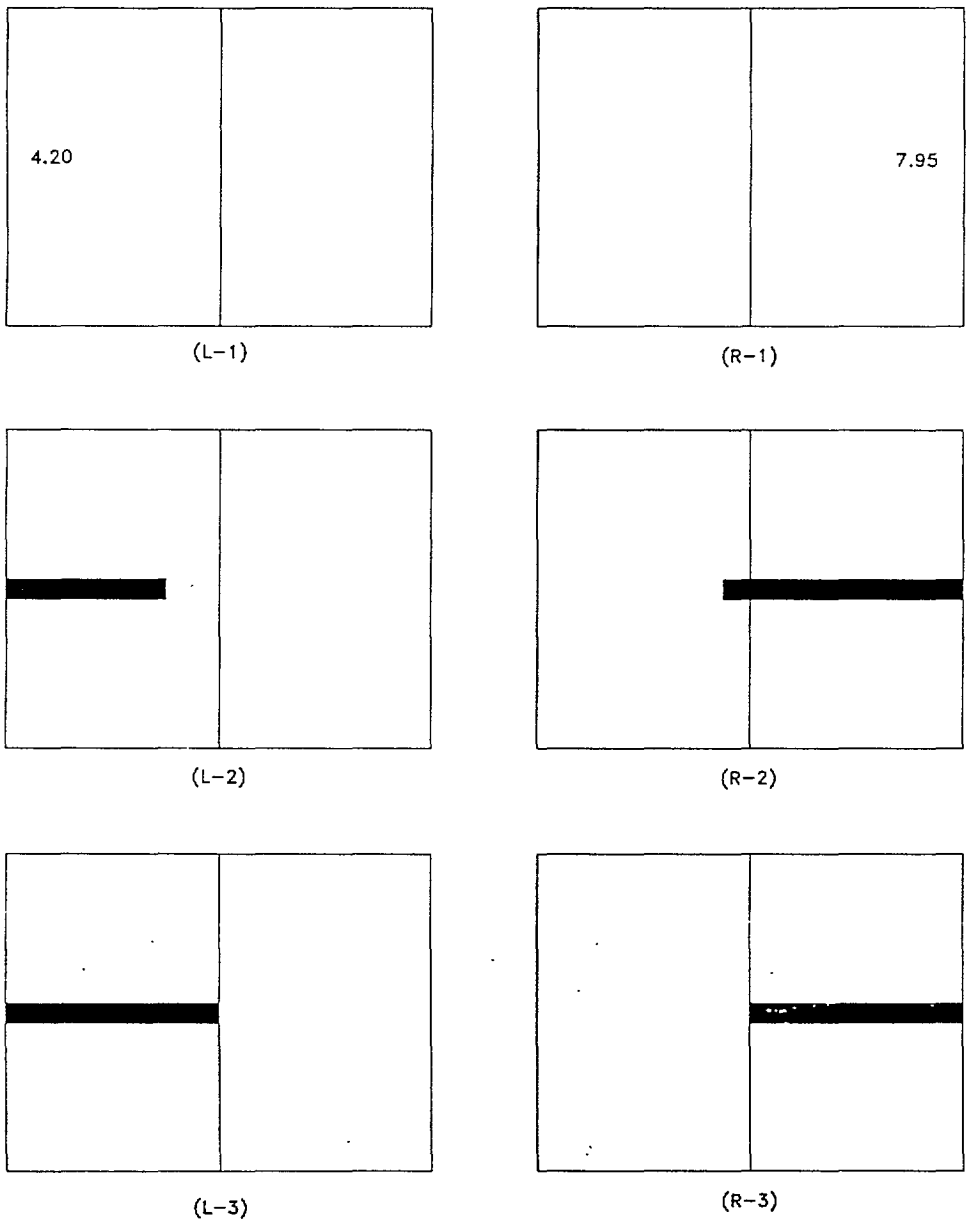

Figure 3-3: Contact force display during the three stages of force control experiments for left and right hands.

of the screen and approached the center of the screen as the subjects exerted forces closer to the target magnitude. After some pilot experiments, the range of the entire display was chosen to be half of the target force range during the graphical feedback stage. The screen resolution was set to VGA mode with 640 by 480 pixels. For the low force target (2N), each pixel corresponds to about 0.0016N. At high target force (8N), the force display resolution was about 0.0063N per pixel. Such high force display resolution should allow the subjects to see the force difference clearly. During the final stage, the graphical bar occupied half the screen and remained the same irrespective of the forces exerted by the subjects. In this stage, the subject was instructed to maintain the target force for 5 seconds based on memory. After the period ended, the screen changed back to the initial state for the next run.

3.3.4 Data analysis

Several measures of the force error between the target force and the forces exerted by the subjects were computed: (1) the standard deviation from the mean force exerted; (2) the absolute error with respect to the target force; (3) the absolute error expressed as a percentage of the target force. The results described below are given in terms of the absolute errors. The force data sampled at 200 samples per second were filtered with a low-pass filter that had a cut-off frequency of 50Hz for noise removal before the force error were calculated. The mean absolute error and the pooled standard deviation [24] were tabulated. Also, only data from the second and third stage of each run were analyzed. The analysis of variance (ANOVA) [31][24][36] was used to find out whether the results were significantly influenced by various factors. The data averaged from three individual trials under each experimental conditions were used for the calculations of the ANOVA table. The statistical analysis was performed by using MATLAB statistics toolbox. The results from different subjects were not averaged in order to observe their differences.

3.4 Results

3.4.1 Force profiles

Typical force exerted by the subjects during the experiments are shown in Figures 3-4, 3-5, and 3-6. The rows of panels are force traces on different specimens whereas the different columns are for different finger conditions. Three force traces are shown in each panel for

the three target forces used. Any force variations at frequencies greater than about 50 Hz are removed by low-pass filtering the recorded force data.

Visual inspection of the data suggests that the differences between data obtained from different specimens are similar. The tracking force from the second stage (5 to 10 seconds from the start) of each run was quite close to the target, especially for the two low force targets. However, the last stage (10 to 15 seconds from the start) of the force traces seemed to have more variability due to the fact that no visual force feedback was given. For example, in Figure 3-4, the forces exerted by subject CH on the rigid specimen dropped considerably during the third stage under finger cot condition. For subject CT, the visual inspection on some trials shown in Figure 3-5 suggested that the data from the third stage (without visual feedback) were considerably different from the second stage (with graphical visual feedback). In almost all the 8N target trials, the force traces during the third stage dropped by a noticeable amount, sometimes more than 2N (25%). This visual inspection suggested that the subject CT had difficulty maintaining constant force without visual feedback. For subject JK, force traces from the third stage also shows considerable deviation from the target force, but were not as severe as those observed for subject CT.

Although the error distributions obtained from the force traces would depend on particular trials, there was a distinct difference between the distributions obtained from the second and third stage for most trials. Shown in Figure 3-7 are distributions of error and absolute error for stage 2 and stage 3 of a typical run. The error distribution for the second stage was typically shaped close to a normal distribution centered around zero. However, the error distribution for the third stage was usually not centered around zero. The corresponding absolute error distributions were shown in the bottom two panels. For trials with continuing drift in the third stage, the error distribution would be quite flat and distributed on one side of zero (see Figure 3-8).

3.4.2 Performance measurement

Due to the large number of experimental parameters involved, a single table which contains all the performance data is not possible. Instead, the results have been grouped by the following three factors: subject, visual feedback availability, and the hands used. The performance measurement using absolute errors for each subject under various experimental parameters are given in Appendix E.

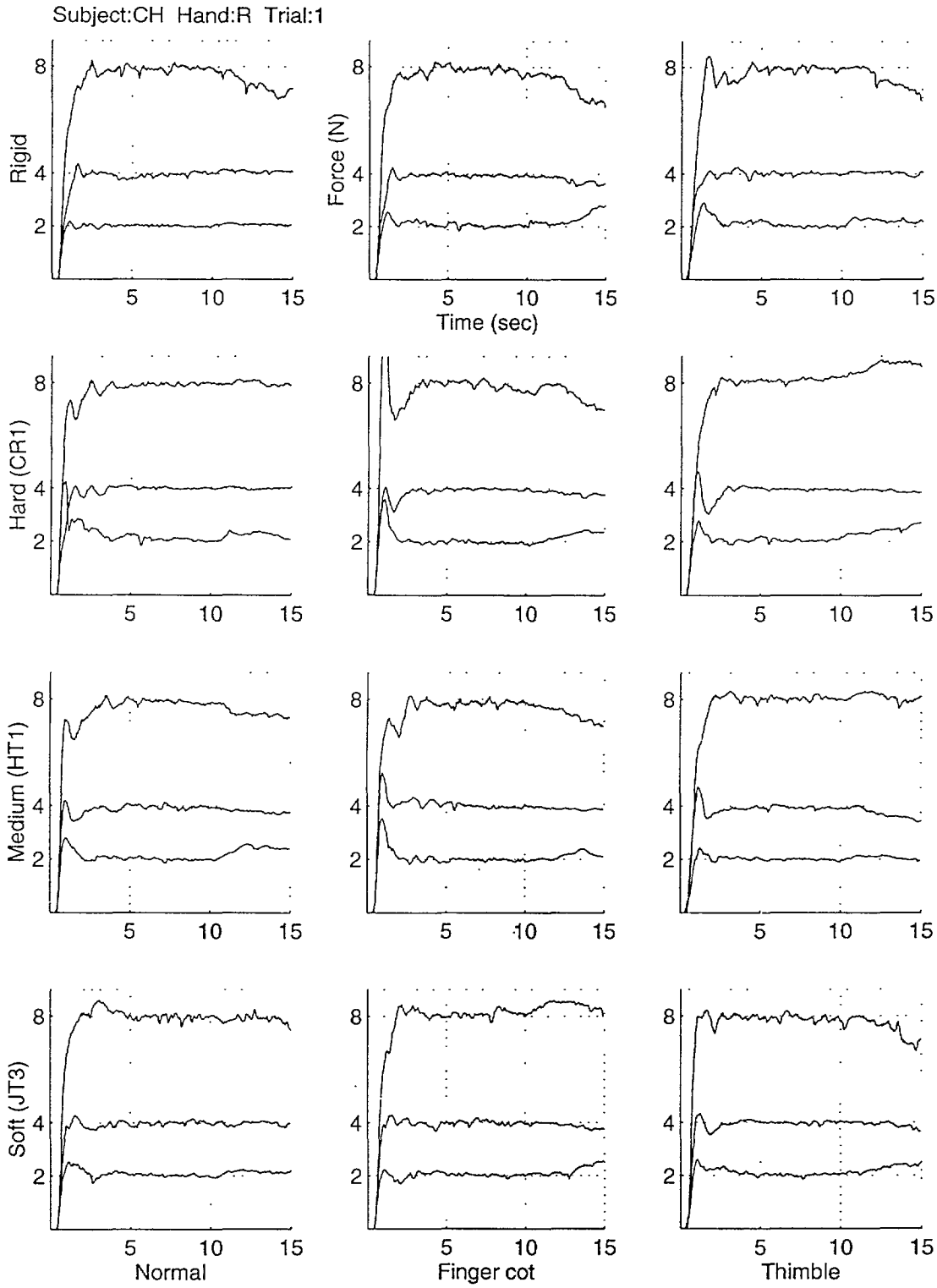

Figure 3-4: Typical force versus time traces for subject CH under different finger conditions on various specimens

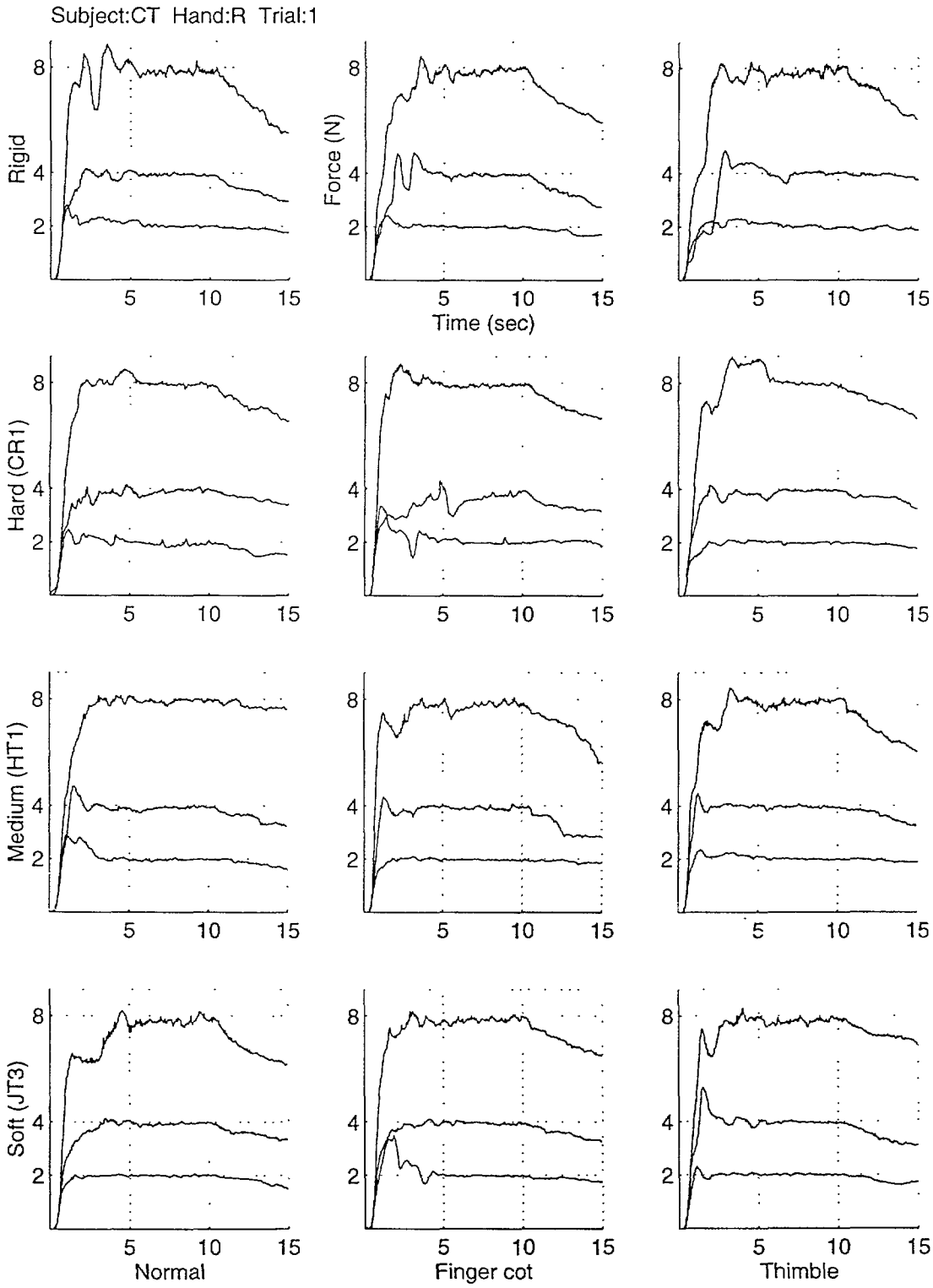

Figure 3-5: Typical force versus time traces for subject CT under different finger conditions on various specimens

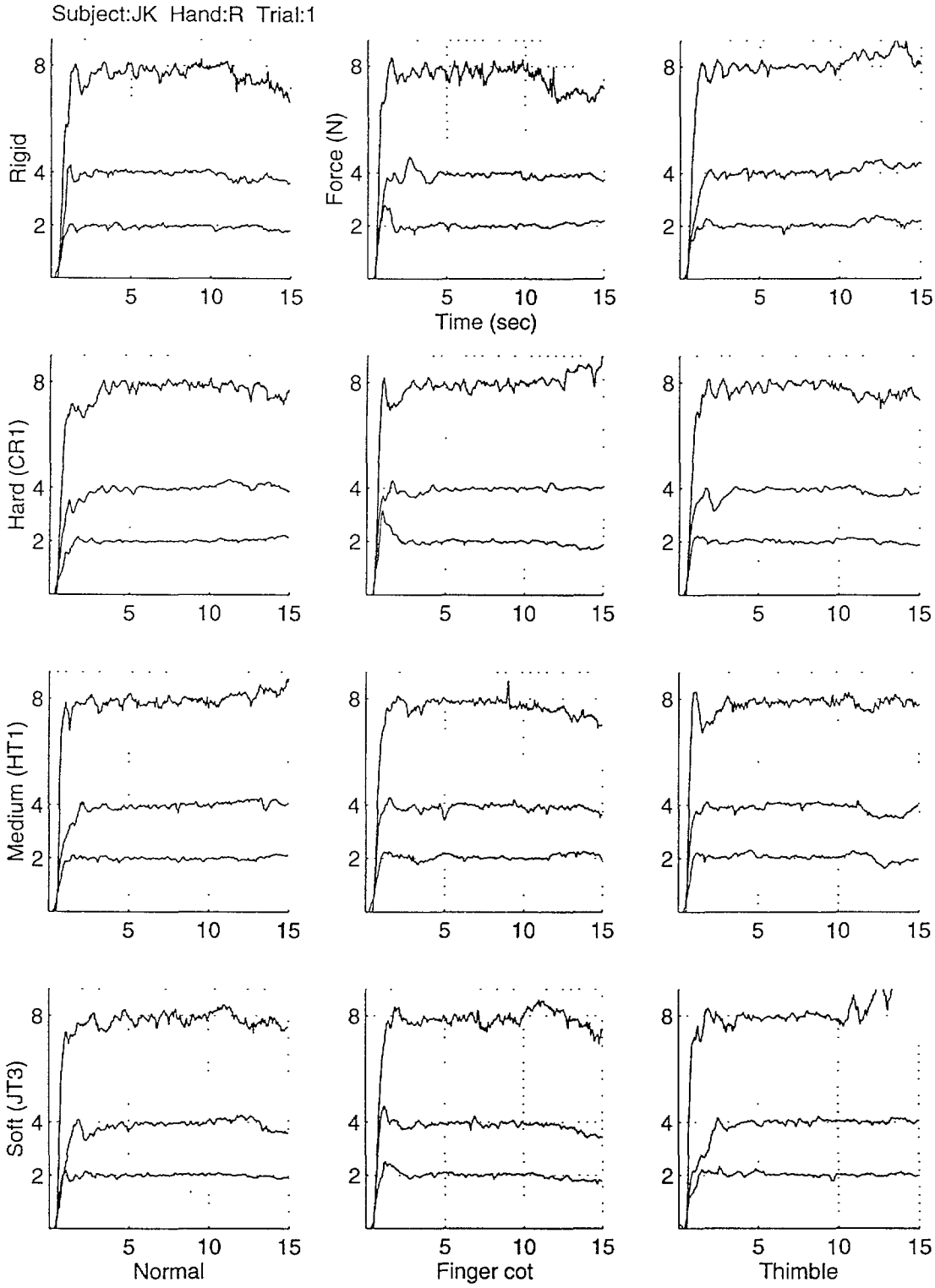

Figure 3-6: Typical force versus time traces for subject JK under different finger conditions on various specimens

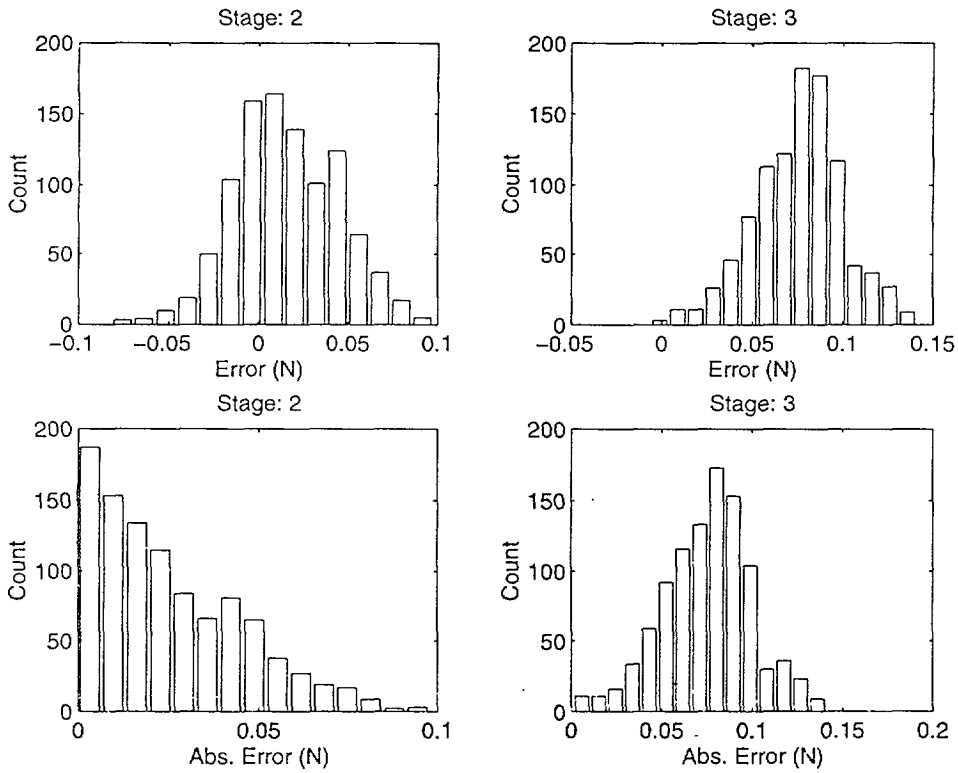

Figure 3-7: A typical error and absolute error distribution for the two stages of an experimental run from a trial conducted on rigid specimen with 2N target force under normal condition by subject CH.

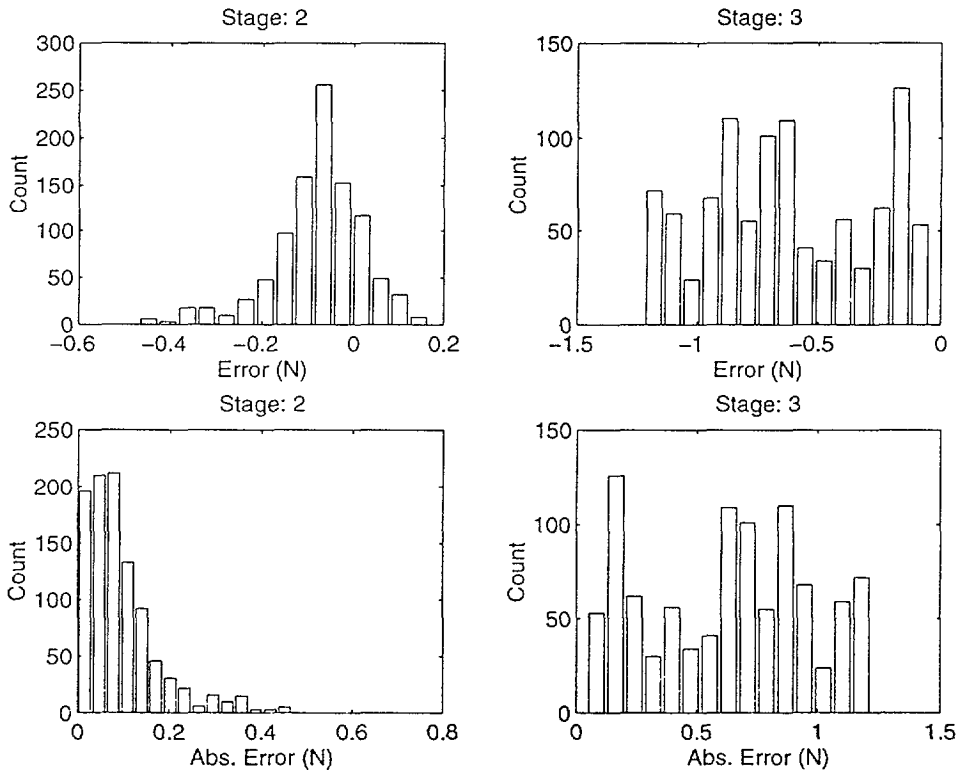

Figure 3-8: A typical error and absolute error distribution for the two stages of an experimental run from a trial conducted on rigid specimen with 8N target force under normal condition by subject CH.

Condition	Force	Absolute Error (N)							
		Rigid		Hard		Medium		Soft	
		Mean	S.D.	Mean	S.D.	Mean	S.D.	Mean	S.D.
Normal	2N	0.035	0.028	0.063	0.046	0.030	0.028	0.036	0.031
Normal	4N	0.054	0.040	0.030	0.023	0.056	0.043	0.067	0.051
Normal	8N	0.093	0.077	0.061	0.047	0.128	0.106	0.073	0.064
Finger cot	2N	0.051	0.046	0.037	0.031	0.032	0.028	0.035	0.035
Finger cot	4N	0.070	0.054	0.035	0.027	0.049	0.037	0.057	0.037
Finger cot	8N	0.165	0.122	0.100	0.089	0.108	0.093	0.160	0.129
Thimble	2N	0.057	0.045	0.057	0.042	0.030	0.024	0.041	0.034
Thimble	4N	0.048	0.041	0.032	0.026	0.060	0.052	0.042	0.030
Thimble	8N	0.128	0.087	0.098	0.059	0.066	0.053	0.110	0.077

Table 3.1: Absolute error in force control for subject CH using right hand index finger with visual feedback.

The tables for the three subjects when visual feedback was present and the right hand was used are shown here in Tables 3.1, 3.2, and 3.3. The mean absolute error was obtained by averaging the mean absolute error of the three experimental runs, with the same number of samples, under the same conditions. The standard deviation (s) was obtained by pooling the standard deviations from the three experimental runs (s_1, s_2, and s_3) using the following formula: $s = \sqrt{({s_1}^2 + {s_2}^2 + {s_3}^2)/3}$.

The performance of all the subjects with the softest specimen when using the right hand, with and without visual force feedback are listed in Tables 3.4 and 3.5. With visual force feedback, the mean absolute error of the three subjects did not differ much given the large variations in the standard deviation. However, without visual feedback, the performance of subject CT is seen to deteriorate more than the other two subjects in most of the conditions.

3.4.3 Statistical tests on experimental parameters

The analysis of variance (ANOVA) was used to find out whether the force control performance was influenced by parameters such as finger contact conditions, specimen compliance, target force magnitude, visual feedback conditions, and the hands used. Data collected using different parameters were grouped together whenever possible for more reliable tests. The complete analysis is presented in Appendix F and the main results are summarized here.

The effects of both specimen softness and finger contact conditions were examined together by using two-way ANOVA table. The data for the three target force magnitudes were grouped

Condition	Force	Absolute Error (N)							
		Rigid		Hard		Medium		Soft	
		Mean	S.D.	Mean	S.D.	Mean	S.D.	Mean	S.D.
Normal	2N	0.034	0.043	0.066	0.043	0.043	0.028	0.021	0.016
Normal	4N	0.066	0.048	0.080	0.060	0.079	0.058	0.063	0.037
Normal	8N	0.147	0.102	0.078	0.063	0.098	0.062	0.171	0.098
Finger cot	2N	0.025	0.031	0.036	0.032	0.030	0.019	0.024	0.021
Finger cot	4N	0.071	0.053	0.171	0.149	0.065	0.045	0.051	0.039
Finger cot	8N	0.188	0.114	0.099	0.051	0.172	0.114	0.122	0.073
Thimble	2N	0.041	0.032	0.027	0.019	0.028	0.024	0.025	0.016
Thimble	4N	0.074	0.065	0.082	0.072	0.048	0.033	0.042	0.024
Thimble	8N	0.142	0.104	0.139	0.152	0.136	0.093	0.137	0.080

Table 3.2: Absolute error in force control for subject CT using right hand index finger with visual feedback.

Condition	Force	Absolute Error (N)							
		Rigid		Hard		Medium		Soft	
		Mean	S.D.	Mean	S.D.	Mean	S.D.	Mean	S.D.
Normal	2N	0.033	0.029	0.024	0.019	0.037	0.028	0.029	0.023
Normal	4N	0.067	0.046	0.049	0.038	0.063	0.050	0.058	0.048
Normal	8N	0.140	0.114	0.114	0.090	0.151	0.108	0.134	0.103
Finger cot	2N	0.040	0.034	0.027	0.022	0.046	0.037	0.034	0.030
Finger cot	4N	0.059	0.048	0.045	0.036	0.068	0.063	0.066	0.054
Finger cot	8N	0.154	0.130	0.121	0.099	0.125	0.089	0.139	0.104
Thimble	2N	0.046	0.044	0.039	0.026	0.051	0.034	0.048	0.047
Thimble	4N	0.056	0.046	0.039	0.032	0.061	0.048	0.066	0.049
Thimble	8N	0.097	0.081	0.094	0.073	0.116	0.088	0.103	0.080

Table 3.3: Absolute error in force control for subject JK using right hand index finger with visual feedback.

Condition	Force	Absolute Error (N)					
		Subject:CH		Subject:CT		Subject:JK	
		Mean	S.D.	Mean	S.D.	Mean	S.D.
Normal	2N	0.036	0.031	0.021	0.016	0.029	0.023
Normal	4N	0.067	0.051	0.063	0.037	0.058	0.048
Normal	8N	0.073	0.064	0.171	0.098	0.134	0.103
Finger cot	2N	0.035	0.035	0.024	0.021	0.034	0.030
Finger cot	4N	0.057	0.037	0.051	0.039	0.066	0.054
Finger cot	8N	0.160	0.129	0.122	0.073	0.139	0.104
Thimble	2N	0.041	0.034	0.025	0.016	0.048	0.047
Thimble	4N	0.042	0.030	0.042	0.024	0.066	0.049
Thimble	8N	0.110	0.077	0.137	0.080	0.103	0.080

Table 3.4: Absolute error in force control for all subjects using right hand index finger with visual feedback on the softest specimen.

Condition	Force	Absolute Error (N)					
		Subject:CH		Subject:CT		Subject:JK	
		Mean	S.D.	Mean	S.D.	Mean	S.D.
Normal	2N	0.123	0.069	0.184	0.139	0.065	0.034
Normal	4N	0.135	0.109	0.509	0.263	0.123	0.085
Normal	8N	0.164	0.132	0.875	0.461	0.475	0.260
Finger cot	2N	0.157	0.119	0.202	0.113	0.117	0.098
Finger cot	4N	0.098	0.072	0.437	0.224	0.204	0.132
Finger cot	8N	0.594	0.265	0.642	0.331	0.306	0.184
Thimble	2N	0.214	0.091	0.127	0.083	0.125	0.121
Thimble	4N	0.104	0.095	0.532	0.335	0.094	0.062
Thimble	8N	0.415	0.321	0.833	0.406	0.455	0.368

Table 3.5: Absolute error in force control for all subjects using right hand index finger without visual feedback on the softest specimen.

together in this analysis. To minimize the effect of target force in the analysis, the performance data was expressed in terms of percentage of the target. Twelve ANOVA tables representing data from different subjects, visual feedback conditions and hands were constructed. Based on results of the overwhelming majority of the ANOVA tables (11/12), the likelihood that the specimen softness and the finger contact conditions played important roles in these tasks was small.

One-way ANOVA tables were constructed to compare target force magnitude factor. The columns stand for the data collected at three target force levels under various specimen and contact interface conditions. For all subjects, there were significant differences between the errors for 2N, 4N, and 8N target force magnitudes. For subject CH, the main difference came from the data for 8N target force. For subjects CT and JK, the differences between 2N and 4N target force magnitudes were big enough to reject the hypothesis that their performance were the same at 1% significance level under both visual force feedback conditions. ANOVA tables using the errors expressed as a percentage of target force were also constructed. With visual force feedback for both subjects CH and JK, the percentage errors were significantly lower when controlling 4N and 8N target force than in controlling 2N target force. For subject CT, the percentage errors were not significantly different under the three different target force levels with visual feedback. However, without visual feedback, the percentage error was significantly higher for subject CT at 8N target force.

To determine the effect of visual feedback, one-way ANOVA tables were constructed by using the performance data, expressed as a percentage of target force, collected from each subject by pooling data from various finger conditions, target force magnitude, and specimen softness. The results rejected the null hypothesis for all three subjects with very high F ratios at 1% significance level and found significant differences between the performances with and without visual force feedback.

To compare the factor of hand used, one-way ANOVA tables were constructed by using the performance data, expressed as a percentage of target force, collected from each subject by pooling data from various finger conditions, target forces, and specimen softness. The results indicate that there was a significant difference between the performance of the two hands of subject JK in controlling forces both with or without visual feedback. For subject CT, there was a significant difference between the performances with the two hands only when the visual feedback was not available. As far as subject CH is concerned, no significant

difference in performance was found between the two hands.

3.5 Discussion

3.5.1 Effects of various experimental parameters

The force control experiments conducted had parameters including the specimen softness, finger contact conditions, the target force magnitude, the hands used, and whether or not the force exerted was visually fed back to the subjects. From the data collected, not all the parameters had significant effects on the controlling of normal contact force with the specimens.

The statistical tests conducted indicate that the finger contact condition as well as the specimen softness did not have significant effects on the results. The target force magnitude did have significant effects when the mean absolute error in force was used in the tests. The percentage error was also used in the statistical tests as the performance index to normalize the error. Both subjects CH and JK had significantly lower percentage error controlling 4N and 8N targets. For subject CT, the difference was less significant among all three target forces. Not surprisingly, when there was visual force feedback, the error was smaller than without feedback for all the subjects. For both subject CH and JK, the percentage error increased from less than 2% at 8N target with visual force feedback to about 6% and 4% without visual force feedback, respectively. In the case of subject CT, the increase, from 2% to 11% at 8N, was more dramatic.

The tests on the hands used show that there were significant differences between the results obtained from two hands of subject JK, whether or not visual force feedback was present. For subject CT, significant difference between the performance with the two hands was found only when visual force feedback was not present. But the tests on subject CH were not able to reject the hypothesis that the performances with the two hands was the same.

In the experiments conducted by Srinivasan and Chen [39], the mean absolute error in tracking constant normal forces up to 1.6N was about 0.04N. The results obtained from this study were similar to that result at 2N (see Table 3.4) for not only the rigid specimen but also for the compliant specimens. However, when the target force magnitude increased to 4N and 8N, the mean absolute error increased for each subject but the mean percentage error (about 2%) did not differ significantly for all the subjects.

3.5.2 Force control in haptic interaction with objects

The objects that we interact with as well as the contact interface conditions can vary quite a lot from one haptic task to another. From the results obtained in this study, we know that our abilities in controlling normal forces of contact with objects of various softnesses under different contact conditions did not differ much across the target forces tested (2N, 4N, and 8N).

The major differences in the abilities of subjects in terms of controlling contact forces under various parameters seemed more obvious when there was no visual force feedback. As observed from the force data of the experimental runs (from 10 to 15 seconds) which did not have visual force feedback, subject CT had more error in controlling the applied force than the other two subjects, even though this subject was as capable in controlling force as the other two during visual feedback stage. The possible explanations include: (1) the subject was not able to sense as well, but because of the visual feedback available at the second stage, the subject performed as well as the other two during that stage; or (2) the subject was not able to remember the forces as well as the other two subjects; thus maintaining a contact force without visual feedback was difficult. In a general haptic discrimination task which typically involves force control without visual force feedback, one might expect that the subjects who cannot control well in the tasks (as experimented here) would not perform as well as other subjects. The softness discrimination experiments presented in the previous chapter shows that the subject whose force control (without visual feedback) performance was not as good as that of the other two subjects did not perform as well in the discrimination tasks also.

We interact with objects daily using both of our hands. The abilities of our finger force control from the two hands may differ just as any other sense. It was found from the statistical tests conducted on the results of these experiments that there were significant differences between the two index fingers of subject JK in controlling normal forces of contact. As pointed out in the Discussion section on softness discrimination, the forces used by the two fingers on the pair of specimens were quite different for subject JK, which is again very consistent with the findings here. Although such differences exist, from the excellent discrimination performance of JK, it seems that our haptic system can compensate for it.

Chapter 4

Contact Visualization

4.1 Abstract

When a finger contacts an object, the extend of the contact region depends on the force applied. As the force increases, the contact grows and the mechanoreceptors under the skin surface respond and convey information about the contact through the nerve pathways to the central nervous system. Contact visualization is a step towards understanding the process of contact development. A real-time imaging setup which consisted of a videomicroscopy system and a tactile stimulator system was developed to observe the region of contact and to perform controlled experiments by using transparent objects. When the finger contacted the transparent specimens, the contact developed gradually. Initially, there were islands of contact. As the contact force increased, the islands got larger and then connected to form finger ridge patterns. However, not all the regions inside the overall contact boundary were in contact even at high forces. In order to analyze the contact images, various image processing techniques were applied and developed to improve the contact images and to determine the contact as distinct from non-contact regions in order to extract contact information. Various contact variables, including nominal area, actual area, percentage contact area, nominal mean pressure, and actual mean pressure, were calculated by using data obtained from the active contact of the fingerpad with a rigid Plexiglass plate. During indentation, the nominal area saturated quickly while the actual area inside the overall contact region increased gradually. During retraction, both the nominal area and the actual area decreased slowly. On the other hand, the variations of the nominal mean contact pressure were gradual during both indentation and retraction. Surprisingly, there was almost a step change in the actual

mean contact pressure at the beginning of contact, after which it was remained almost constant during indentation and reduced gradually during retraction. The percentage contact area, obtained by dividing the actual area by the nominal area, increased gradually during indentation but remained almost constant during retraction. When soft specimens of varying compliance were used, the nominal contact area observed using low magnification was about the same for all the specimens when the forces were less than 1N. At high contact forces, low magnification settings used to record the entire contact region resulted in poor image quality due to the deformation of the specimens. When high magnifications were used to capture only portions of the contact region, the percentage contact areas for the softer specimens were found to be higher than those for harder specimens. From the visualization of the fingerpad actively slipping against a flat Plexiglas plat, it was observed that the motions of the finger ridges near the boundaries of contact moved relative to the plate, which caused the finger ridges to stretch at the leading edge and compress at the trailing edge. These relative movements of the finger ridges will most likely cause the mechanoreceptors underneath the skin to respond and, through the central nervous system, convey to the brain information about the incipience of slip. The brain can then activate the motor subsystem to take appropriate actions to avoid objects from slipping through our fingers. One reasonable hypothesis for the boundaries to slip first is that the pressure distribution on the contact region is in fact not uniform. If the contact pressure in the middle was higher and decreased until it reached the boundary of contact, the observed slip phenomenon can be explained in terms of Coulomb friction. The visualization system and the image processing techniques developed in this study can be applied to other biomechanical experiments involving fingers, such as for the automated fingerprint identification system involving image capture, enhancement, and data compression.

4.2 Introduction

In studying various aspects of the human sense of touch, it is important to understand the biomechanics of contact during manual interactions with objects. During the process of finger-object contact for exploration or manipulation, the mechanoreceptors underneath the skin are an important source of information. Since these sensors are embedded underneath the finger ridges, visualizing the contact region will help us understand what kind of mechanistic

information is available to the tactile sensors. As the finger comes in contact with an object, the contact region develops gradually. The overall area as well as the details inside the contact boundary vary with properties of the object, properties of the finger, and the forces of interaction. Therefore, the objective of this study were to develop systems to enable visualization of the contact region and to find out how contact information such as contact forces, the overall contact area, and the percentage contact area change during the course of contact.

After contact of the fingerpad with an object, a fingerprint is often left on the surface of the object. It is not too difficult to obtain a latent fingerprint left behind by fingers on a variety of objects [19] [14]. In general, for latent fingerprinting, one will need tools and materials such as some talcum powder, a fine paintbrush, clear cellophane tape, and a shiny black paper. By dusting the object with talcum powder, blowing on the talcum power gently, and brushing the powdered spots lightly, a pattern will show and cellophane tape can be used to lift it up and put it on the shiny black paper for examination. Although it is not too difficult, one will have to practice this a few times till one gets the hang of it. This simple procedure takes a lot of time and is only good for latent fingerprints and is not suitable for dynamic and real-time observations which are necessary to capture the progress of contact. To find out the contact area, ink fingerprinting would work just fine for some applications that requires the overall contact area. For a more detailed level of study on the contact region, however, a more capable system is called for. Thus a videomicroscopy system which can achieve such goals was developed. In addition, to perform controlled contact tasks, a tactile stimulator system was also developed, which was used to control the motion of a transparent object to indent a finger which is stationary (passive touch). With the two systems integrated together, the development of the contact region between the fingerpad and objects can be examined in a controlled manner in real-time.

Studies on various aspects of haptic interactions have utilized the information obtained from the contact region. For example, contact area estimation was used to relate to the perceived curvature in the research conducted by Goodwin *et al* [18] on the tactile discrimination of curvature. They estimated the area of contact between skin and objects with different curvature by ink fingerprinting. They found that as the curvature increased, the contact area decreased. And lower contact force resulted in a decrease in contact area. In the study on human discrimination of thickness, Ho [7] estimated the contact area between finger

and plates of various thickness by ink fingerprinting and the data was used in finite element analysis to compute the deformed plate curvature. By using the videomicroscopy system developed in this study, Dandekar [10] conducted experiments to perform 3D reconstruction of the primate fingerpads for finite element analysis and also measured surface deformation of human fingertip *in vivo* with indenters of various sizes and shapes.

In this study, the focus was on the visualization of the contact region with objects of differing compliance. This chapter includes descriptions of the various devices developed which enable such observations, image processing techniques applied to enhance or visualize the image data, observations of the slip phenomenon between finger and rigid Plexiglas, and also presents data obtained from controlled contact experiments with soft objects. The visualization systems developed in the study, the accompanying image processing and visualization software, and the results on contact region development can be applied to other biomechanical experiments involving fingers and also to the automated fingerprint identification systems [19] for image capture, enhancement, and data compression.

4.3 Methods

4.3.1 Videomicroscopy system

A videomicroscopy system capable of real-time imaging was developed to observe the region of the human finger in contact with transparent objects. Figure 4-1 is a schematic diagram of the system which includes a fiber optic light source, a gray scale CCD camera, a zoom lens, a video monitor, and a frame grabber hosted by a 80486 personal computer.

The contact region is illuminated by a Fostec Model 8375 fiber optic light source. For high magnification images, the light illuminates the contact region coaxially through the beam splitter and zoom lens. For low magnification images, an alternative light is used as indicated in the figure. The Unitron 1:6.5 zoom lens provides a range of magnifications of the contact region, enabling the overall contact area as well as the details of islands of contact with a few finger ridges to be imaged. The output of the high resolution Hitachi Model KP-M1U CCD camera is displayed on a Hitachi video monitor. The camera output can also be digitized by a BitFlow VESA local-bus VideoRaptor frame grabber in the 80486 personal computer.

Using this videomicroscopy system, video data can be digitized in real-time and transferred from the frame grabber to the computer system memory. The amount of digitized

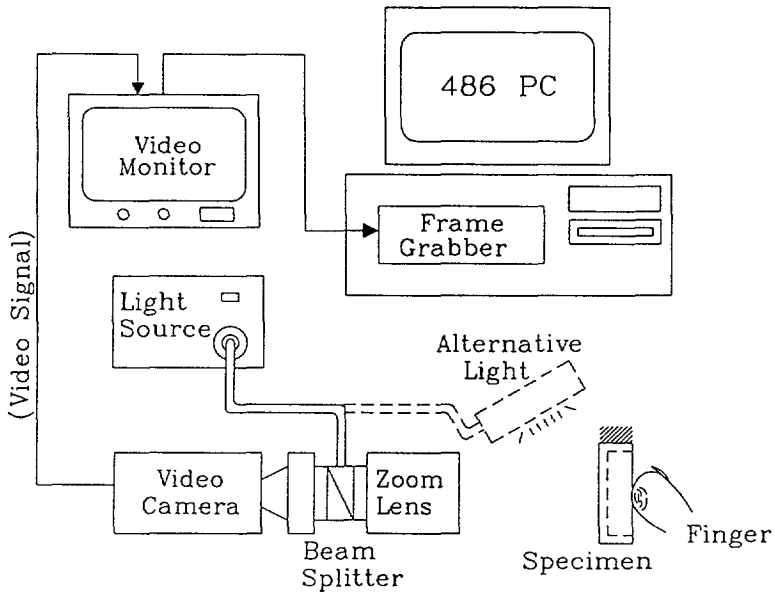

Figure 4-1: The videomicroscopy system.

video data is thus limited to the available memory in the computer system. For a typical 640x480 8-bit gray scale image resolution, the 16MB memory inside the computer can hold about 54 frames of video which amounts to about 1.8 seconds of data if digitized at a rate of 30 frames per second. Observations made from daily contact tasks suggest that the development of a typical finger-object contact usually has a time span of less than 2 seconds. For slower contact speed (the contact region will also vary slowly), the video acquisition rate can be reduced to accommodate a longer period of contact without sacrificing either the duration or the accuracy of the analysis.

4.3.2 Tactile stimulator system

A tactile stimulator was developed to investigate the contact phenomena in a controlled manner. Figure 4-2 is a diagram of the tactile stimulator system. This linear stepper motor based tactile stimulator is used to carry a specimen to indent a stationary finger at a given velocity. The Industrial Device Corporation (IDC) NS2T205A-2 linear electric cylinder together with a IDC S5101 micro-stepping drive has a step size of less than 1 micrometer which makes it easy to achieve high precision.

As indicated in Figure 4-2, the motor is controlled by a 80386 personal computer with a custom digital input/output interface. By changing the frequency of the step pulses sent to the motor, the speed of indentation can be accurately controlled. The timing of the step

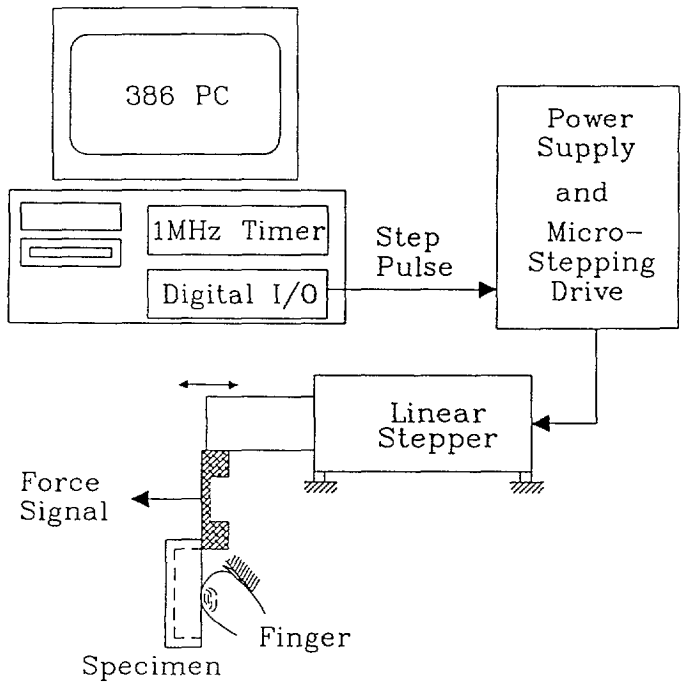

Figure 4-2: The tactile stimulator system.

frequency is controlled via a 1MHz custom timing interface.

In order to observe the contact forces between the specimen and the human finger, a strain gage based single degree of freedom force sensor was built and mounted between the specimen holder and the motor cylinder. Binocular spring element was used to construct the sensor because it is more rigid and less sensitive to location of force application. Four strain gages, made by Measurements Group, were mounted on the top and bottom surfaces of the force sensor near the center of the two holes of the binocular to form a full bridge. The force signal was amplified by a signal conditioner before it was digitized by a data acqusition system in a computer.

4.3.3 Real-time imaging setup

Both the videomicroscopy and the tactile stimulator systems can be used by themselves to collect useful data. For example, the videomicroscopy system was used for the 3D reconstruction of the fingerpad and observe the surface deformation of the fingertips under a variety of indentors [10]. The integration of the two systems which would provide synchronized force and video data collection is one of the important goals of this research.

Since digitizing the video data and controlling the stimulator both require constant at-

tention of the central processing unit of the computer (CPU), two computers were used to meet the two needs. In such a design, the synchronization of the two tasks was a major concern. This problem can be solved by having an accurate custom timer interface on both computers and use digital input/output interfaces to allow communication between them for synchronization. Figure 4-3 shows a schematic of the integrated system. The communication between the two computers is achieved by sending command data through the custom digital input/output interfaces installed on both computers. The 80386 PC is dedicated to the motion control of the stimulator while the 80486 PC records both video and force data during contact. The 80386 PC receives parameters such as motor speed and travel distance from the 80486 PC and executes the command accurately, by using the 1MHz timer, after receiving the start signal. On the other hand, the 80486 PC coordinates the experiment and collects video and force data according to its own time base which is the same custom timing interface as the one in the 80386 PC.

As a result of this integration, the two computer systems work together with their own control software and the setup is capable of a video rate of at least 20 frames per second and a force rate of 1000 samples per second. However, such high data rate can only be sustained for a short period of time, usually a little less than 2 seconds, because of the amount of system memory available on the 80486 computer to store the digitized image (about 300 KByte per frame). Typical contact duration of tasks such as softness discrimination takes about 1 second. Therefore, the 2 second capture time allowed by this setup is sufficient for achieving the goals of the investigations.

4.3.4 Active and passive touch experiments

Performing active and passive touch experiments to obtain contact information is a crucial step towards the understanding of the mechanical inputs to the mechanoreceptors under the skin. The real-time imaging setup (Figure 4-3) was used to visualize the contact region and record the contact forces. In passive touch experiments, the finger was attached to a stationary finger holder and the tactile stimulator applied specimens to the finger at controlled velocity of 2.4mm/sec. During active touch experiments, the subject's finger was not constrained. Instead of moving the tactile stimulator, the subjects moved their finger to touch the stationary specimen.

Transparent rigid Plexiglas and compliant silicon rubber specimens were used in the

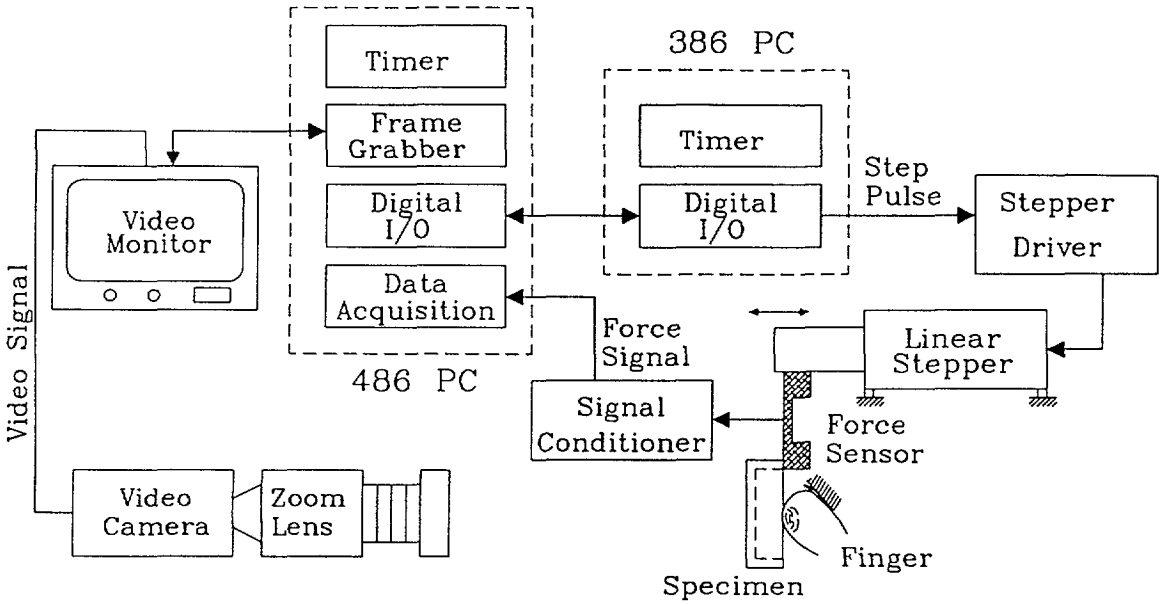

Figure 4-3: The real-time imaging setup.

experiments. By adjusting the amount of diluent GE SF96-50 mixed to fixed proportions of GE RTV615A and RTV615B silicon rubber components, the compliance of the specimen can be varied. The procedure and method used to cast and calibrate the specimens are described in detail in the Methods section on softness discrimination experiments. Three soft specimens with objective compliance value of 0.086mm/N (specimen code AB4), 0.188mm/N (code BA4), and 0.304mm/N (code CA4) were used. The transparent rigid Plexiglas used had a thickness of 1/4 inch.

The custom-made binocular force sensor was used to record the contact force. The sensor has a range of 40N and the data is digitized by a 12-bit data acquisition board at the rate of 1000 samples per second. Due to its binocular design, the sensor is not very sensitive to the location of load application. The contact region was captured into the 80486 PC system memory at a rate of 20 frames per second. In passive touch experiments, the recording was carried out for the indentation portion. In the active touch experiments, the recording time span was about 2 seconds and required coordination between the subjects and the experimenter for a good capture. Three repetitions were performed for the passive touch experiments; the active touch experiments were repeated until three satisfactory sequences were captured.

4.3.5 Observations of slip

In addition to the recording of the contact region during passive indentation and active touch experiments with compliant specimens, the videomicroscopy system can also be used to visualize a variety of contact related phenomena. For example, the study of slip requires visualization at the finger ridge level.

For observations on slip, the subject first contacted the rigid Plexiglas and then stroked it back and forth with the fingerpad in the horizontally direction. The subject repeatedly performed the actions and a two second capture was initialized at the appropriate time to record a part of the process. Due to the setup limitations, only active touch experiments on slip are possible. This is because, to have controlled passive slip, another motor to control a second degree of freedom is required. Also, a more quantitative study of slip requires shear force measurements. In the experiments described here, the phenomenon of slip was observed and the sequence of images obtained was analyzed. Even with limitation of the available setup, the understanding of slip at the ridge level is enhanced by these observations. It also provided good evidence on the nature of force distribution over the contact region.

4.4 Contact image processing

In the context of tactile sense, the portion of the fingerpad that is in contact with the object is especially important since the mechanoreceptors under that region will generate most of the nerve impulses transmitted to the central nervous system. The images acquired from the videomicroscopy system are of high enough contrast as to be visible to the human eye when appropriate lighting is used. In order to provide qualitative visualization and to perform quantitative analysis of the images, algorithms for enhancing and extracting the contact regions were developed. This section is devoted to the techniques used in this study in order to enhance contact images, separate the contact area from the non-contact area, and visualize various contact phenomena.

4.4.1 Simple thresholding

When appropriate lighting is used, the regions of the finger that are in contact with the specimen have lower image intensity than the regions that are not in contact. This suggests the use of a simple thresholding of the image intensity to determine the contact area. The

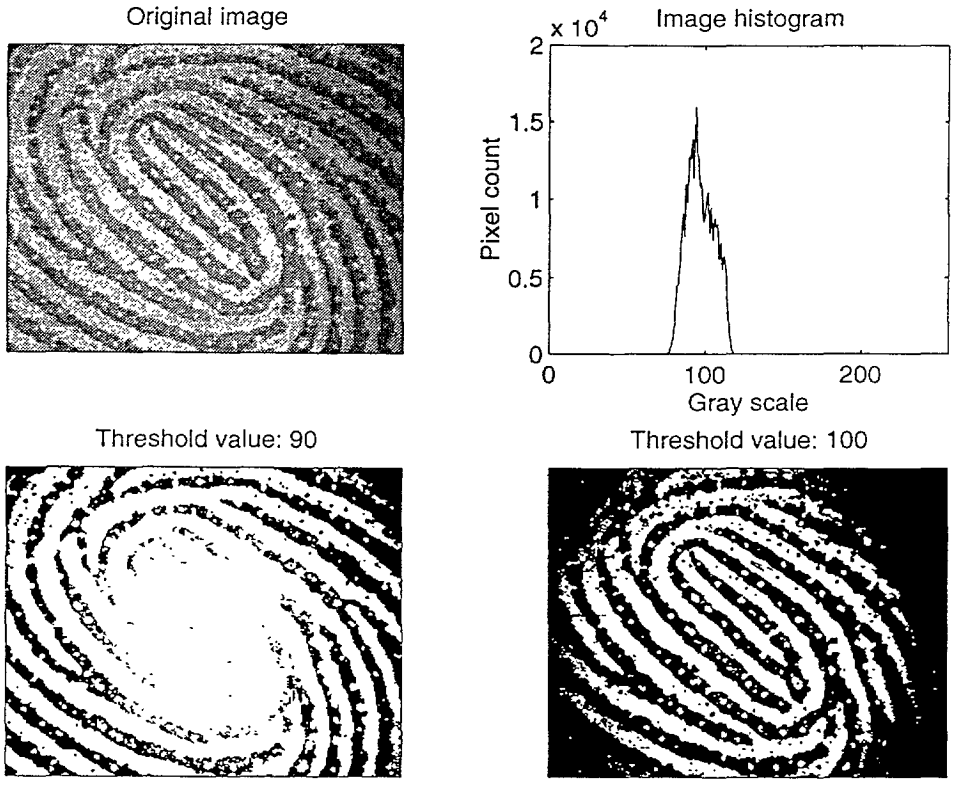

Figure 4-4: Application of simple thresholding to obtain the contact area.

threshold value can be picked out from the image histogram, which is the distribution of gray levels in an image. A higher gray scale value in the distribution corresponds to a brighter pixel. If the pixel at a particular location has a lower gray level than the threshold, it is in contact. Otherwise, it is not.

A typical result of applying such a technique to obtain the contact area is shown in Figure 4-4. The upper left graph shows a contact image of a fingerpad with rigid Plexiglas. The histogram of the image is shown at the upper right. The simple thresholding method requires one to pick a gray scale value to convert the original image into a binary image consisting only of contact and non-contact pixels. Although human eyes can easily pick out the contact region in the image because of our sophisticated visual system, it is difficult to pick a gray level from the image histogram to perform the thresholding operation. The bottom two graphs show the result of using two different threshold values. A threshold value of 90 seems too low because it cannot convert the middle region into a binary image properly. If the threshold value is increased to a higher value of 100 in order to convert the center part properly, the boundaries become too dark.

By taking a closer look at the original image and comparing the gray levels of the white region in the center and that of the boundaries, one realizes that the background of the image has non-uniform gray values. Since the illumination of the image is not perfectly uniform, contact regions in an area of high illumination may have equal or greater intensity than non-contact regions in the area of low illumination. Therefore, the simple operation of thresholding cannot convert the pixels into contact or non-contact regions satisfactorily. However, if the effect of non-uniform illumination can be eliminated by other techniques, then thresholding can be applied to obtain the contact area reliably.

4.4.2 Homomorphic processing

One way of removing the non-uniform lighting is to apply homomorphic processing [29][17] [1]. Homomorphic processing can be used to reduce the dynamic range of the image and enhance the local contrast. The resulting image has uniform illumination, thereby facilitating the use of the thresholding method to determine the area of contact.

The gray level of a contact image $f(n_1, n_2)$ can be modeled as

$$f(n_1, n_2) = i(n_1, n_2)r(n_1, n_2), \tag{4.1}$$

where $i(n_1, n_2,)$ represents the illumination of the image at location (n_1, n_2) and $r(n_1, n_2)$ represents the reflectance of the object. In this case, the illumination $i(n_1, n_2)$ varies slowly across the image with a low spatial frequency of one cycle per image. The reflectance $r(n_1, n_2)$ contains the details of the fingerprint whose fundamental frequency is determined by the number of finger ridges present in the image. Since equation 4.1 cannot be used directly to perform a Fourier transform operation in order to separate the two components, we can convert it from a product to a sum by taking the logarithm of equation 4.1:

$$log(f(n_1, n_2)) = log(i(n_1, n_2)) + log(r(n_1, n_2)). \tag{4.2}$$

Now, because of linearity, we can filter the *log* of $f(n_1, n_2)$ to remove the illumination effects. After that, we can exponentiate the result to obtain $r(n_1, n_2)$. A block diagram for applying homomorphic processing is illustrated in Figure 4-5.

[1] The homomorphic processing technique was developed with the help of Eric Foxlin and Robert Stadler and the author wishes to gratefully acknowledge their assistance.

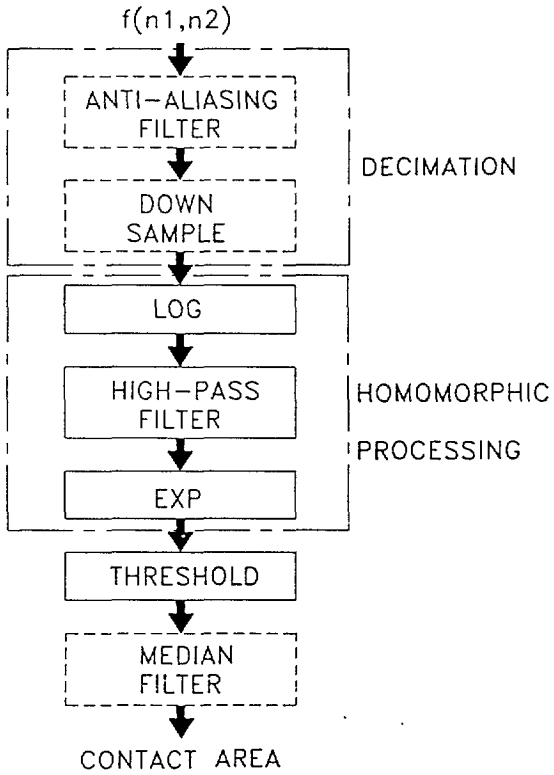

Figure 4-5: A block diagram for applying homomorphic processing to determine the contact area.

If the homomorphic processing successfully removes the illumination effects, the unimodal histogram (Figure 4-4) of the original image should be in the form of a bimodal histogram. One mode represents the finger ridges that are in contact and the other mode represents the regions that are not in contact. We can then choose a threshold value between the two modes so that the contact areas in the image are black and non-contact areas are white. Any significant noise will be converted into impulsive noise by the thresholding. A median filter can serve to remove the noise before counting the pixels. The actual contact area can be calculated by applying a calibration constant which represents the area of a single pixel. For high magnification images which contain only a few finger ridges, the frequency of the ridges is closer to the illumination frequency. In those cases, either a filter with very sharp cutoff must be used or a decimation on the images must be performed in order to separate the two areas(Figure 4-5).

The implementation of the algorithm is accomplished by using the software package MATLAB in conjunction with custom developed C programs. The frequency transform method was used for the filter design. It begins with the design of an optimal 1-dimensional filter using the Parks-McClellan algorithm. For an image that is 640 pixels wide, the illumination frequency is $\pi/320$ (one cycle per image). If there are 10 finger ridges in the image, the fundamental frequency will be $\pi/32$. So, the filter must pass $\pi/32$ but filter $\pi/320$. The 1-dimensional frequency response is later converted into a 2-dimensional frequency response with the McClellan transformation. The high-pass filtering operation is performed in the frequency domain by multiplying the Fourier transformed image and the high-pass filter. Then the inverse Fourier transform operation converts the result back into the spatial domain.

Figure 4-6 shows the same original image shown in Figure 4-4 and the resulting image after homomorphic processing, its histograms and the thresholded image. In addition to checking that the histogram is now bimodal, the results of the image processing can also be verified by eye to see how well they represent the true contact area shown in the original image.

4.4.3 Scan-line processing

In real-time applications, reducing the amount of time required to process the image data is critical. For example, for a robot equipped with a vision system or a high resolution tactile sensor array to manipulate an object like the humans do, the recognition time is critical.

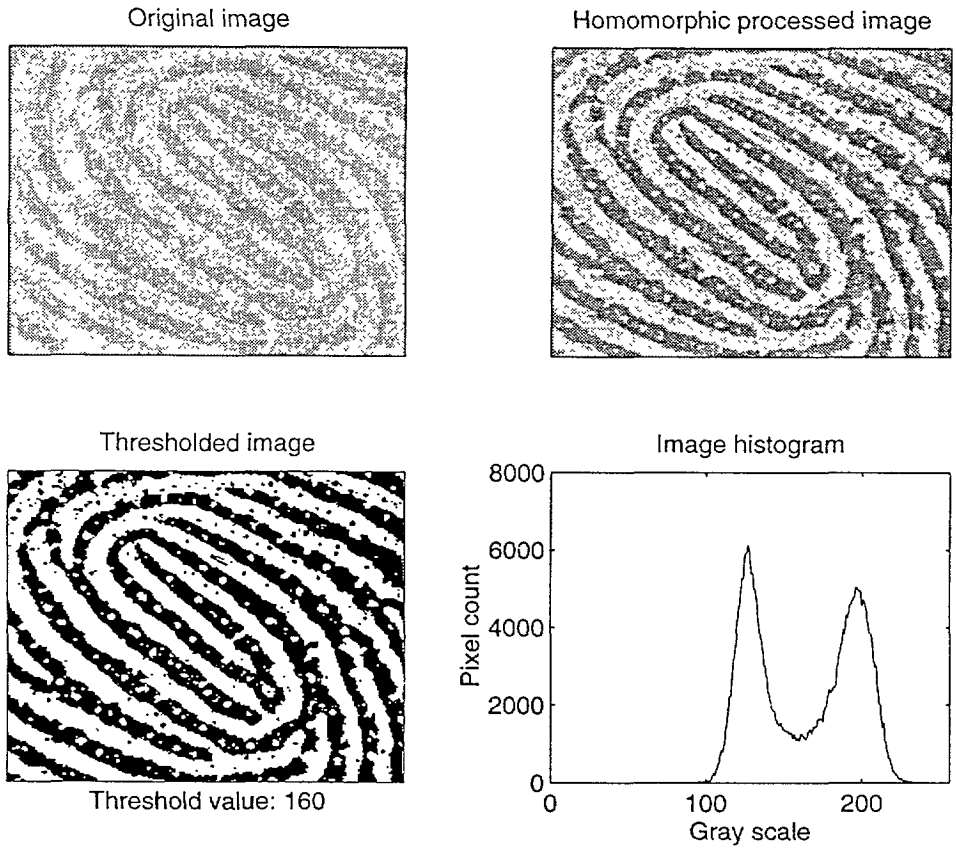

Figure 4-6: Apply homomorphic processing to image.

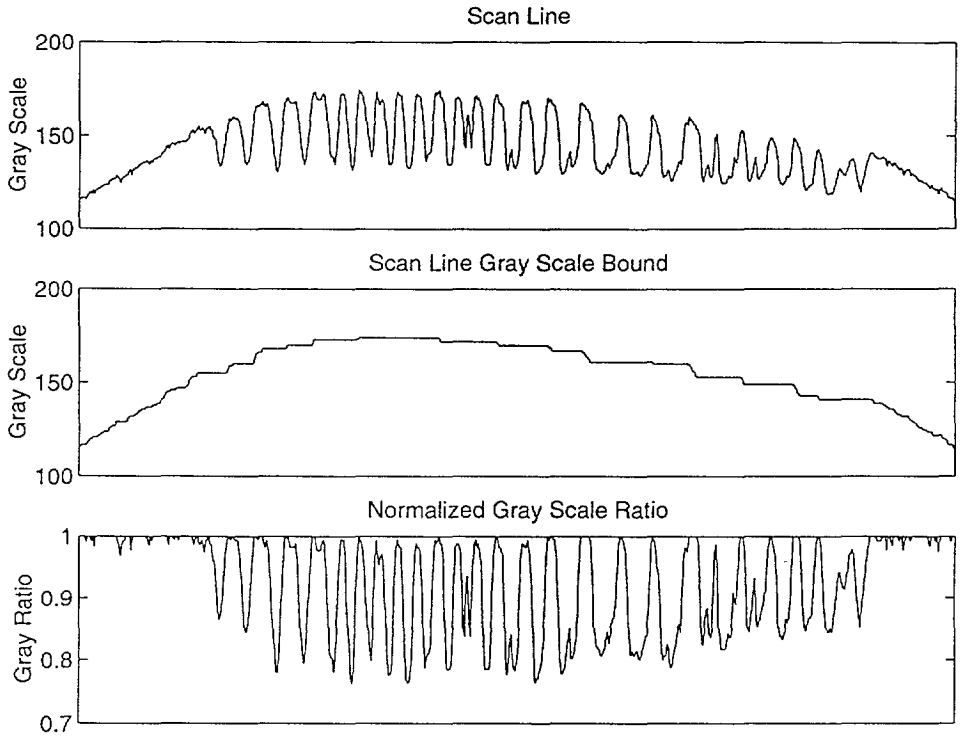

Figure 4-7: The scan-line processing on a fingerprint line.

The same is true for finger print security systems. In real-time inspection or target detection applications, optical correlators are typically used to achieve the required speed [2][5][6]. If using optical correlators is not practical, scan-line processing seems to be the best choice. By processing the image line by line using simple operations, it is possible to achieve real-time performance.

The idea of scan-line processing is generated from the image model used in homomorphic processing, image calibration, and other techniques such as top-hat and well transform for peak and valley detection [1]. In the case of top-hat transform, the bright peaks of an image are revealed. The top-hat image is created by first applying an opening operation which removes protruding peaks from the image. Then a dual-image point process is used to subtract the top-hat image from the original image. The result is an image in which the bright peaks appear.

The scan-line processing method used here first estimates the background image intensity by bounding the scan-line to be processed. The first step is to find the location of the maximum intensity value on the scan-line. Then a background is constructed from the history of searching for the maximum location starting from both ends of the scan line. The result is

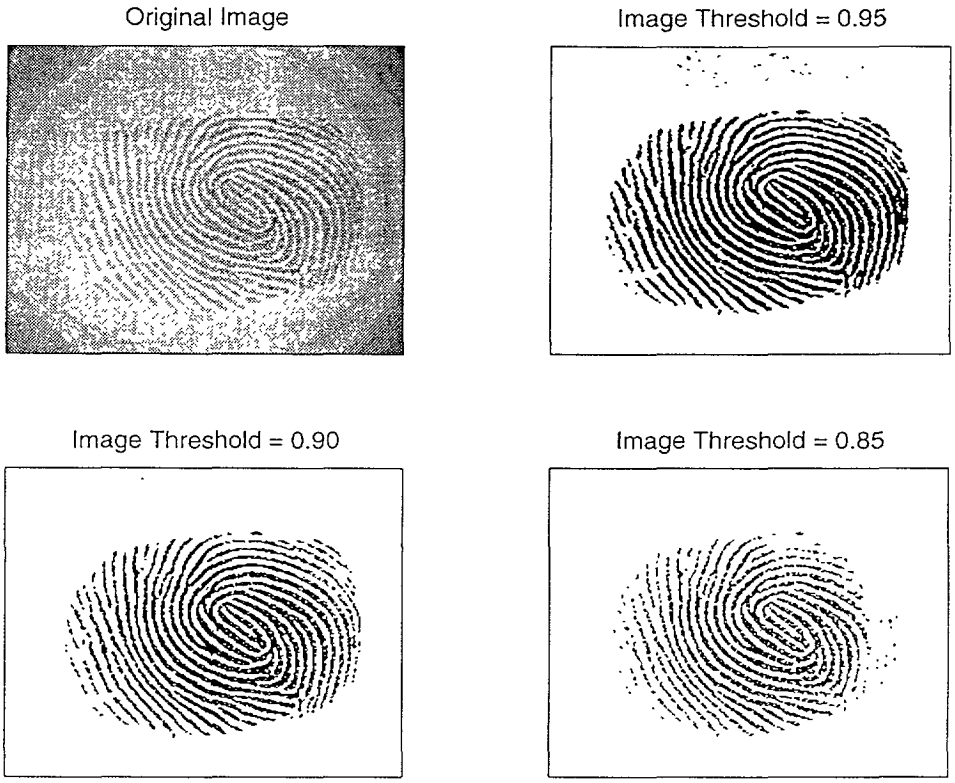

Figure 4-8: Results of applying the scan-line processing to a fingerprint image with different threshold values.

usually a dome shaped background with steps. The third step is to divide the original scan-line by this estimated background. The result is a gray scale ratio between 0 and 1. A high contrast image would result in scan-lines in which the contact pixels would have gray scale values closer to 0 than the result from a low contrast image. Afterwards, a threshold ratio can be used to convert the scan-line into binary images. Figure 4-7 illustrates an original scan-line, a constructed background and their ratio. The results of the scan-line processing and thresholding are shown in Figure 4-8 where three different threshold percentages values were used.

When the borders contain finger ridges, error will occur from the method outlined above because the gray scale ratio will be close to 1 when it should ideally be lower than 1. For images containing a substantial amount of noise, a low-pass filtering on the scan-line would improve the thresholding result. This technique is suitable when the fingerprint does not occupy the whole image, as in the case of real-time automated fingerprint recognition or security systems. It efficiently converts the gray-scale image into binary in real time, thus

reducing the data size to one eighth of the original. For most applications, the size of the resulting image can be reduced by compressing the binary image using algorithms such as LZW [30]. An image size reduction of about 30 was achieved in pilot trials with fingerprint images. With the possibility of real-time binarization of the original fingerprint images, the automated fingerprint recognition systems [32][9] could be speeded up.

4.4.4 Morphological processing

Image morphology involves pixel level processing that helps to clarify and simplify objects of interest[1][17]. It can be applied to obtain outlines or skeletons of an object by emptying the interior or reducing the thickness of the object. For binary images, binary morphological processing uses logical operators such as AND and OR on neighboring pixels to obtain a resulting image. In this study, it is used to obtain the boundaries of the finger ridges for the purpose of visualization of contact phenomena.

Erosion and dilation are two fundamental morphological operations. A 3 x 3 mask size is usually used for the operation. Suppose a binary image is composed of black and white pixels, with the object represented by white pixels. To erode away the boundaries of the object, the erosion operation is called for. If a pixel and its eight neighbors are all white, the corresponding pixel is white in the eroded image; otherwise, the corresponding pixel in the resulting image is black. When erosion is performed on a pixel inside an object, it has no effect. However, if the pixel is on the boundary of an object, since its neighboring pixels consists of both object and background, it will be converted into a background pixel. If there is random noise consisting of only a few pixels, they will be eroded away also. Dilation does the opposite to the image: a pixel in the dilated image is white if any of the pixels defined by the mask is white in the original image. It helps to make the object bigger and fill in tiny holes inside the object.

Different combinations of the erosion and dilation operations produce different effects. The opening operation is an erosion operation followed by a dilation operation to remove single-pixel noise spikes. The closing operation is a dilation operation followed by an erosion to fill small holes and gaps. When an eroded image is subtracted from the original image by using a dual-image point process, the result is the outline of the objects in an image. Figure 4-9 shows the outline of the fingerprint images created by the outlining process. The image shown was first thresholded by scan-line thresholding with a threshold value of 0.95.

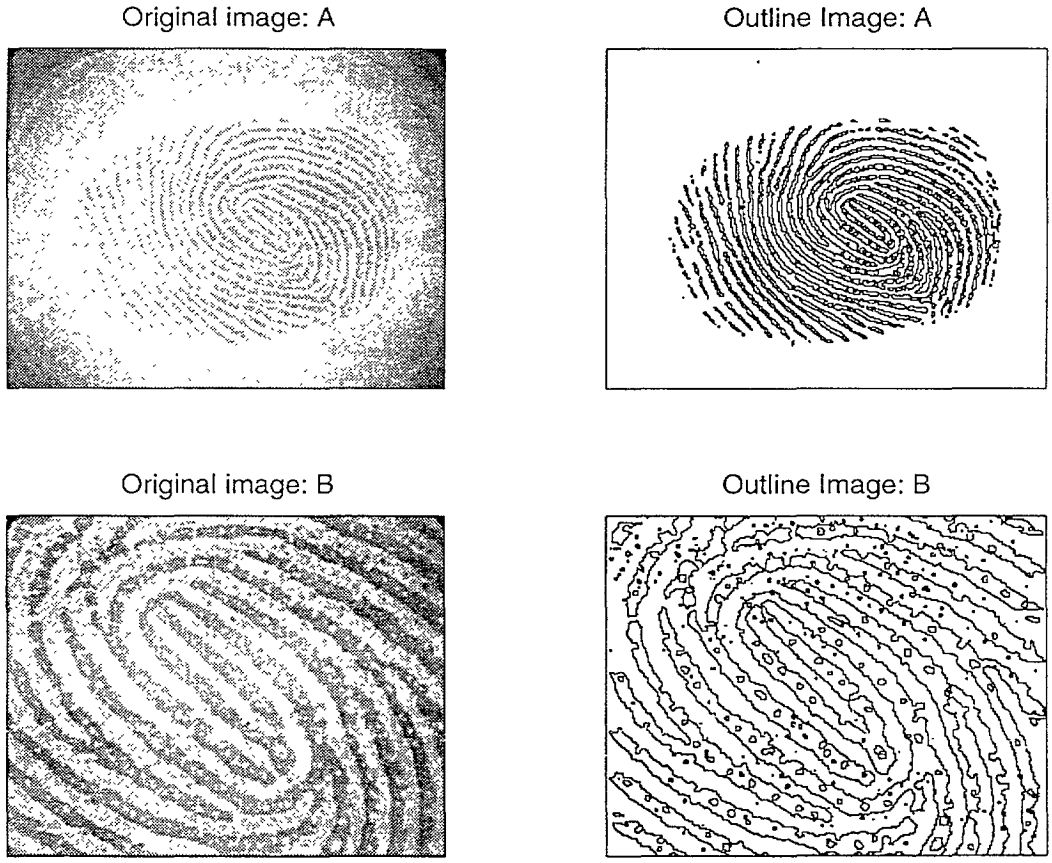

Figure 4-9: Results of applying binary morphological processing to obtain the outline of the fingerprint contact regions.

A dilation followed by an erosion operation was used to reduce the noise. Two more erosion operations were performed and the resulting image was subtracted from the noise reduced binary image to create the outline image.

4.5 Implications on the mechanics of contact

4.5.1 Overall (Nominal) and actual contact areas

When the finger comes in contact with objects, the contact region gradually develops. At first, there are islands of contact corresponding to contact points on each of the finger ridges. As the normal force of contact increases, the islands grow bigger and the overall (nominal) contact boundary grows as well. The islands of contact eventually get connect together result in the fingerprint patterns. Figure 4-10 shows part of a sequence of images obtained when a fingerpad actively contacted a Plexiglas plate. The image sequence was recorded at a rate of 20 frames per second under low magnification and compressional force of contact was recorded at 1000 samples per second. Therefore, there were 50 force samples within a single frame. The corresponding mean forces exerted during an image frame are also shown in the figure. The growth of the overall contact boundary can be seen by comparing consecutive frames. To quantitatively describe the growth of the contact region, the overall area of the contact boundary and the actual areas inside the contact region can be useful measures.

To obtain the overall area, the border of the image region occupied by the fingerprint needs to be extracted. The border extraction was performed in two steps. First, the original contact images were converted into binary images by using scan-line thresholding or homomorphic processing. Then, an estimate of the border was obtained by using a technique similar to the wedge-ring detection method broadly used in pattern recognition [9]. In this modified wedge-ring method, the original image was partitioned by using wedges and rings formed by concentric circles and radial lines. Figure 4-11 shows the wedge-ring pattern that was used to count the contact pixels and obtain the contact region boundary. The actual pattern consisted of more rings and wedges than in the one shown. The numbers were determined by using typical images and by adjusting on the basis of visual inspection of the extracted boundary smoothness. The contact pixels from a binary image were used to first calculate the approximate center of the contact region by using the averaged coordinates. Then the wedge-ring pattern centered around the contact center was superimposed to collect contact

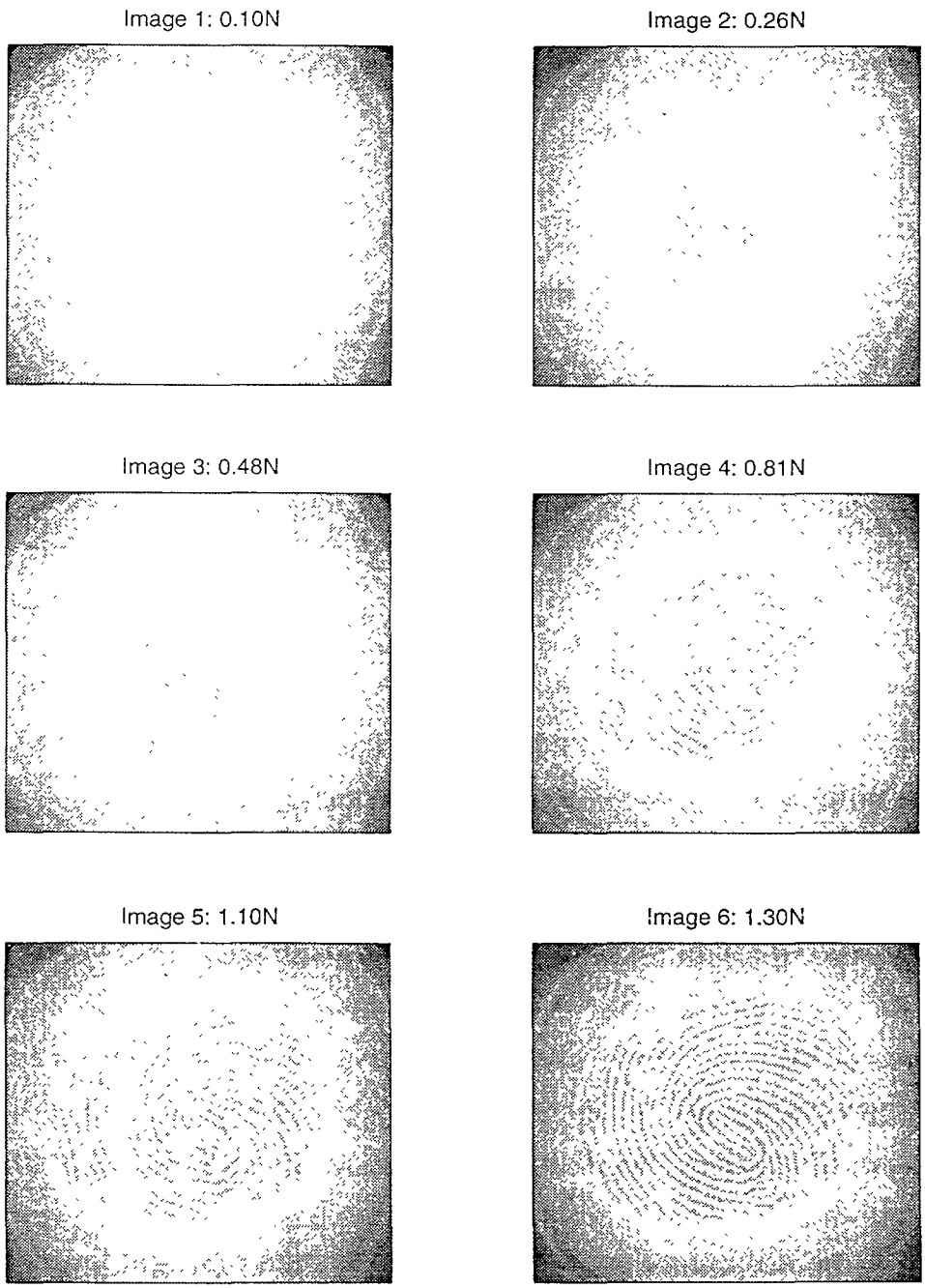

Figure 4-10: A sequence of images of contact between a fingerpad and Plexiglas specimen.

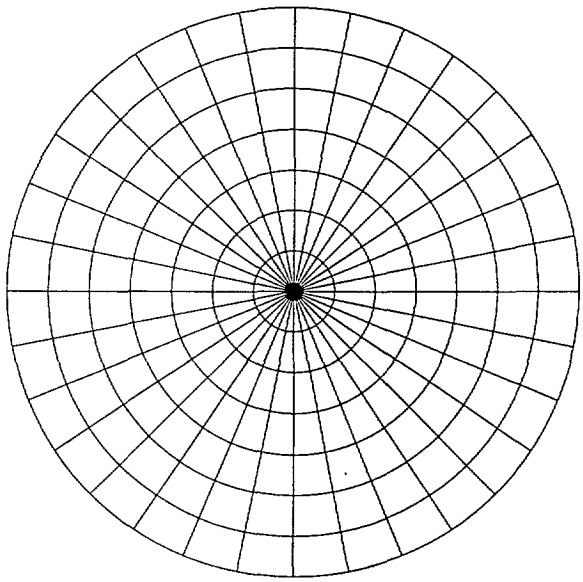

Figure 4-11: The wedge-ring pattern used in contact region boundary extraction.

pixels within each cell. Once the pixels were assigned to the appropriate cells by determining their distance and angles with respect to the center of the contact region, the cumulative sum of contact pixels within the cells along each wedge starting from the center was obtained. An estimate of the boundary can be made based on the ring radius inside which most of the contact pixels reside. A typical ratio of 99% was used to avoid noise existing outside the border, which also showed up as contact pixels. The number of wedges and rings used would roughly determine the errors in the boundary estimation. Figure 4-12 shows a binary contact image and the result of the boundary points estimated by using the above procedure. The number of wedges and rings used were 48 and 80, respectively. In general, using more than 30 wedges and 60 rings will generate satisfactory estimates for the border. However, if the number of wedges is too many, the resulting boundaries may not vary smoothly.

The total number of pixels inside the boundary were estimated from the coordinates of the border points and that of the contact region center. Calibration of image size was performed before the contact images were obtained. The calibration constants depend on the magnification of the images and can be found by imaging a reticle which has calibration patterns and by counting the corresponding number of pixels that occupy a known area. The overall contact area estimates can then be obtained by applying the calibration constant which represents a unit pixel area for a particular contact image sequence.

Although the overall contact area is a number which represents the nominal size of the

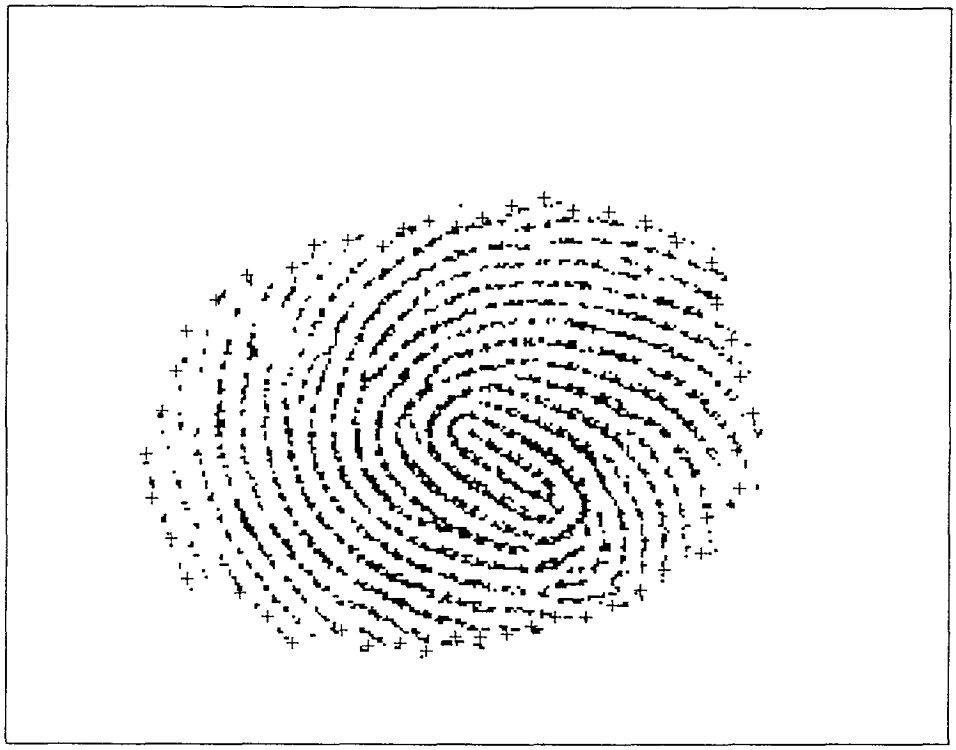

Figure 4-12: An estimate of the overall contact region boundary using the modified wedge-ring method.

contact region, the actual area of contact inside the contact boundary is as important. For example, given a contact force, a nominal mean pressure can be determined if the overall contact area is known. However, from results of visualizing the contact region, we know that not all regions inside the contact boundary are actually in contact. Therefore, the nominal mean pressure can be considerably less than the actual mean pressure if the actual contact area is only a small portion of the overall area. The actual area in contact can be estimated by counting the contact pixels after thresholding, although such estimates may have inherently higher errors due to the fact that low magnification was used to acquire the overall area. By using high magnification capture of the central portion of the contact images, the actual area estimations will be more accurate owing to higher resolution. However, depending on the locus of the image within the contact region, the percentage contact can vary since the finger ridge pattern is different in different parts of the fingerpad.

The following illustrates various pieces of information available during contact by using data from active touch experiments on fingerpad contacting with a rigid Plexiglas plate under low magnification. Figures 4-13 and 4-14 show several variables plotted against time and

force for subject CH. The profiles of the plotted variables are divided into two phases: the indentation phase and the retraction phase. The indentation is marked with crosses whereas the retraction portion is marked with circles. Since the first few frames digitized did not contain contact images, the calculations were done for the frames which had a mean force larger than 0.1N.

In Figure 4-13, the first graph shows the force profile which reached its maximum value just before the 1 second time mark. The corresponding nominal contact area increased as the force increased during the indentation with an initial rapid increase followed by a slower rate as shown, it saturated even before the contact forces reached the maximum. By comparing the nominal area with the actual contact area, it can be observed that during the later part of the indentation, the actual area kept on increasing even after the overall contact saturated. The actual area divided by the nominal area is shown as the percentage of contact inside the nominal contact area: it increased during the indentation phase and seemed to stay constant in the figure during the retraction phase. The mean nominal contact pressure was obtained by dividing the contact forces by the nominal contact area. The shape of the mean nominal pressure is close to that of the force profile. On the other hand, when the actual contact area was used for pressure calculations, the mean actual pressure obtained showed qualitatively different characteristics from the mean nominal pressure. Unlike the nominal pressure which rose very fast durint indentation, the increase in the actual pressure was slow. The pressure drop-off rate for both nominal and actual was about the same during retraction. Since the percentage contact inside the overall area ranged from 10 % at the beginning to 25 % during the retraction, the actual pressure was at least 4 times as large as the nominal pressure. Figure 4-14 provides a different view of the data obtained. The difference between the two phases of contact is more dramatic when plotted against force. Given the same amount of force, the contact information strongly depends on whether it was in the indentation phase or the retraction phase. The only variable which was similar during the two phases was the nominal contact pressure.

4.5.2 Contact areas with soft specimens

The real-time imaging setup was used to observe the contact areas of the fingerpad with objects of various compliances during passive indentation. Passive touch experiments were conducted by using the tactile stimulator to move the specimen by 3mm from the point of

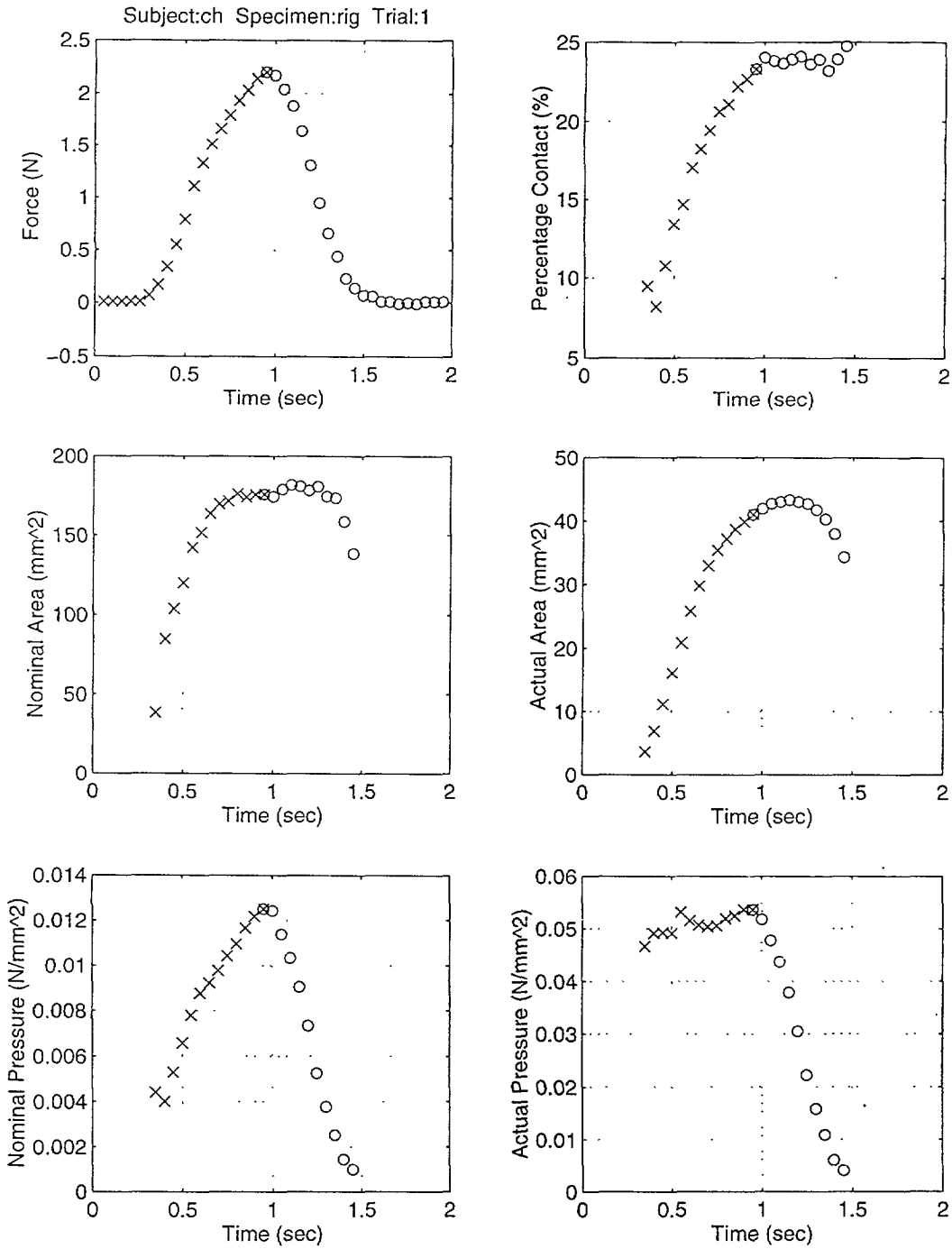

Figure 4-13: Various contact variables, plotted against time, calculated from the image and force data obtained using low magnification.

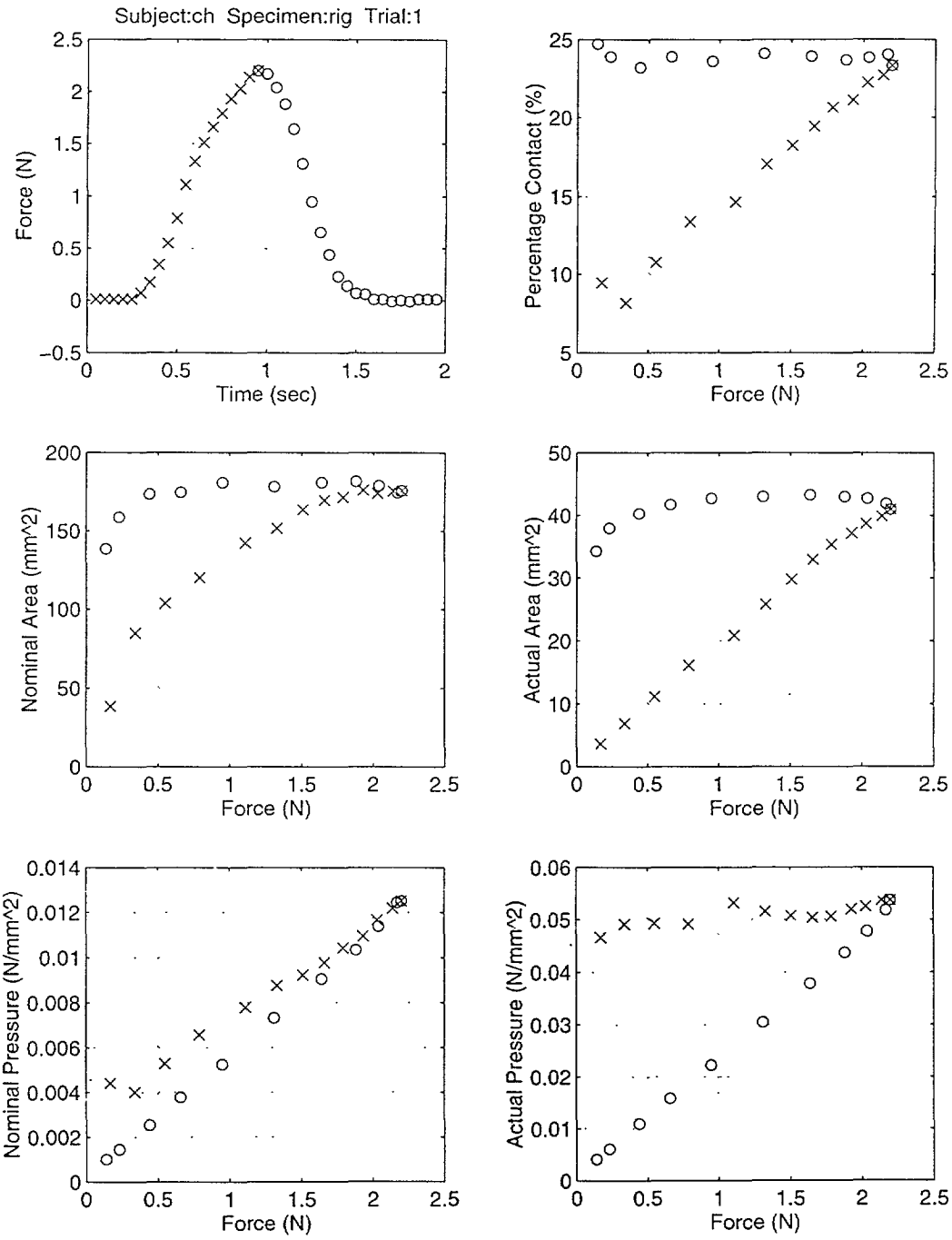

Figure 4-14: Various contact variables, plotted against contact force, calculated from the image and force data obtained using low magnification.

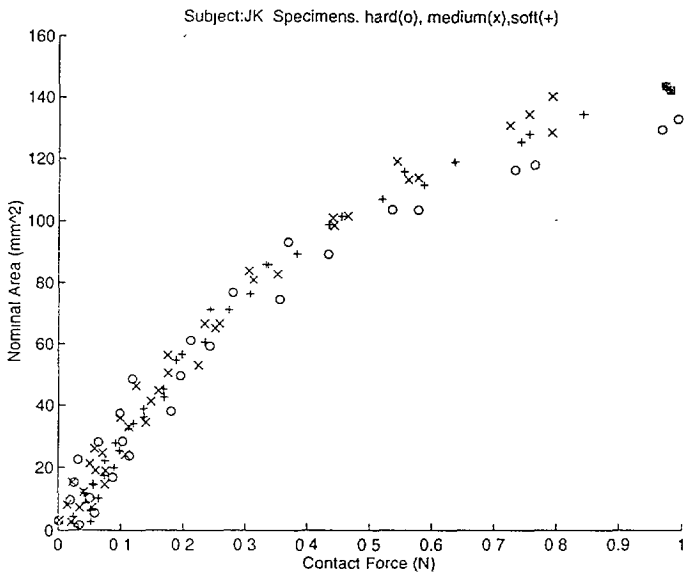

Figure 4-15: Nominal contact area versus contact force for specimens of various softnesses for subject JK.

barely touching to indent the stationary finger at a constant speed of 2.4mm/sec. The overall contact areas were obtained by using low magnification to capture the entire contact region when the forces were less than 1N. At higher contact forces, the low magnification images obtained to capture the entire contact region were of poor quality due to the deformation of the specimens. Therefore, the percentage contact areas were obtained separately using high magnification. Since the real-time imaging setup does not have a large depth of focus at high magnification, the focus was adjusted to about half of the range of specimen motion to obtain acceptable images during indentation.

The overall contact boundaries were extracted manually since the automatic method did not give satisfactory results for all the images due to the presence of noise and specimen deformation. The area calculations were performed on the manually extracted borders which were obtained by using MATLAB software GINPUT function. The overall area versus mean contact force curves for all the specimens were about the same when the contact force was less than about 1N. Figure 4-15 shows the results of nominal contact area versus the contact forces from three trials, plotted with the same symbol, of passive touch experiments with various specimens, plotted with different symbols, for subject JK.

To have higher resolution in the data analysis, the percentage contact areas for soft specimens were obtained with higher magnification. By using homomorphic processing, the

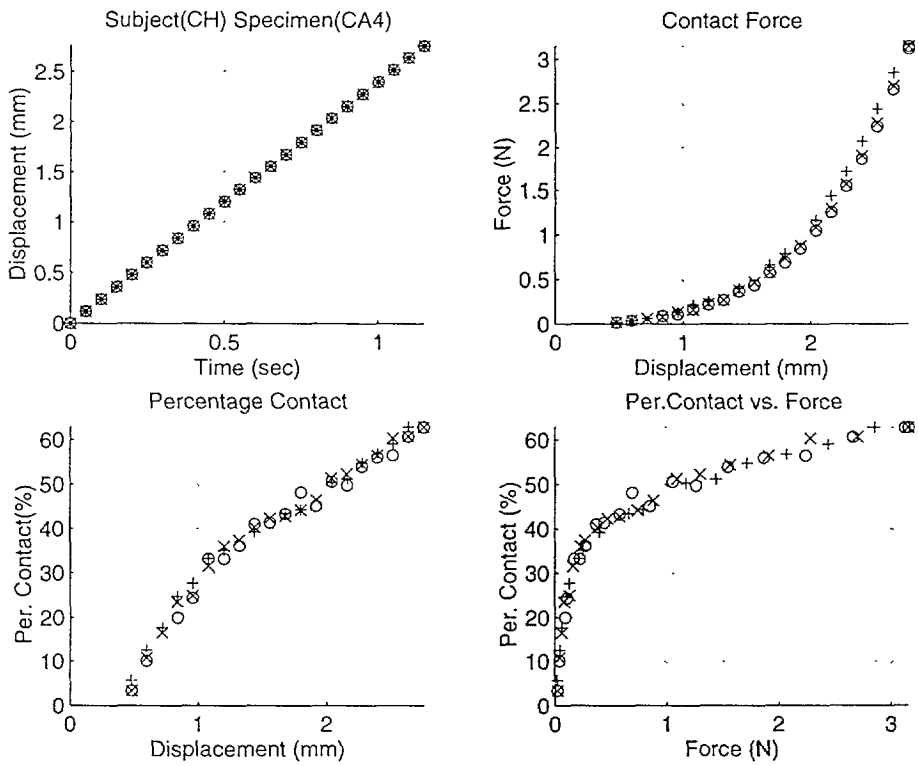

Figure 4-16: Percentage contact data from three trials for subject CH in contact with the soft specimen CA4(0.304mm/N).

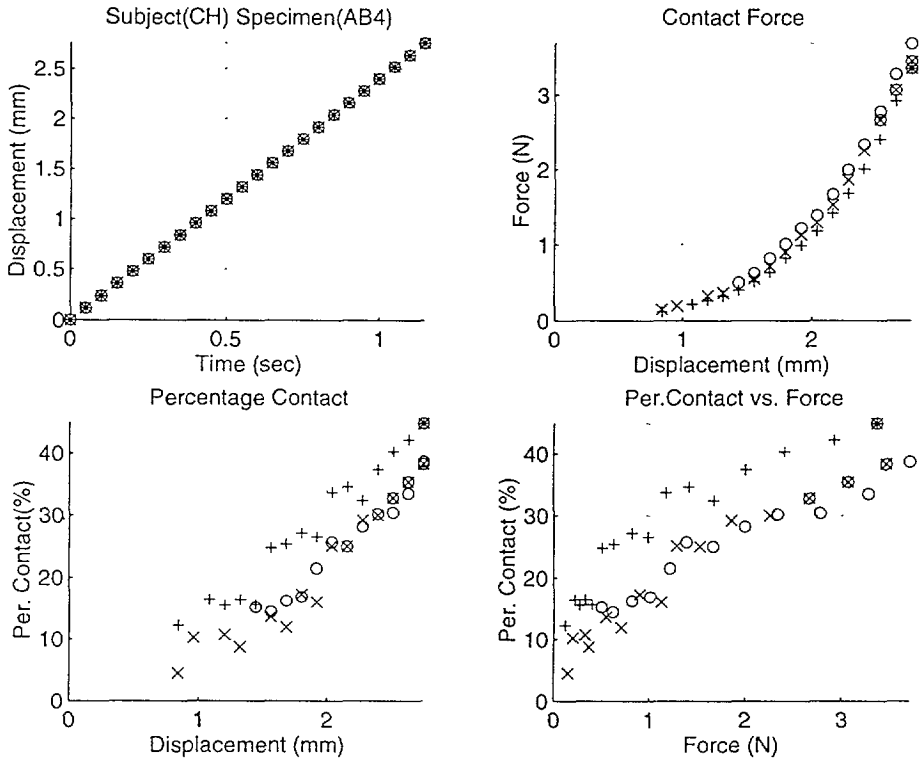

Figure 4-17: Percentage contact data from three trials for subject CH in contact with the hard specimen AB4(0.086mm/N).

portions that were in contact were separated from the portions that were not in contact. Figure 4-16 shows the results of three trials, plotted using three different symbols, from contact experiments using a compliant object (CA4) which has an objective compliance of 0.304mm/N. The mean contact force during each image frame increased as the specimen was indented into the finger by the stimulator. The corresponding percentage contact area grew with increased depth of indentation. Since the data was processed using homomorphic processing, the percentage results which are less than 15% or more than 85% are considered unreliable because the processed image histogram was approximately unimodal in the corresponding frames and an appropriate threshold value could not be found easily. Also, even if the resulting histogram is bimodal, a threshold value which differs slightly would give slightly different results. Therefore, errors of a few percent are expected and should be kept in mind when interpreting the data. The data from the three trials, shown in different symbols, are very consistent as indicated by the small variations in the results. The percentage contact rose quickly to 40% with a contact force of only 0.25N. As the contact force increased to 3N, the percentage contact rose more gradually to about 60%.

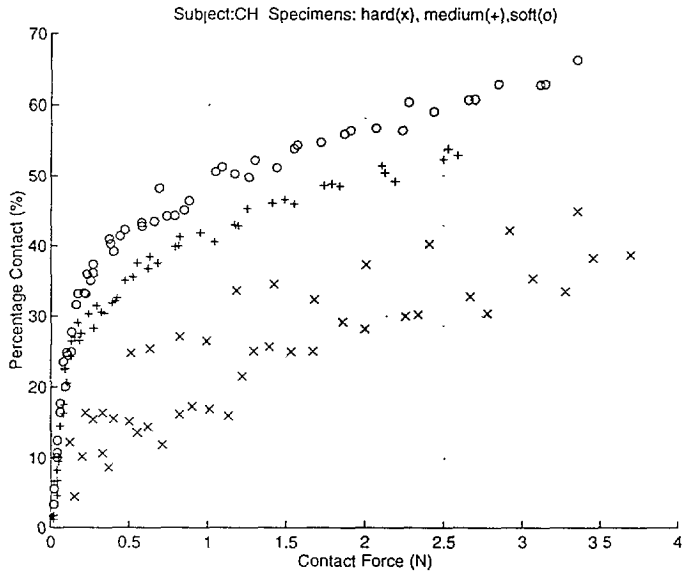

Figure 4-18: Percentage contact results from various soft specimens used for subject CH.

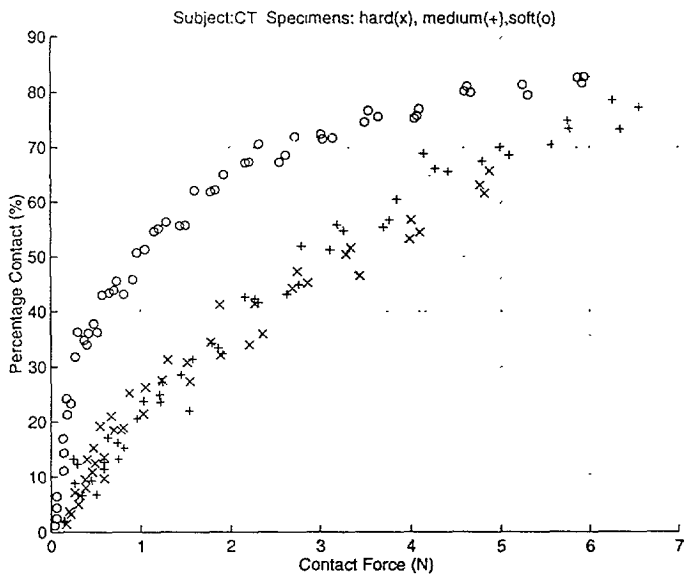

Figure 4-19: Percentage contact results from various specimens used for subject CT.

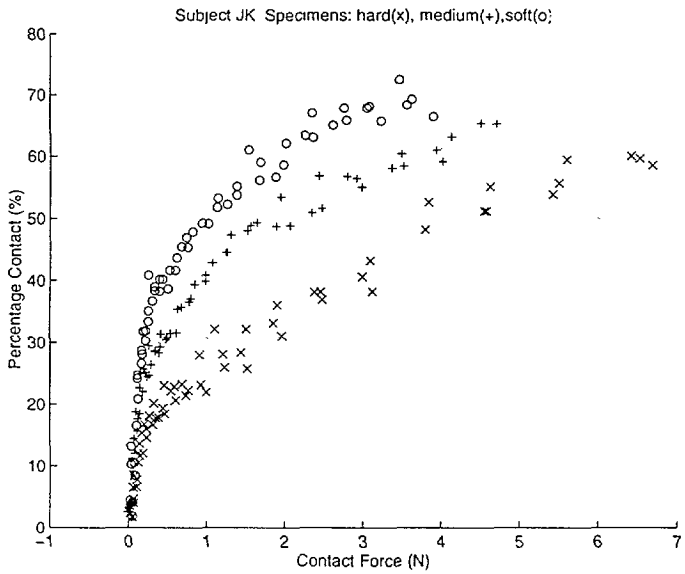

Figure 4-20: Percentage contact results from various specimens used for subject JK.

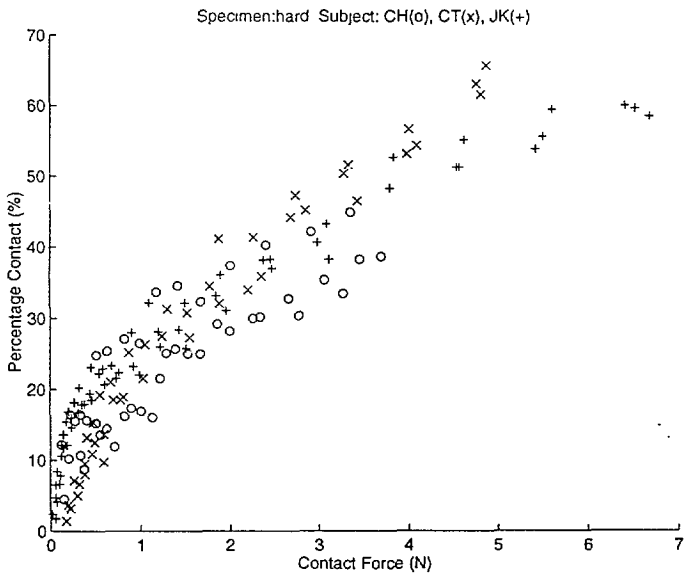

Figure 4-21: Comparison of percentage contact results from various subjects for the hard specimen.

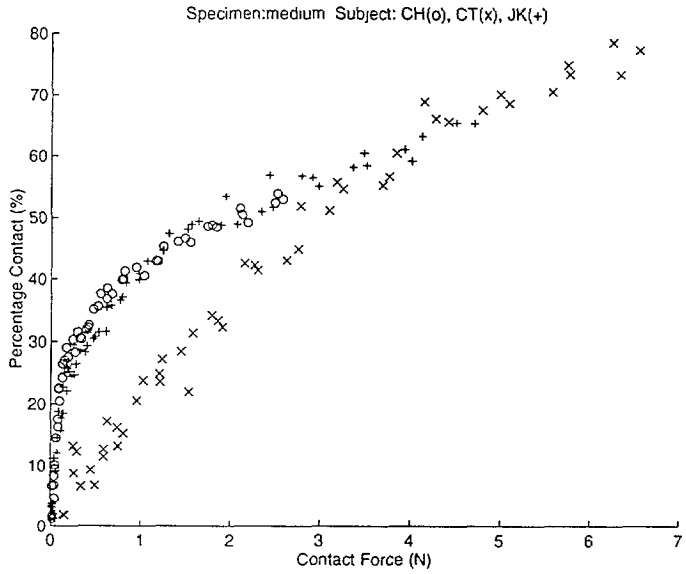

Figure 4-22: Comparison of percentage contact results from various subjects for the medium specimen.

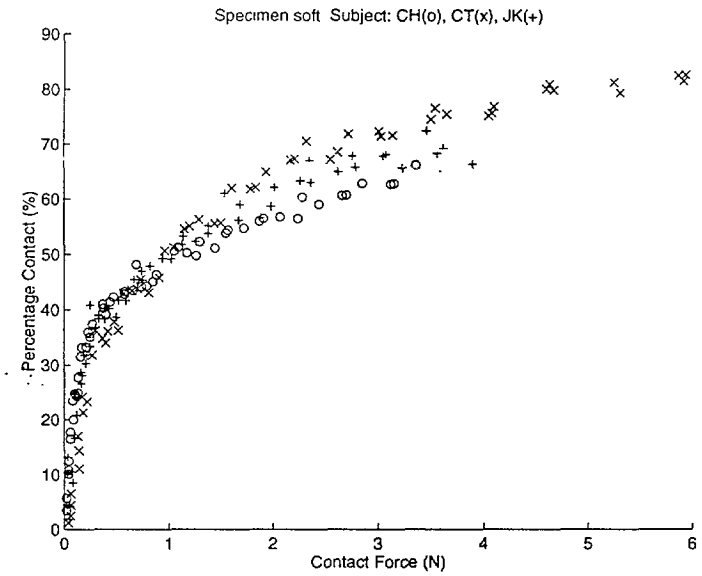

Figure 4-23: Comparison of percentage contact results from various subjects for the soft specimen.

The results of contact experiments with harder specimen AB4 which has an objective compliance of only 0.086mm/N are shown in Figure 4-17. For the three trials conducted, there is slightly more variability among the results compared to those for the soft specimen. The resulting percentage contact was only about 40% at 3N force, which is significantly less than that for the soft specimen. The results for the three different soft specimens used are compared in Figure 4-18 for subject CH. The results from subject CT and JK for various specimens are shown in Figures 4-19 and 4-20, respectively. The percentage contact area is generally lower for the specimens with lower objective compliance. Comparison of the results for the three subjects in contact with various specimens used is shown in Figures 4-21 to 4-23. Although there is some variability among the results for different subjects, the effect of subject was not as obvious as the effect of specimens.

4.5.3 Description of slip

To observe contact phenomena accompanying slip, the videomicroscopy system was setup to record the contact region as the subject actively stroked the fixed Plexiglas specimen across the field of view of the camera. By viewing the image sequence composed of frames taken 50 msec apart, one realizes that as the shear force applied on the finger increases, slip between the fingerpad and the plate starts from the border of the contact region. The region which remains stationary in the center shrinks as time progresses. Eventually, the whole contact region slides as a whole across the surface of the plate and the image of the contact region remains unchanged as in rigid body translation. The figures described below illustrate this phenomenon in greater detail.

The relative motion of the finger ridges can be observed by comparing the scan-lines of two adjacent frames. In Figure 4-24, images A and B are 50 msec apart in time. Although they look very similar to the eye, there are slight differences in the locations of the finger ridges, especially in the left and right portions of the image. The gray scale variations on line 240, the middle horizontal line of the 640 by 480 size images, is plotted in the lower left graph. The gray-scale variation from image A is plotted as a solid line and that from image B is plotted as a dotted line. The dotted line mostly coincides with the solid line in the middle portion of the scan line and leads the solid line on the two sides. The differences of the two scan-lines are shown in the lower right graph.

The movement of the finger ridges in consecutive frames is depicted in Figure 4-25. The

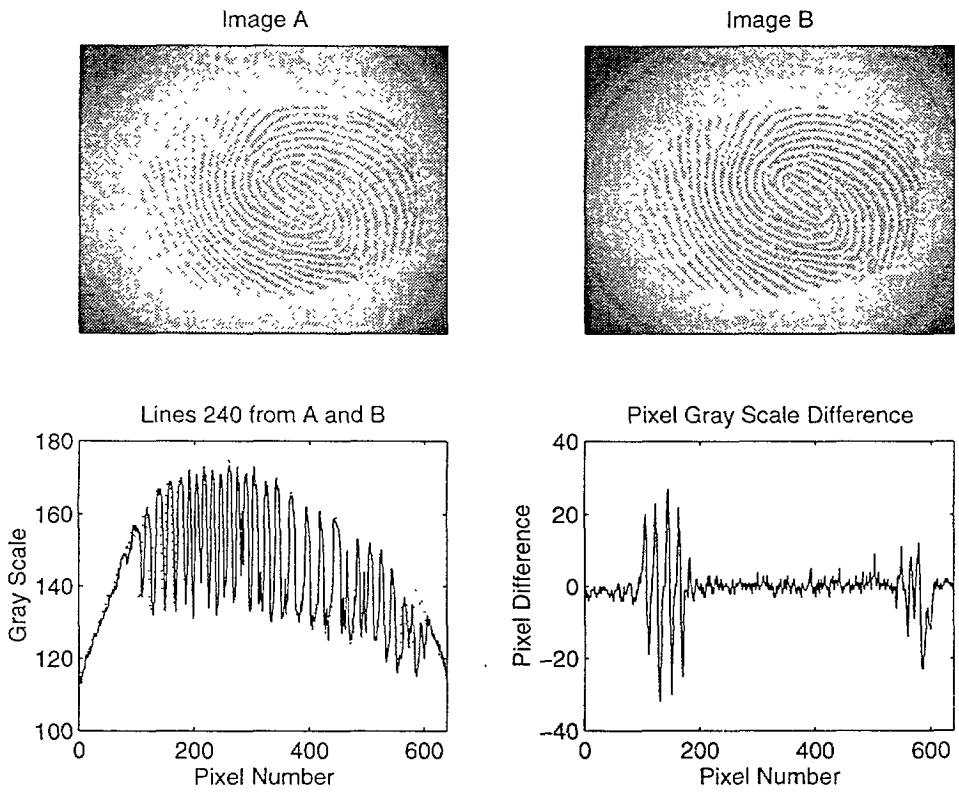

Figure 4-24: Typical images and scan-lines from contact between a fingerpad and a Plexiglas plate when slip started to occur on the boundary.

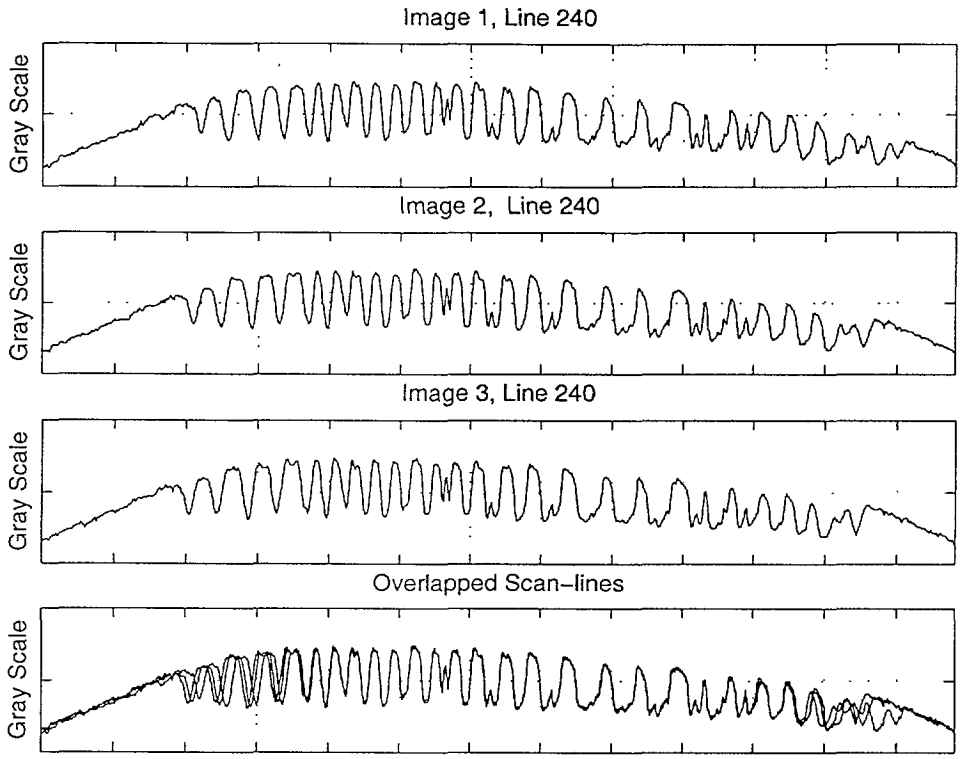

Figure 4-25: Comparison of gray scale values on a scan-line in a sequence of images at the incipience of slip.

top three graphs consist of gray scale variation on a scan-line in the center of three consecutive images while the bottom graph is a superposition of the three. Grid lines are provided for easy comparison of finger ridges. By comparing the finger ridges, it is concluded that the middle region has not moved yet in all the three frames which occur over 150 msec in time, whereas the two ends have already moved an observable amount. The distances between ridges on the left side of the graph are stretched whereas the middle region is still stationary. In contrast, the distances between the ridges on the right are compressed.

Although this phenomenon of slip starting from the boundary and propagating inwards can be seen vividly by playing the recorded image sequences in real-time, it is difficult to present such results in stationary pictures on a single page. By superimposing the finger ridge outlines of the image sequences, such effects can be seen more easily. The left hand graphs of Figure 4-26 are three images from the slip sequence. The outlines of the finger ridges are obtained by morphological operations, as explained in the image processing section. In the upper right graph, the outlines of the first image is shown. In the middle, the outlines of both first and second images are shown. This is created by performing a logical OR operation

from the two outline images. In the bottom, the outlines generated from the three frames are shown. By comparing the three outline graphs, one sees immediately that the regions in the middle have not moved while the borders have moved an appreciable amount.

4.6 Discussion

4.6.1 Contact phenomena

The development of contact

Based on the images and force data obtained from the low magnification experiments using a rigid Plexiglas plate, our understanding of the development of contact has been enhanced. By combining the information available in variables such as nominal (overall) contact areas, actual contact areas, and contact forces, various pieces of information generated during contact can be calculated (see Figures 4-13 and 4-14). Surprisingly, the actual contact area increased slowly as compared to the nominal area during the indentation, which indicates presence of viscoelasticity in the fingerpad. At the same time, the actual mean contact pressure did not vary much as compared to the rate of change in nominal mean contact pressure. On the other hand, the percentage contact increased during the indentation phase and remained roughly constant during the retraction phase.

The results from visualization of contact region showed a considerable difference between loading and unloading in terms of contact pressure, contact area and the percentage contact inside the nominal contact region. Soft tissues which make up the fingerpad can be modeled according to Fung's [16] quasi-linear viscoelastic model, which was proposed to explain the mechanical properties of biological tissues with a response consisting of an elastic response and a reduced relaxation function. The increased actual area of contact during the loading phase can also be thought of as more and more springs coming into contact from each of the finger ridge (small contact islands growing bigger and getting connected and the ridges growing fatter due to increases in the contact force applied). During the unloading phase, however, the same springs do not retract due to viscoelastic effects (as shown by the slow decrease of actual contact area in Figure 4-14). Instead, it is likely that the stiffness of each spring reduces as the contact force is reduced. Eventually, the ridges get thinner and disconnect and finally disappear.

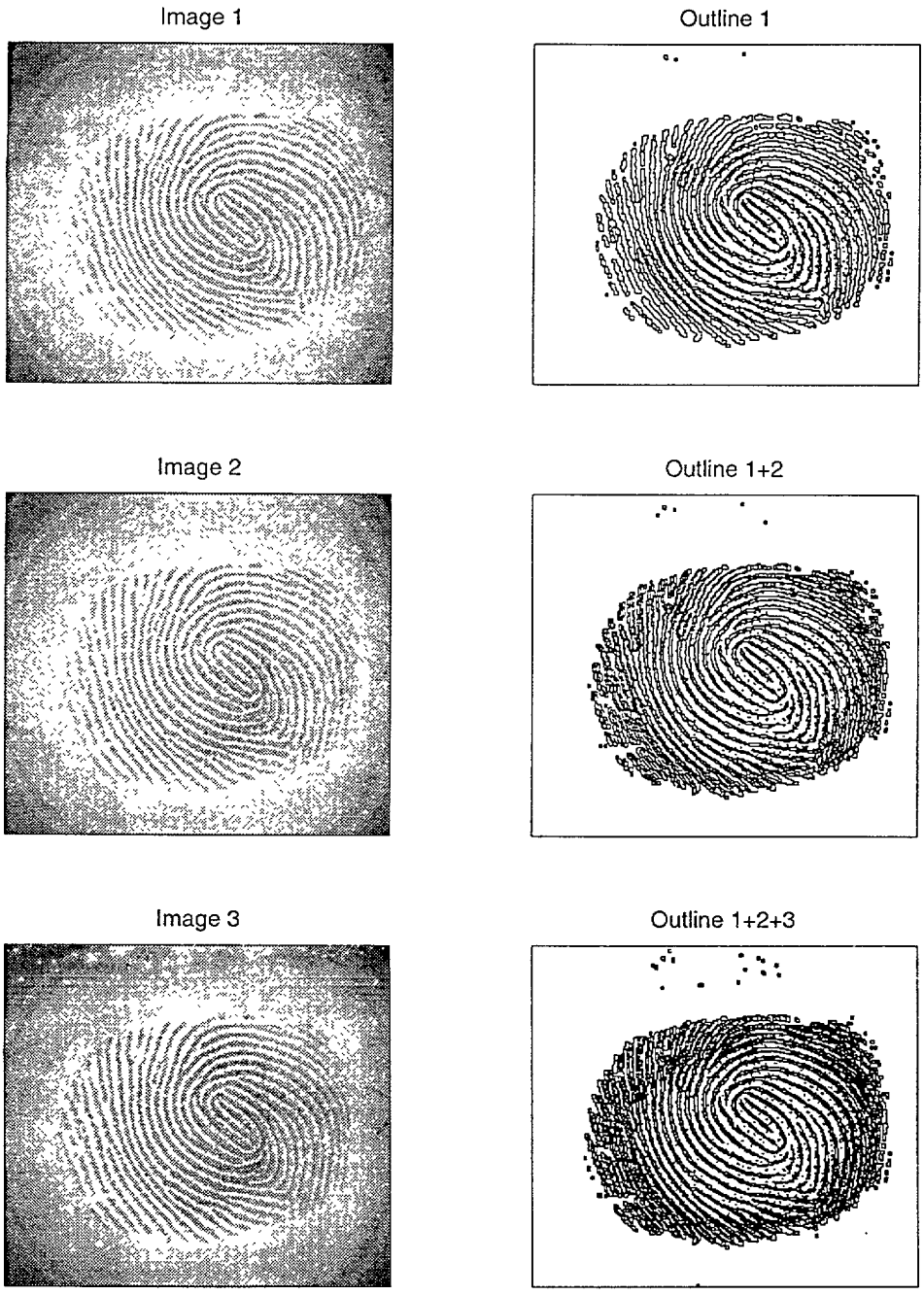

Figure 4-26: Visualizing the slip sequence in action by combining images processed by the outlining procedure.

The hypothesis of pressure distribution

Although the contact information discussed used mean pressure inside the contact region, the actual distribution is quite likely to be non-uniform. Without high resolution pressure sensor arrays, the pressure distribution cannot be measured directly. The pressure distribution that one would expect from contact mechanics [23] is parabolic in nature, assuming that the materials in contact are linear.

If we assume that the material properties of the individual finger ridges are similar, the static friction coefficient between the finger ridges and the Plexiglas would also be similar. During active slip, we observed that the boundaries of the contact region slipped first, whereas the center of the contact region remained stationary. One reasonable hypothesis for the border to slip first is that the pressure distribution on the contact region is in fact not uniform. The pressure in the middle is probably higher than that in the surround, as expected from mechanics. Therefore, the shear force overcomes the static friction at the borders first and the middle slipped only when the shear force fully overcame the frictional forces. In addition, during such a process, the finger ridge distances in the front portion of the motion get stretched because the middle region has not moved yet and the ridges on the back portion of the fingerpad get compressed. From a neurophysilogical viewpoint, the skin stretching and compression could be sensed by the mechanoreptors in order to detect the incipience of slip (Srinivasan *et al* [43]).

4.6.2 Contact information available for softness discrimination

During softness discrimination experiments using normal fingers to perform discrimination, the subjects had tactile information from the contact region in addition to kinesthetic information. From the visualization of fingerpad contact with soft specimens, we know that the overall contact areas were about the same for the hard (0.086mm/N), medium (0.188mm/N), and soft (0.304mm/N) specimens when the contact forces were up to 1N (Figure 4-15). The percentage contact areas were, however, significantly different (Figures 4-18, 4-19, and 4-20) for specimens of various softness. Thus, if we assume that the overall contact areas were about the same for the different specimens even for higher contact forces, the percentage contact areas and/or the pressure distributions could be the cues for subjects to discriminate object softness.

Since the subjects reported that the discriminations were based on the indentation portion of the contact, the retraction portion of the fingerpad contact was not important for this task. When the subjects wore thimbles, the contact interface conditions were different from the normal finger conditions. The tactile information which allowed the subjects to have fine softness discriminability was eliminated and the subjects' performance degraded significantly. When the subjects had thin (0.06mm) finger cots on, the performance was not statistically different from the normal finger, which suggests that the finger ridge level details are not important for discriminating the specimens used.

4.6.3 The role of contact mechanics in haptic interaction

During haptic interaction with objects, be it exploration or manipulation, tactile sensory information originates directly from the contact region. The development of contact region depends not only on the gross properties of objects and fingers, but also on the detailed mechanics of contact, the underlying pressure distributions, as well as the history of the contact. For a seemingly simple task such as handling an egg during its transportation from the refrigerator to the kitchen counter, our fingers need to exert the right amount of force to not break or drop the egg.

From the visualization of the slip phenomenon, we see that slipping of the finger ridges near the boundaries of contact occured first, which caused the finger ridges to stretch in front and compress near the back. These relative movements of the finger ridges will most likely cause the mechanoreceptors underneath the skin to respond and, through the central nervous system, notify the brain about the incipience of slip, so that the brain can activate the motor subsystem to take appropriate actions to avoid objects from slipping through our fingers.

During indentation, the fast growth of the overall (nominal) contact region allows the contact forces to be distributed across a large region in a short period of time to provide stable contact. The actual area of contact developed more slowly in the meantime, as described in the sections on contact areas. The retraction or unloading portion of the contact showed mechanisms that provide as large an area of contact as possible by reducing the actual pressure, but maintaining the overall contact area for a prolonged period of time to provide stable contact.

With these additional insights provided by this study on contact visualization, it seems clear that the same kind of contact process which depends a lot on the mechanics of contact

has to happen in order to achieve successful haptic interaction with more complex objects as well. It may also be helpful to design robotic fingers to have similar relationship among contact forces, nominal areas, and actual areas.

Chapter 5

Conclusions

5.1 Main results

5.1.1 Softness discrimination

To measure the abilities of humans in discriminating softness with their fingerpads by active touch (with eyes closed), a specimen presenter system was built to randomly present the softness specimens for the discrimination task. Two experimental paradigms involving one and two index fingers were used; three finger-contact interface conditions were tested (normal, finger cot, and rigid thimble). The results from the three different finger conditions show that the fine detailed finger ridge level tactile information is not necessary for the task because discrimination with the finger cot is as good as with the normal finger (see Tables 2.3 and 2.4). But when thimbles were present, the dramatic degradation in discriminability demonstrated the absolute necessity of tactile information to achieve normal resolution.

In order to look into the strategies and underlying mechanisms used during the softness discrimination process, an experimental paradigm involving the two index fingers from both hands was used. The performance under both normal and finger cot conditions improved, which could be attributed to the fact that in this paradigm, the subjects need only to rely on immediately available sensory information and not on memory. When the peak forces applied with normal finger on the two specimens by each subject are compared, three different strategies stand out: (1) to achieve the same amount of deformation of the two specimens by exerting higher forces on the harder specimen, (2) to compare the contact information obtained by applying the same amount of pressure on both specimens (thus higher peak

forces on the softer specimen), and (3) to apply the same amount of peak forces on both specimens and compare the deformations.

Although one of the subjects consistently applied higher forces with the right hand, the subject's performance did not seem to be affected, implying that the brain can compensate for such differences.

5.1.2 Force control

In the force control experiments, subjects were asked to achieve and maintain a constant contact force by pressing their fingerpads on specimens with the following experimental parameters: object softness, contact interface condition (normal, finger cot, thimble), target force magnitude (2N, 4N, 8N), visual feedback availability, and the hand used. Statistical tests on the results indicated that the errors from tracking with visual feedback was significantly lower than when the subjects had to maintain the force without visual feedback. The abilities of the subjects to control forces on specimens of various softness under the three finger contact interface conditions were not significantly different. The errors were higher when controlling a higher target force. In addition, significant differences were found between the force control abilities of the two hands for the subject who showed handedness in the softness discrimination experiments.

5.1.3 Contact visualization

A real-time imaging setup which integrated a videomicroscopy system with a tactile stimulator system by means of a custom made communication interface was developed. This system allowed both the contact images and the contact forces to be digitized in real-time. This setup was used for visualizations of the overall and actual contact areas as well as for detailed observation of the phenomenon of slip.

Various image processing techniques were developed and applied in order to obtain contact information from the digitized images. The images of the contact regions were improved by first applying homomorphic processing for contrast enhancement and then performing a global thresholding or scan-line processing. Homomorphic processing is better suited for images with larger contact regions, since it is likely to produce a a bimodal histogram which benefits the thresholding step for converting the original image into a binary image consisting of contact and non-contact regions. The overall contact area in each image was estimated

by using a modified wedge-ring approach to determine the approximate boundaries of the contact images obtained with low magnification.

Based on the images and force data obtained from the low magnification experiments using rigid Plexiglas, and examining the mean pressure on the contact regions, various sources of tactile information such as overall contact areas, actual contact areas, percentage contact, nominal mean pressure, and actual mean pressure were calculated. Surprisingly, the actual contact area increased much more slowly than the nominal area during the indentation. But the actual contact pressure did not vary as much as the nominal contact pressure during indentation. On the other hand, the percentage contact increased steadily during the indentation and remained roughly constant during retraction.

The results of visualization of the fingerpad in contact with soft specimens showed that the overall contact areas were about the same for various specimens for contact forces up to 1N. However, the percentage contact area inside the contact region obtained from high magnification images showed significant differences for the hard (0.086mm/N), medium (0.188mm/N), and soft (0.304mm/N) specimens.

From the visualization of the slip between the fingerpad and a rigid Plexiglas plate, it was shown that slipping first occured only near the boundaries of contact, which caused the finger ridges to stretch in front and compress near the back. These relative movements of the finger ridges most likely cause the mechanoreceptors underneath the skin to respond and, through the central nervous system, notify the brain about the incipience of slip. The brain can then activate the motor subsystem to take appropriate action to avoid slipping of objects through our fingers.

5.2 Implications and applications

5.2.1 Human haptic interaction with soft objects

Although the process of the haptic interaction with objects, which generally involves multimodal perception, and intersensory integration during exploration or manipulation, is complicated, our understanding of the process has been improved by this investigation of the phenomenon from three different perspectives: discriminability, force control, and contact visualization.

The abilities, at the behavioral level, to distinguish fine differences in object softness

without useful visual and auditory information are likely to depend on both tactual perception and motor control. The subject with poorer performance in controlling forces without visual feedback of force, also did not do as well in discrimination when compared to the other subjects. Memory does play a role in discriminability as shown from the significant improvement in the results for all subjects when using both index fingers to discriminate the two specimens. Although subjects may exhibit handedness as shown from the differences in force control ability of the two fingers and the large difference of forces used during discrimination, the ability to discriminate was not impaired, which indicates that the brain was able to accommodate for handedness during the cognition process.

Since tactile information is essential to achieve normal softness resolution, the mechanisms for discrimination must rely on the spatio-temporal profiles of various contact variables. However, as seen in the visualization experiments, our finger has the property of developing the nominal contact area quickly even with a small force. The overall contact areas were about the same for specimens of different softness for forces up to 1N. But the actual contact areas were very different, based on high resolution images obtained with high magnification. Assuming that the overall contact areas were also about the same for specimens of different softnesses at higher contact forces, the information used during discrimination is probably the spatio-temporal distribution of the pressure over the nominal contact region. According to Srinivasan and LaMotte [42][40][41], this information can be signaled by mechanoreceptors of the type SAI (Merkel cells) and RAI (Meissner corpuscles).

5.2.2 The pressure distribution hypothesis

If the material properties of the individual finger ridges are assumed to be similar, the static friction coefficient between individual finger ridges and the Plexiglas would also be similar. In the visualization of the slip phenomenon, we observed that the boundaries of the contact region moved first whereas the center of the contact slipped last. The slip front moved gradually inwards during the process and then disappeared, at which time the finger ridges seemed to translate as a rigid body. One reasonable hypothesis for the boundaries to slip first is that the pressure distribution on the contact region is in fact not uniform. If the contact pressure in the middle is higher and decreased either linearly or non-linearly until it reached the edge, the observed slip phenomenon can be explained as due to Coulomb friction laws.

5.2.3 Slip detection

During the slip process, the finger ridges at the boundaries overcome the static Coulomb friction first and moved relative to the center of the contact region. The middle portion only slipped when the total shear force overcame the total frictional force. The inter-ridge distance in the front portion of the contact region got stretched because the middle region had not moved yet. In contrast, the ridges on the back portion of the fingerpad got compressed. From a neurophysiological viewpoint, the skin stretching and compressing could be the mechanical stimulus sensed by the mechanoreceptors and the corresponding neural impulses transmitted to the brain could be used for slip detection and prevention.

5.2.4 Dexterous robot finger design

If we imagine the human as the ultimate robot, then building a dexterous robot should borrow as much of the human system design or functionality as possible. During object manipulation, the control of contact forces is a major concern. An ideal dexterous robot finger should be able to maintain stable contact with objects having a wide range of properties. Although an intelligent control system which drives such a robot can use force sensors available in the various joints to sense the environmental properties and to perform dexterous manipulations, it would be beneficial to construct robot fingers that can exhibit some of the desired contact phenomena revealed in this study. The development of a robot fingerpad with a fast growth of the overall (nominal) contact region as contact forces are increased allows the contact forces to be distributed across a large region in a short period of time to provide stable contact. The actual area of contact needs to develop gradually, in the meantime, so as to provide a gradual increase in contact pressure. During the retraction or unloading portion of the contact, if the mechanisms were to maintain a large area of contact even when force dropped, the actual pressure would reduce and the contact would be more stable. The other benefit of providing a large contact surface as opposed to a point contact (as in the case of a rigid robot finger) is to simultaneously avoid crushing of objects with the same amount of force but lower pressure and prevent slip with a lower force to conserve energy.

5.2.5 Biomechanical visualization

The videomicroscopy and tactile stimulator systems developed during this study are powerful tools to investigate the underlying mechanics of contact. The videomicroscopy system was used by Dandekar [10], a recent Ph.D. from Touchlab, MIT, to successfully obtain images of the fingertip required for 3D reconstruction and the surface deformation experiments which were useful in verifying finite element models of the fingertip. The real-time imaging setup has proven to be very useful in revealing the underlying mechanics of contact. Several pieces of contact information, such as the overall contact area, actual contact area, nominal contact pressure, and actual pressure, were measured based on the image and force data. The observations of slip led to the hypothesis of non-uniform pressure distribution within the contact region which is yet to be proved in the future, possibly with high resolution tactile sensor arrays. Other possible experiments include observations of the finger ridge deformation as the fingerpad performs scanning motion to detect surface irregularities.

5.2.6 Automated fingerprint identification system

Automated fingerprint identification systems could benefit from the results of this study. In terms of real-time fingerprint image acquisition, the developed videomicroscopy system is capable of not only static images but also dynamic images. The slip phenomenon, prerecorded for each individual using the system, can be used as test. Such operation reduces the risk of beating the system with artificial impostor fingers, which would not have the same mechanical properties as live, real, fingers of a particular individual. The scan-line processing techniques can be implemented in real-time to convert the fingerprint images into binary format, for identification or storage purposes. As for image storage, a typical compression ratio of 30 was obtained by applying LZW compression algorithms, widely used in Unix systems, to the binary fingerpad images to achieve lossless compression. With lossless compression, the minute details of the finger ridges, sweat pores, and the small islands between ridges can be preserved. These techniques can be used to replace the high quality lossy compression standard, Wavelet Scalar Quantization (WSQ) [3] [4], currently adopted by the Federal Bureau of Investigation (FBI).

Appendix A

Softness Discrimination: Analysis of Applied Forces

This section presents the graphs similar to Figure 2-13 for the peak forces used in S-2AFC discrimination tasks. Peak forces on soft specimens versus peak forces on hard specimens for subjects CH, CT, and JK under normal, finger cot, and thimble conditions are plotted. The four panels are for the four specimen pairs. The data were pooled from 3 experimental runs, 64 trials each, conducted for each of the experimental conditions. The percentage of correct calls, confusion matrix (labeled CM), and force-specimen-correctness matrix (labeled FsM) are also shown in each panel.

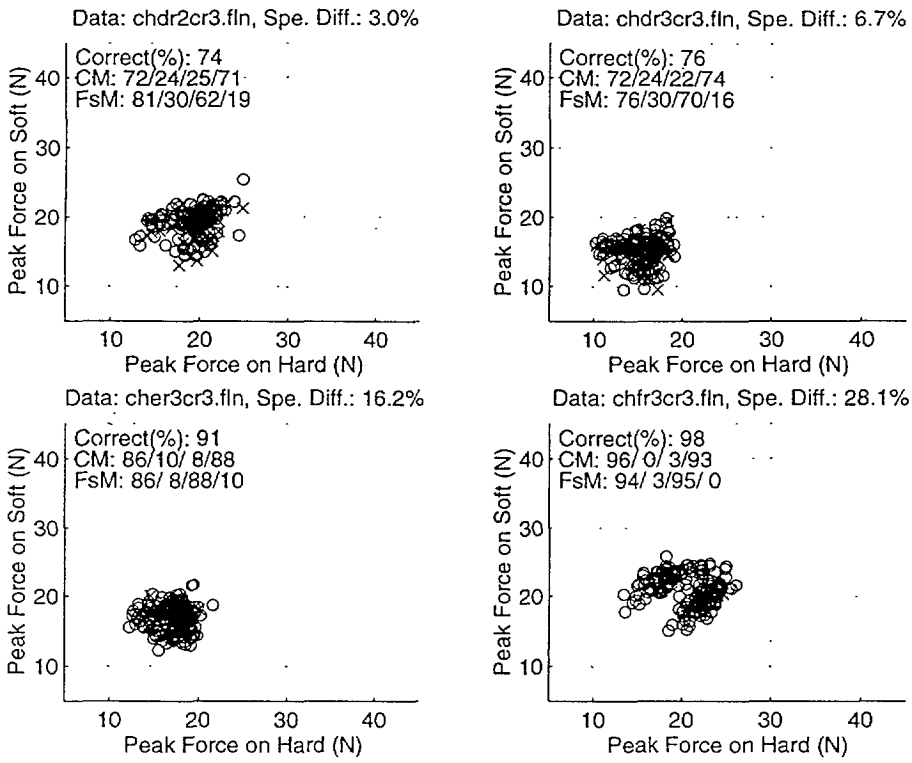

Figure A-1: S-2AFC Peak force plot for subject CH under normal condition.

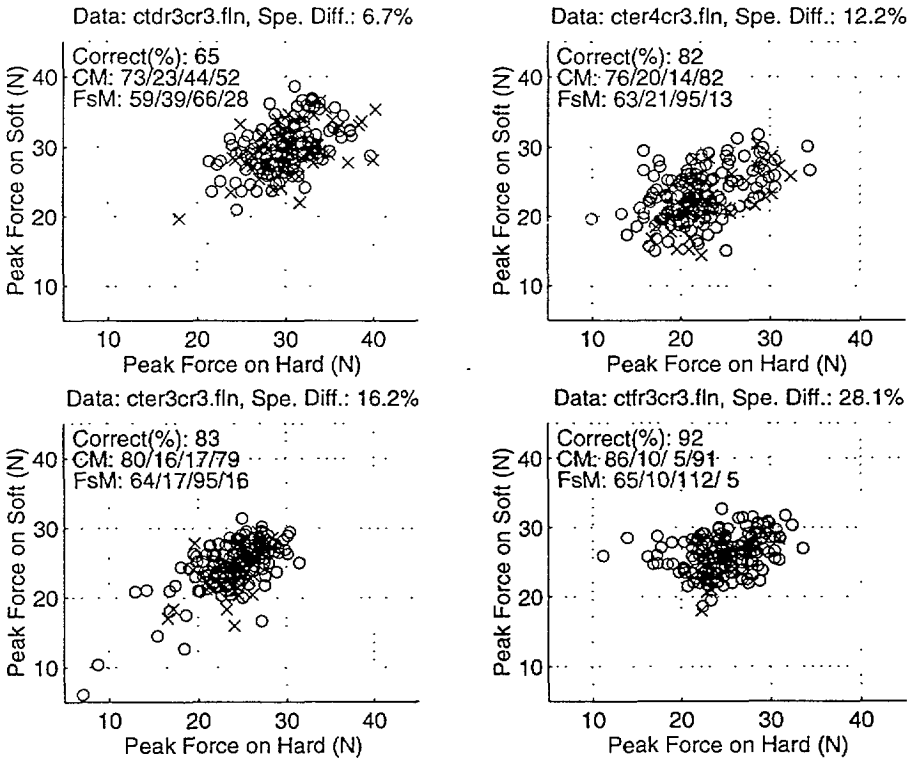

Figure A-2: S-2AFC Peak force plot for subject CT under normal condition.

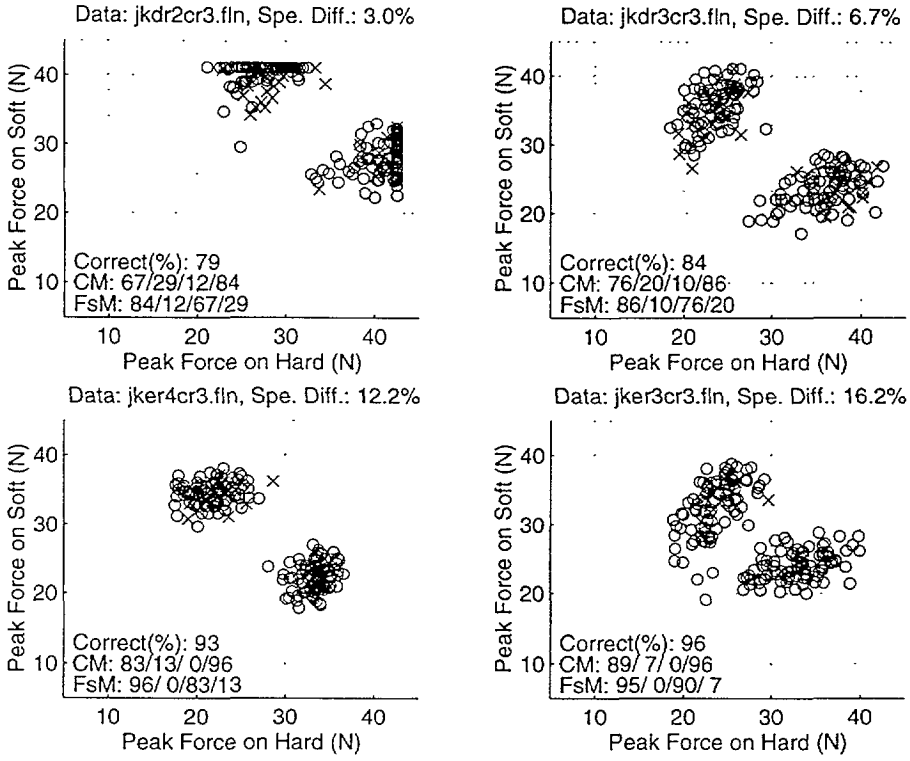

Figure A-3: S-2AFC Peak force plot for subject JK under normal condition.

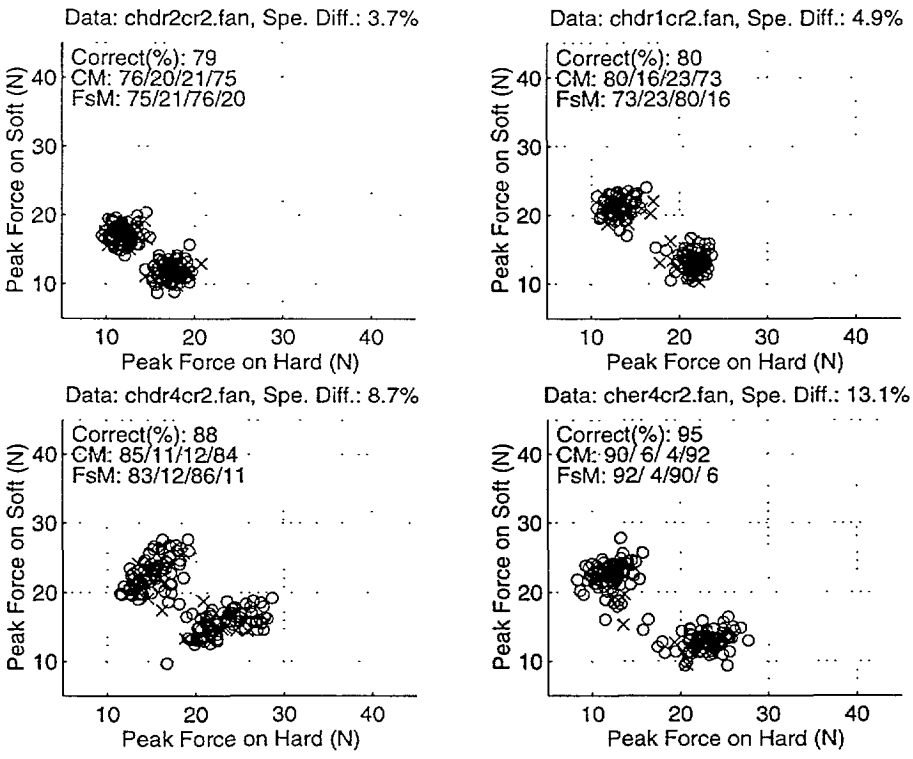

Figure A-4: S-2AFC Peak force plot for subject CH under finger cot condition.

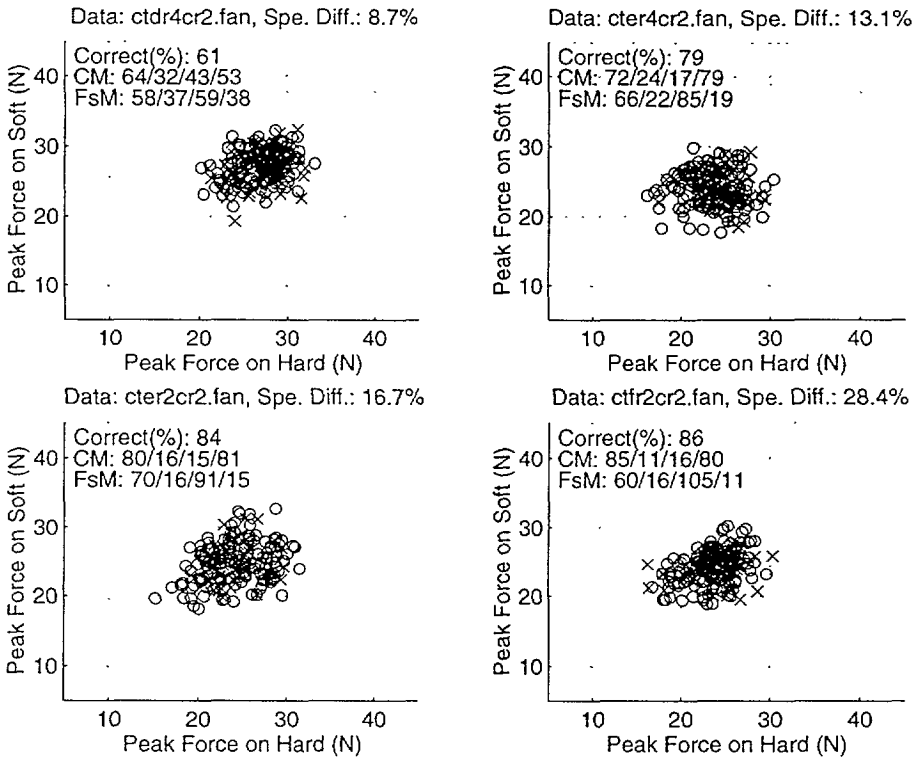

Figure A-5: S-2AFC Peak force plot for subject CT under finger cot condition.

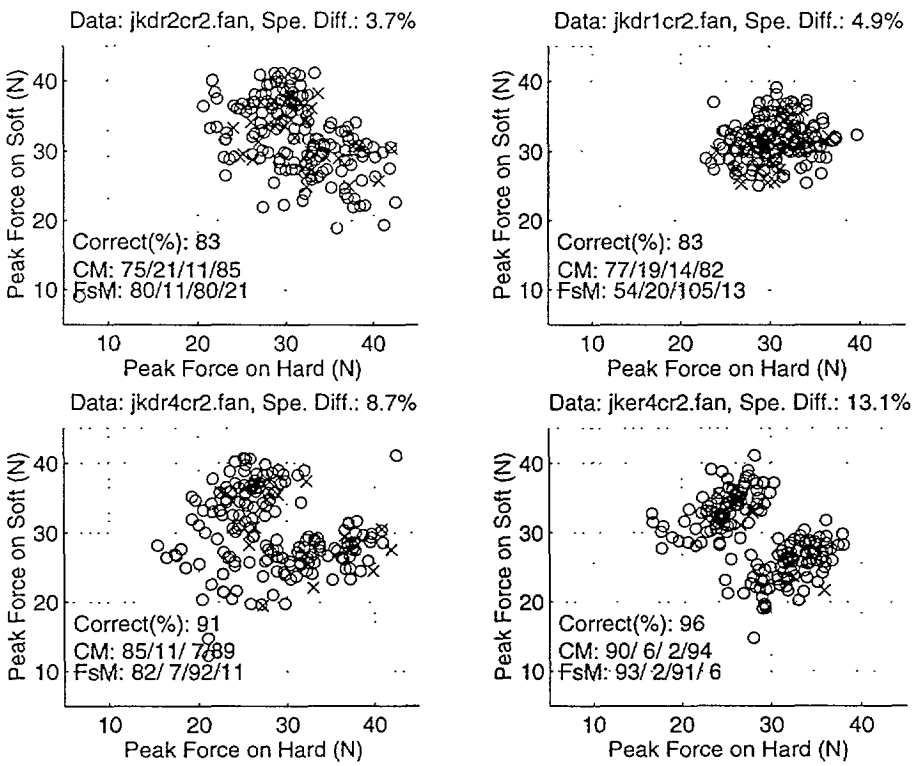

Figure A-6: S-2AFC Peak force plot for subject JK under finger cot condition.

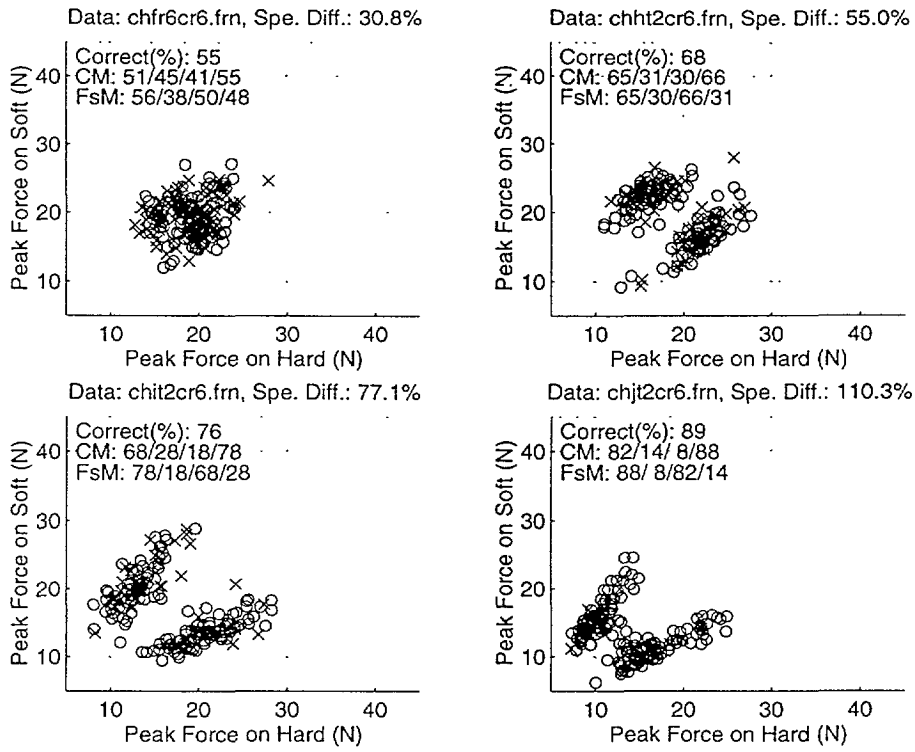

Figure A-7: S-2AFC Peak force plot for subject CH under thimble condition.

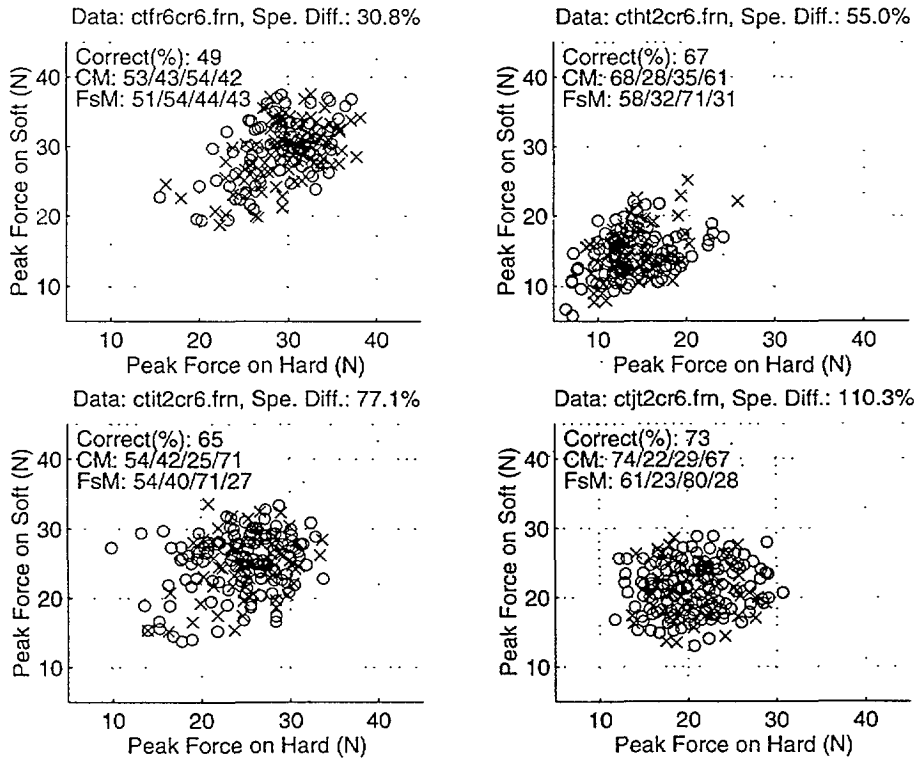

Figure A-8: S-2AFC Peak force plot for subject CT under thimble condition.

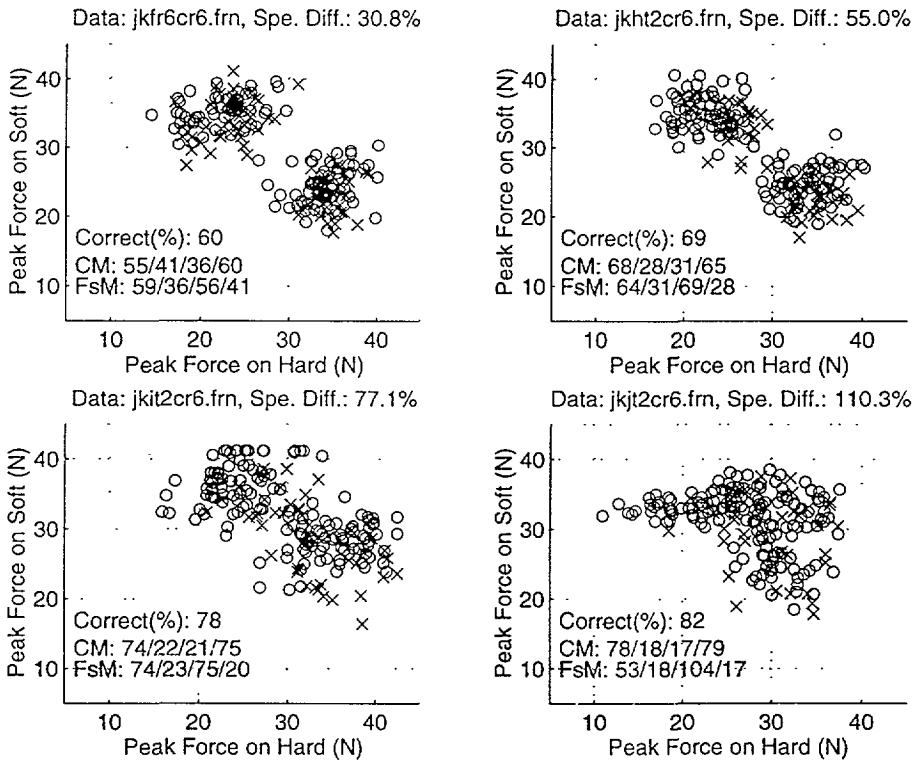

Figure A-9: S-2AFC Peak force plot for subject JK under thimble condition.

Appendix B

Softness Discrimination: JND Data

The discrimination results from an experimental run was represented by a confusion matrix. The matrices from three runs of 64 trials each was pooled together for the calculation of the sensitivity index d' and the response bias β for a given comparison specimen. Recall that the JND value is defined as the difference of stimuli which corresponds to a d' value of 1. The JND value for a particular subject under a given finger condition was then obtained by averaging the estimates of JND from the four comparison specimens. The data points which had a d' value less than 0.5 was not included in the mean JND calculations and their estimated JND values are enclosed in brackets.

Specimen	DR1	DR5	ER1	FR1
Difference	2.6%	7.1%	13.5%	31.7%
Confusion Matrix	55 41 29 67	74 22 20 76	74 22 17 79	92 4 1 95
d'	0.70	1.55	1.67	4.04
β	-0.17	-0.04	-0.09	-0.29
JND (%)	3.8	4.6	8.1	7.8
$MeanJND = 6.1\%$				

Table B.1: 1I-2AFC discrimination results for subject CH under normal condition (Standard: CR1 [0.304mm/N])

Specimen	DR2	DR4	ER4	ER2
Difference	3.7%	8.7%	13.1%	16.7%
Confusion Matrix	78 18 13 83	69 27 14 82	91 5 6 90	88 8 7 89
d'	1.99	1.63	3.16	2.84
β	-0.11	-0.24	0.05	-0.04
JND (%)	1.9	5.3	4.1	5.9
$MeanJND = 4.3\%$				

Table B.2: 1I-2AFC discrimination results for subject CH under finger cot condition (Standard: CR2 [0.298mm/N])

Specimen	ER4	FR4	HT2	IT2
Difference	14.7%	27.2%	53.3%	75.2%
Confusion Matrix	54 42 37 59	54 42 27 69	68 28 28 68	76 20 18 78
d'	0.45	0.74	1.10	1.70
β	-0.08	-0.21	-0.00	-0.04
JND (%)	[32.7]	36.9	48.7	44.3
$MeanJND = 43.3\%$				

Table B.3: 1I-2AFC discrimination results for subject CH under thimble condition (Standard: CR4 [0.293mm/N])

Specimen	DR2	DR3	ER3	FR3
Difference	3.0%	6.7%	16.2%	28.1%
Confusion Matrix	72 24 25 71	72 24 22 74	86 10 8 88	96 0 3 93
d'	1.32	1.42	2.64	4.43
β	0.02	-0.03	-0.06	0.35
JND (%)	2.3	4.8	6.1	6.3
$MeanJND = 4.9\%$				

Table B.4: S-2AFC discrimination results for subject CH under normal condition (Standard: CR3 [0.300mm/N])

Specimen	DR2	DR1	DR4	ER4
Difference	3.7%	4.9%	8.7%	13.1%
Confusion Matrix	76 20 21 75	80 16 23 73	85 11 12 84	90 6 4 92
d'	1.59	1.68	2.35	3.27
β	0.02	0.13	0.03	-0.10
JND (%)	2.4	2.9	3.7	4.0
$MeanJND = 3.2\%$				

Table B.5: S-2AFC discrimination results for subject CH under finger cot condition (Standard: CR2 [0.298mm/N])

Specimen	FR6	HT2	IT2	JT2
Difference	30.8%	55.0%	77.1%	110.3%
Confusion Matrix	51 45 41 55	65 31 30 66	66 30 26 70	82 14 8 88
d'	0.26	0.95	1.10	2.44
β	-0.05	-0.02	-0.06	-0.16
JND (%)	[117.7]	58.1	70.2	45.3
$MeanJND = 57.9\%$				

Table B.6: S-2AFC discrimination results for subject CH under thimble condition (Standard: CR6 [0.290mm/N])

Specimen	DR1	ER1	FR1	HT6
Difference	2.6%	13.5%	31.7%	47.9%
Confusion	46 50	55 41	77 19	92 4
Matrix	32 64	28 68	22 74	4 92
d'	0.38	0.73	1.59	3.64
β	-0.24	-0.18	0.05	0.00
JND (%)	[7.0]	18.5	19.9	13.8
$MeanJND = 17.4\%$				

Table B.7: 1I-2AFC discrimination results for subject CT under normal condition (Standard: CR1 [0.304mm/N])

Specimen	DR4	ER4	ER2	FR2
Difference	8.7%	13.1%	16.7%	28.4%
Confusion	60 36	67 29	70 26	72 24
Matrix	35 61	22 74	29 67	17 79
d'	0.66	1.26	1.13	1.60
β	-0.01	-0.11	0.05	-0.13
JND (%)	13.1	10.4	14.8	17.7
$MeanJND = 14.0\%$				

Table B.8: 1I-2AFC discrimination results for subject CT under finger cot condition (Standard: CR2 [0.298mm/N])

Specimen	FR4	HT2	IT2	JT2
Difference	27.2%	53.3%	75.2%	108.0%
Confusion	58 38	52 44	63 33	72 24
Matrix	48 48	36 60	22 74	17 79
d'	0.26	0.42	1.14	1.45
β	0.13	-0.11	-0.17	-0.05
JND (%)	[102.99]	[126.06]	65.8	74.5
$MeanJND = 70.2\%$				

Table B.9: 1I-2AFC discrimination results for subject CH under thimble condition (Standard: CR4 [0.293mm/N])

Specimen	DR3	ER4	ER3	FR3
Difference	6.7%	12.2%	16.2%	28.1%
Confusion Matrix	73 23 44 52	76 20 14 82	80 16 17 79	86 10 5 91
d'	0.81	1.87	1.89	2.88
β	0.30	-0.12	0.02	-0.18
JND (%)	8.3	6.6	8.6	9.7
$MeanJND = 8.3\%$				

Table B.10: S-2AFC discrimination results for subject CT under normal condition (Standard: CR3 [0.300mm/N])

Specimen	DR4	ER4	ER2	FR2
Difference	8.7%	13.1%	16.7%	28.4%
Confusion Matrix	69 27 42 54	72 24 17 79	80 16 15 81	85 11 16 80
d'	0.74	1.60	1.98	2.17
β	0.21	-0.13	0.02	0.12
JND (%)	11.8	8.2	8.5	13.1
$MeanJND = 10.4\%$				

Table B.11: S-2AFC discrimination results for subject CT under finger cot condition (Standard: CR2 [0.298mm/N])

Specimen	FR6	HT2	IT2	JT2
Difference	30.8%	55.0%	77.1%	110.3%
Confusion Matrix	53 43 54 42	68 28 35 61	60 36 27 69	74 22 29 67
d'	-0.03	0.89	0.90	1.26
β	0.14	0.10	-0.13	0.11
JND (%)	[*]	61.5	86.0	87.6
$MeanJND = 78.4\%$				

Table B.12: S-2AFC discrimination results for subject CT under thimble condition (Standard: CR6 [0.290mm/N])

Specimen	DR1	DR5	ER1	FR1
Difference	2.6%	7.1%	13.5%	31.7%
Confusion Matrix	69 27 29 67	64 32 28 68	77 19 9 87	88 8 10 86
d'	1.10	0.98	2.17	2.64
β	0.03	-0.06	-0.24	0.06
JND (%)	2.4	7.3	6.2	12.0
$MeanJND = 7.0\%$				

Table B.13: 1I-2AFC discrimination results for subject JK under normal condition (Standard: CR1 [0.304mm/N])

Specimen	DR2	DR4	ER4	ER2
Difference	3.7%	8.7%	13.1%	16.7%
Confusion Matrix	61 35 20 76	68 28 19 77	86 10 3 93	86 10 9 87
d'	1.16	1.40	3.12	2.58
β	-0.23	-0.15	-0.30	-0.03
JND (%)	3.2	6.2	4.2	6.5
$MeanJND = 5.0\%$				

Table B.14: 1I-2AFC discrimination results for subject JK under finger cot condition (Standard: CR2 [0.298mm/N])

Specimen	FR4	HT2	IT2	JT2
Difference	27.2%	55.0%	75.2%	108.0%
Confusion Matrix	42 54 23 73	57 39 19 77	66 30 15 81	69 27 5 91
d'	0.55	1.09	1.50	2.20
β	-0.43	-0.31	-0.26	-0.52
JND (%)	49.4	50.7	50.2	49.0
$MeanJND = 49.8\%$				

Table B.15: 1I-2AFC discrimination results for subject JK under thimble condition (Standard: CR4 [0.293mm/N])

Specimen	DR2	DR3	ER4	ER3
Difference	3.0%	6.7%	12.2%	16.2%
Confusion Matrix	67 29 12 84	76 20 10 86	83 13 0 96	89 7 0 96
d'	1.67	2.07	3.67	4.02
β	-0.32	-0.22	-0.73	-0.55
JND (%)	1.8	3.3	3.3	4.0
$MeanJND = 3.1\%$				

Table B.16: S-2AFC discrimination results for subject JK under normal condition (Standard: CR3 [0.300mm/N])

Specimen	DR2	DR1	DR4	ER4
Difference	3.7%	4.9%	8.7%	13.1%
Confusion Matrix	75 21 11 85	77 19 14 82	85 11 7 89	90 6 2 94
d'	1.98	1.90	2.66	3.57
β	-0.20	-0.10	-0.13	-0.25
JND (%)	1.9	2.6	3.3	3.7
$MeanJND = 2.9\%$				

Table B.17: S-2AFC discrimination results for subject JK under finger cot condition (Standard: CR2 [0.298mm/N])

Specimen	FR6	HT2	IT2	JT2
Difference	30.8%	55.0%	77.1%	110.3%
Confusion Matrix	55 41 36 60	68 28 31 65	75 21 19 77	78 18 17 79
d'	0.50	1.01	1.62	1.81
β	-0.07	0.05	-0.04	-0.02
JND (%)	61.4	54.6	47.5	60.9
$MeanJND = 56.1\%$				

Table B.18: S-2AFC discrimination results for subject JK under thimble condition (Standard: CR6 [0.290mm/N])

Appendix C

Statistical Tests on Softness Discrimination JND Data

The analysis of variance (ANOVA) method [31][24][36] was used to find out whether the results on softness discrimination were influenced by factors such as finger conditions and experimental paradigms. The JND estimates from the pooled data for each of the comparison specimens were used for the calculations of the ANOVA table. To compare any two JND results obtained under different circumstances, the *Student's t* test was used. The statistical analysis was performed by using MATLAB statistics toolbox.

C.1 1I-2AFC experiments

A two-way ANOVA was performed using subjects and conditions as the two factors. The thimble condition was not included because the data range is very different and it is clear that there is a significant difference between thimble and the other two conditions. Table C.1 lists the data used for the ANOVA analysis. The ANOVA table generated by using MATLAB software function *anova2* is shown in Table C.2. The ANOVA analysis provided tests for the following three hypotheses. First, the conditions differ in performance. Second, the subjects differ in performance. Third, there is an interaction between the subjects and conditions. The ANOVA table provides a means to look at variations between groups and variations within groups. The column SS in the table stands for sum of squares. The df column is the degrees of freedom for the factors. There are 3 subjects, therefore the df for columns is 2 $(3-1)$. There are 2 conditions, so the df for rows is 1 $(2-1)$. The column MS was

Condition	Subject		
	CH	CT	JK
Normal	3.8/4.6/8.1/7.8	7.0/18.5/19.9/13.8	2.4/7.3/6.2/12.0
Finger cot	1.9/5.3/4.1/5.9	13.1/10.4/14.8/17.7	3.2/6.2/4.2/6.5

Table C.1: 1I-2AFC data used for the two-way ANOVA table.

ANOVA Table

Source	SS	df	MS	F
Columns	416.3	2	208.2	17.92
Rows	13.37	1	13.37	1.151
Interaction	1.558	2	0.7791	0.06707
Error	209.1	18	11.62	
Total	640.3	23		

Table C.2: 1I-2AFC ANOVA table. The rows represent the conditions and the columns represent the subjects.

obtained by dividing SS by df. The F ratio was obtained by dividing the MS value for Columns, Rows, and Interaction by the MS value for Error. By looking up F-distribution table [47] with degree of freedom pairs of (2,18), (1,18), and (2,18), the 1% points of F ratios from the table were 6.01, 8.28, and 6.01. Therefore, only the first hypothesis was rejected because the F value from the ANOVA table (18.46) was larger than the F value (6.01) from the F distribution. There was significant difference between the subjects at 1% significance level (the significance is the probability of observing the given result by chance given that the hypothesis is true). However, the differences between normal and finger cot conditions and the interactions of subjects and conditions were small, as shown by the small F ratio from analysis of variance.

A box plot of the softness discrimination JND values obtained under normal and finger cot conditions of the 1I-2AFC paradigm is shown in Figure C-1. The box has lines at the lower quartile, median, and upper quartile values. The whiskers are lines extending from each end of the box to show the extent of data.

Three t tests were performed on the data given in Table C.1 between the subjects' performance under normal and finger cot conditions by using the *ttest2* function of the MATLAB software. Significant differences of the mean JNDs, at 5% significance level, were repor-

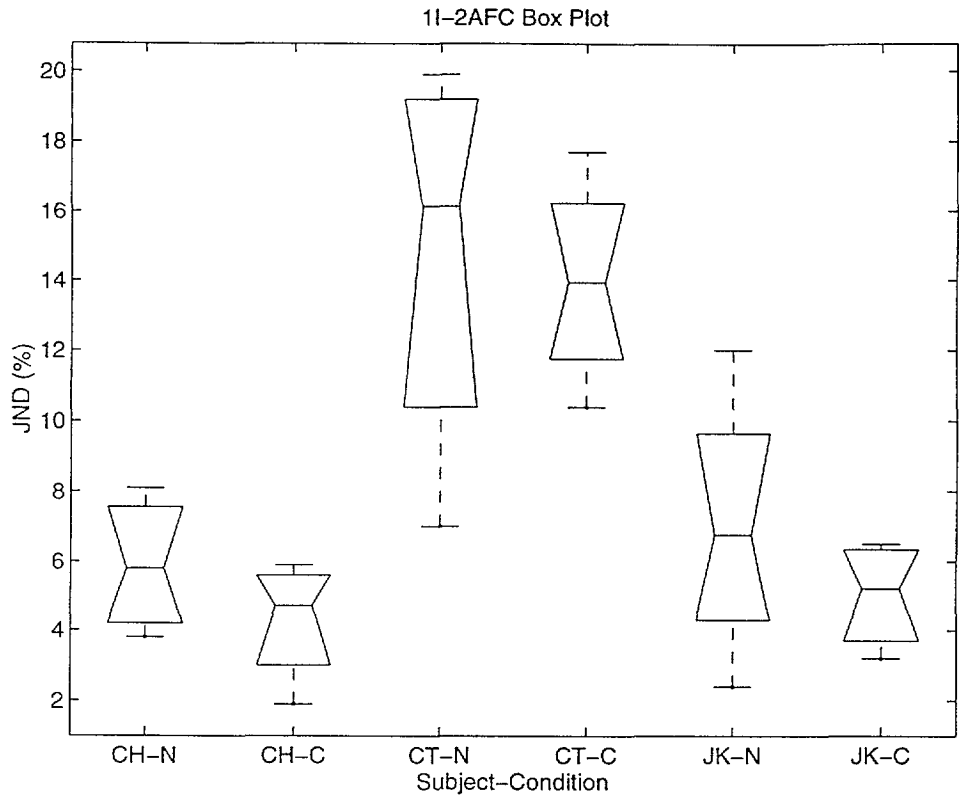

Figure C-1: A box plot of the softness discrimination JND values obtained under normal(N) and finger cot(C) conditions of the 1I-2AFC paradigm.

ted between subjects (CH,CT) under normal condition and between subjects (CH,CT) and (JK,CT) under finger cot condition.

C.2 S-2AFC experiments

The same type of analysis used on the 1I-2AFC data was performed on the data from S-2AFC experiments. A two-way ANOVA was performed by using subjects and conditions as the two factors. The thimble condition was not included because the data range is very different and it is clear that there is a significant difference between thimble and the other two conditions. Table C.3 lists the data used for the ANOVA analysis. The ANOVA table generated by using MATLAB software function *anova2* is shown in table C.4. There was significant difference between the subjects at 1% significance level (the significance is the probability of observing the given result by chance given that the hypothesis is true). However, the differences between normal and finger cot conditions and the interactions of subjects and conditions were small

Condition	Subject		
	CH	CT	JK
Normal	2.3/4.8/6.1/6.3	8.3/6.6/8.6/9.7	1.8/3.3/3.3/4.0
Finger cot	2.4/2.9/3.7/4.0	11.8/8.2/8.5/13.1	1.9/2.6/3.3/3.7

Table C.3: S-2AFC data used for the two-way ANOVA table.

ANOVA Table

Source	SS	df	MS	F
Columns	185.6	2	92.79	42.95
Rows	0.04167	1	0.04167	0.01929
Interaction	14.16	2	7.08	3.278
Error	38.88	18	2.16	
Total	238.7	23		

Table C.4: S-2AFC ANOVA table. The rows represent the conditions and the columns represent the subjects.

as shown by the small F ratio from the analysis of variance.

A box plot of the softness discrimination JND values obtained under normal and finger cot conditions of the S-2AFC paradigm is shown in Figure C-2. Three t tests were performed on the data given in Table C.3 between the subjects performance under normal and finger cot conditions by using the *ttest2* function of the MATLAB software. Significant differences of the mean JNDs, at 5% significance level, were reported between subjects (CH,CT) and (JK,CT) under both normal and finger cot conditions.

C.3 Comparison of JND among different paradigms

To compare the effect of the two experimental paradigms, data from the three subjects under both normal and finger cot conditions were used. Pooling data from all the subjects together allows us to examine the differences between the two paradigms with higher reliability.

The ANOVA table generated is shown in Table C.5. The two paradigms are represented by the rows in the table. The columns represent the six groups of data from the three subjects under both normal and finger cot conditions. The F ratio (16.21) obtained was higher than the value (7.39) from the F distribution table with degrees of freedom (1,36) at 1% significance

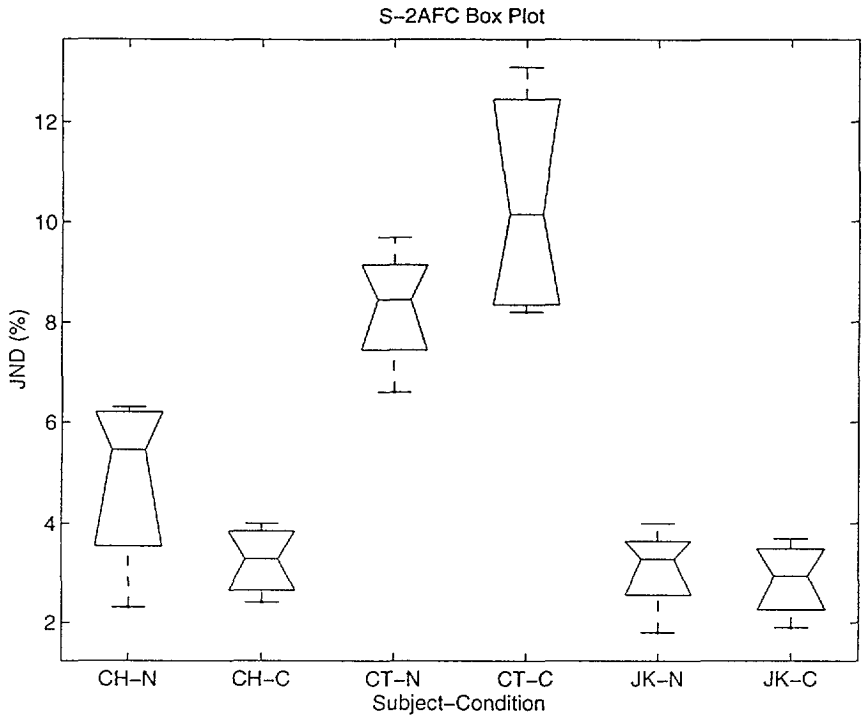

Figure C-2: A box plot of the softness discrimination JND values obtained under normal(N) and finger cot(C) conditions of the S-2AFC paradigm.

level. Therefore, we conclude the results from the 1I-2AFC experiments are significantly different from the results from S-2AFC experiments at 1% significance level.

The individual box plots that compare JNDs from the two paradigms for the three subjects are graphed in Figure C-3, Figure C-4, and Figure C-5, respectively. The results from the two different experimental paradigms are plotted side by side for both normal and finger cot conditions. From the box lines (indicating the lower quartile, median, and the upper quartile) and the whiskers (indicating the extent of the data), we can see that the variation in the JND values are lower in the S-2AFC paradigm than in the 1I-2AFC paradigm. Therefore, S-2AFC experiments is different from a hypothetical two interval, two alternative, forced choice paradigm (2I-2AFC) which would have higher variations in the JND values than the 1I-2AFC experiments.

ANOVA Table

Source	SS	df	MS	F
Columns	591.5	5	118.3	17.42
Rows	110.1	1	110.1	16.21
Interaction	43.79	5	8.758	1.29
Error	244.5	36	6.791	
Total	989.9	47		

Table C.5: ANOVA table to compare 1I-2AFC and S-2AFC paradigms. The rows represent the experimental paradigms and the six columns represent three subjects under both normal and finger cot conditions.

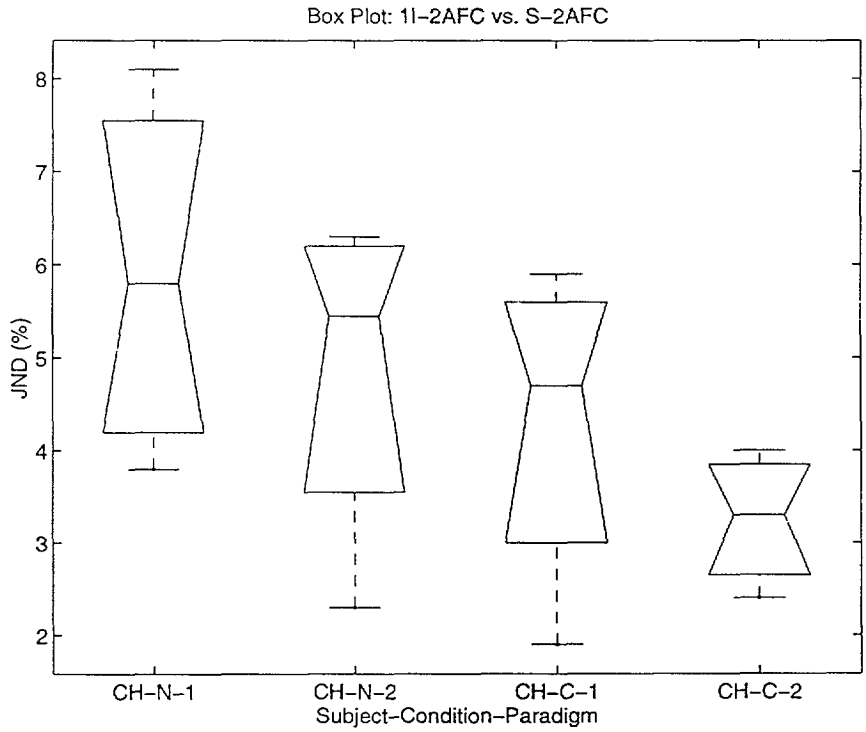

Figure C-3: Box plot of the JND values obtained under both normal(N) and finger cot(C) conditions using 1I-2AFC(1) and S-2AFC(2) paradigms for subject CH.

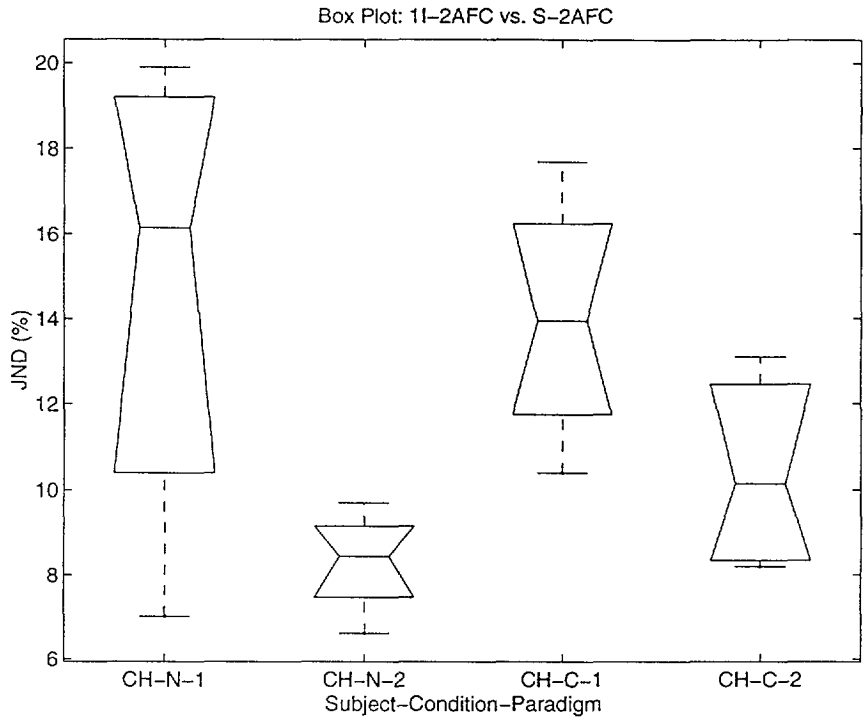

Figure C-4: Box plot of the JND values obtained under both normal(N) and finger cot(C) conditions using 1I-2AFC(1) and S-2AFC(2) paradigms for subject CT.

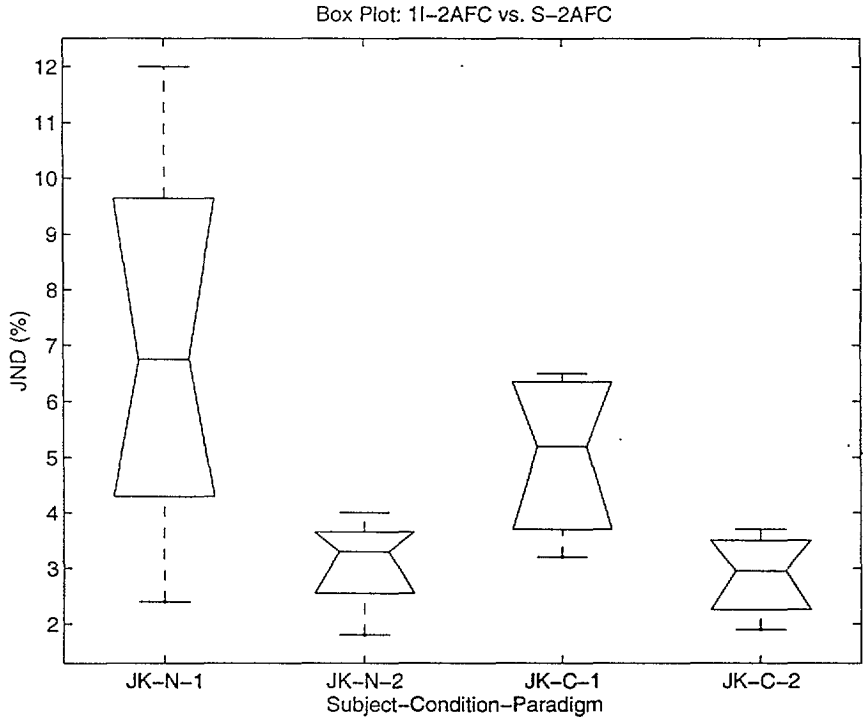

Figure C-5: Box plot of the JND values obtained under both normal(N) and finger cot(C) conditions using 1I-2AFC(1) and S-2AFC(2) paradigms for subject JK.

Appendix D

Force Control Data

Presented in this appendix are the data recorded during the force control experiments under various conditions. For each subject, three trials of force data under the same conditions are plotted on three separate pages. There are four rows to each graph which represent the specimens used. Going from top to bottom are rigid, hard, medium, and soft specimens. The Plexiglas was used as the rigid specimen and the three compliant specimens chosen had objective compliances of 0.304mm/N (hard), 0.455mm/N (medium), and 0.608mm/N (soft). The three columns represent the data from normal, finger cot, and thimble conditions. The subject, hand, and trial number are printed on the upper-left corner of the force versus time graphs.

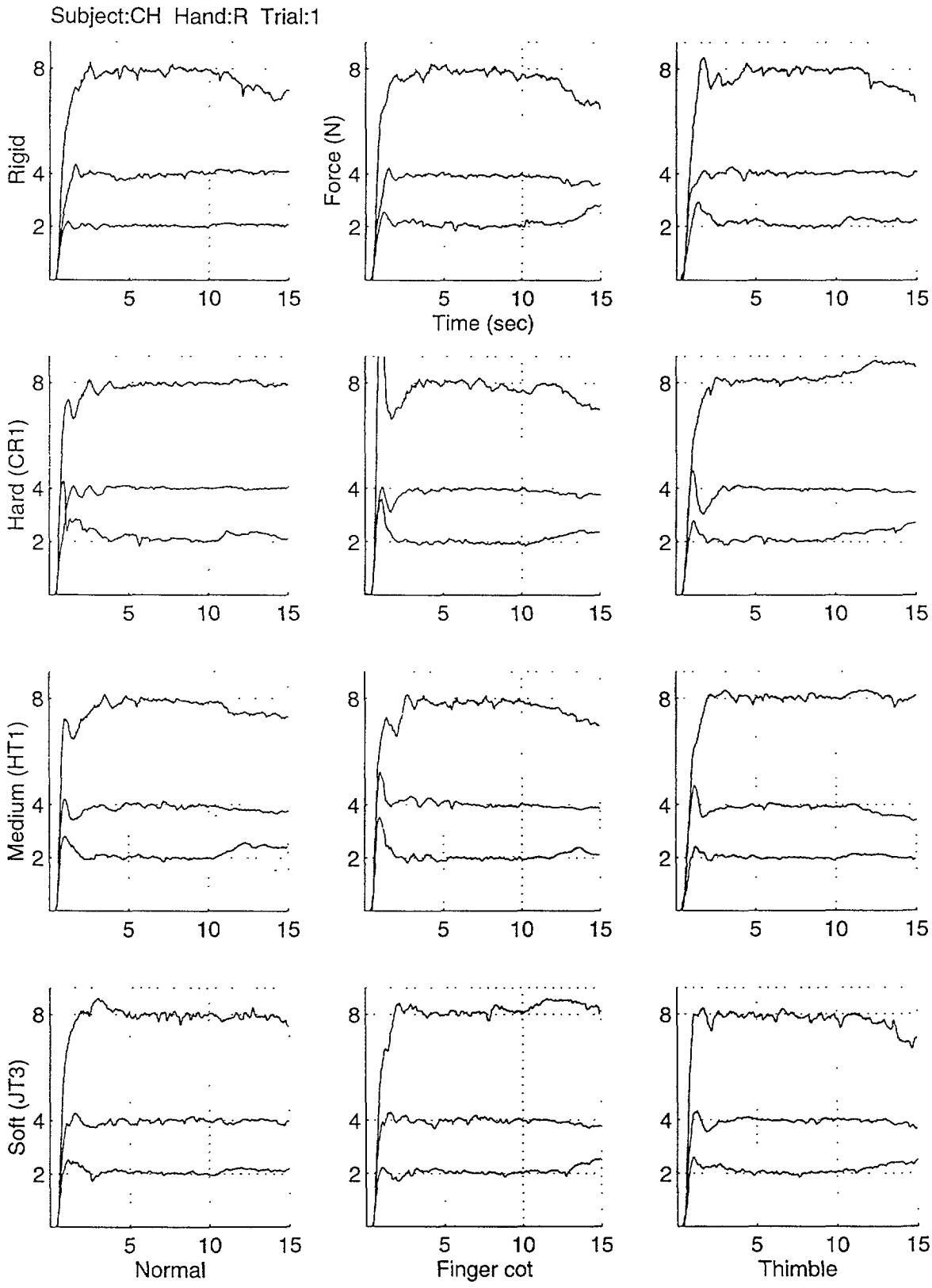
Subject:CH Hand:R Trial:1
Rigid
Hard (CR1)
Medium (HT1)
Soft (JT3)
Force (N)
Time (sec)
Normal
Finger cot
Thimble
2
4
8
5
10
15

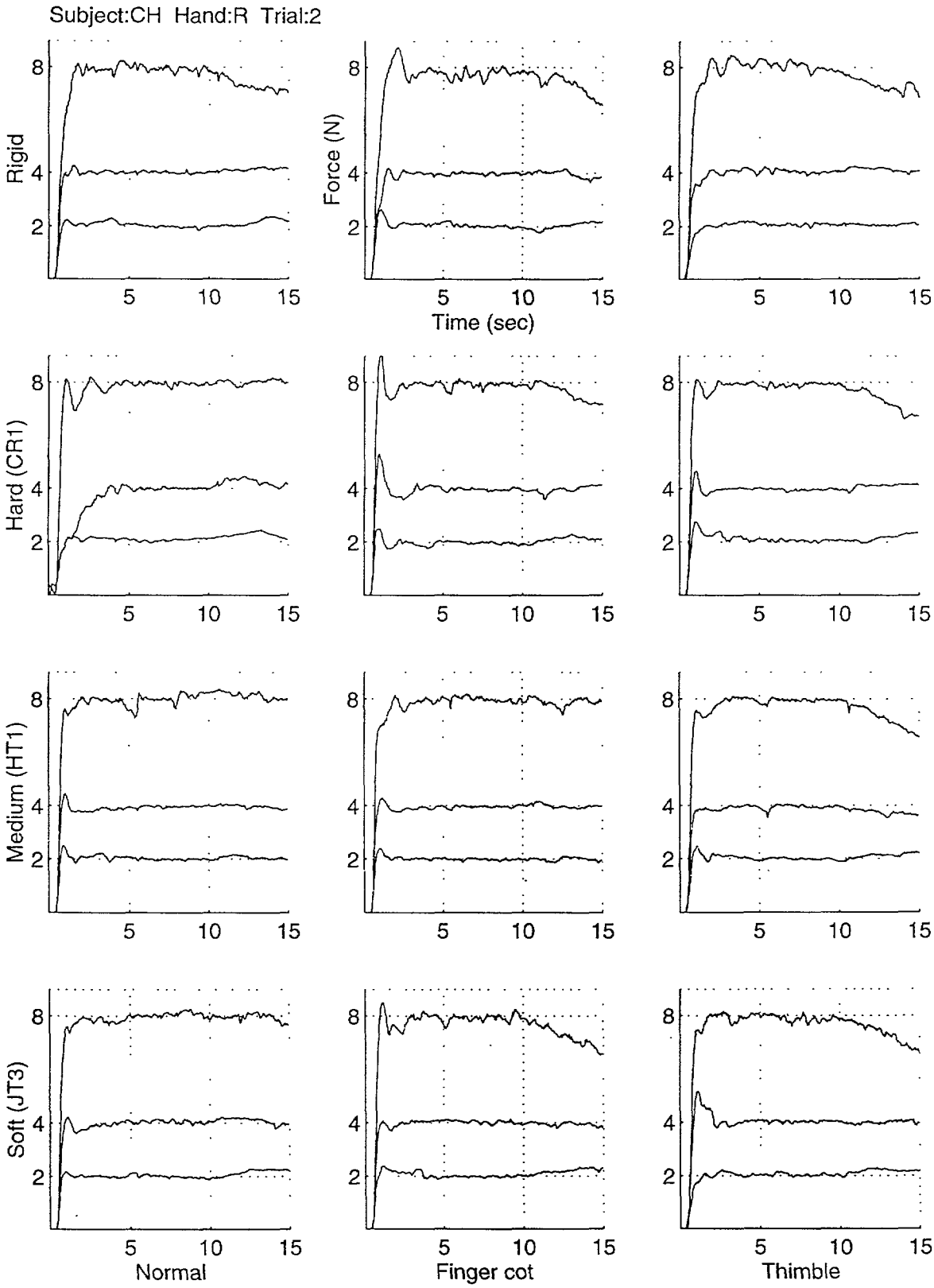
Subject:CH Hand:R Trial:2
Rigid
Force (N)
Hard (CR1)
Medium (HT1)
Soft (JT3)
Time (sec)
Normal
Finger cot
Thimble

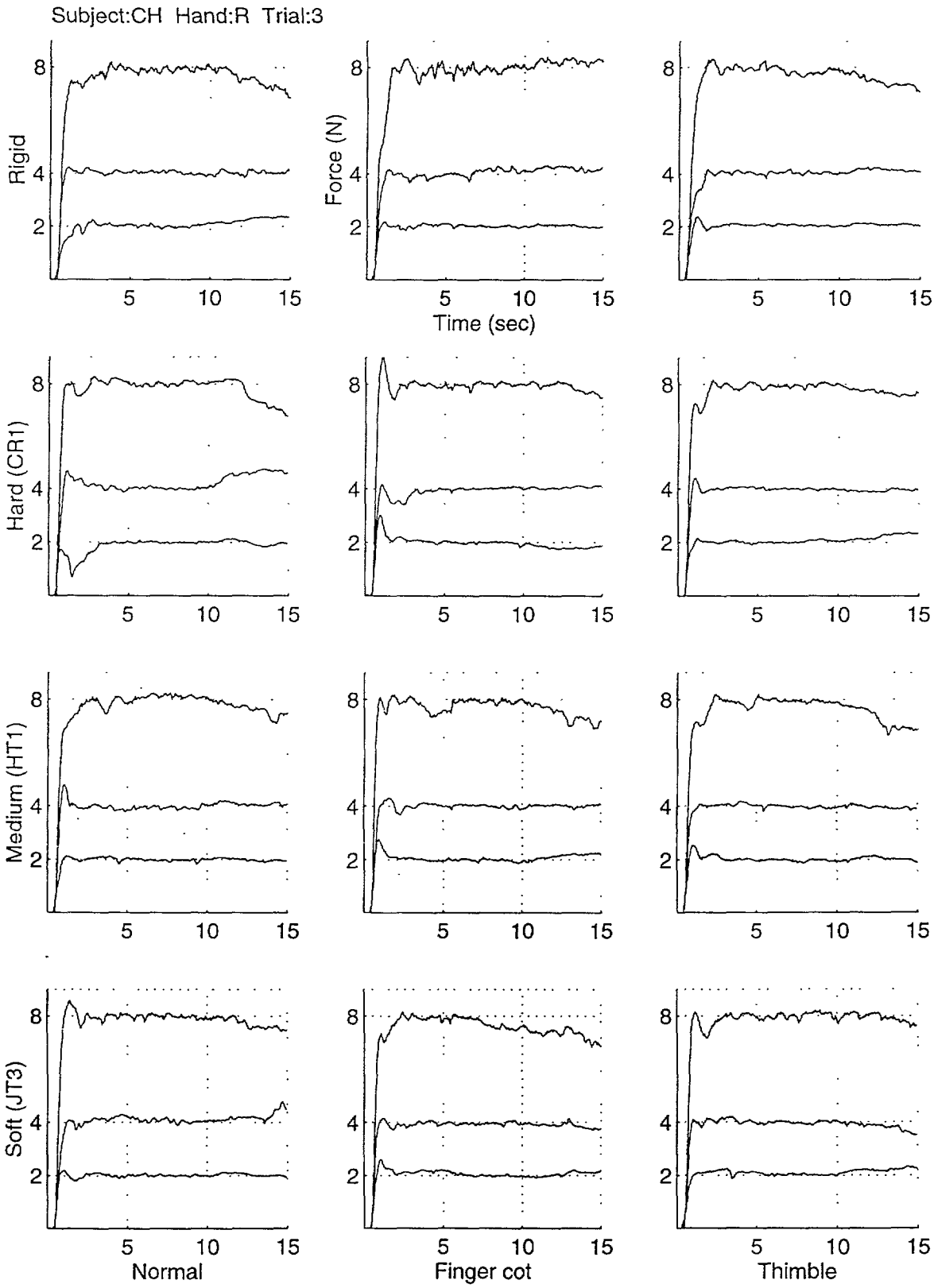
Subject:CH Hand:R Trial:3
Rigid
Force (N)
Hard (CR1)
Medium (HT1)
Soft (JT3)
Time (sec)
Normal
Finger cot
Thimble

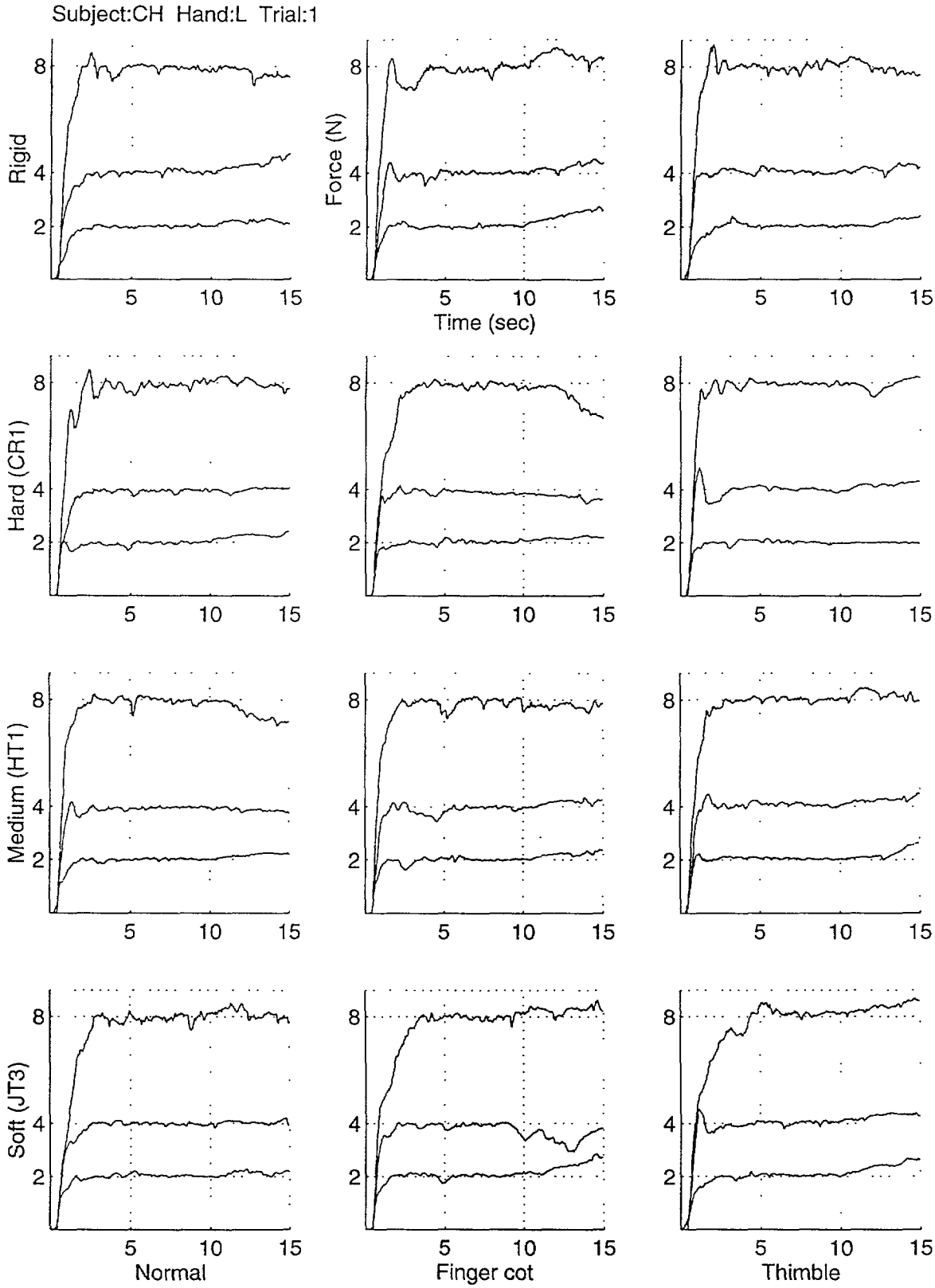
Subject:CH Hand:L Trial:1
Rigid
Hard (CR1)
Medium (HT1)
Soft (JT3)
Force (N)
Time (sec)
Normal
Finger cot
Thimble
2
4
8
5
10
15

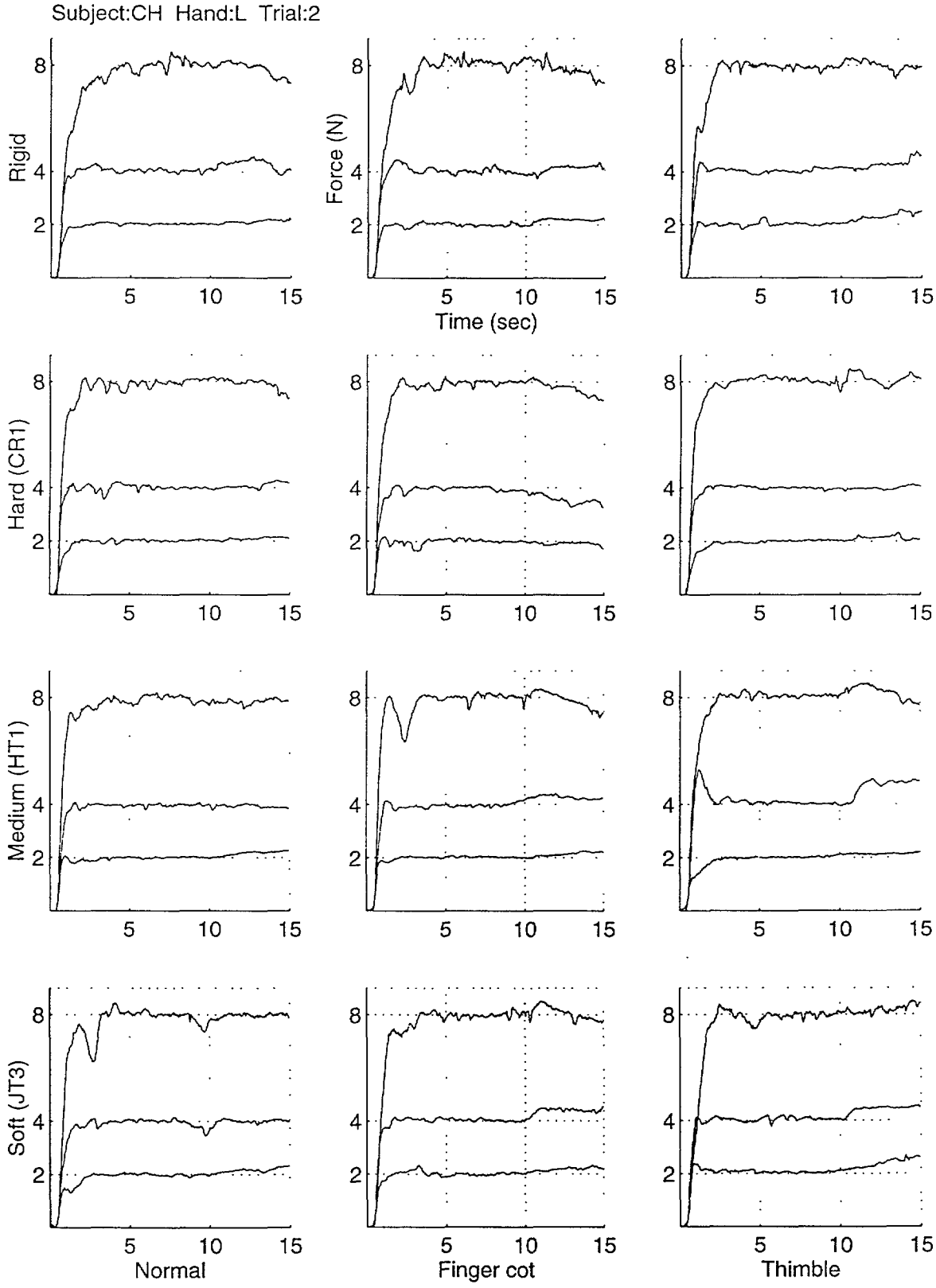
Subject:CH Hand:L Trial:2
Force (N)
Time (sec)
Rigid
Hard (CR1)
Medium (HT1)
Soft (JT3)
Normal
Finger cot
Thimble

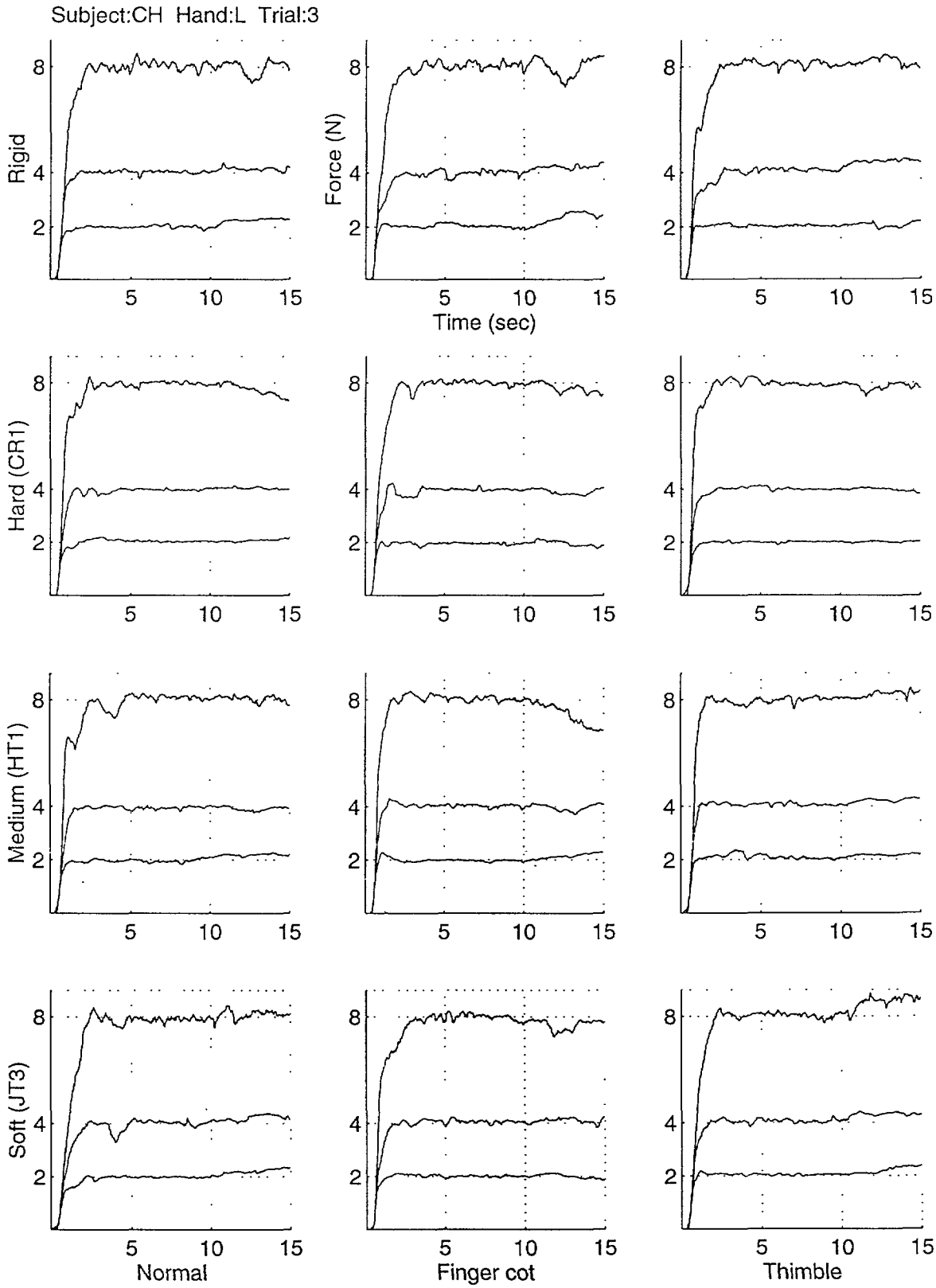
Subject:CH Hand:L Trial:3
Rigid
Hard (CR1)
Medium (HT1)
Soft (JT3)
Force (N)
Time (sec)
Normal
Finger cot
Thimble
2
4
8
5
10
15

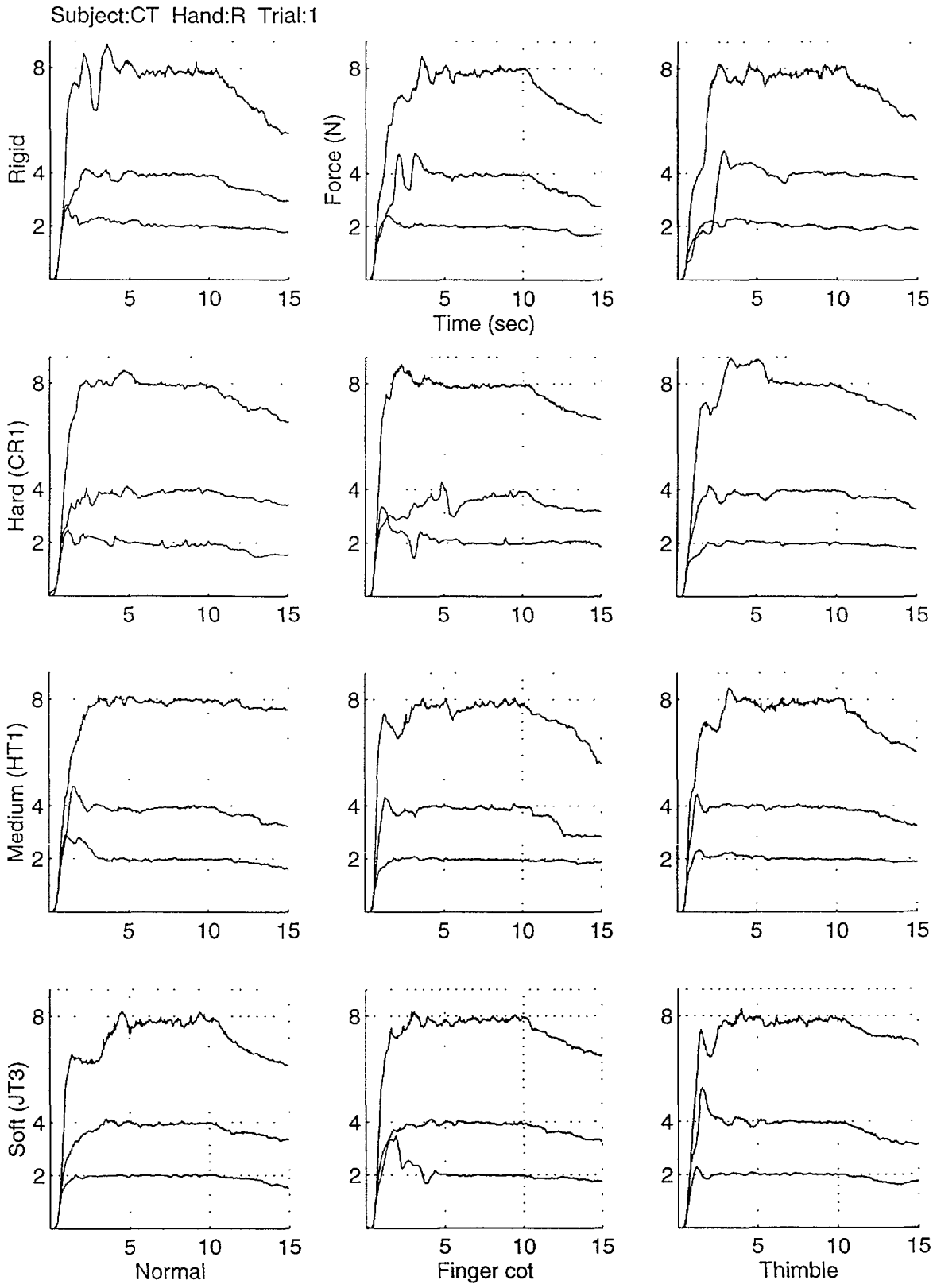
Subject:CT Hand:R Trial:1
Rigid
Force (N)
Hard (CR1)
Medium (HT1)
Soft (JT3)
Time (sec)
Normal
Finger cot
Thimble

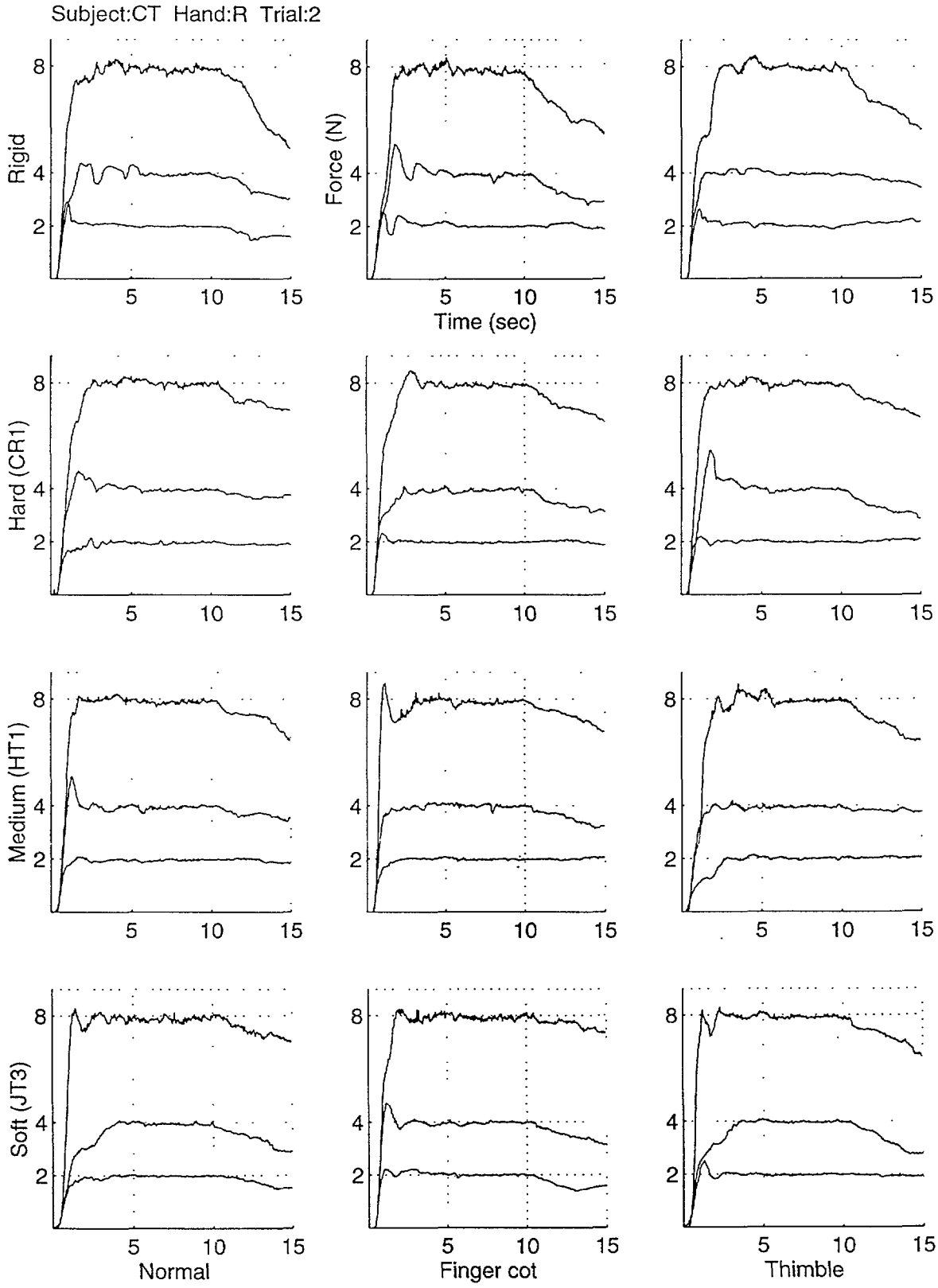
Subject:CT Hand:R Trial:2
Rigid
Hard (CR1)
Medium (HT1)
Soft (JT3)
Force (N)
Time (sec)
Normal
Finger cot
Thimble
2
4
8
5
10
15

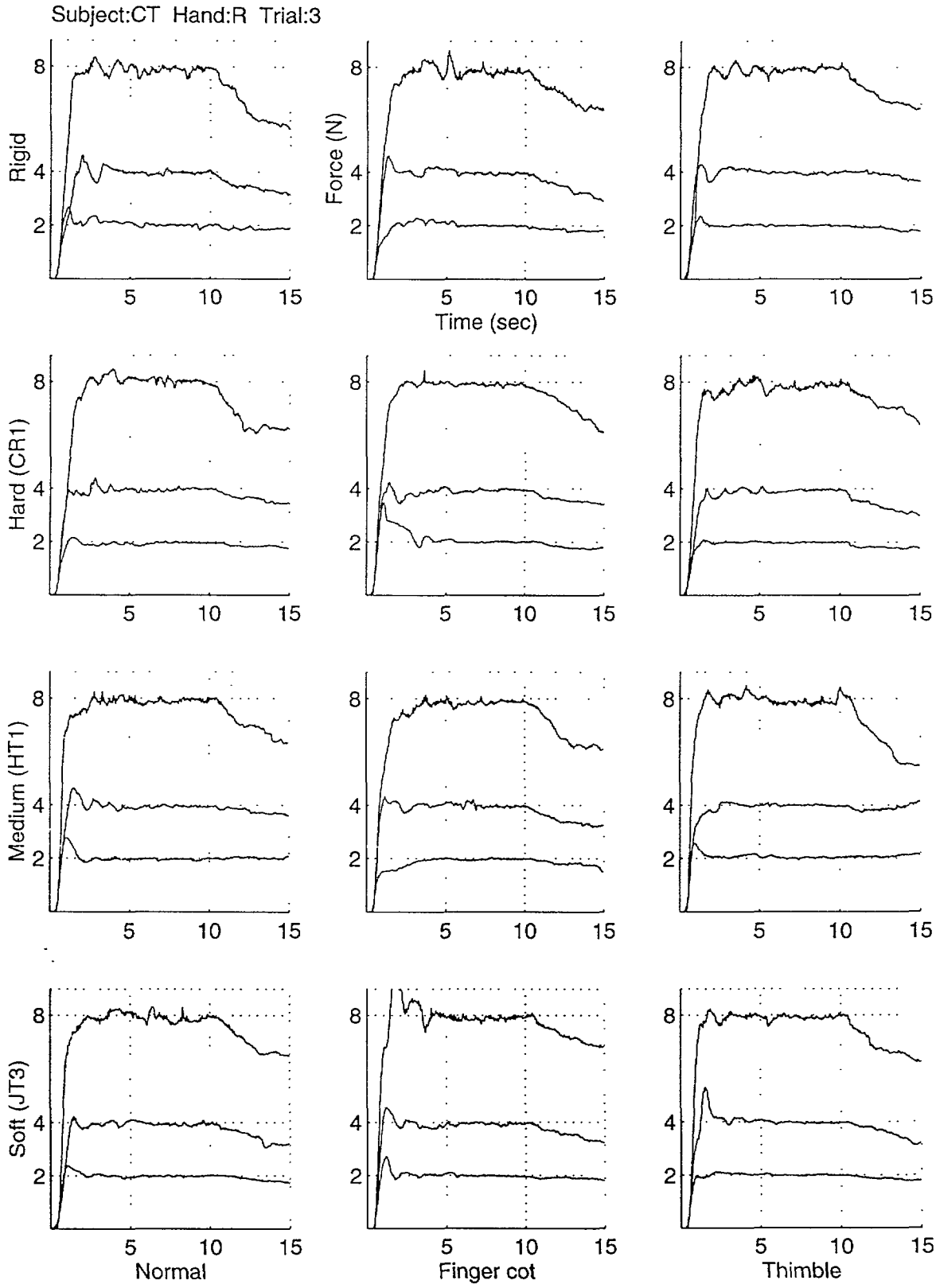
Subject:CT Hand:R Trial:3
Rigid
Force (N)
Hard (CR1)
Medium (HT1)
Soft (JT3)
Time (sec)
Normal
Finger cot
Thimble

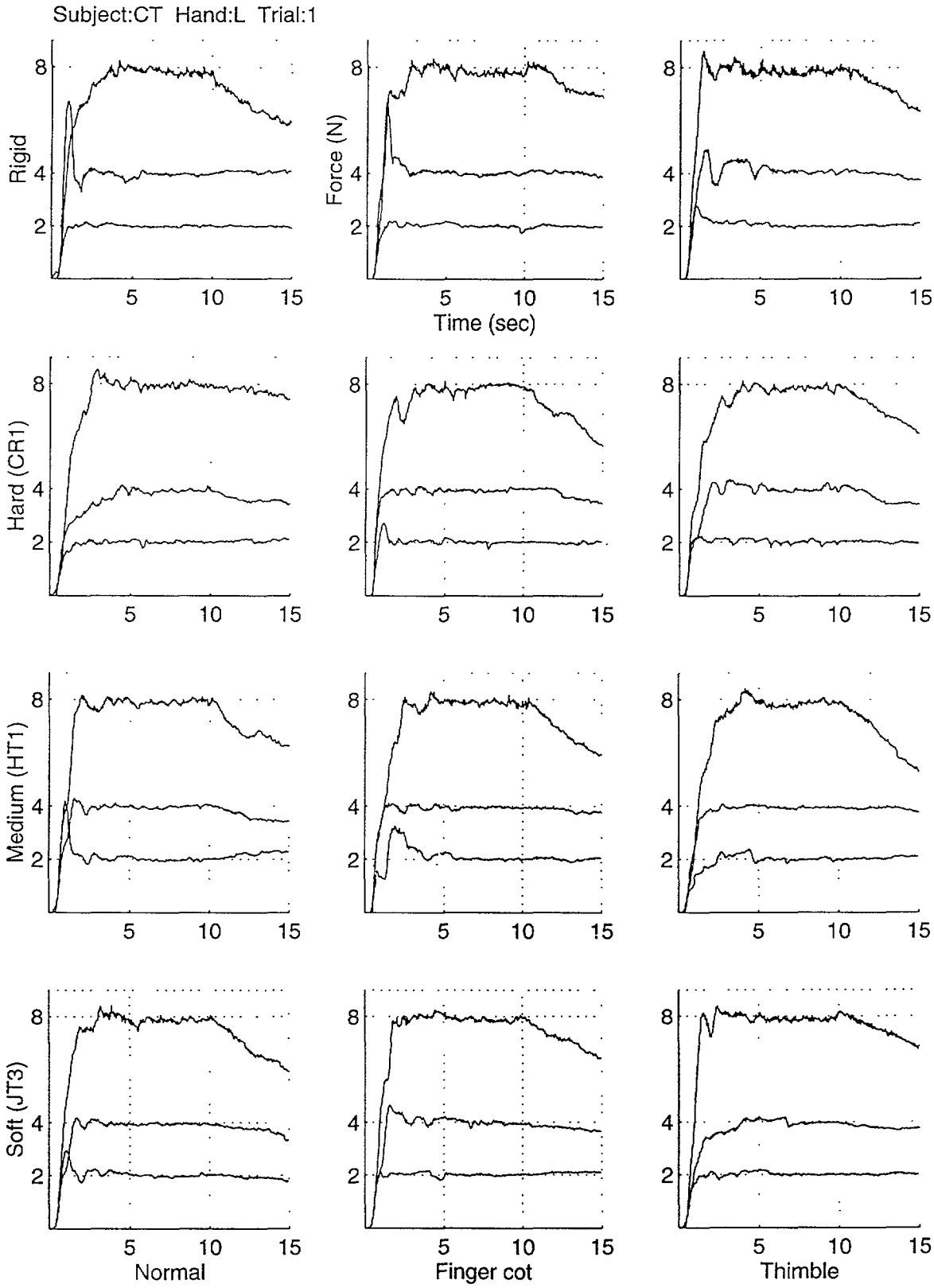
Subject:CT Hand:L Trial:1
Rigid
Force (N)
Hard (CR1)
Medium (HT1)
Soft (JT3)
Time (sec)
Normal
Finger cot
Thimble

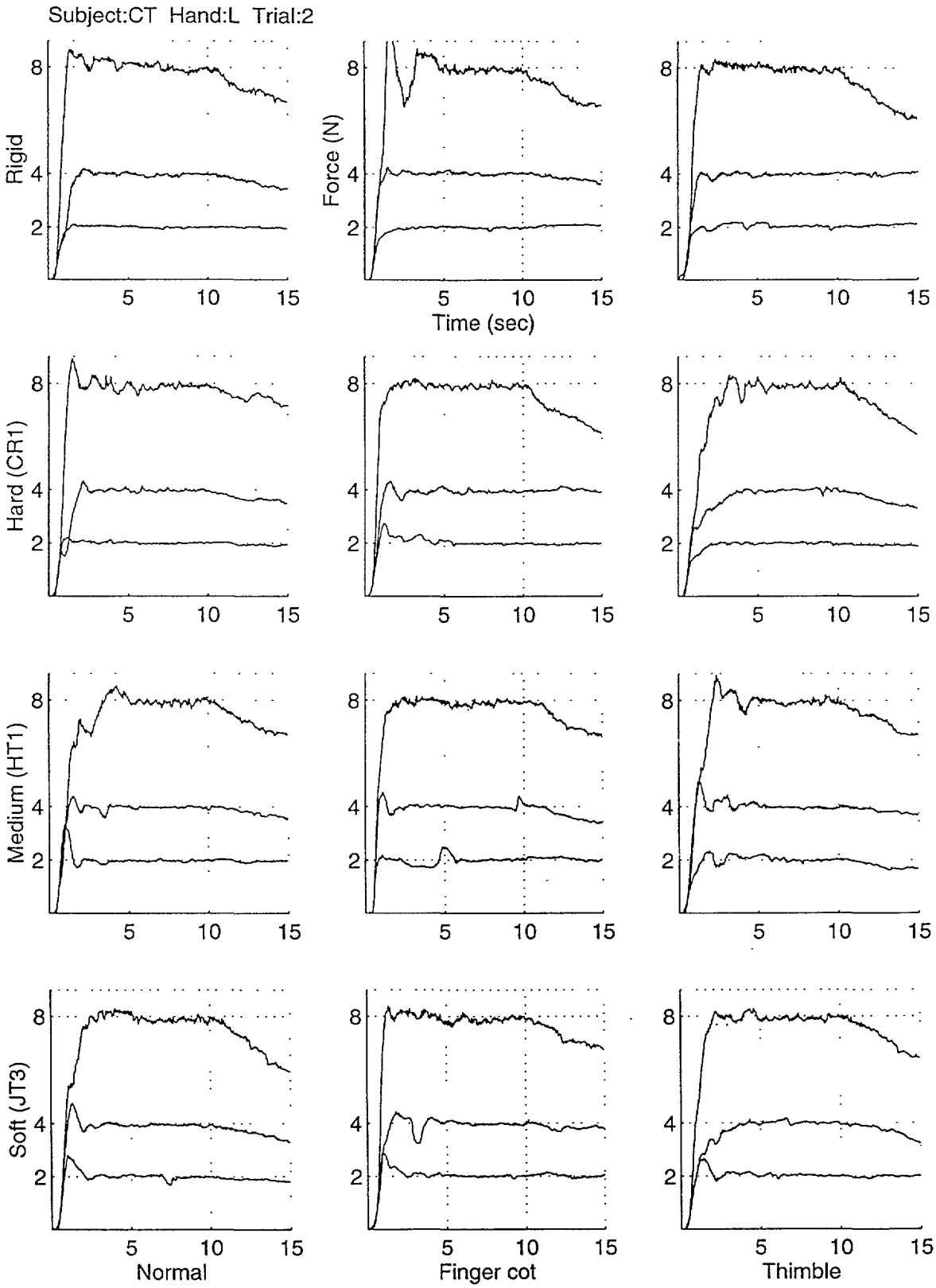
Subject:CT Hand:L Trial:2
Rigid
Hard (CR1)
Medium (HT1)
Soft (JT3)
Force (N)
Time (sec)
Normal
Finger cot
Thimble
2
4
8
5
10
15

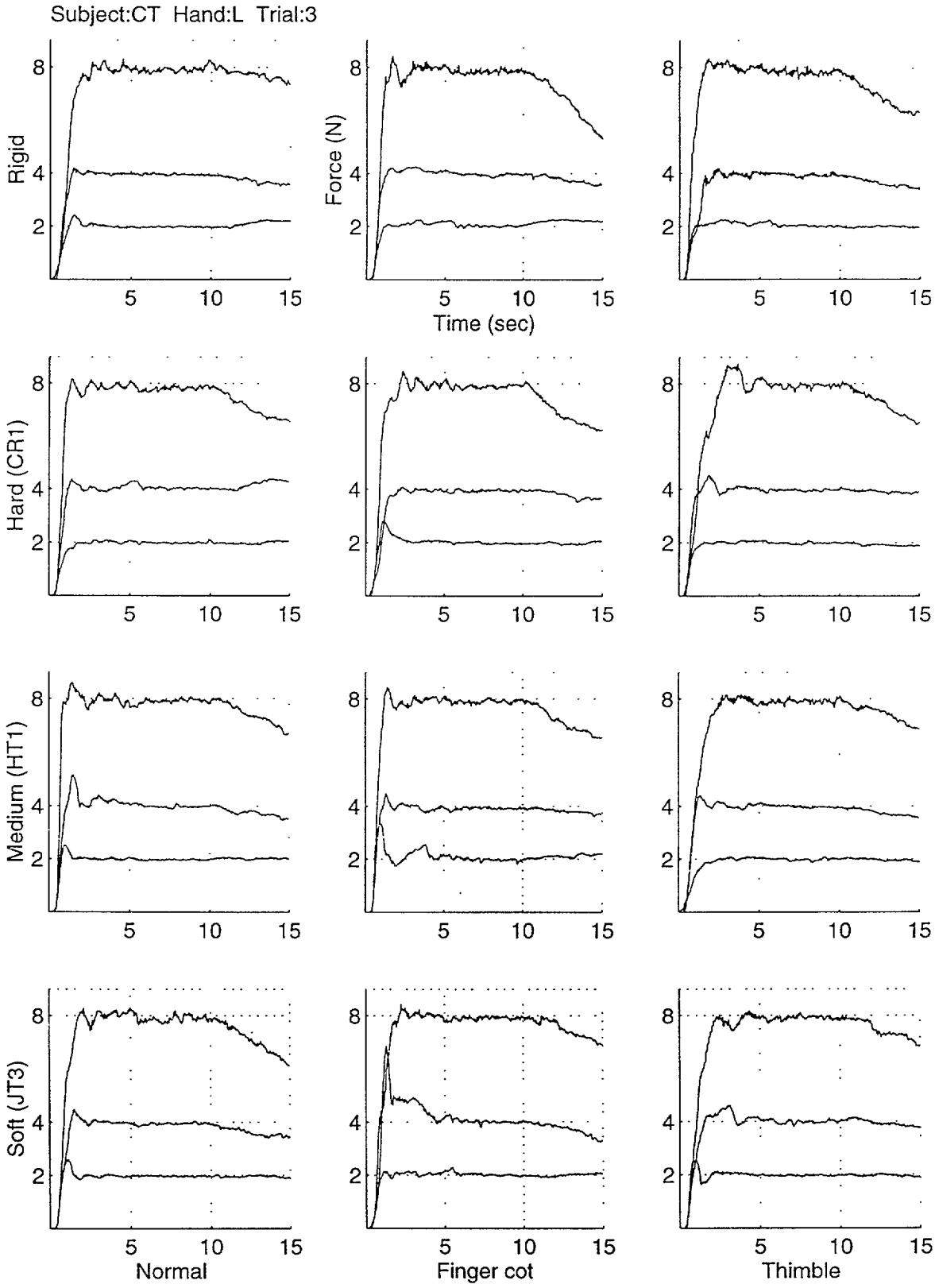
Subject:CT Hand:L Trial:3
Rigid
Hard (CR1)
Medium (HT1)
Soft (JT3)
Force (N)
Time (sec)
Normal
Finger cot
Thimble
2
4
8
5
10
15

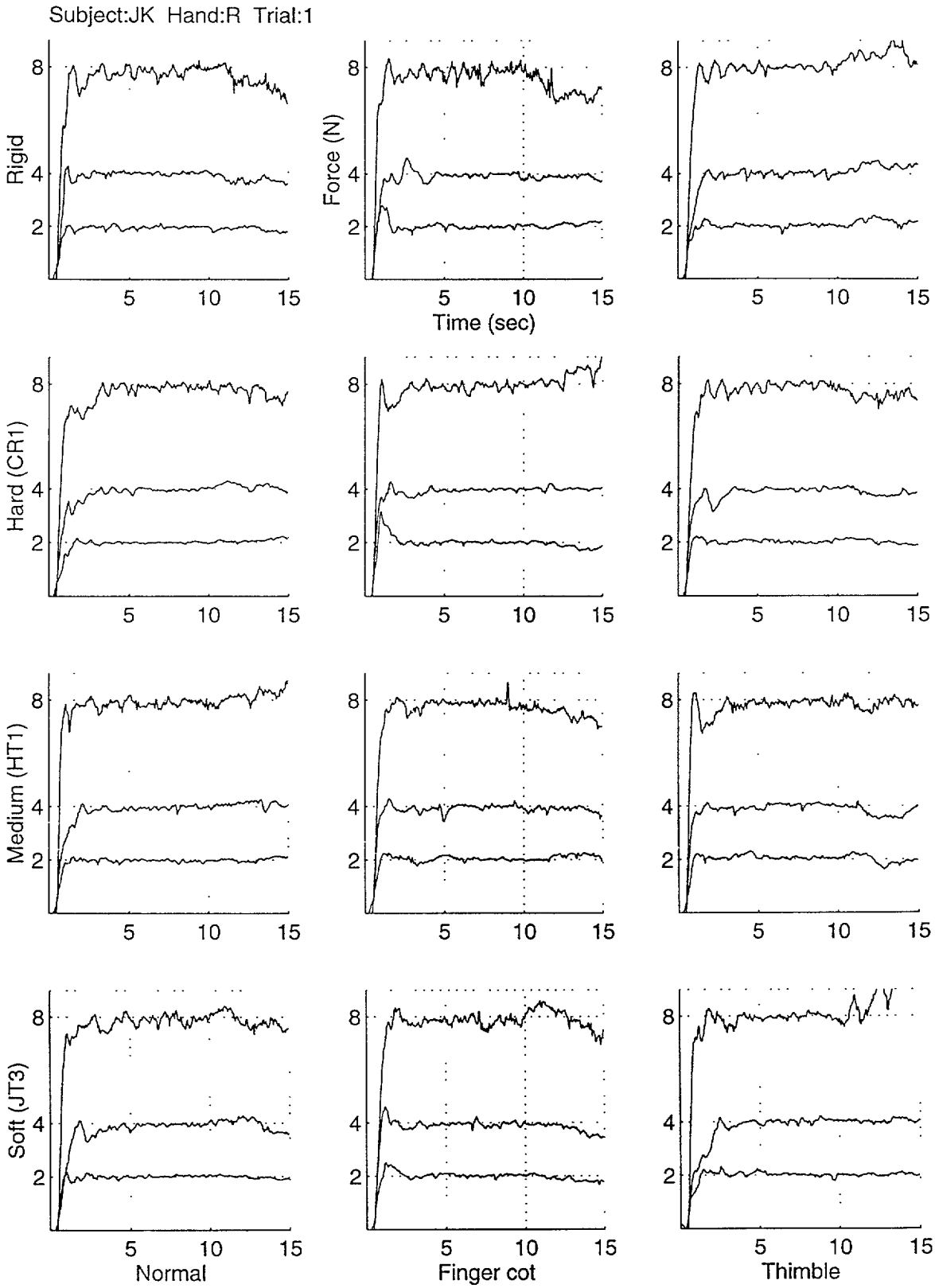
Subject:JK Hand:R Trial:1
Rigid
Force (N)
Hard (CR1)
Medium (HT1)
Soft (JT3)
Time (sec)
Normal
Finger cot
Thimble
2
4
8
5
10
15

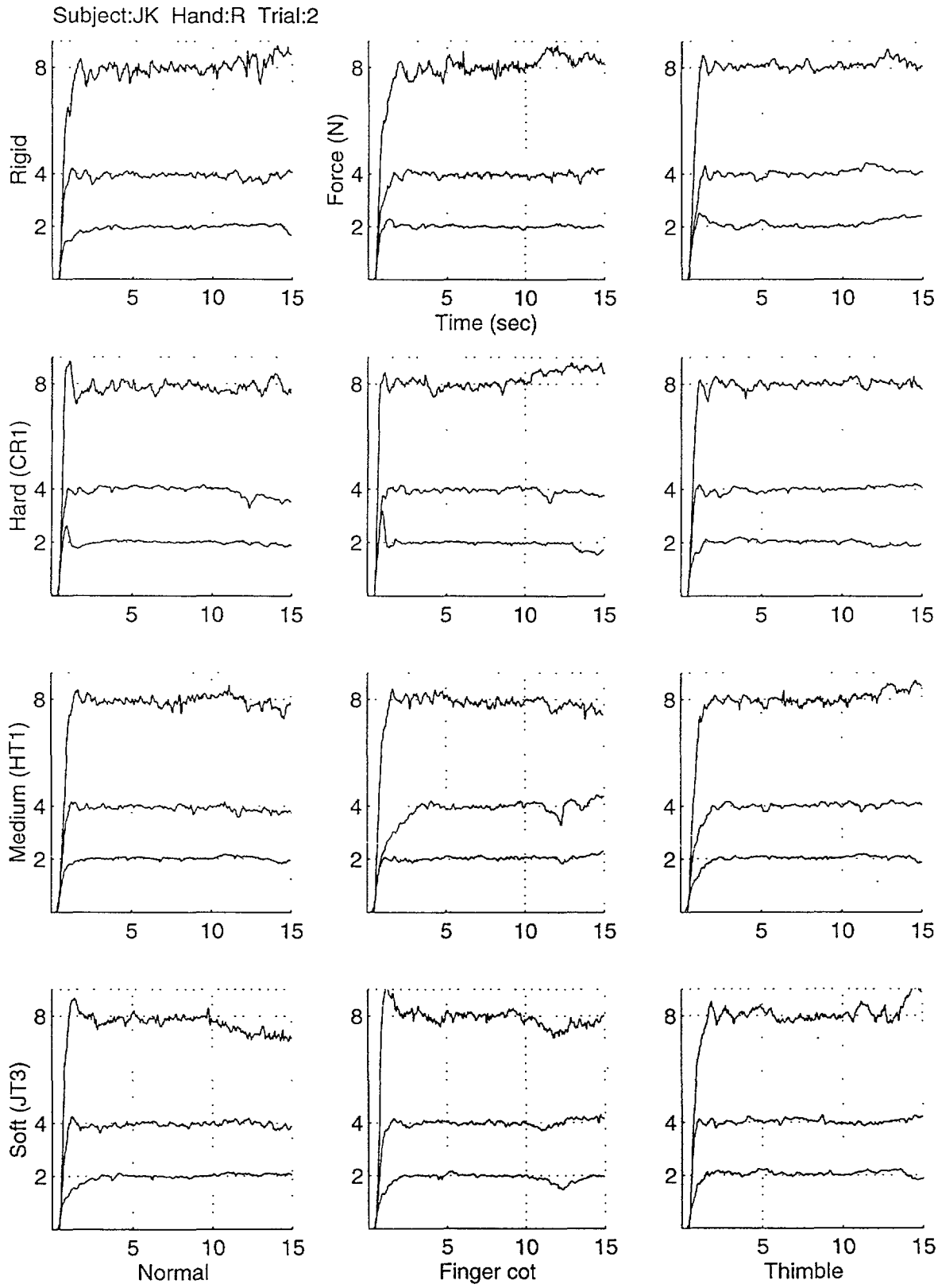
Subject:JK Hand:R Trial:2
Rigid
Hard (CR1)
Medium (HT1)
Soft (JT3)
Force (N)
Time (sec)
Normal
Finger cot
Thimble
2
4
8
5
10
15

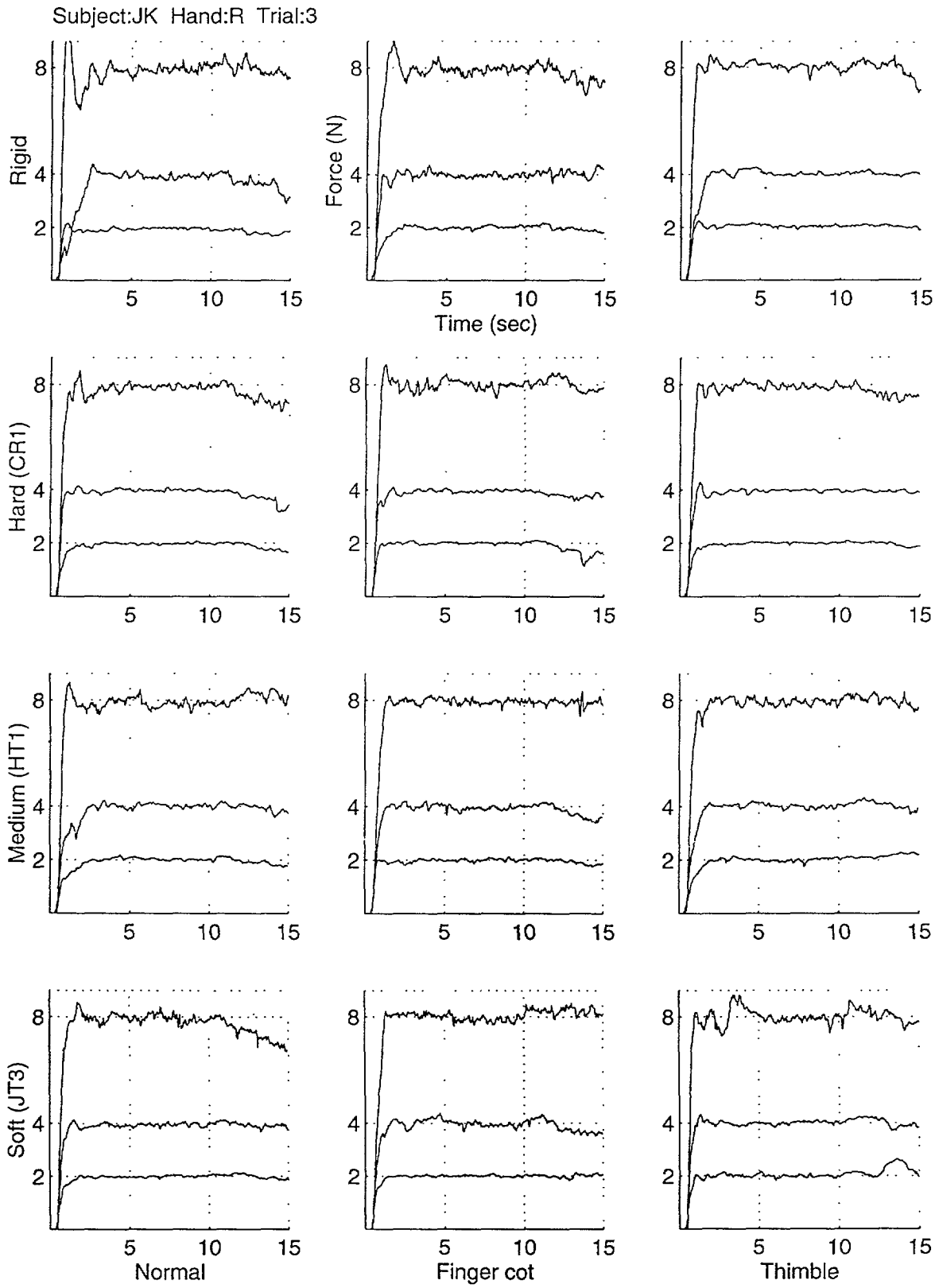
Subject:JK Hand:R Trial:3
Rigid
Force (N)
Hard (CR1)
Medium (HT1)
Soft (JT3)
Time (sec)
Normal
Finger cot
Thimble
2
4
8
5
10
15

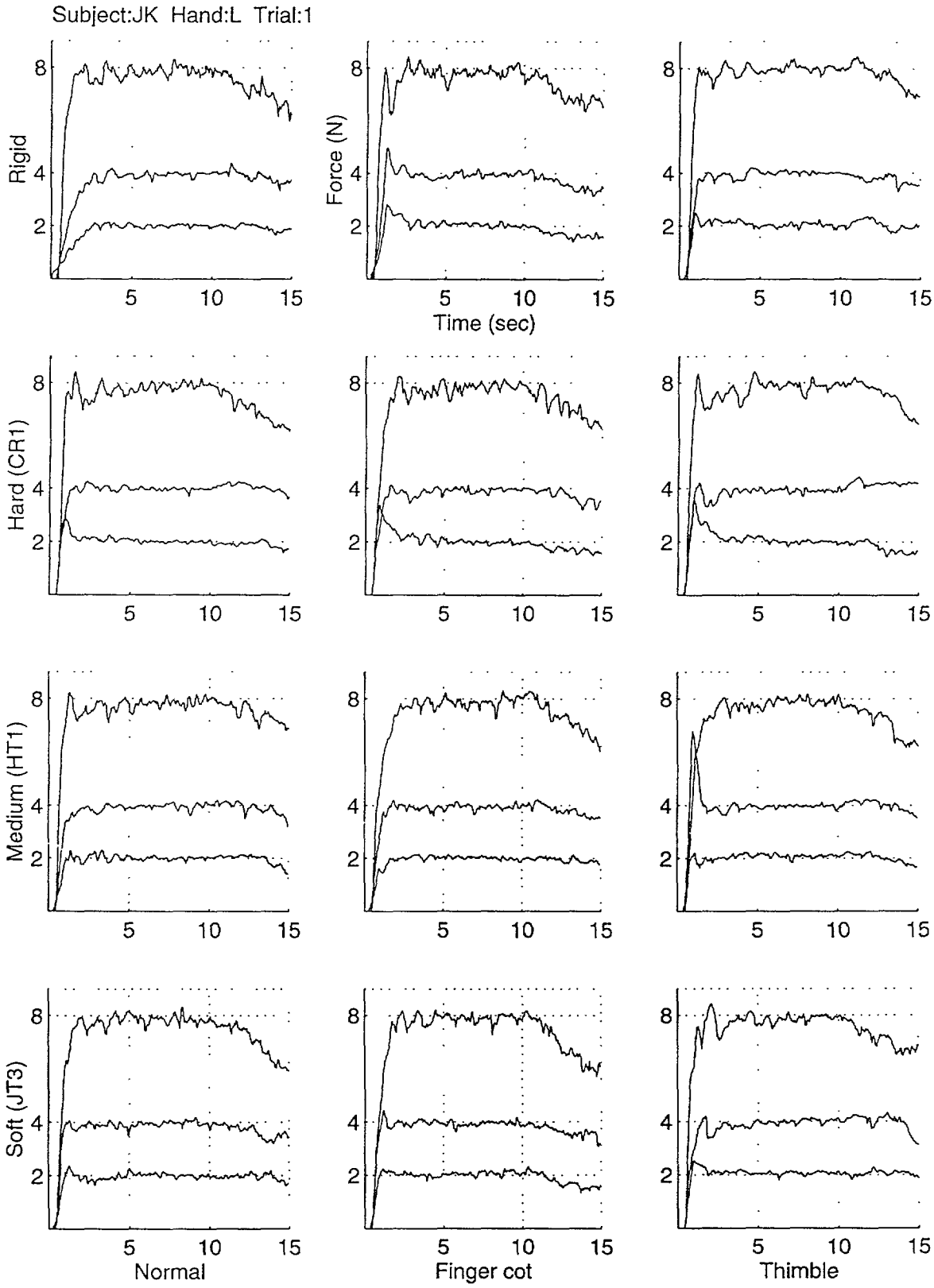
Subject:JK Hand:L Trial:1
Rigid
Force (N)
Hard (CR1)
Medium (HT1)
Soft (JT3)
Time (sec)
Normal
Finger cot
Thimble
2
4
8
5
10
15

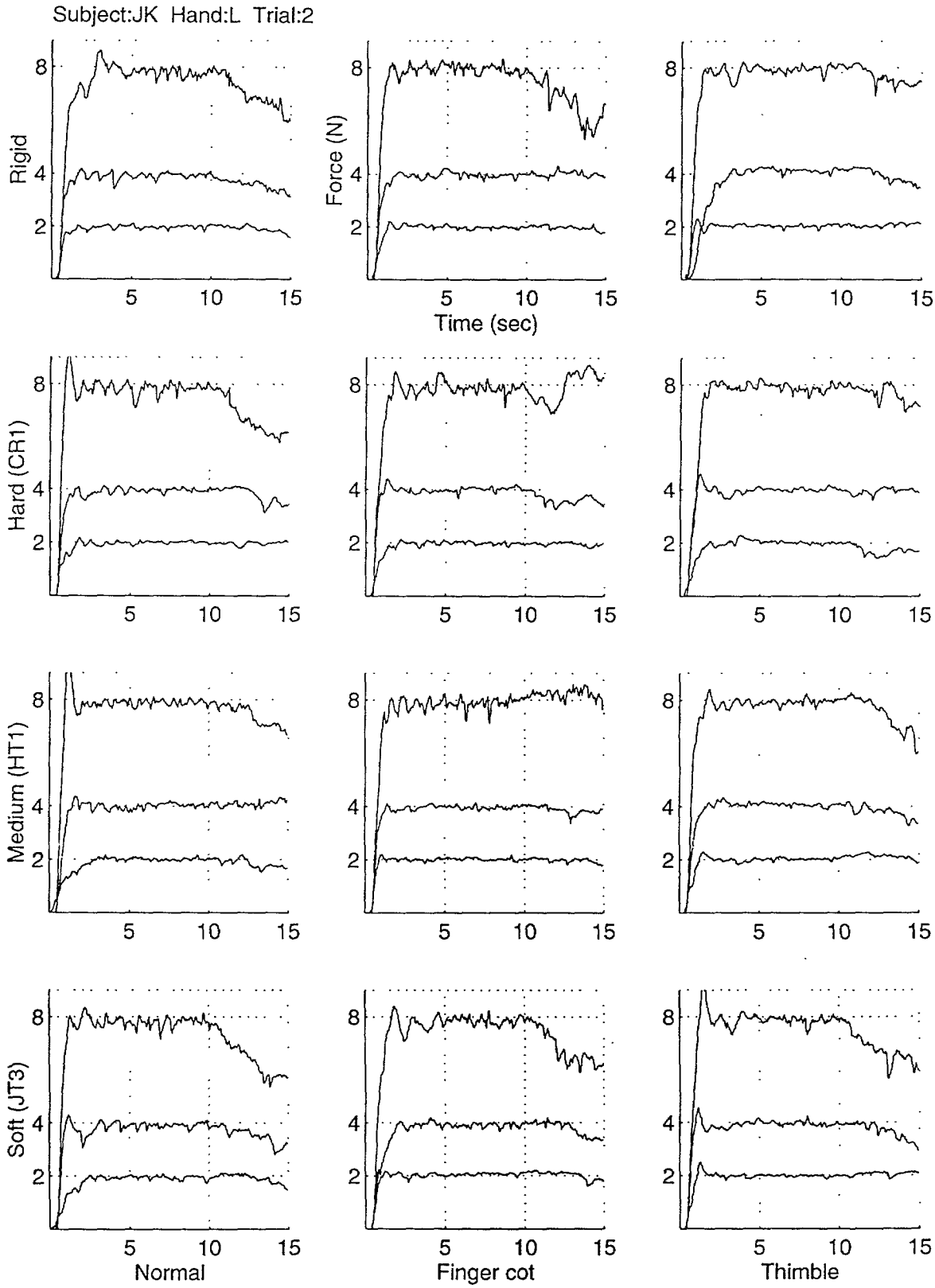
Subject:JK Hand:L Trial:2
Rigid
Hard (CR1)
Medium (HT1)
Soft (JT3)
Force (N)
Time (sec)
Normal
Finger cot
Thimble
2
4
8
5
10
15

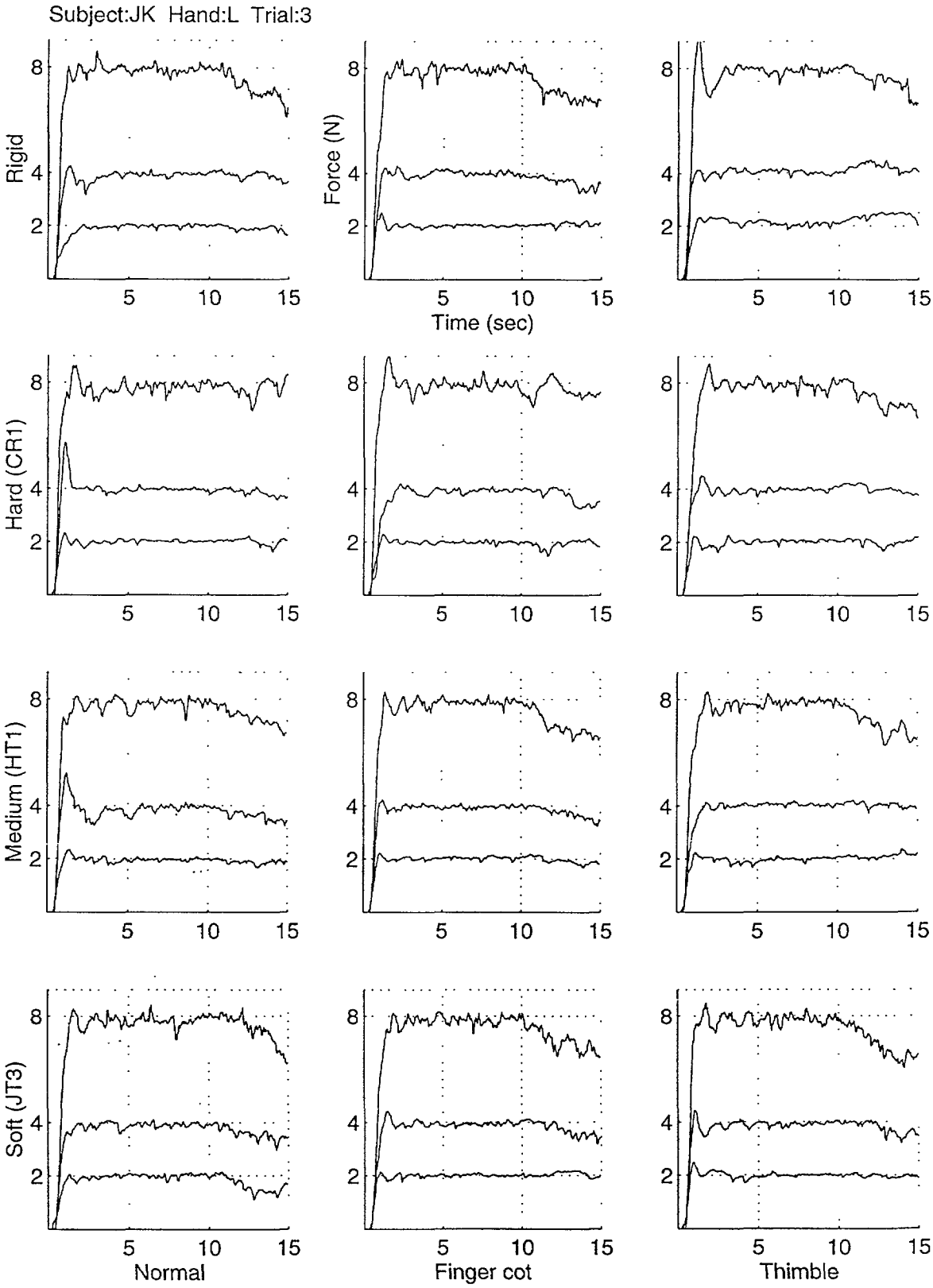
Subject:JK Hand:L Trial:3
Rigid
Force (N)
Hard (CR1)
Medium (HT1)
Soft (JT3)
Time (sec)
Normal
Finger cot
Thimble

Appendix E

Force Control Performance Measures

The force data digitized at 200 samples per second were filtered with a low-pass filter which had a cut-off frequency of 50Hz for noise removal before the force error was calculated. Also, only the data from the second and third stage of each run were analyzed. During the second stage, the subject had visual force feedback; during the third stage, the visual feedback was turned off. The mean absolute error and the pooled standard deviation were tabulated. The mean absolute error was obtained from 3 experimental runs of 1000 data points during each stage. The standard deviation (s) was obtained by pooling the standard deviations from the three experimental runs (s_1, s_2, and s_3) according to the following formula: $s = \sqrt{({s_1}^2 + {s_2}^2 + {s_3}^2)/3}$.

Condition	Force	Absolute Error (N)							
		Rigid		Hard		Medium		Soft	
		Mean	S.D.	Mean	S.D.	Mean	S.D.	Mean	S.D.
Normal	2N	0.035	0.028	0.063	0.046	0.030	0.028	0.036	0.031
Normal	4N	0.054	0.040	0.030	0.023	0.056	0.043	0.067	0.051
Normal	8N	0.093	0.077	0.061	0.047	0.128	0.106	0.073	0.064
Finger cot	2N	0.051	0.046	0.037	0.031	0.032	0.028	0.035	0.035
Finger cot	4N	0.070	0.054	0.035	0.027	0.049	0.037	0.057	0.037
Finger cot	8N	0.165	0.122	0.100	0.089	0.108	0.093	0.160	0.129
Thimble	2N	0.057	0.045	0.057	0.042	0.030	0.024	0.041	0.034
Thimble	4N	0.048	0.041	0.032	0.026	0.060	0.052	0.042	0.030
Thimble	8N	0.128	0.087	0.098	0.059	0.066	0.053	0.110	0.077

Table E.1: Absolute error in force control for subject CH using right hand index finger with visual feedback.

Condition	Force	Absolute Error (N)							
		Rigid		Hard		Medium		Soft	
		Mean	S.D.	Mean	S.D.	Mean	S.D.	Mean	S.D.
Normal	2N	0.162	0.094	0.191	0.090	0.150	0.101	0.123	0.069
Normal	4N	0.093	0.050	0.261	0.133	0.107	0.059	0.135	0.109
Normal	8N	0.586	0.301	0.210	0.218	0.331	0.182	0.164	0.132
Finger cot	2N	0.148	0.144	0.182	0.096	0.111	0.083	0.157	0.119
Finger cot	4N	0.171	0.098	0.107	0.067	0.062	0.038	0.098	0.072
Finger cot	8N	0.519	0.341	0.314	0.267	0.400	0.247	0.594	0.265
Thimble	2N	0.121	0.053	0.266	0.120	0.082	0.051	0.214	0.091
Thimble	4N	0.105	0.054	0.090	0.041	0.195	0.121	0.104	0.095
Thimble	8N	0.533	0.274	0.520	0.264	0.506	0.336	0.415	0.321

Table E.2: Absolute error in force control for subject CH using right hand index finger without visual feedback.

Condition	Force	Absolute Error (N)							
		Rigid		Hard		Medium		Soft	
		Mean	S.D.	Mean	S.D.	Mean	S.D.	Mean	S.D.
Normal	2N	0.037	0.026	0.033	0.026	0.035	0.025	0.038	0.031
Normal	4N	0.054	0.045	0.048	0.044	0.047	0.039	0.069	0.077
Normal	8N	0.125	0.104	0.086	0.079	0.106	0.083	0.107	0.117
Finger cot	2N	0.048	0.039	0.043	0.039	0.033	0.030	0.041	0.033
Finger cot	4N	0.062	0.058	0.065	0.040	0.056	0.043	0.071	0.075
Finger cot	8N	0.136	0.095	0.069	0.058	0.100	0.113	0.081	0.069
Thimble	2N	0.040	0.041	0.029	0.025	0.041	0.034	0.048	0.027
Thimble	4N	0.074	0.052	0.037	0.035	0.065	0.044	0.071	0.047
Thimble	8N	0.110	0.080	0.076	0.057	0.068	0.052	0.108	0.090

Table E.3: Absolute error in force control for subject CH using left hand index finger with visual feedback.

Condition	Force	Absolute Error (N)							
		Rigid		Hard		Medium		Soft	
		Mean	S.D.	Mean	S.D.	Mean	S.D.	Mean	S.D.
Normal	2N	0.188	0.076	0.138	0.056	0.175	0.068	0.168	0.083
Normal	4N	0.252	0.144	0.069	0.060	0.091	0.056	0.111	0.073
Normal	8N	0.218	0.174	0.178	0.155	0.237	0.193	0.129	0.101
Finger cot	2N	0.324	0.160	0.113	0.052	0.154	0.086	0.210	0.135
Finger cot	4N	0.204	0.102	0.263	0.119	0.176	0.074	0.345	0.162
Finger cot	8N	0.314	0.172	0.329	0.286	0.335	0.262	0.256	0.150
Thimble	2N	0.182	0.117	0.051	0.044	0.167	0.113	0.316	0.158
Thimble	4N	0.280	0.124	0.092	0.057	0.375	0.193	0.326	0.103
Thimble	8N	0.180	0.121	0.168	0.132	0.227	0.130	0.351	0.171

Table E.4: Absolute error in force control for subject CH using left hand index finger without visual feedback.

Condition	Force	Absolute Error (N)							
		Rigid		Hard		Medium		Soft	
		Mean	S.D.	Mean	S.D.	Mean	S.D.	Mean	S.D.
Normal	2N	0.034	0.043	0.066	0.043	0.043	0.028	0.021	0.016
Normal	4N	0.066	0.048	0.080	0.060	0.079	0.058	0.063	0.037
Normal	8N	0.147	0.102	0.078	0.063	0.098	0.062	0.171	0.098
Finger cot	2N	0.025	0.031	0.036	0.032	0.030	0.019	0.024	0.021
Finger cot	4N	0.071	0.053	0.171	0.149	0.065	0.045	0.051	0.039
Finger cot	8N	0.188	0.114	0.099	0.051	0.172	0.114	0.122	0.073
Thimble	2N	0.041	0.032	0.027	0.019	0.028	0.024	0.025	0.016
Thimble	4N	0.074	0.065	0.082	0.072	0.048	0.033	0.042	0.024
Thimble	8N	0.142	0.104	0.139	0.152	0.136	0.093	0.137	0.080

Table E.5: Absolute error in force control for subject CT using right hand index finger with visual feedback.

Condition	Force	Absolute Error (N)							
		Rigid		Hard		Medium		Soft	
		Mean	S.D.	Mean	S.D.	Mean	S.D.	Mean	S.D.
Normal	2N	0.157	0.103	0.179	0.105	0.079	0.073	0.184	0.139
Normal	4N	0.565	0.275	0.308	0.140	0.311	0.160	0.509	0.263
Normal	8N	1.400	0.849	0.931	0.436	0.609	0.371	0.875	0.461
Finger cot	2N	0.130	0.075	0.082	0.058	0.098	0.068	0.202	0.113
Finger cot	4N	0.646	0.338	0.507	0.207	0.568	0.304	0.437	0.224
Finger cot	8N	1.303	0.560	0.833	0.441	0.957	0.520	0.642	0.331
Thimble	2N	0.101	0.058	0.100	0.054	0.060	0.038	0.127	0.083
Thimble	4N	0.156	0.110	0.541	0.240	0.221	0.135	0.532	0.335
Thimble	8N	1.137	0.568	0.742	0.360	1.156	0.660	0.833	0.406

Table E.6: Absolute error in force control for subject CT using right hand index finger without visual feedback.

Condition	Force	Absolute Error (N)							
		Rigid		Hard		Medium		Soft	
		Mean	S.D.	Mean	S.D.	Mean	S.D.	Mean	S.D.
Normal	2N	0.029	0.020	0.032	0.030	0.035	0.023	0.040	0.044
Normal	4N	0.051	0.042	0.066	0.057	0.045	0.034	0.054	0.034
Normal	8N	0.132	0.080	0.133	0.083	0.106	0.077	0.145	0.086
Finger cot	2N	0.045	0.051	0.034	0.034	0.053	0.076	0.036	0.038
Finger cot	4N	0.048	0.036	0.065	0.039	0.063	0.054	0.057	0.053
Finger cot	8N	0.154	0.083	0.114	0.087	0.105	0.071	0.113	0.075
Thimble	2N	0.044	0.046	0.038	0.034	0.042	0.040	0.034	0.033
Thimble	4N	0.069	0.058	0.056	0.043	0.048	0.029	0.053	0.041
Thimble	8N	0.162	0.094	0.132	0.081	0.117	0.073	0.105	0.063

Table E.7: Absolute error in force control for subject CT using left hand index finger with visual feedback.

Condition	Force	Absolute Error (N)							
		Rigid		Hard		Medium		Soft	
		Mean	S.D.	Mean	S.D.	Mean	S.D.	Mean	S.D.
Normal	2N	0.055	0.046	0.053	0.033	0.087	0.062	0.074	0.044
Normal	4N	0.206	0.126	0.283	0.127	0.267	0.157	0.320	0.160
Normal	8N	0.821	0.375	0.537	0.283	0.830	0.432	1.011	0.598
Finger cot	2N	0.104	0.040	0.036	0.023	0.073	0.047	0.057	0.033
Finger cot	4N	0.149	0.102	0.155	0.139	0.207	0.141	0.207	0.144
Finger cot	8N	0.902	0.565	1.111	0.562	0.896	0.530	0.682	0.380
Thimble	2N	0.051	0.031	0.063	0.031	0.096	0.080	0.033	0.024
Thimble	4N	0.166	0.103	0.262	0.176	0.158	0.095	0.193	0.137
Thimble	8N	0.998	0.531	0.878	0.519	0.872	0.557	0.607	0.407

Table E.8: Absolute error in force control for subject CT using left hand index finger without visual feedback.

Condition	Force	Absolute Error (N)							
		Rigid		Hard		Medium		Soft	
		Mean	S.D.	Mean	S.D.	Mean	S.D.	Mean	S.D.
Normal	2N	0.033	0.029	0.024	0.019	0.037	0.028	0.029	0.023
Normal	4N	0.067	0.046	0.049	0.038	0.063	0.050	0.058	0.048
Normal	8N	0.140	0.114	0.114	0.090	0.151	0.108	0.134	0.103
Finger cot	2N	0.040	0.034	0.027	0.022	0.046	0.037	0.034	0.030
Finger cot	4N	0.059	0.048	0.045	0.036	0.068	0.063	0.066	0.054
Finger cot	8N	0.154	0.130	0.121	0.099	0.125	0.089	0.139	0.104
Thimble	2N	0.046	0.044	0.039	0.026	0.051	0.034	0.048	0.047
Thimble	4N	0.056	0.046	0.039	0.032	0.061	0.048	0.066	0.049
Thimble	8N	0.097	0.081	0.094	0.073	0.116	0.088	0.103	0.080

Table E.9: Absolute error in force control for subject JK using right hand index finger with visual feedback.

Condition	Force	Absolute Error (N)							
		Rigid		Hard		Medium		Soft	
		Mean	S.D.	Mean	S.D.	Mean	S.D.	Mean	S.D.
Normal	2N	0.114	0.074	0.087	0.080	0.084	0.054	0.065	0.034
Normal	4N	0.230	0.173	0.221	0.176	0.124	0.087	0.123	0.085
Normal	8N	0.344	0.254	0.311	0.212	0.217	0.148	0.475	0.260
Finger cot	2N	0.072	0.048	0.173	0.160	0.098	0.070	0.117	0.098
Finger cot	4N	0.109	0.081	0.125	0.087	0.186	0.144	0.204	0.132
Finger cot	8N	0.513	0.292	0.330	0.187	0.289	0.177	0.306	0.184
Thimble	2N	0.151	0.104	0.078	0.046	0.128	0.068	0.125	0.121
Thimble	4N	0.158	0.106	0.105	0.067	0.156	0.117	0.094	0.062
Thimble	8N	0.299	0.207	0.291	0.149	0.213	0.156	0.455	0.368

Table E.10: Absolute error in force control for subject JK using right hand index finger without visual feedback.

Condition	Force	Absolute Error (N)							
		Rigid		Hard		Medium		Soft	
		Mean	S.D.	Mean	S.D.	Mean	S.D.	Mean	S.D.
Normal	2N	0.044	0.037	0.036	0.030	0.042	0.034	0.059	0.051
Normal	4N	0.075	0.070	0.054	0.043	0.089	0.090	0.084	0.067
Normal	8N	0.170	0.121	0.174	0.158	0.166	0.144	0.195	0.152
Finger cot	2N	0.047	0.038	0.044	0.036	0.049	0.033	0.059	0.042
Finger cot	4N	0.071	0.056	0.069	0.060	0.067	0.052	0.083	0.064
Finger cot	8N	0.140	0.118	0.159	0.131	0.141	0.131	0.149	0.118
Thimble	2N	0.065	0.050	0.046	0.040	0.060	0.039	0.044	0.033
Thimble	4N	0.082	0.050	0.064	0.048	0.061	0.043	0.071	0.054
Thimble	8N	0.116	0.098	0.149	0.126	0.115	0.097	0.150	0.125

Table E.11: Absolute error in force control for subject JK using left hand index finger with visual feedback.

Condition	Force	Absolute Error (N)							
		Rigid		Hard		Medium		Soft	
		Mean	S.D.	Mean	S.D.	Mean	S.D.	Mean	S.D.
Normal	2N	0.101	0.084	0.088	0.072	0.139	0.114	0.199	0.165
Normal	4N	0.240	0.155	0.174	0.171	0.206	0.146	0.389	0.255
Normal	8N	0.839	0.506	0.828	0.511	0.575	0.352	0.972	0.617
Finger cot	2N	0.145	0.097	0.138	0.104	0.085	0.059	0.169	0.110
Finger cot	4N	0.266	0.187	0.307	0.229	0.208	0.159	0.291	0.225
Finger cot	8N	1.016	0.536	0.585	0.341	0.648	0.399	1.041	0.613
Thimble	2N	0.195	0.100	0.198	0.145	0.130	0.072	0.071	0.048
Thimble	4N	0.227	0.141	0.132	0.080	0.156	0.125	0.258	0.248
Thimble	8N	0.416	0.331	0.489	0.393	0.777	0.533	1.009	0.523

Table E.12: Absolute error in force control for subject JK using left hand index finger without visual feedback.

Appendix F

Statistical Tests on Force Control Performance Measures

The analysis of variance (ANOVA) method was used to find out whether the force control performance was influenced by factors such as target force magnitude, finger contact conditions, and specimens. The performance data from Appendix E were used for all the tests performed. All the statistical analyses were performed by using MATLAB statistics toolbox.

F.1 Specimen softness and finger contact conditions

The effects of both specimen softness and finger contact conditions were examined together by using two-way ANOVA. The data from the three subjects for the two visual force feedback conditions and two hands were analyzed separately (a total of 12 combinations). In other words, the data for the three target force magnitudes were grouped together in this analysis. Visual observations of the subjects' performance indicated that they seemed to have higher error at high target force magnitude. To minimize the effect of target force in the analysis, the performance data was expressed in terms of percentage of the target.

The results of the analysis could not reject the hypothesis that there was no effects of specimen softness and of the contact conditions in all but one circumstances (1 out of 12 tests). In that only circumstance, the ANOVA resulted in rejecting the hypothesis of no specimen effect for subject JK under visual force feedback. Based on results of the majority of the conditions tested, the likelihood that the specimen softness and the finger contact conditions played important roles in the force control tasks was small. Therefore, the following analysis

used data pooled from the different specimen softnesses as well as various contact interface conditions.

F.2 Target force magnitude

One-way ANOVA tables were constructed to compare target force magnitude factor. The columns stands for the data collected at three target force levels under various specimens and contact interface conditions. The reason for pooling data from those two factors is to increase the reliability of the analysis. Table F.1 and Table F.2 list the data pooled for the two visual force feedback conditions. The resulting ANOVA tables are shown in Tables F.3 and Table F.4. The hypothesis tested here is that target force magnitude did not significantly affect the results in either conditions. Taking the F ratios obtained from the two ANOVA tables (32.06 and 36.59) and comparing them to the F distribution with the same degree of freedoms (2,33), both hypotheses were rejected at 1 % significance level. The target force magnitude was found to be a significant factor that affected control performance. However, when only comparing data from 2N and 4N target force, the hypothesis could not be rejected under both visual force feedback conditions. Thus, the main differences came from the 8N target force runs for subject CH.

The corresponding box plots which show the spread of the data for the two tables are shown in Figure F-1 and Figure F-2. The box has lines at the lower quartile, median, and upper quartile values. The whiskers are lines extending from each end of the box to show the extent of the rest of the data if they were less than 1.5 times the interquartile ranges (IQR). Otherwise, whiskers end at the most extreme observations, still lie within 1.5 times IQR of the quartiles and the remaining observations were plotted as outliers.

For subjects CT and JK, there were also significant differences between 2N, 4N, and 8N target force magnitudes. In addition, the differences between 2N and 4N target force magnitudes were big enough to reject the hypothesis that their performance were the same at 1% significance level with and without visual force feedback. The box plots for the two subjects under those two conditions are shown in Figure F-3, Figure F-4, and Figure F-5, Figure F-6, respectively.

On the other hand, comparison can be made after the absolute errors were divided by the target force magnitudes and the performance is measured in terms of the percentage error.

Specimen	Finger Condition	Mean Absolute Error (N)		
		Target: 2N	Target: 4N	Target: 8N
Rigid	Normal	0.035	0.054	0.093
Rigid	Finger cot	0.051	0.070	0.165
Rigid	Thimble	0.057	0.048	0.128
Hard	Normal	0.063	0.030	0.061
Hard	Finger cot	0.037	0.035	0.100
Hard	Thimble	0.057	0.032	0.098
Medium	Normal	0.030	0.056	0.128
Medium	Finger cot	0.032	0.049	0.108
Medium	Thimble	0.030	0.060	0.066
Soft	Normal	0.036	0.067	0.073
Soft	Finger cot	0.035	0.057	0.160
Soft	Thimble	0.041	0.042	0.110

Table F.1: Data used for computing a one-way ANOVA table to determine the significance of target force magnitude for subject CH with visual feedback when using the right hand.

For both subjects CH and JK, the percentage errors were significantly lower when controlling 4N and 8N target force than when controlling 2N target force with visual force feedback (see Figure F-7 and Figure F-9). For subject CT, the percentage errors were not significantly different under the three different target force levels with visual feedback (see Figure F-8). The comparisons for the performance achieved at different target force magnitude without visual feedback were conducted in a similar fashion. The results are shown in Figure F-10, Figure F-11, and Figure F-12.

The qualitative effect of target force magnitude as observed from the box plots can be summarized as follows: When the mean absolute error is used as the performance index, higher target force generally increases both the mean absolute error and the standard deviation of the absolute error. However, for subject CH, the performance at 2N and 4N with or without visual feedback were about the same. When the mean absolute error expressed in percentage is used as the performance index, higher target force did not increase the error in general, except for subject CT without visual force feedback.

F.3 Visual feedback

One-way ANOVA tables were constructed using the performance data, expressed in percentage of target force, collected from each subject, to compare the effect of visual feedback

Specimen	Finger Condition	Mean Absolute Error (N)		
		Target: 2N	Target: 4N	Target: 8N
Rigid	Normal	0.162	0.093	0.586
Rigid	Finger cot	0.148	0.171	0.519
Rigid	Thimble	0.121	0.105	0.533
Hard	Normal	0.191	0.261	0.210
Hard	Finger cot	0.182	0.107	0.314
Hard	Thimble	0.266	0.090	0.520
Medium	Normal	0.150	0.107	0.331
Medium	Finger cot	0.111	0.062	0.400
Medium	Thimble	0.082	0.195	0.506
Soft	Normal	0.123	0.135	0.164
Soft	Finger cot	0.157	0.098	0.594
Soft	Thimble	0.214	0.104	0.415

Table F.2: Data used for computing one-way ANOVA table to determine the significance of target force magnitude for subject CH without visual feedback when using the right hand.

ANOVA Table

Source	SS	df	MS	F
Columns	0.03064	2	0.01532	32.06
Error	0.01577	33	0.0004778	
Total	0.04641	35		

Table F.3: ANOVA table to determine the significance of target force magnitude for subject CH with visual feedback when using right hand. The columns represent the data obtained from three target forces under various finger and specimen conditions.

ANOVA Table

Source	SS	df	MS	F
Columns	0.6386	2	0.3193	36.59
Error	0.288	33	0.008727	
Total	0.9266	35		

Table F.4: ANOVA table to determine the significance of target force magnitude for subject CH without visual feedback when using right hand. The columns represent the data obtained from three target forces under various finger and specimen conditions.

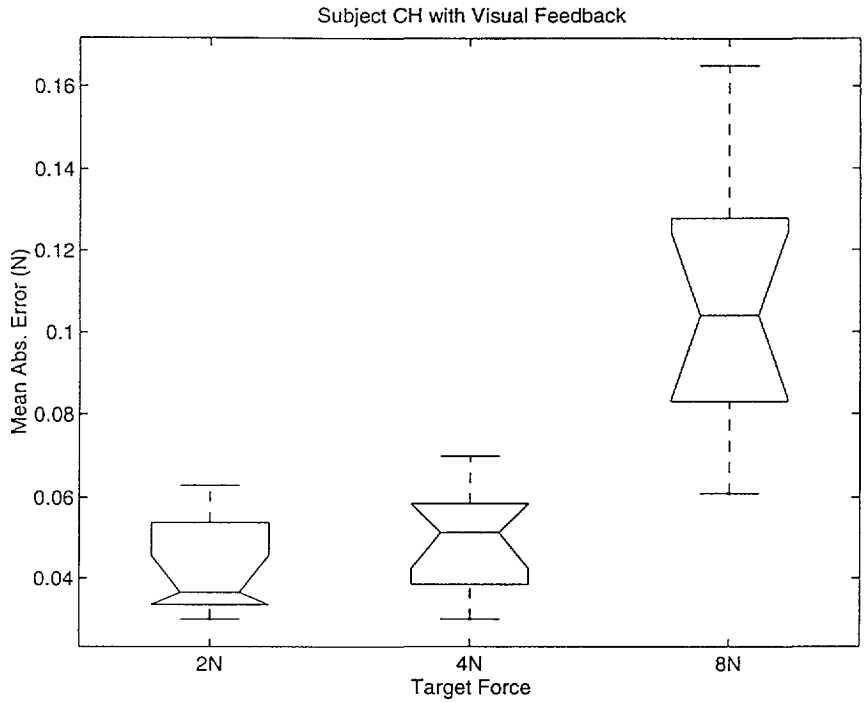

Figure F-1: Box plot of data pooled from various finger and specimen conditions for subject CH with visual feedback when using the right hand.

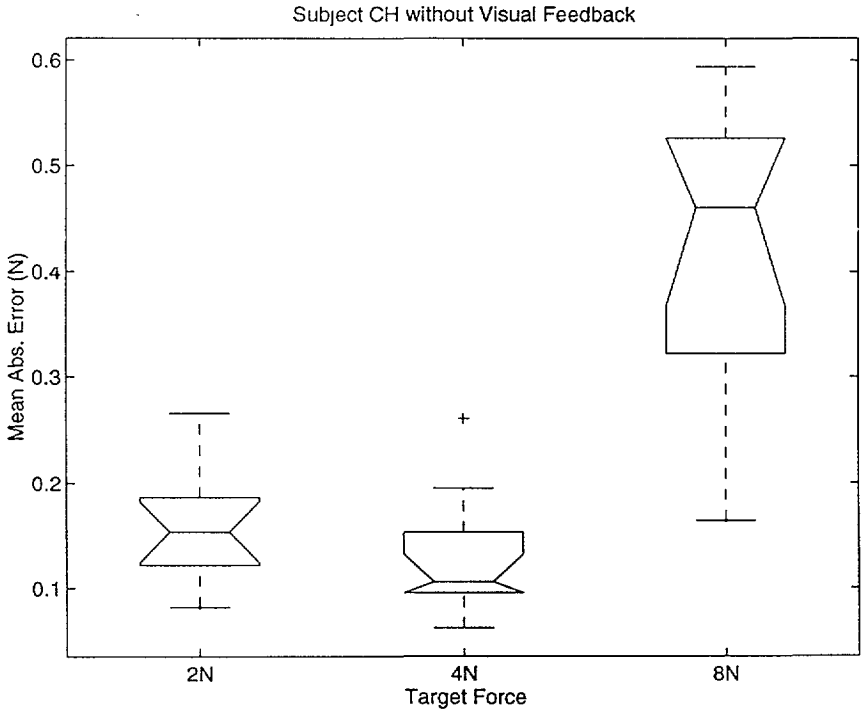

Figure F-2: Box plot of data pooled from various finger and specimen conditions for subject CH without visual feedback when using the right hand.

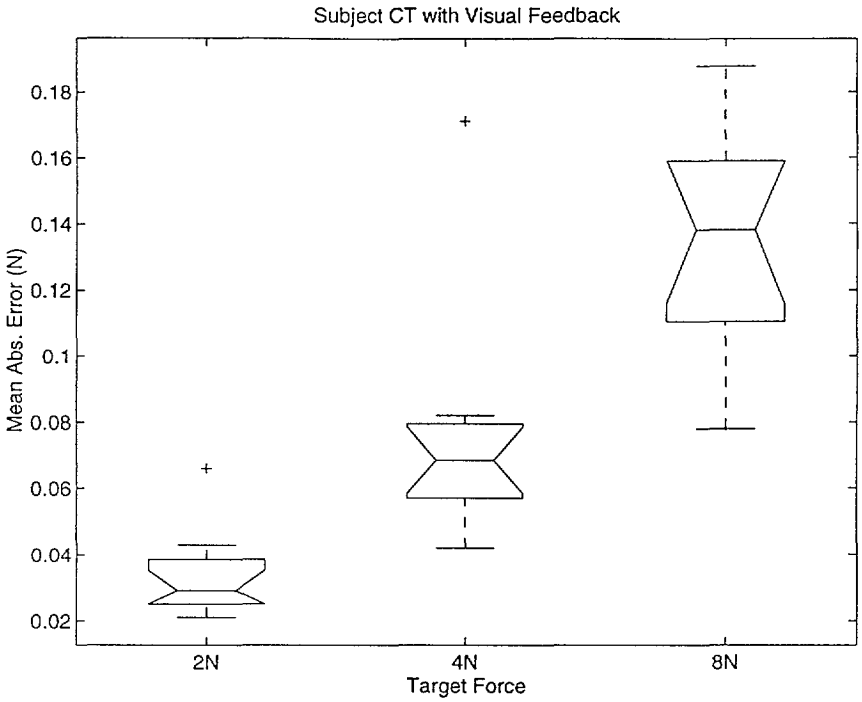

Figure F-3: Box plot of data pooled from various finger and specimen conditions for subject CT with visual feedback when using the right hand.

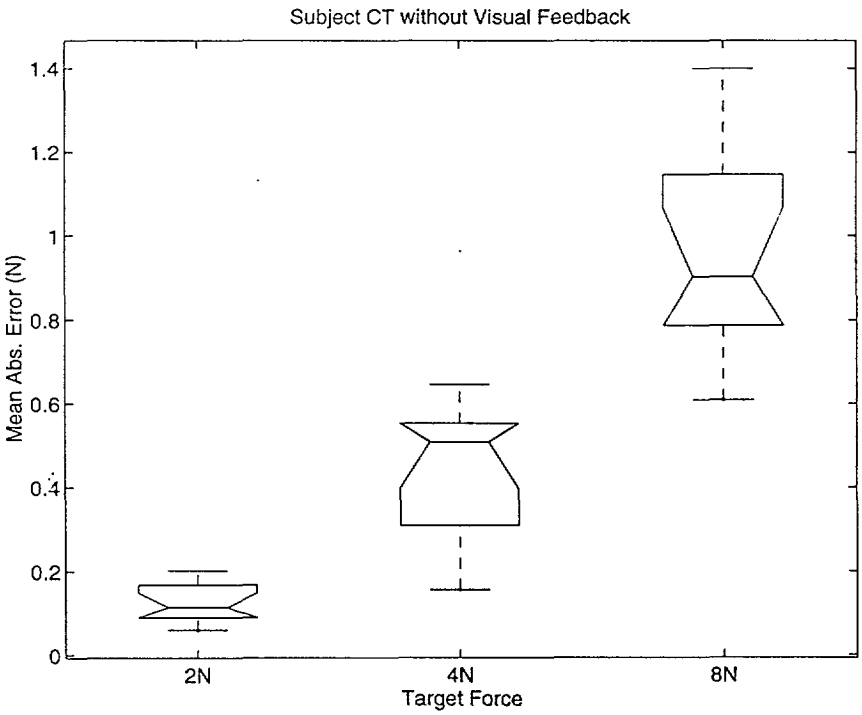

Figure F-4: Box plot of data pooled from various finger and specimen conditions for subject CT without visual feedback when using the right hand.

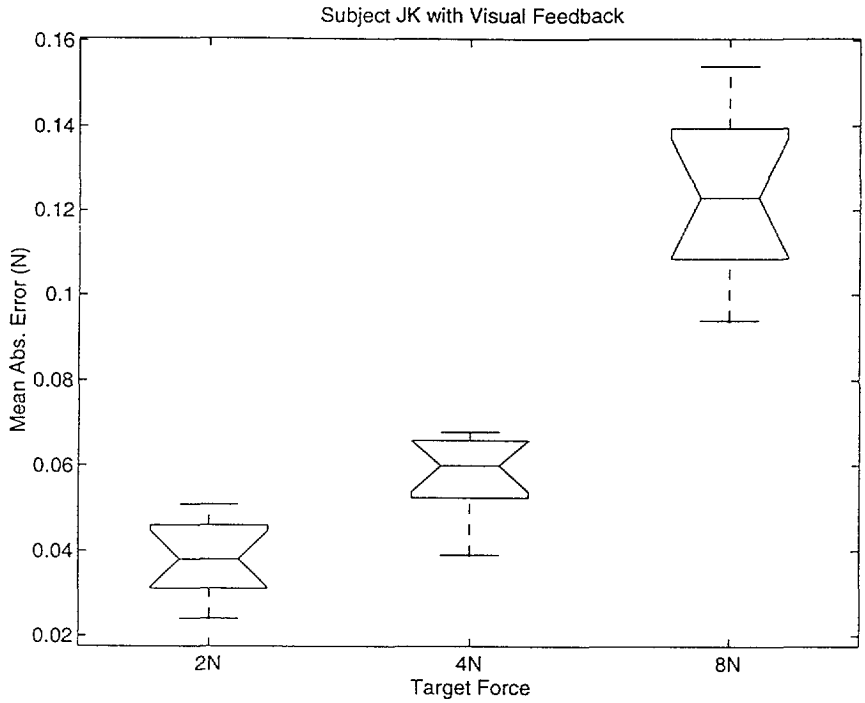

Figure F-5: Box plot of data pooled from various finger and specimen conditions for subject JK with visual feedback when using the right hand.

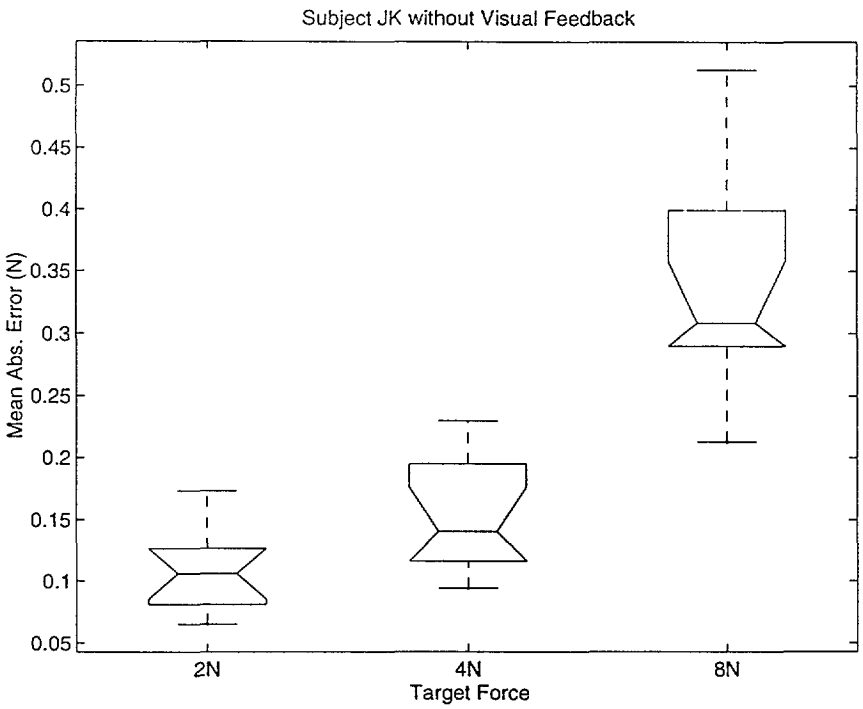

Figure F-6: Box plot of data pooled from various finger and specimen conditions for subject JK without visual feedback when using the right hand.

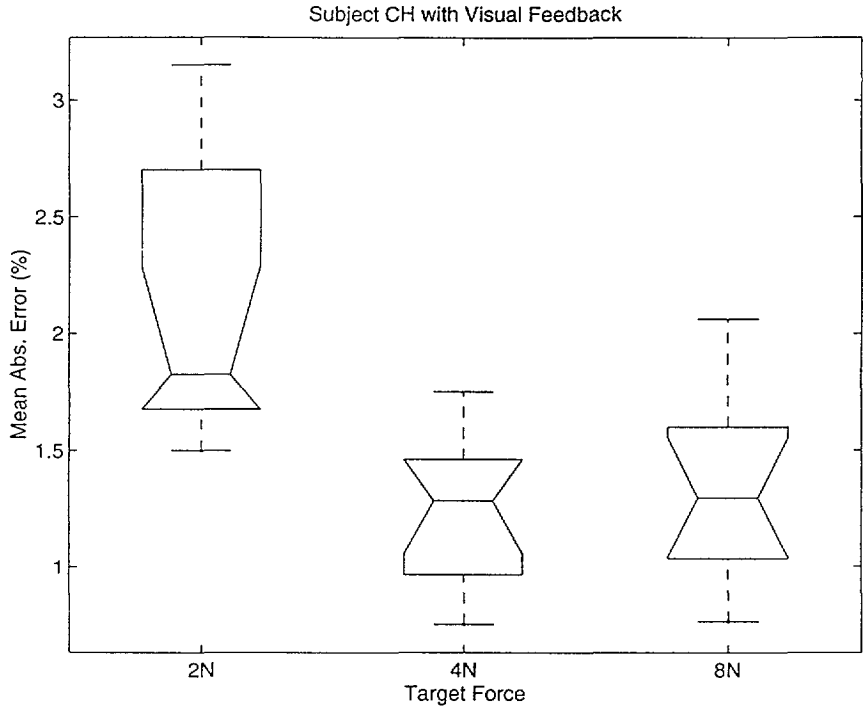

Figure F-7: Box plot of data, expressed in percentage, pooled from various finger and specimen conditions for subject CH with visual feedback when using the right hand.

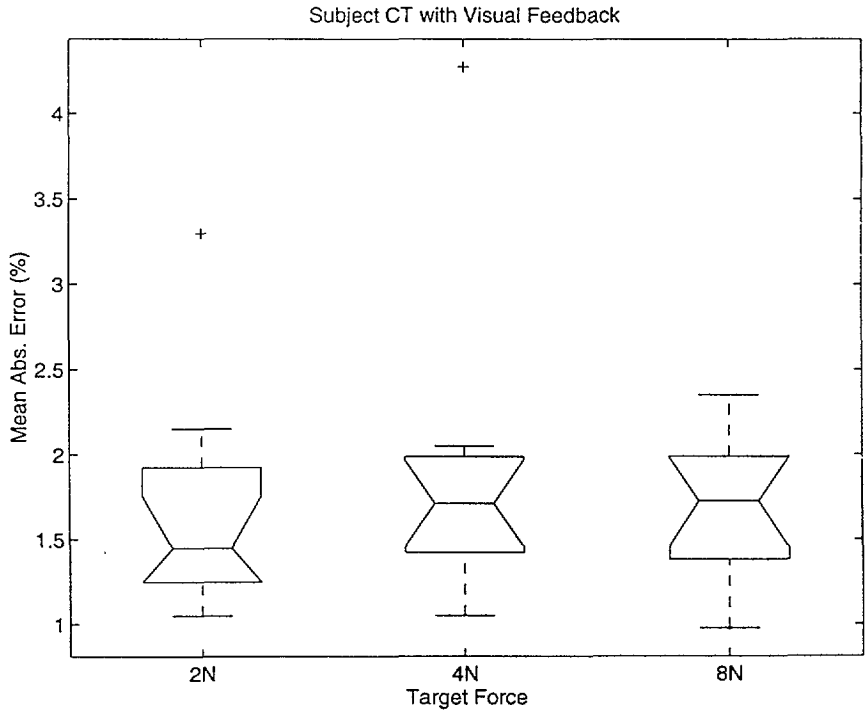

Figure F-8: Box plot of data, expressed in percentage, pooled from various finger and specimen conditions for subject CT with visual feedback when using the right hand.

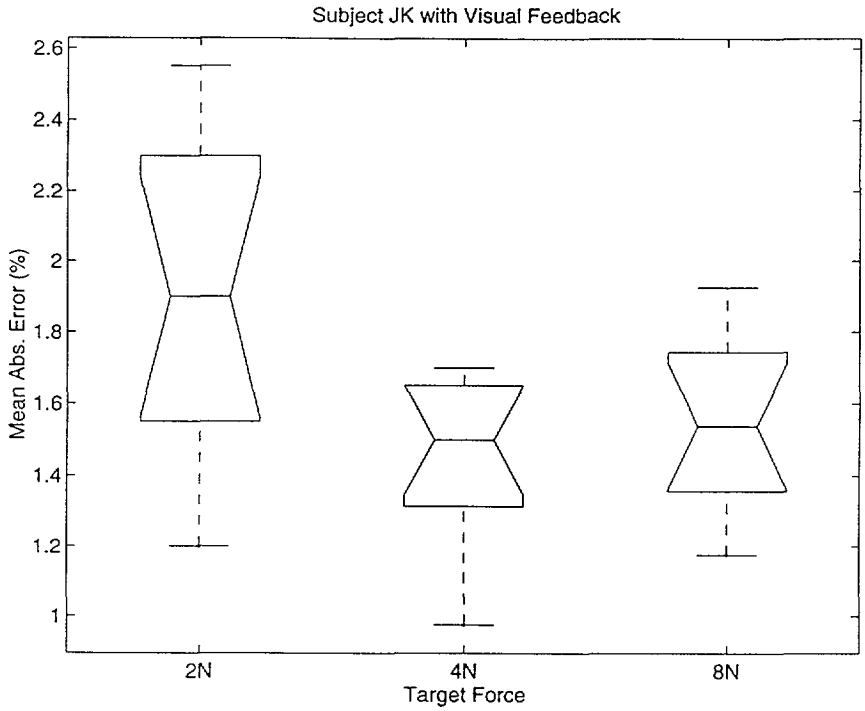

Figure F-9: Box plot of data, expressed in percentage, pooled from various finger and specimen conditions for subject JK with visual feedback when using the right hand.

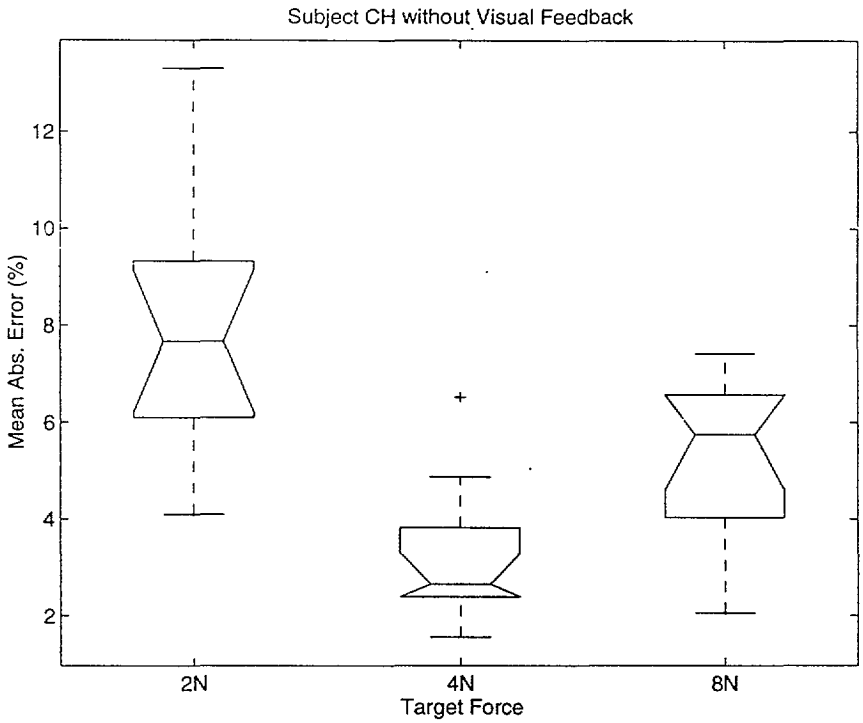

Figure F-10: Box plot of data, expressed in percentage, pooled from various finger and specimen conditions for subject CH without visual feedback when using the right hand.

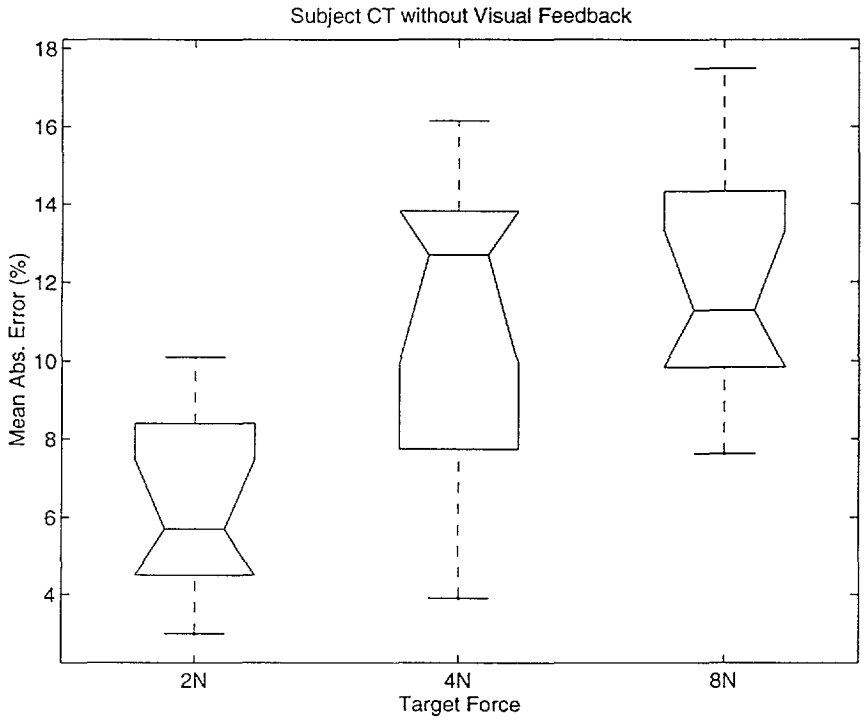

Figure F-11: Box plot of data, expressed in percentage, pooled from various finger and specimen conditions for subject CT without visual feedback when using the right hand.

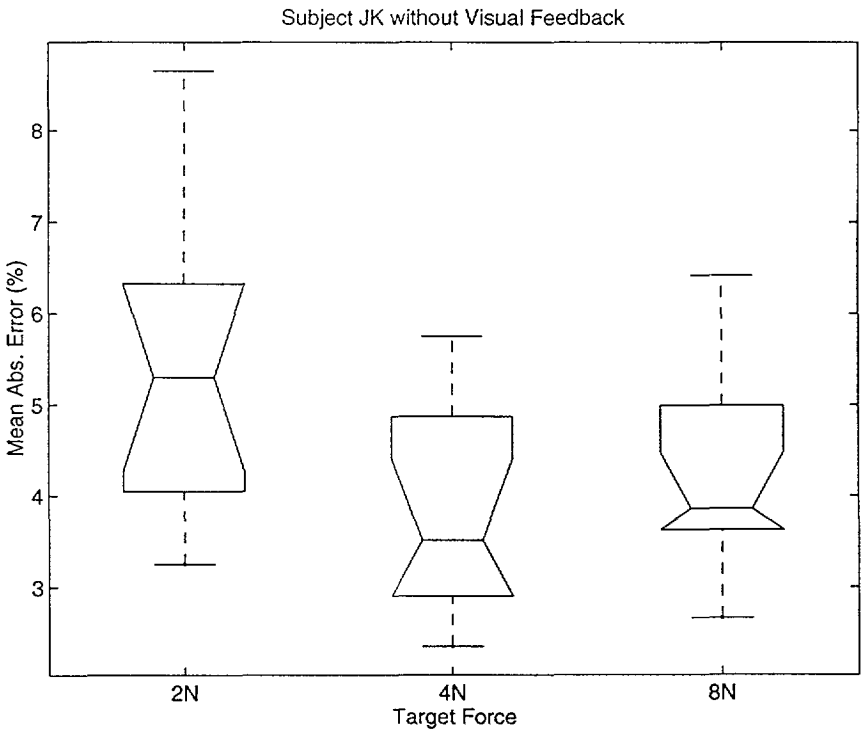

Figure F-12: Box plot of data, expressed in percentage, pooled from various finger and specimen conditions for subject JK without visual feedback when using the right hand.

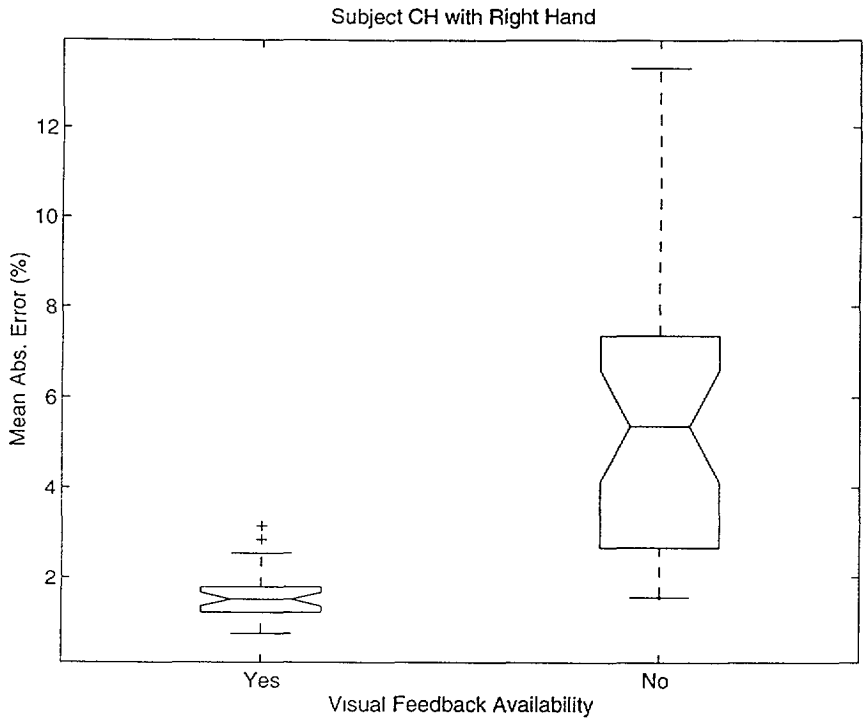

Figure F-13: Box plot of data, expressed in percentage, pooled from various interface, force, and specimen conditions for subject CH when using the right hand.

by pooling data from various finger conditions, target forces, and specimen softnesses. The columns stand for the data collected with different force feedback conditions. The hypothesis tested here is that the presence or absence of feedback did not significantly affect the results. The ANOVA results rejected the hypothesis for all three subjects with very high F ratios at 1% significance level. Therefore, there is a significant difference between whether or not visual force feedback was available. Figure F-13, Figure F-14, and Figure F-15 show the box plots for the right hand of the three subjects.

F.4 Hand used

One-way ANOVA tables were constructed using the performance data, expressed in percentage of target force, collected from each subject to compare the effect of visual feedback by pooling data from various finger conditions, target forces, and specimen softness with visual feedback. The columns stand for the data collected with different hands. The hypothesis tested here is that the two hands did not significantly affect the results. The resulting ANOVA tables which reject the hypothesis at 1% significance level are listed in Tables F.5, F.6,

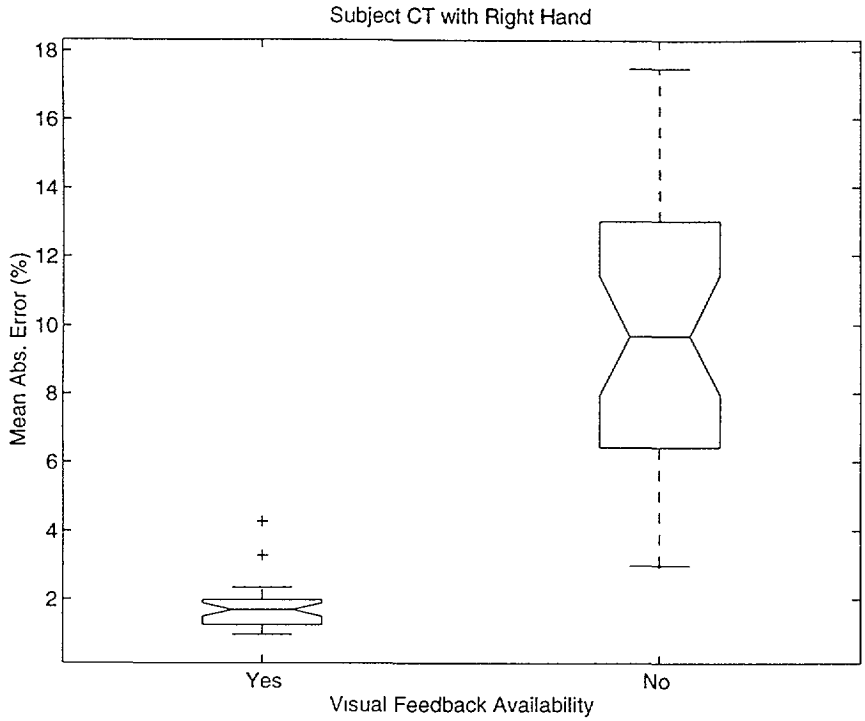

Figure F-14: Box plot of data, expressed in percentage, pooled from various interface, force, and specimen conditions for subject CT when using the right hand.

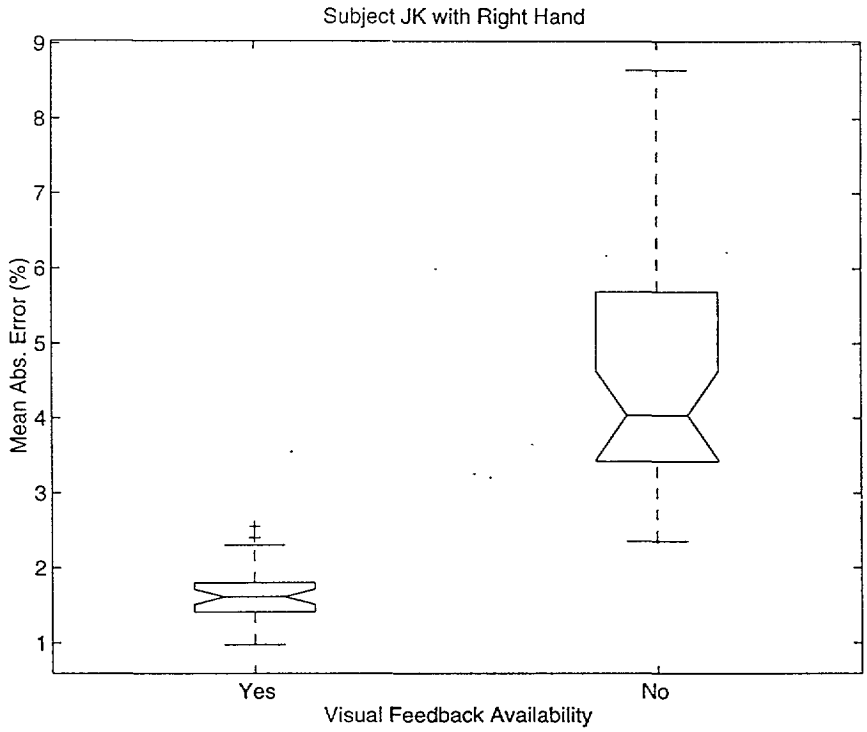

Figure F-15: Box plot of data, expressed in percentage, pooled from various interface, force, and specimen conditions for subject JK when using the right hand.

ANOVA Table

Source	SS	df	MS	F
Columns	199.9	1	199.9	14.3
Error	978.6	70	13.98	
Total	1179	71		

Table F.5: ANOVA table to determine the significance of the hand used for subject CT without visual feedback. The columns represent data, in percentage, obtained from various target forces under various finger and specimen conditions.

ANOVA Table

Source	SS	df	MS	F
Columns	3.369	1	3.369	20.17
Error	11.69	70	0.167	
Total	15.06	71		

Table F.6: ANOVA table to determine the significance of the hand used for subject JK with visual feedback. The columns represent data, in percentage, obtained from various target forces under various finger and specimen conditions.

and F.7. The tables correspond to the data of subject CT without visual feedback and subject JK with and without visual feedback.

Therefore, there was a significant difference between the performance of the two hands of subject JK in force control with and without visual feedback. For subject CT, there was a difference when the visual feedback was not available. As far as subject CH is concerned, the performance was not significantly different for the two hands. Figure F-16 to Figure F-21 show the box plots for the three subjects using different hands with and without visual feedback.

ANOVA Table

Source	SS	df	MS	F
Columns	162.5	1	162.5	33.77
Error	336.9	70	4.813	
Total	499.4	71		

Table F.7: ANOVA table to determine the significance of the hand used for subject JK without visual feedback. The columns represent data, in percentage, obtained from various target forces under various finger and specimen conditions.

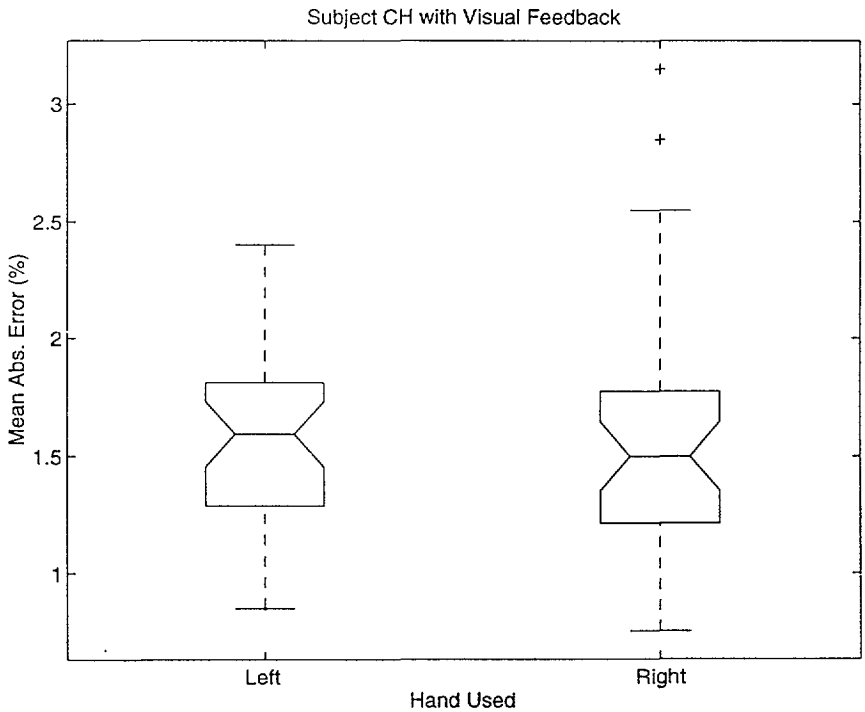

Figure F-16: Box plot of data, expressed in percentage, pooled from various interface, force, and specimen conditions for subject CH when using the right hand.

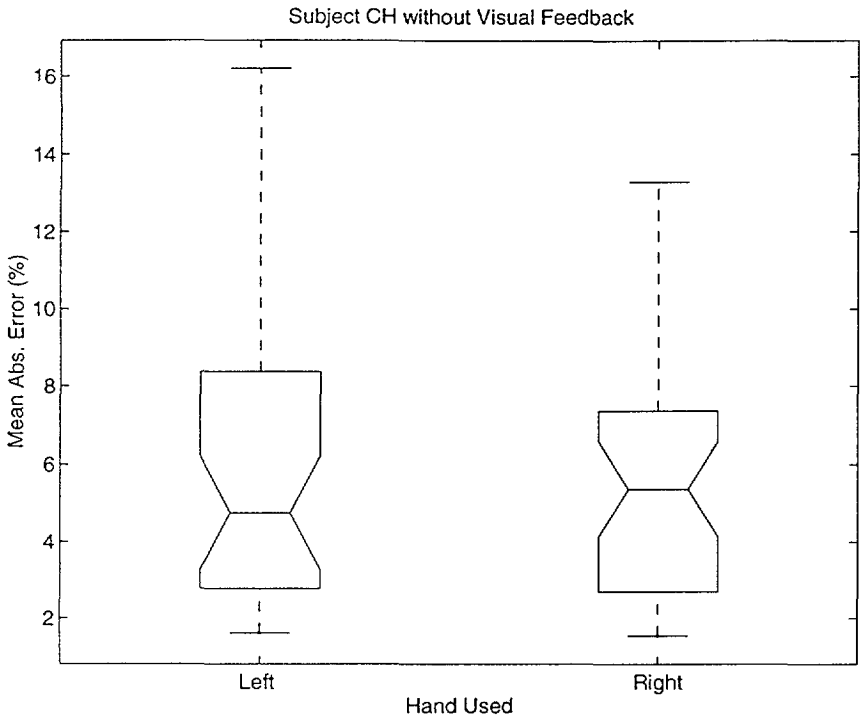

Figure F-17: Box plot of data, expressed in percentage, pooled from various interface, force, and specimen conditions for subject CH when using the left hand.

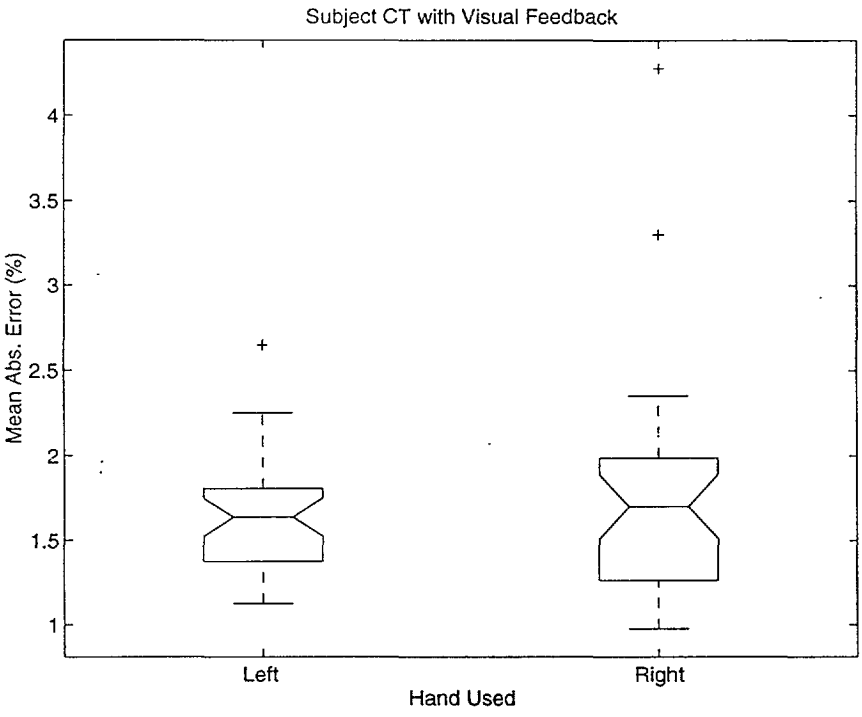

Figure F-18: Box plot of data, expressed in percentage, pooled from various interface, force, and specimen conditions for subject CT when using the right hand.

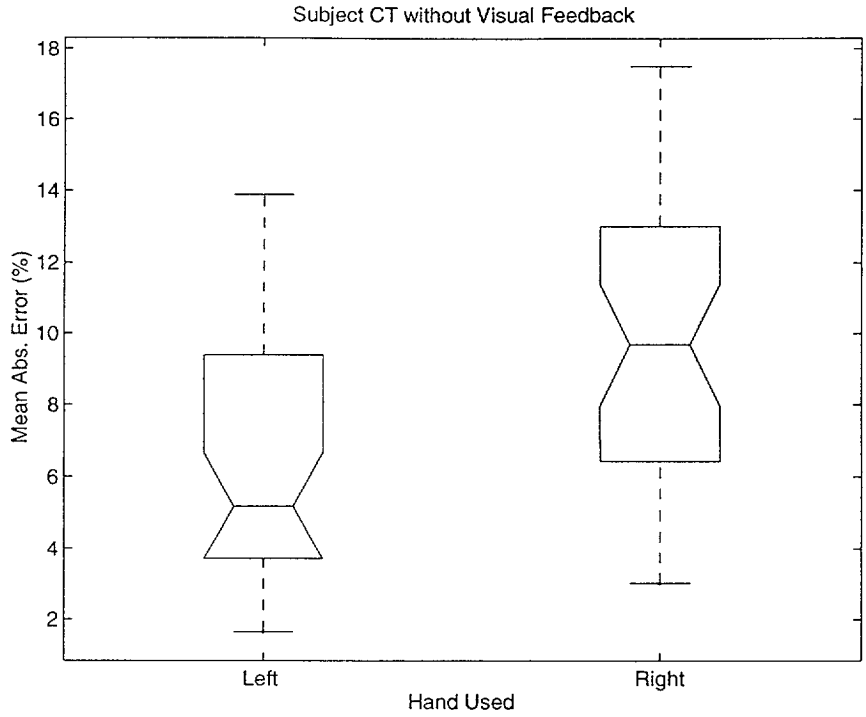

Figure F-19: Box plot of data, expressed in percentage, pooled from various interface, force, and specimen conditions for subject CT when using the left hand.

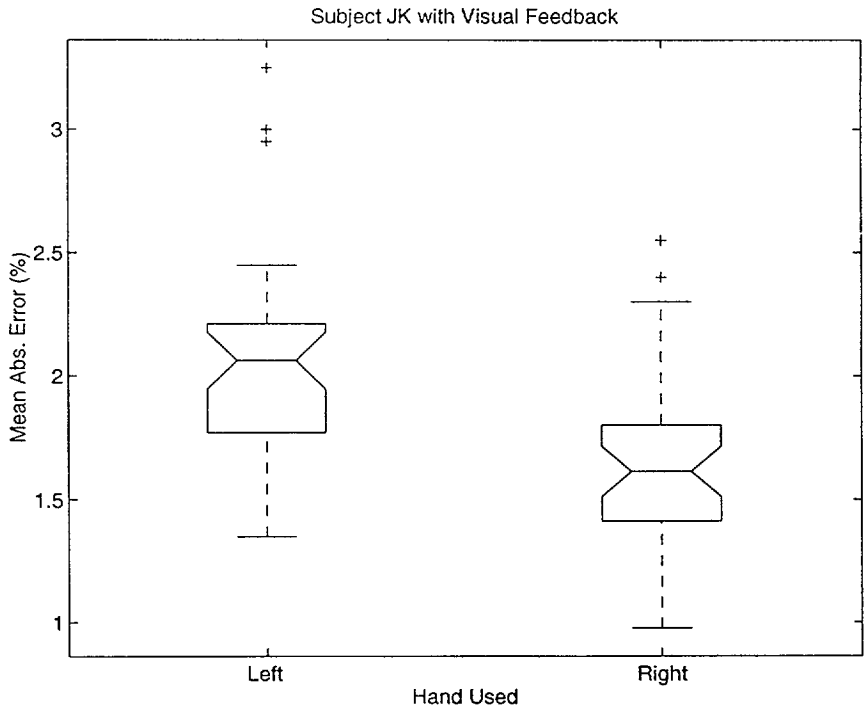

Figure F-20: Box plot of data, expressed in percentage, pooled from various interface, force, and specimen conditions for subject JK when using the right hand.

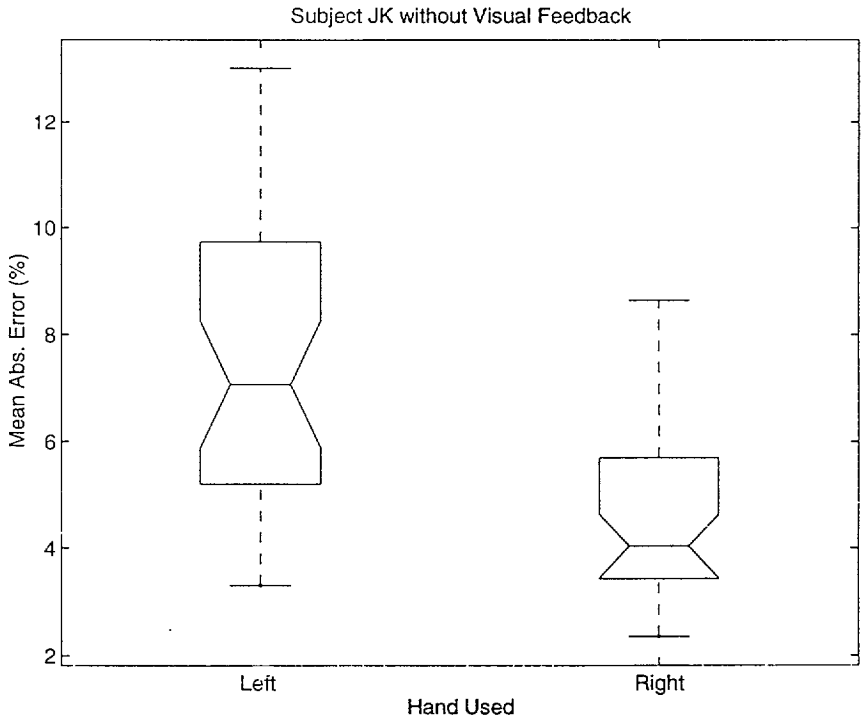

Figure F-21: Box plot of data, expressed in percentage, pooled from various interface, force, and specimen conditions for subject JK when using the right hand.

Appendix G

Contact Visualization Analysis

Presented in this appendix are the data analyzed during the contact visualization experiments under various conditions. For the low magnification experiments on overall contact regions, the results are plotted in two ways. In the first figure, the various pieces of contact information are plotted against time; in the second, the same information is plotted against force. The video and force data were collected at a rate of 20 and 1000 samples per seconds, respectively. In the figures, the mean force during each frame was used as the force magnitude.

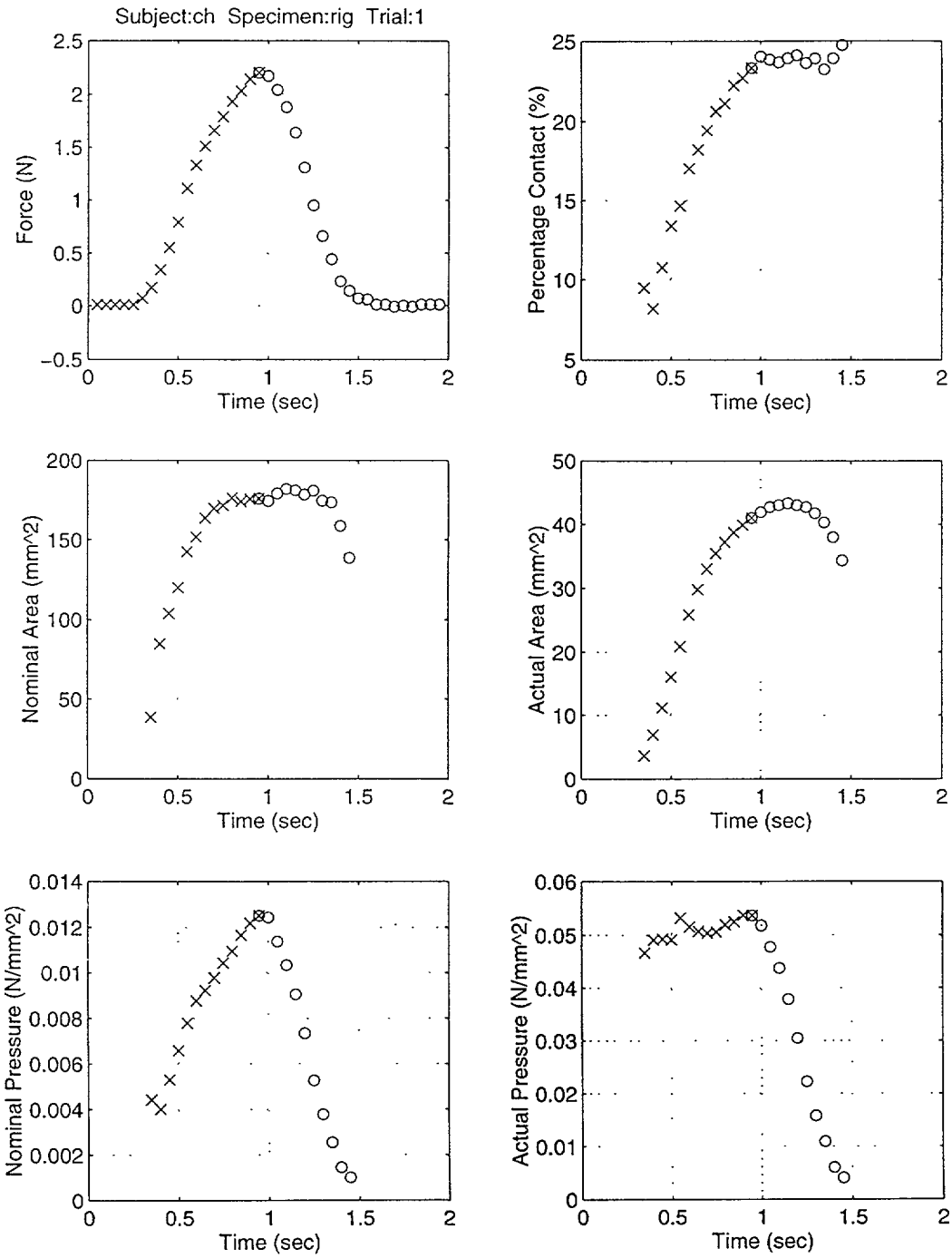

Figure G-1: Various contact variables, plotted against time, calculated from the image and force data obtained using low magnification (Subject:CH, Trial:1).

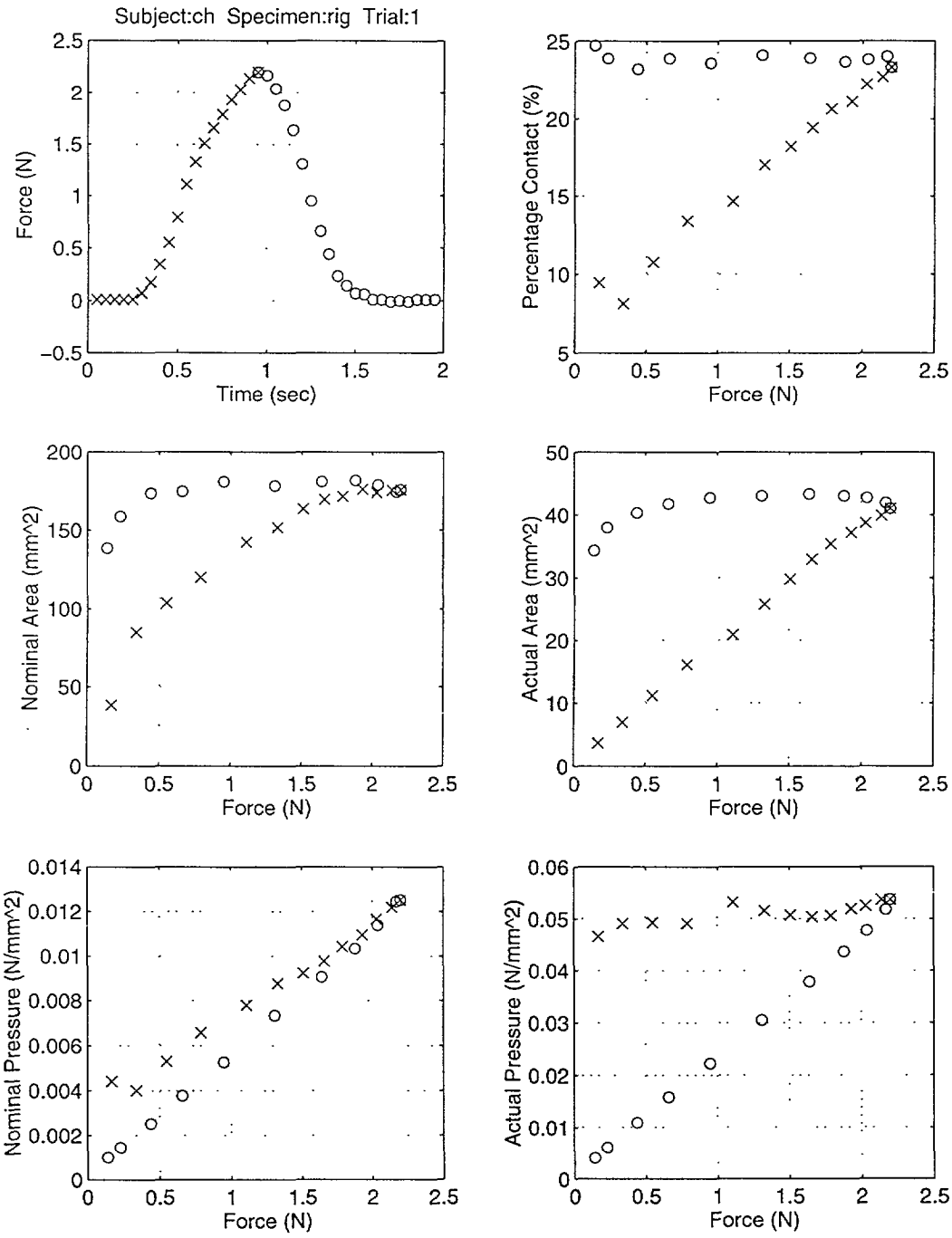

Figure G-2: Various contact variables, plotted against contact force, calculated from the image and force data obtained using low magnification (Subject:CH, Trial:1).

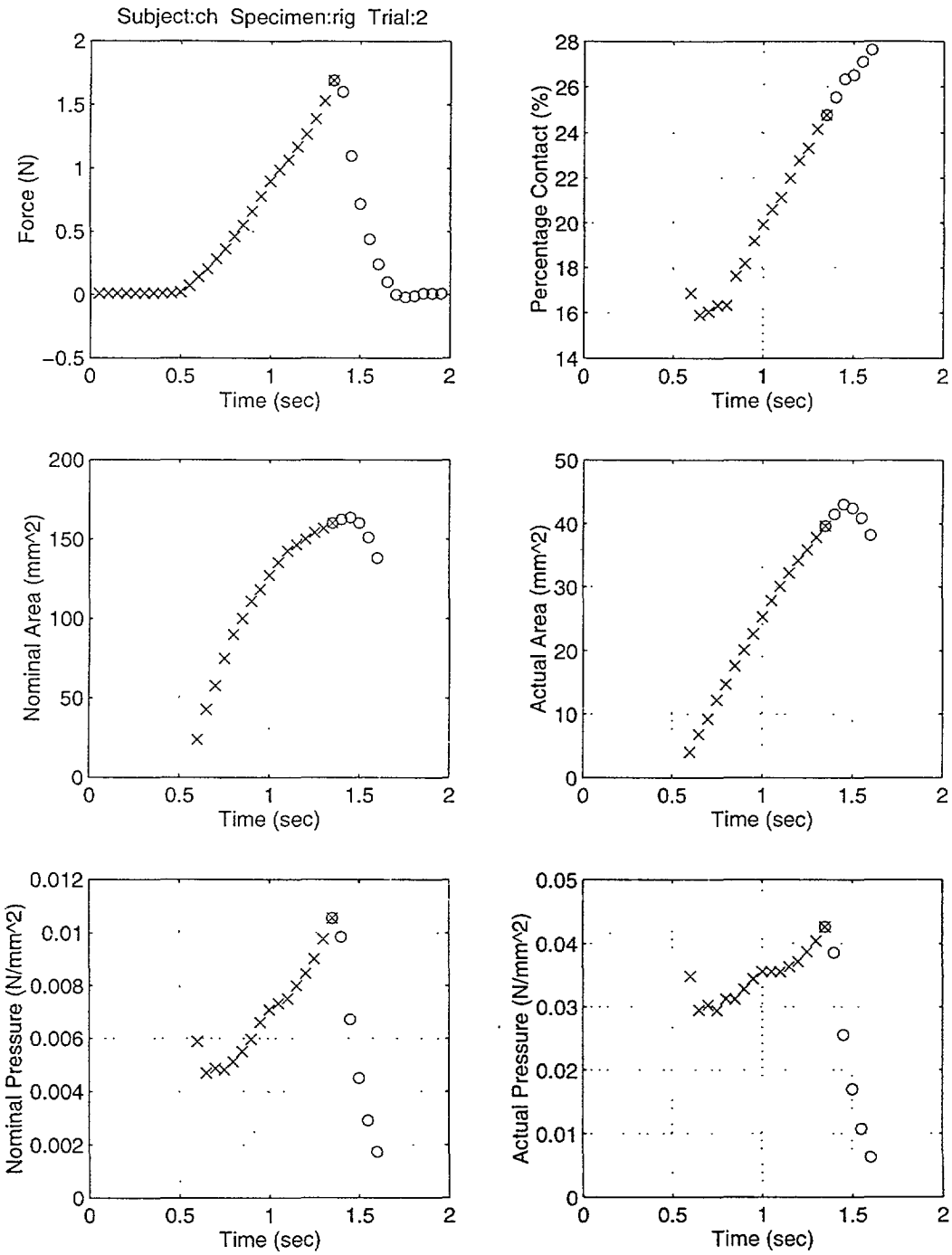

Figure G-3: Various contact variables, plotted against time, calculated from the image and force data obtained using low magnification (Subject:CH, Trial:2).

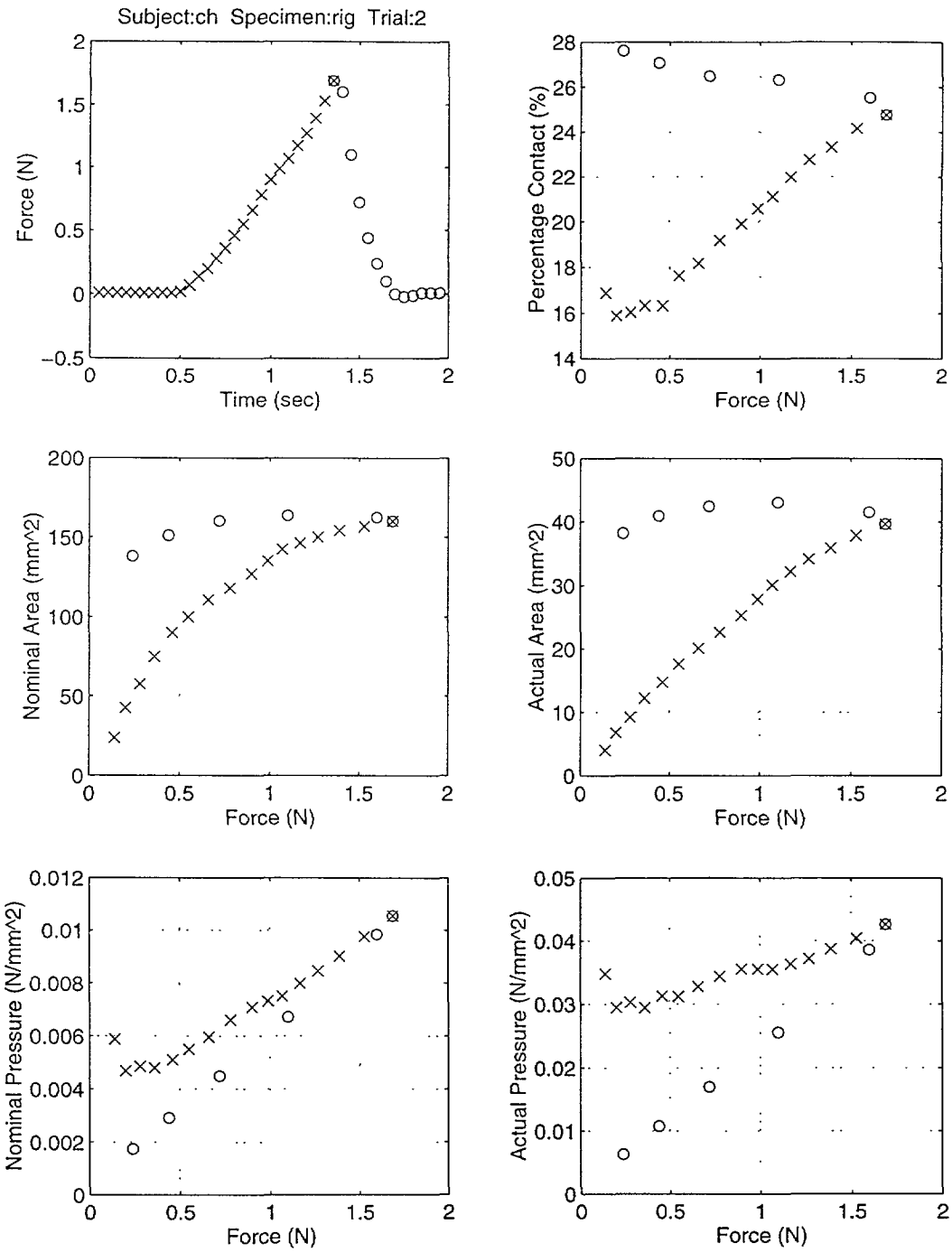

Figure G-4: Various contact variables, plotted against contact force, calculated from the image and force data obtained using low magnification (Subject:CH, Trial:2).

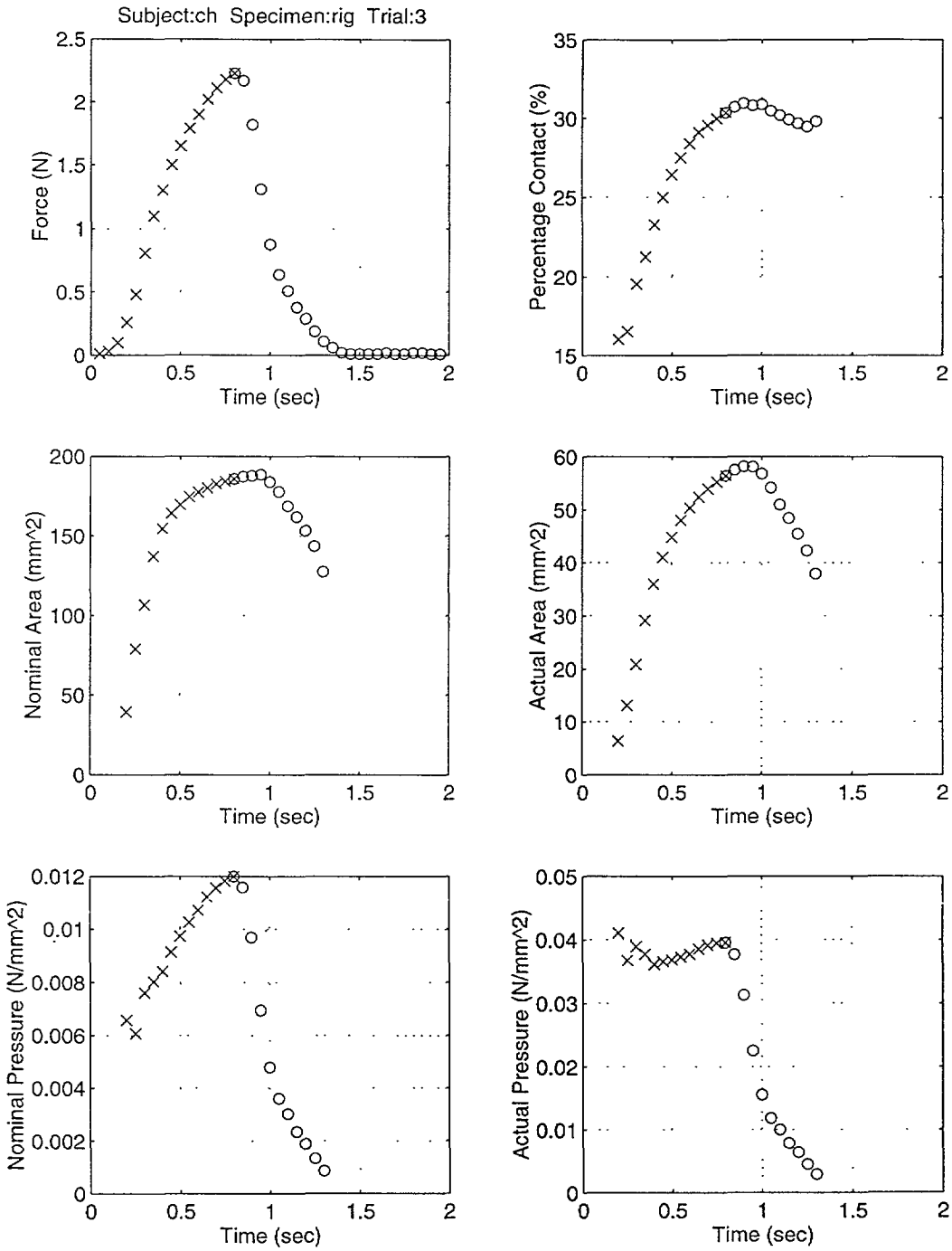

Figure G-5: Various contact variables, plotted against time, calculated from the image and force data obtained using low magnification (Subject:CH, Trial:3).

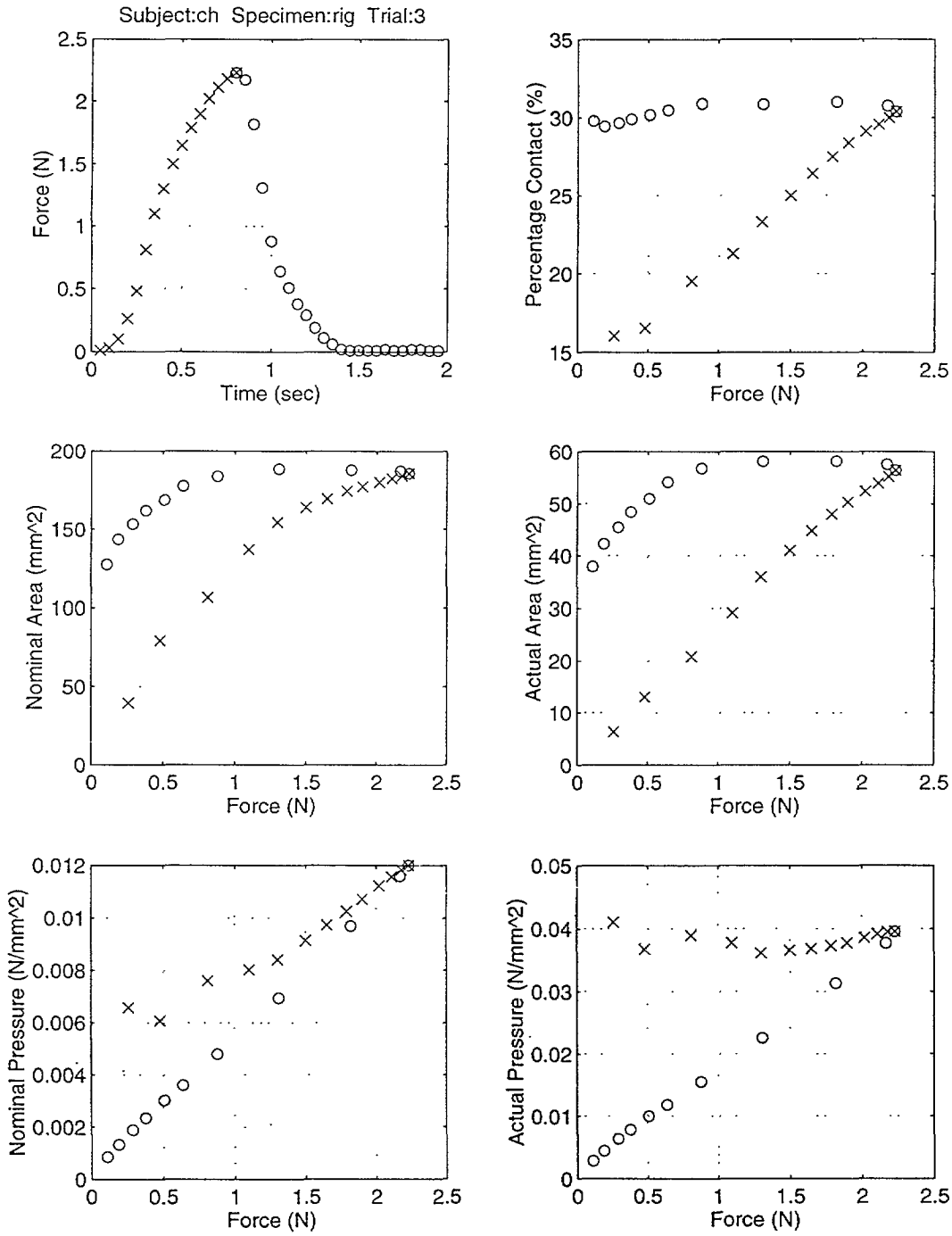

Figure G-6: Various contact variables, plotted against contact force, calculated from the image and force data obtained using low magnification (Subject:CH, Trial:3).

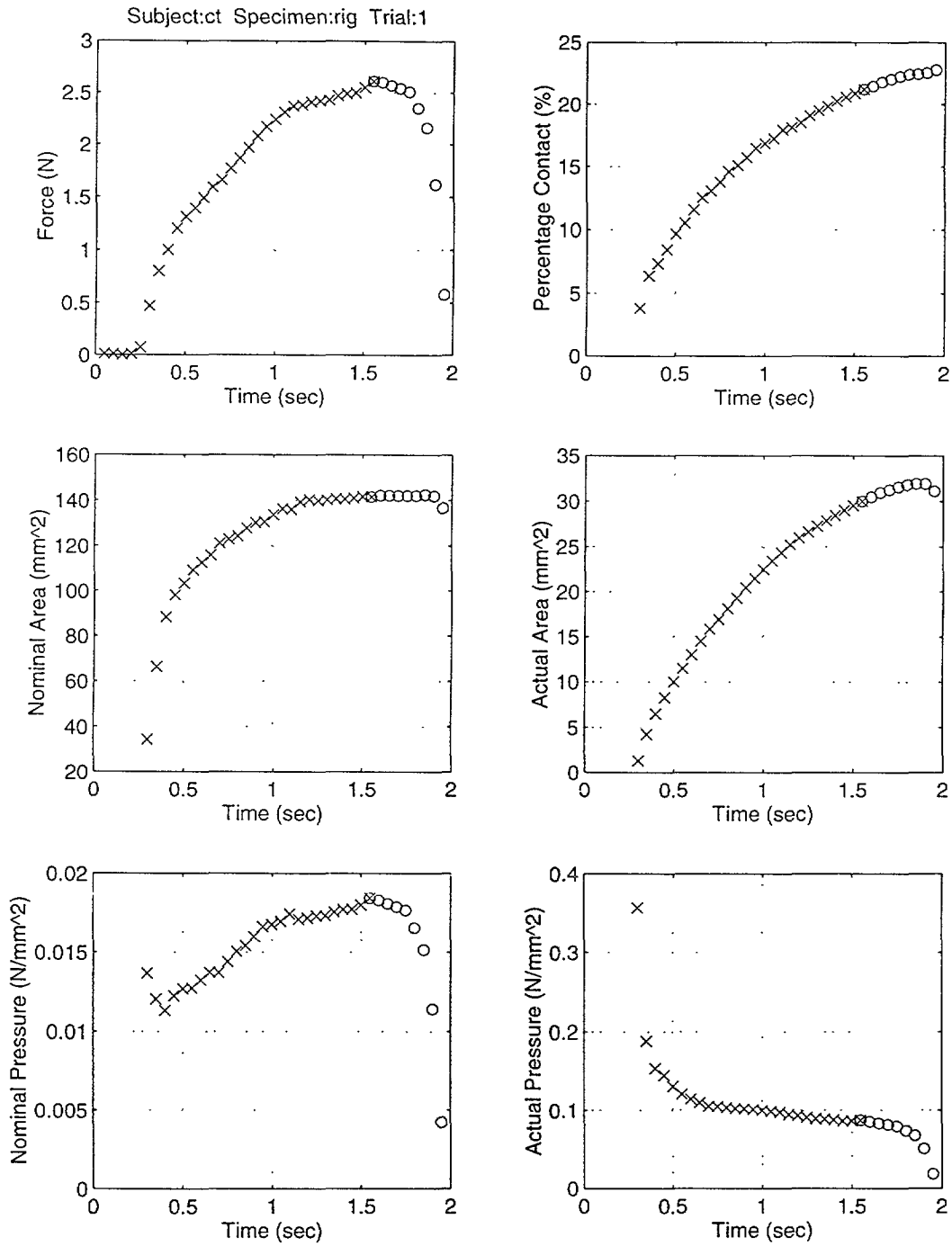

Figure G-7: Various contact variables, plotted against time, calculated from the image and force data obtained using low magnification (Subject:CT, Trial:1).

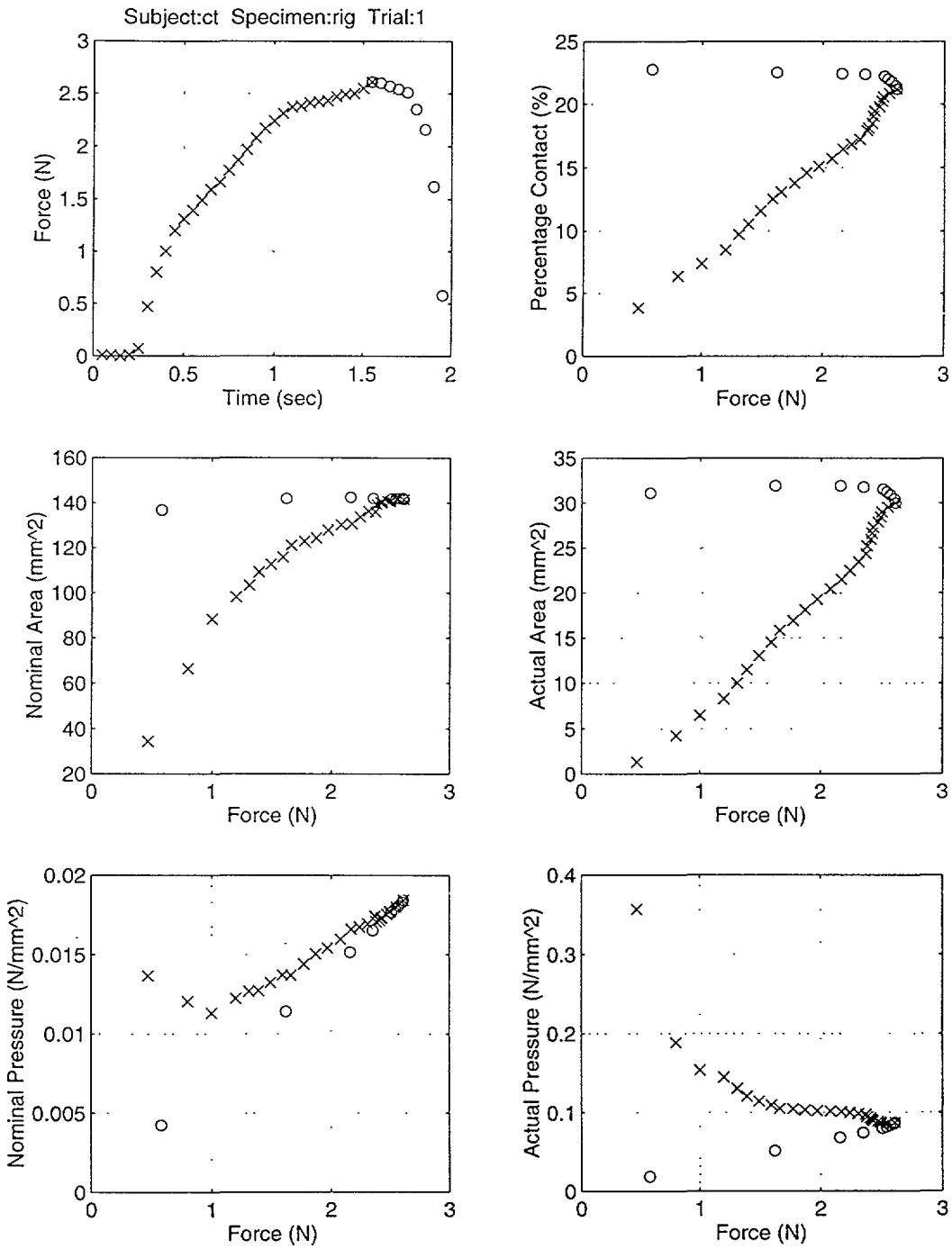

Figure G-8: Various contact variables, plotted against contact force, calculated from the image and force data obtained using low magnification (Subject:CT, Trial:1).

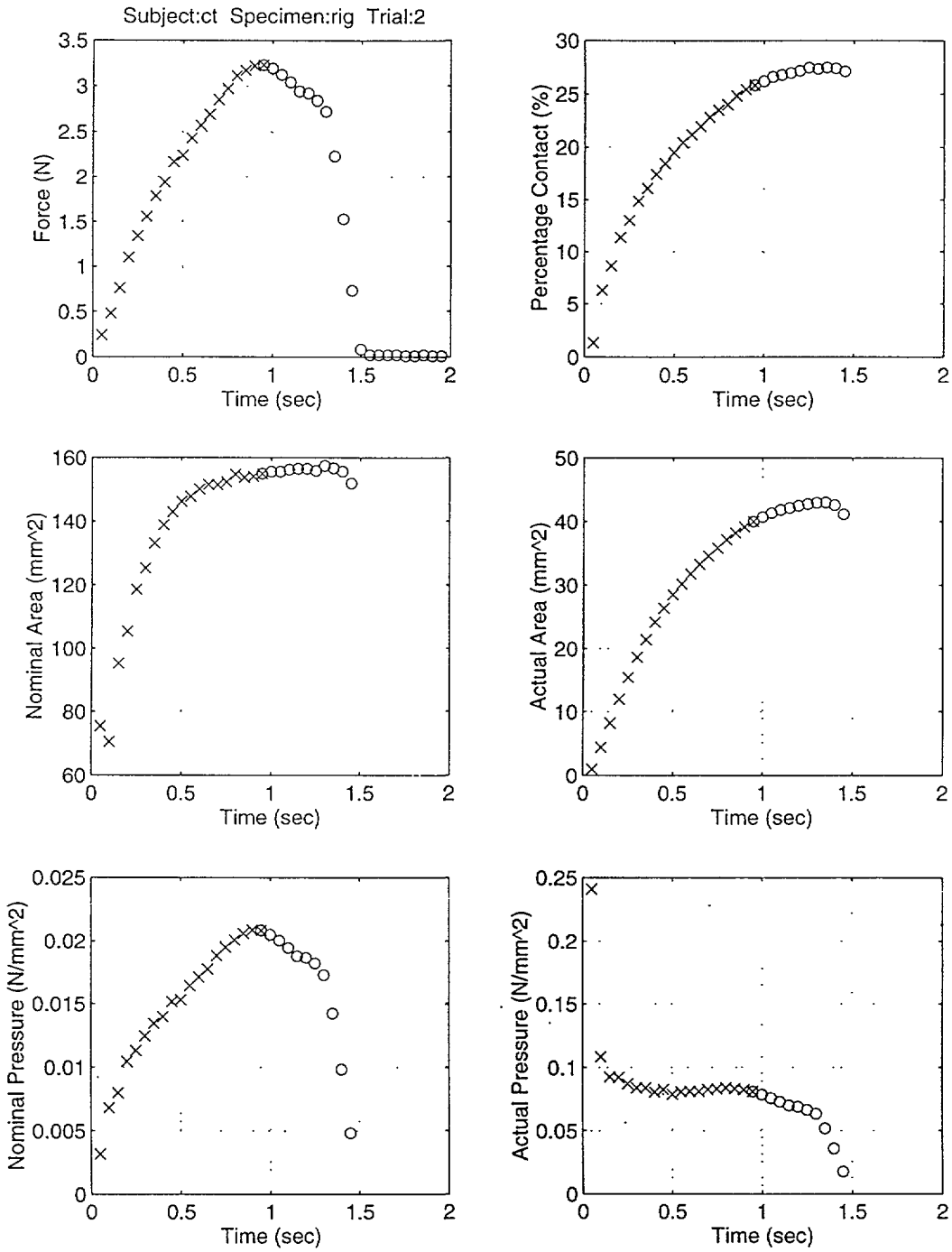

Figure G-9: Various contact variables, plotted against time, calculated from the image and force data obtained using low magnification (Subject:CT, Trial:2).

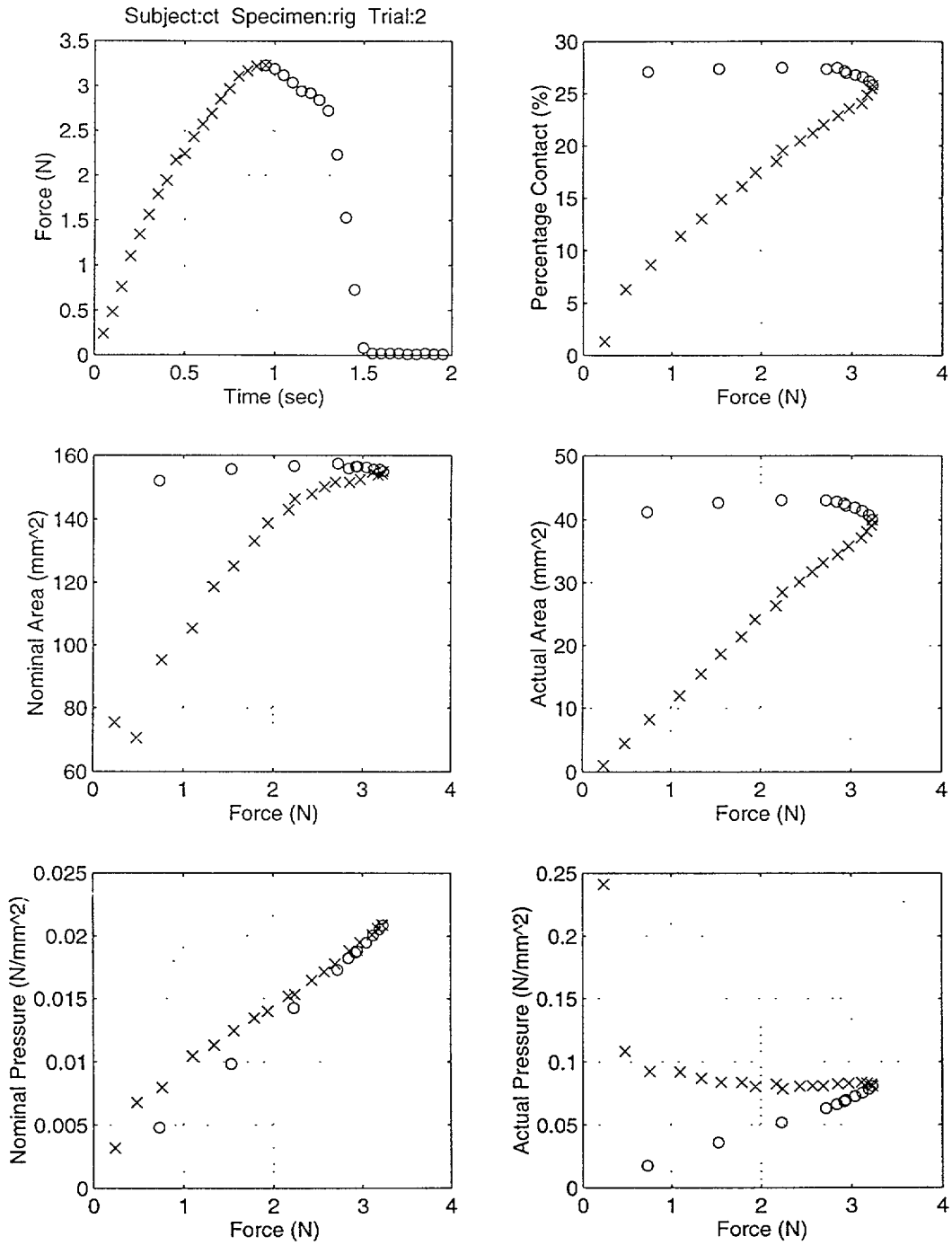

Figure G-10: Various contact variables, plotted against contact force, calculated from the image and force data obtained using low magnification (Subject:CT, Trial:2).

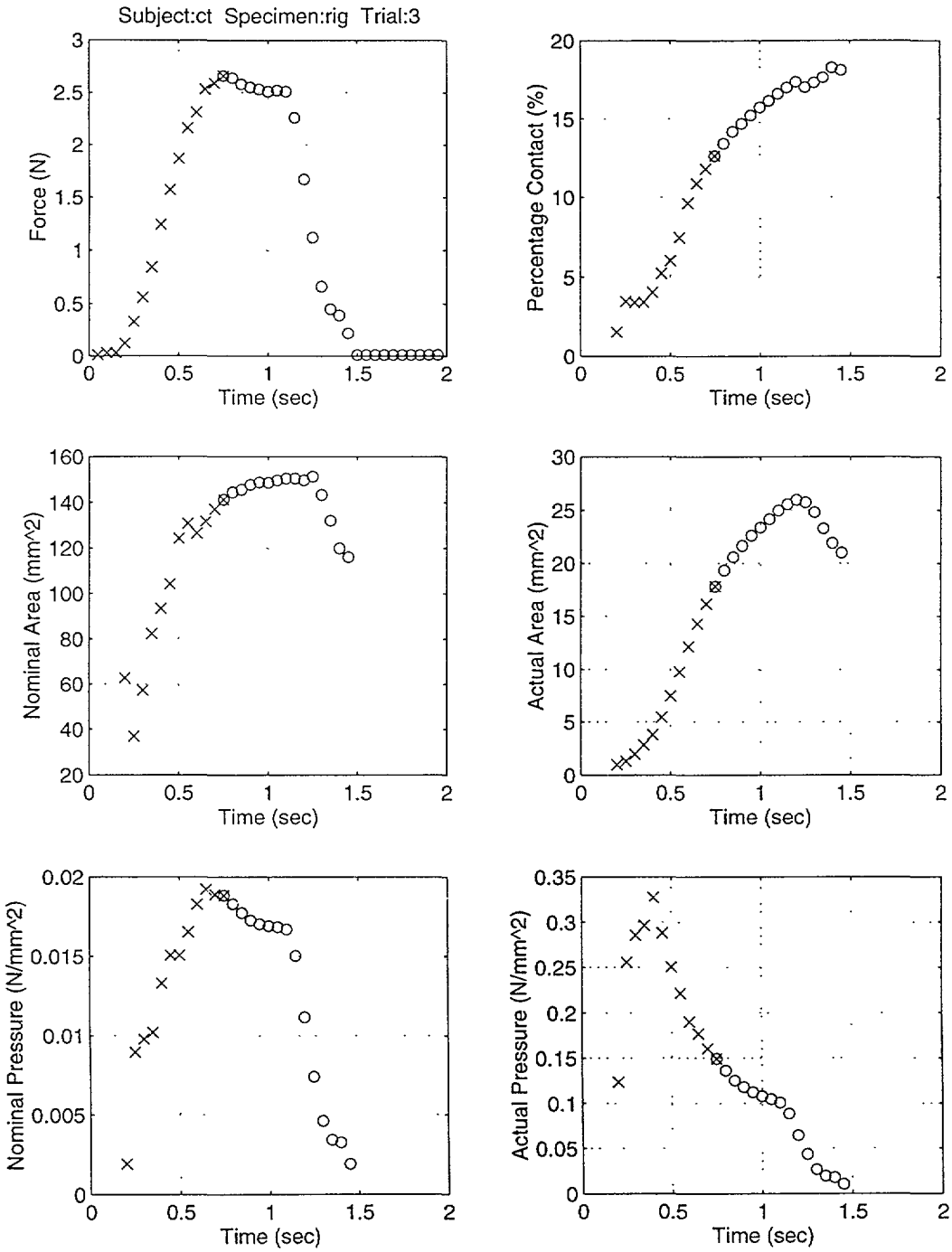

Figure G-11: Various contact variables, plotted against time, calculated from the image and force data obtained using low magnification (Subject:CT, Trial:3).

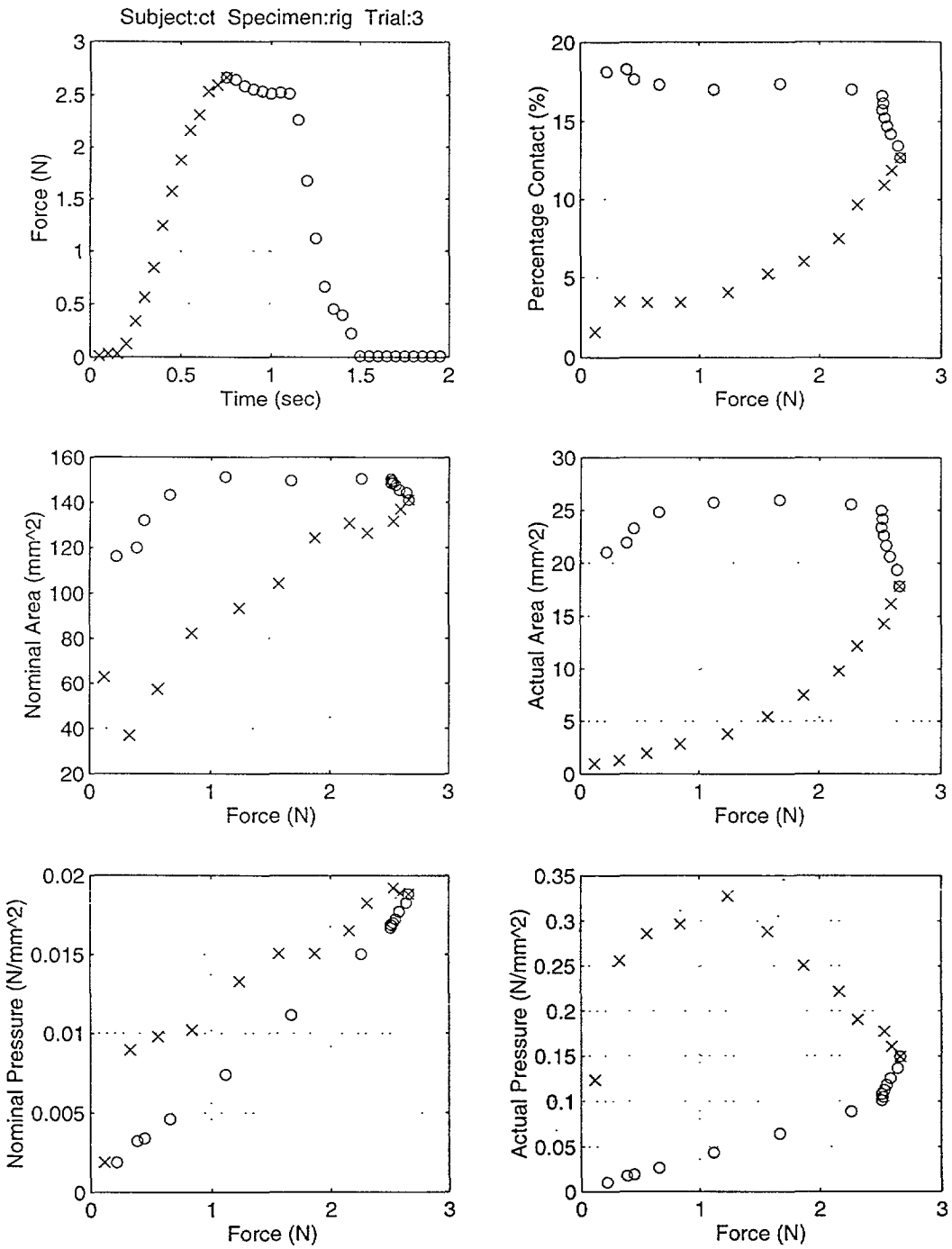

Figure G-12: Various contact variables, plotted against contact force, calculated from the image and force data obtained using low magnification (Subject:CT, Trial:3).

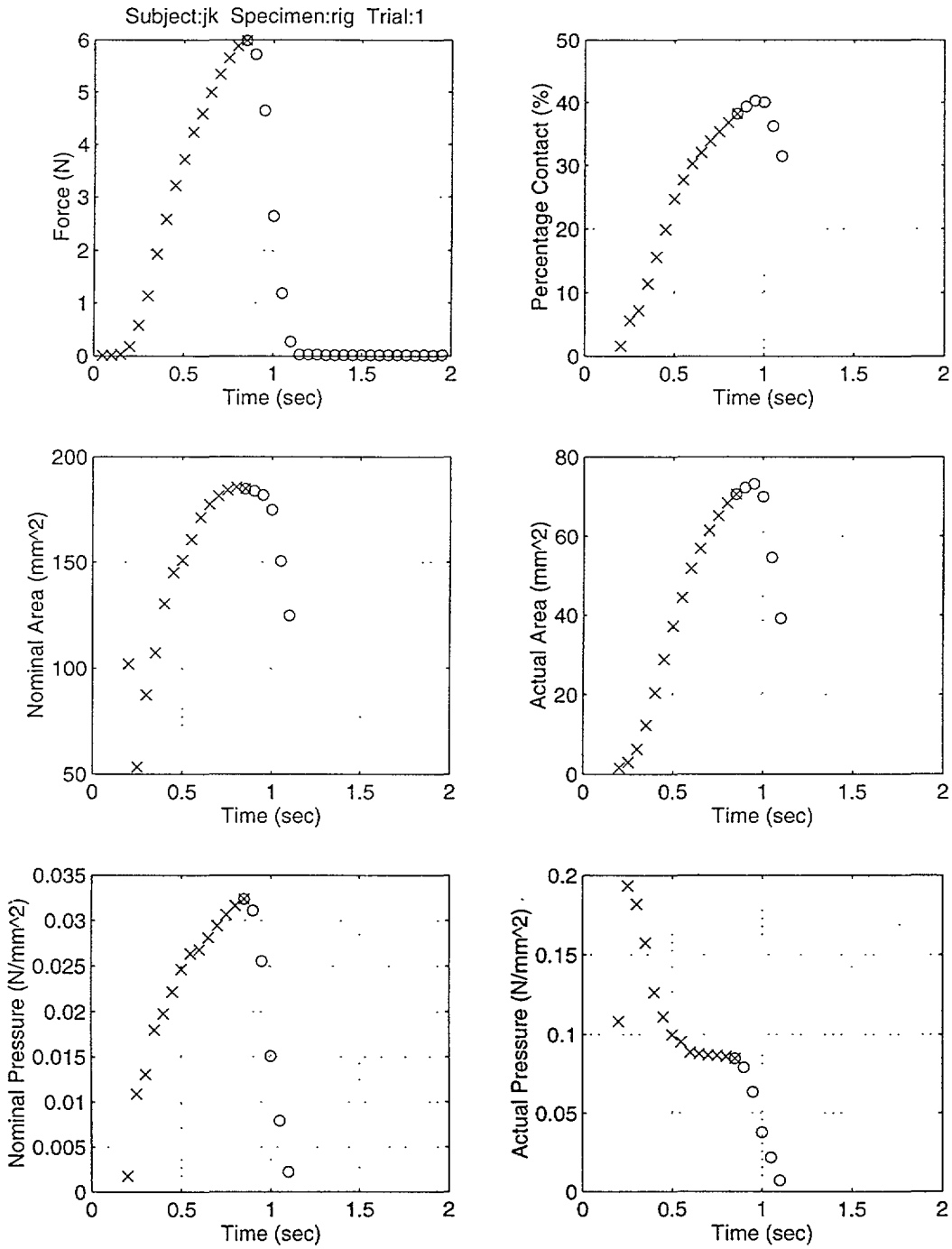

Figure G-13: Various contact variables, plotted against time, calculated from the image and force data obtained using low magnification (Subject:JK, Trial:1).

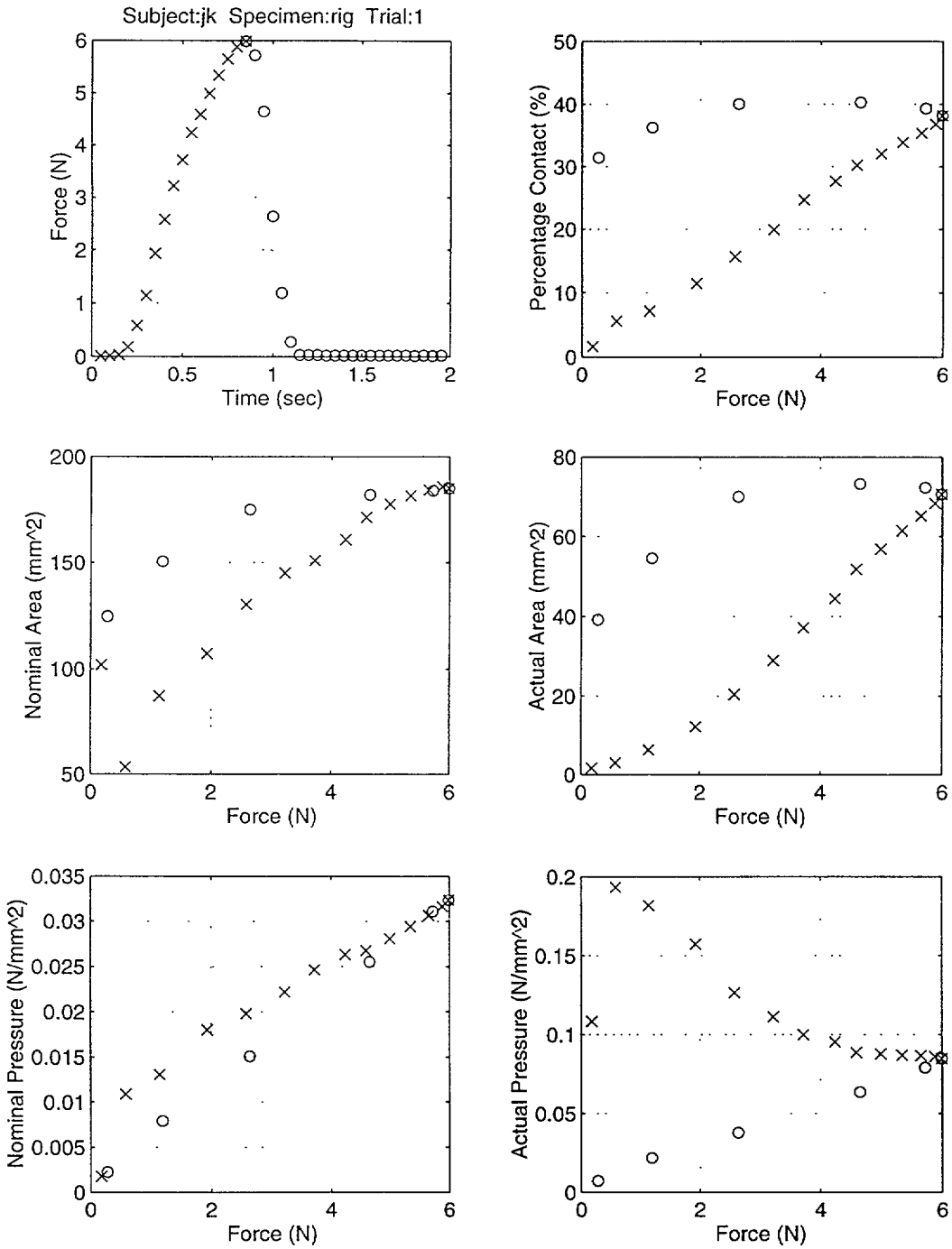

Figure G-14: Various contact variables, plotted against contact force, calculated from the image and force data obtained using low magnification (Subject:JK, Trial:1).

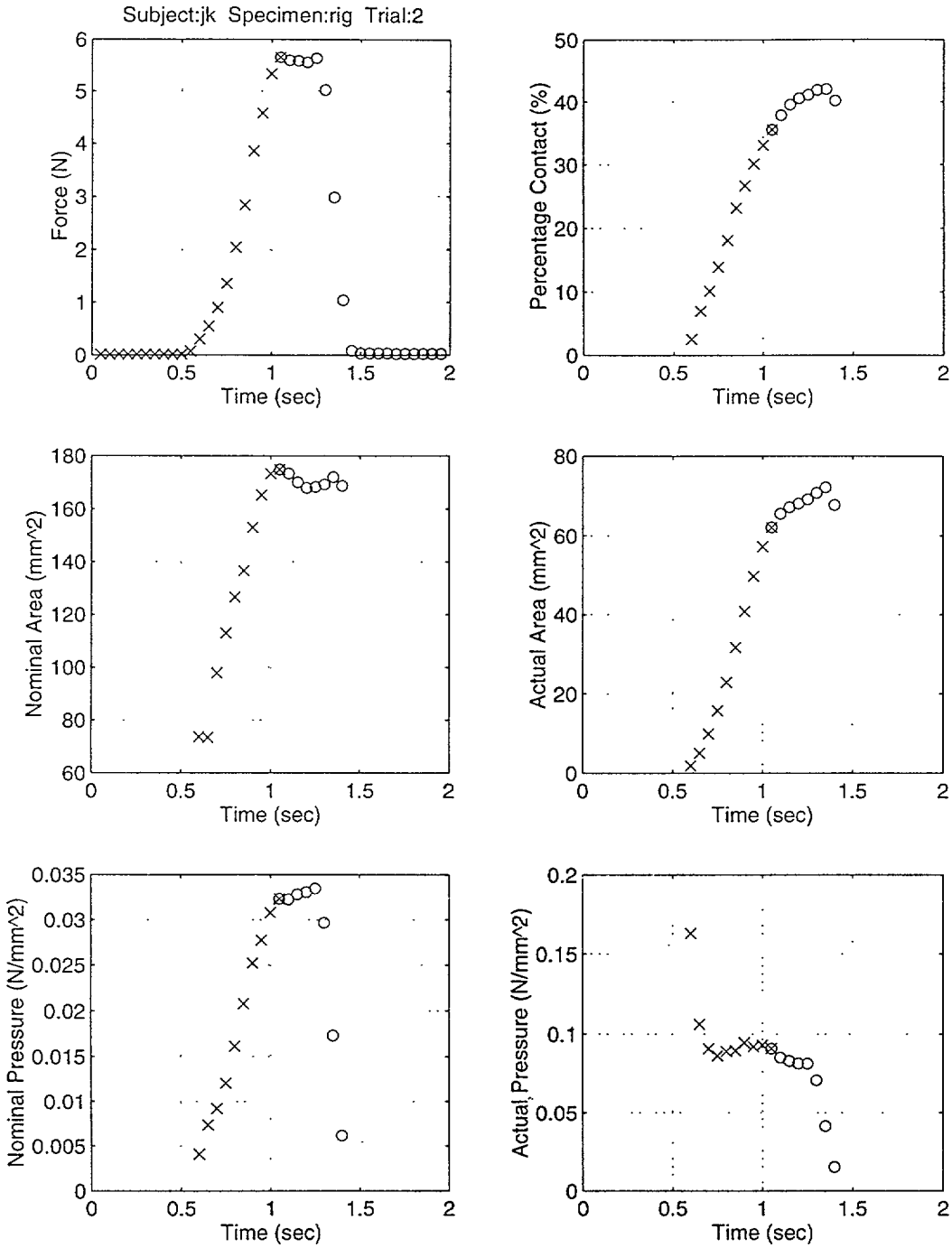

Figure G-15: Various contact variables, plotted against time, calculated from the image and force data obtained using low magnification (Subject:JK, Trial:2).

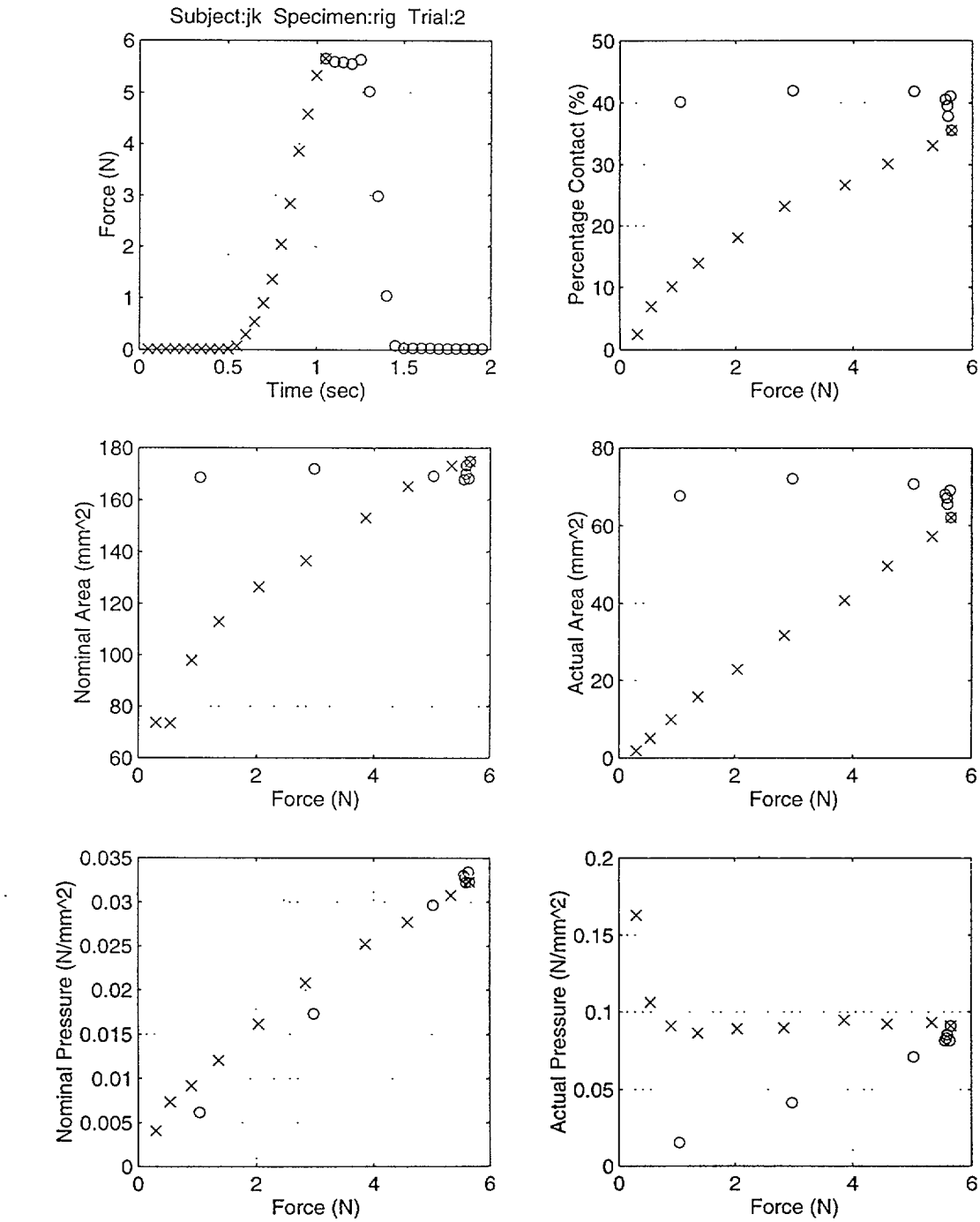

Figure G-16: Various contact variables, plotted against contact force, calculated from the image and force data obtained using low magnification (Subject:JK, Trial:2).

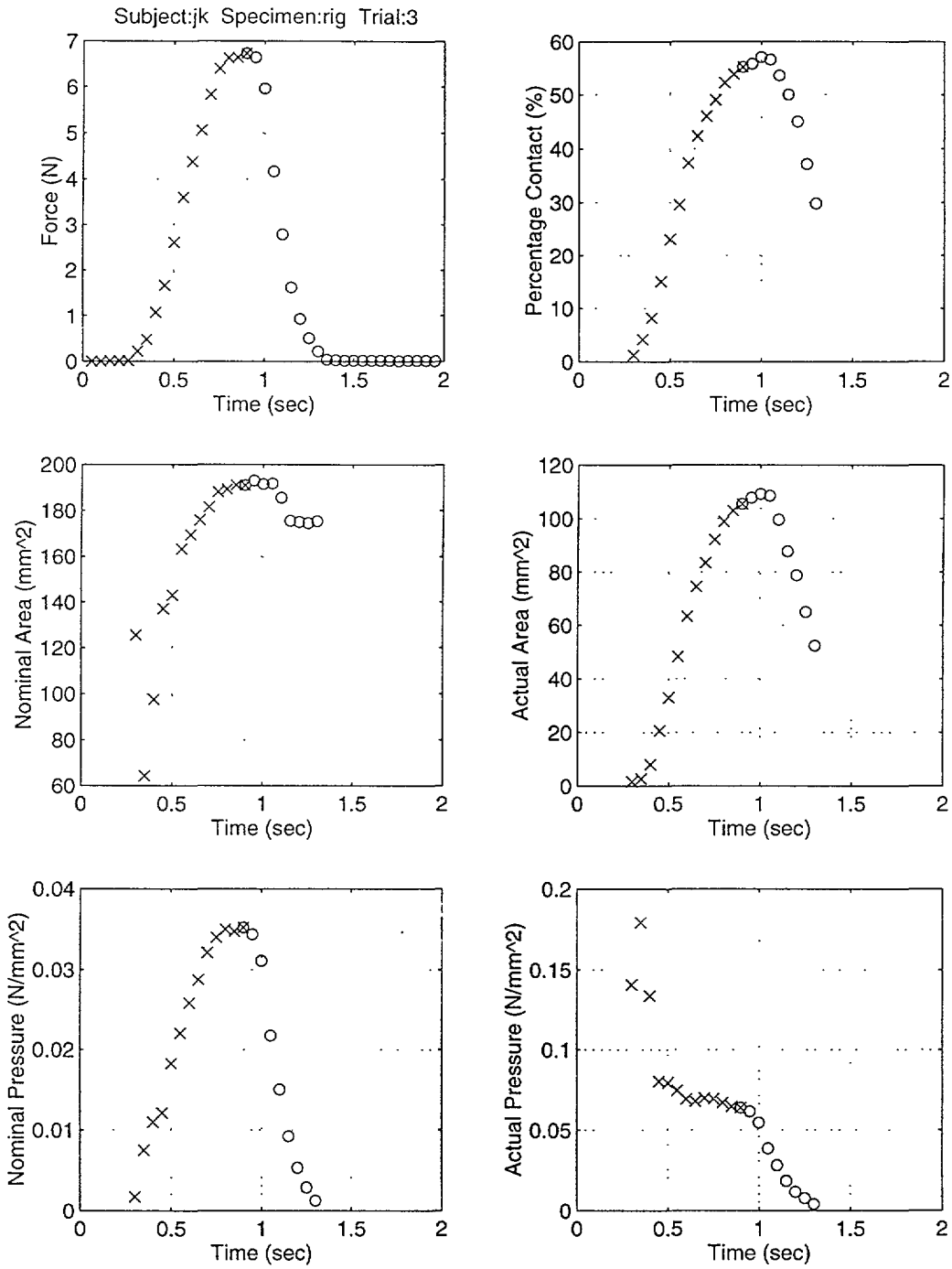

Figure G-17: Various contact variables, plotted against time, calculated from the image and force data obtained using low magnification (Subject:JK, Trial:3).

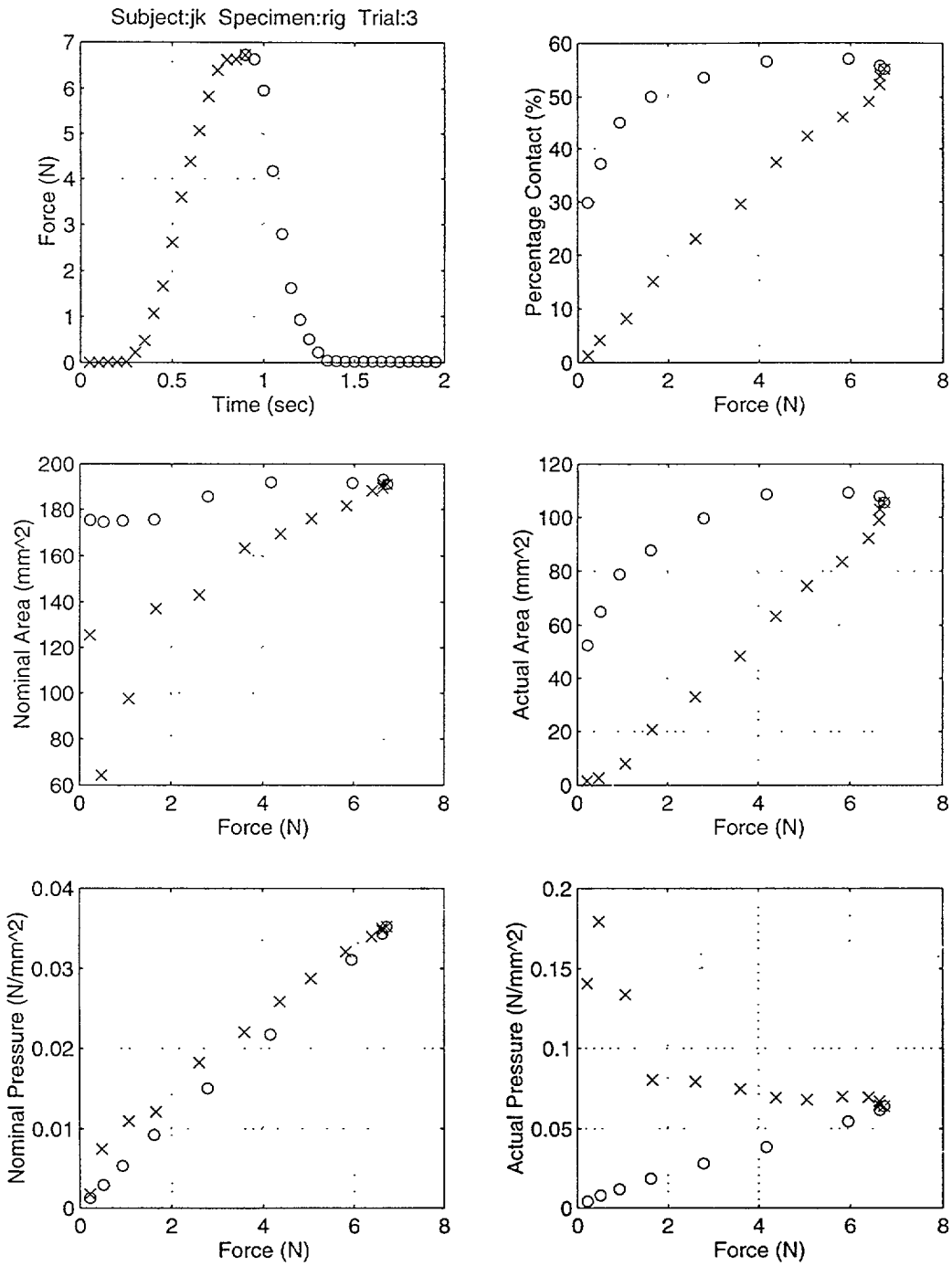

Figure G-18: Various contact variables, plotted against contact force, calculated from the image and force data obtained using low magnification (Subject:JK, Trial:3).

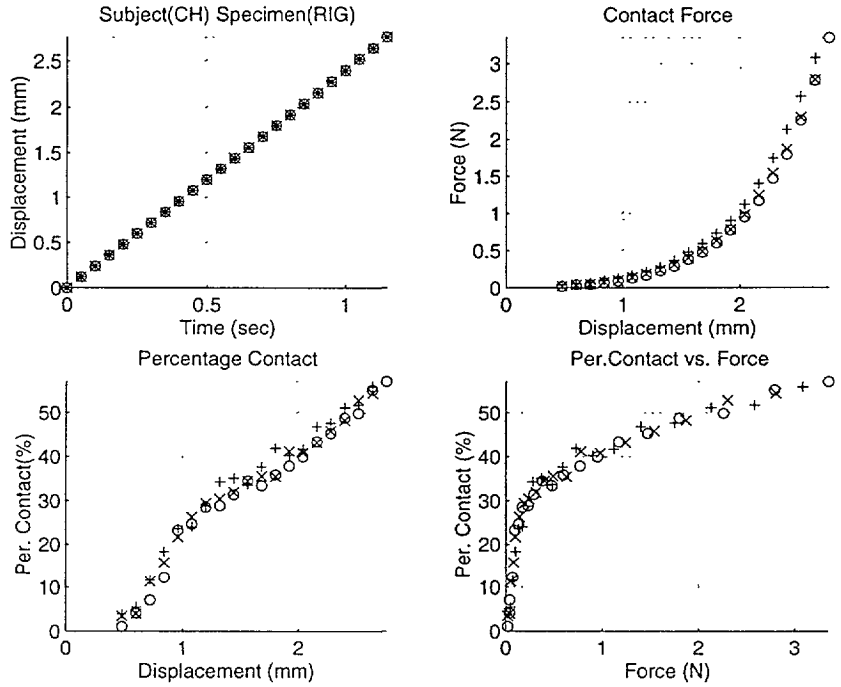

Figure G-19: Percentage contact area calculated from the image and force data obtained using high magnification (Subject:CH, Specimen: rigid).

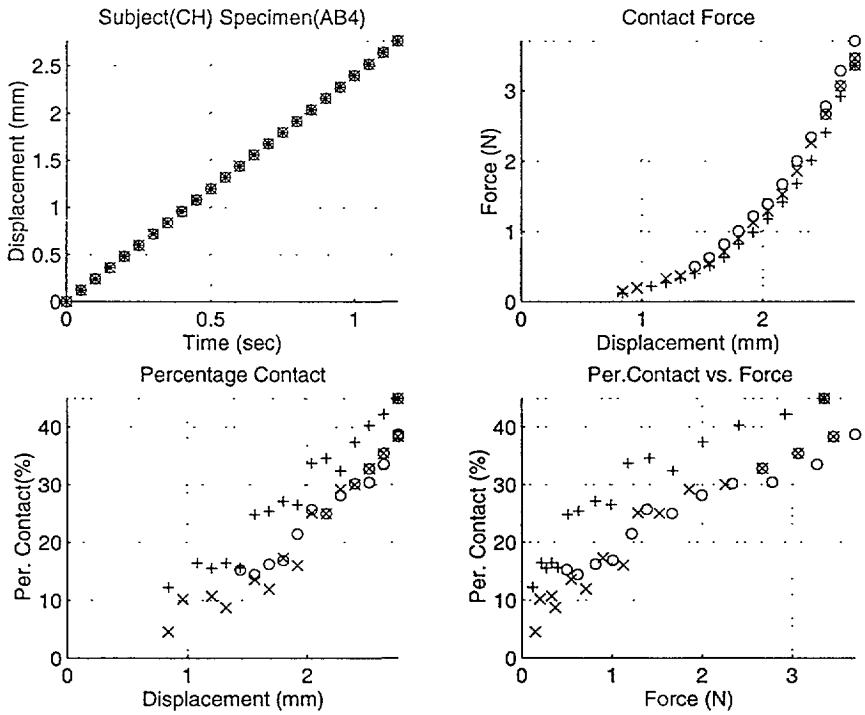

Figure G-20: Percentage contact area calculated from the image and force data obtained using high magnification (Subject:CH, Specimen:hard).

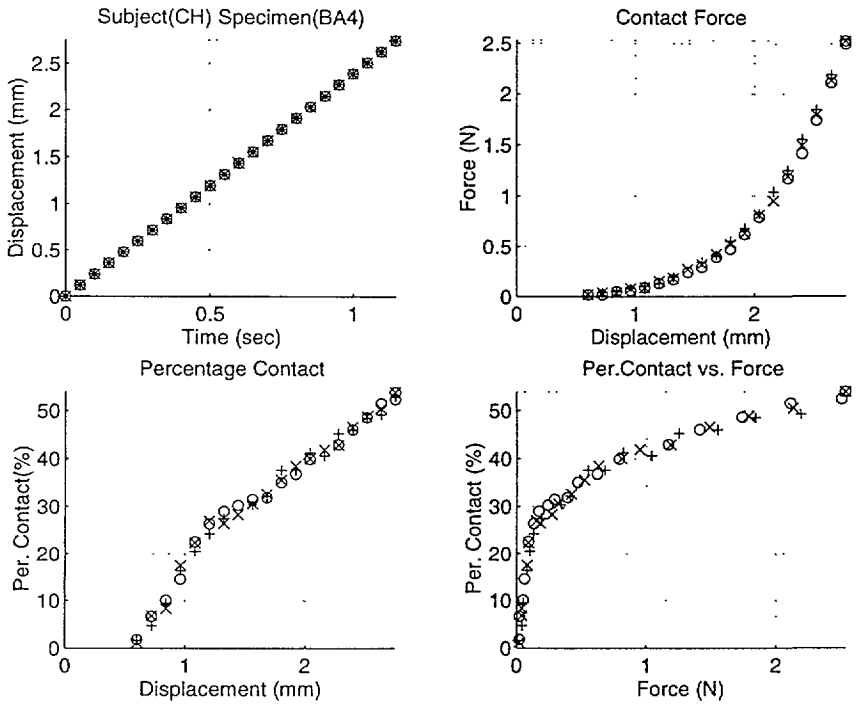

Figure G-21: Percentage contact area calculated from the image and force data obtained using high magnification (Subject:CH, Specimen:medium).

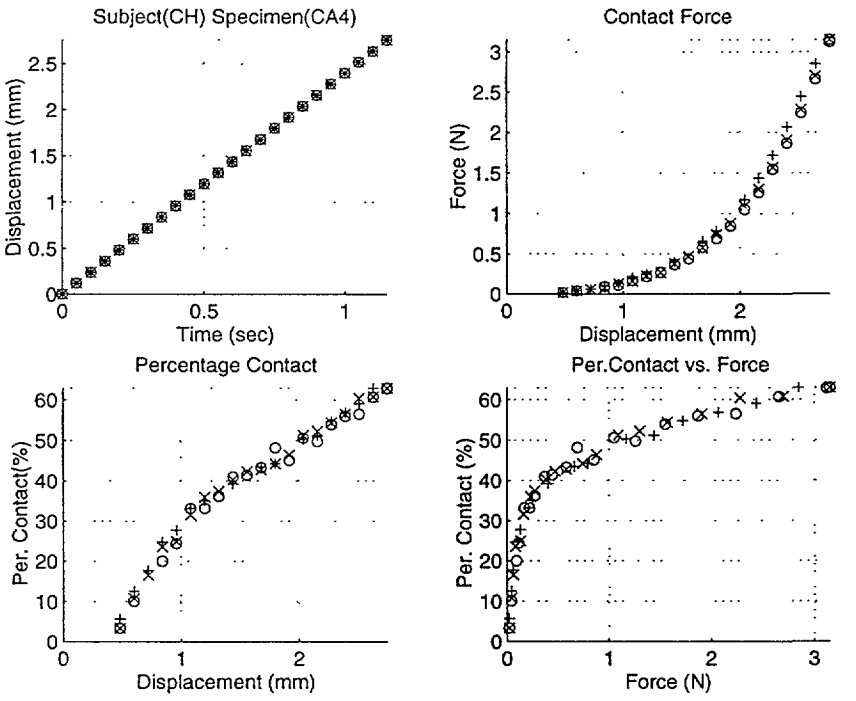

Figure G-22: Percentage contact area calculated from the image and force data obtained using high magnification (Subject:CH, Specimen:soft).

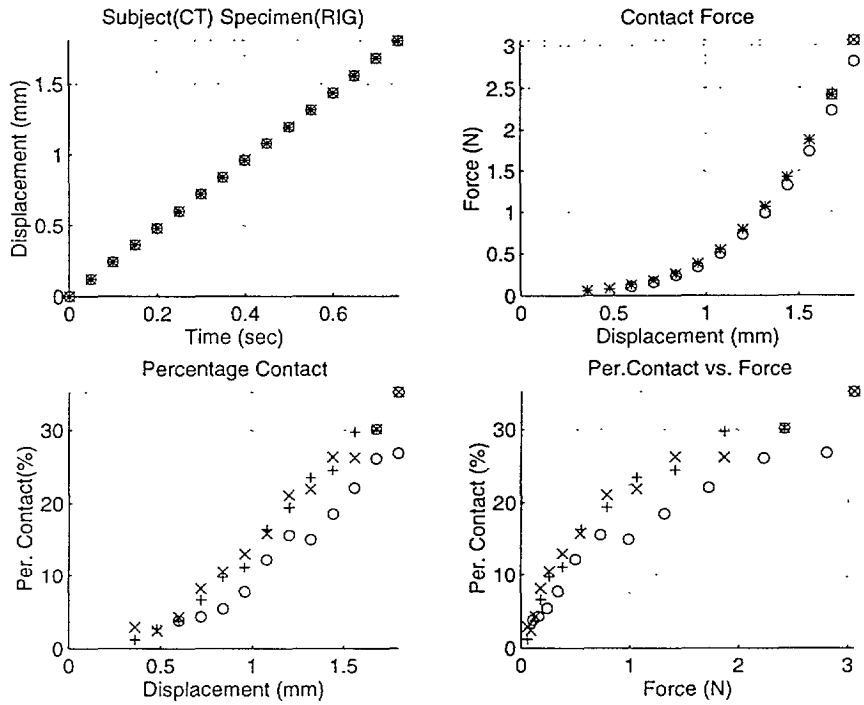

Figure G-23: Percentage contact area calculated from the image and force data obtained using high magnification (Subject:CT, Specimen: rigid).

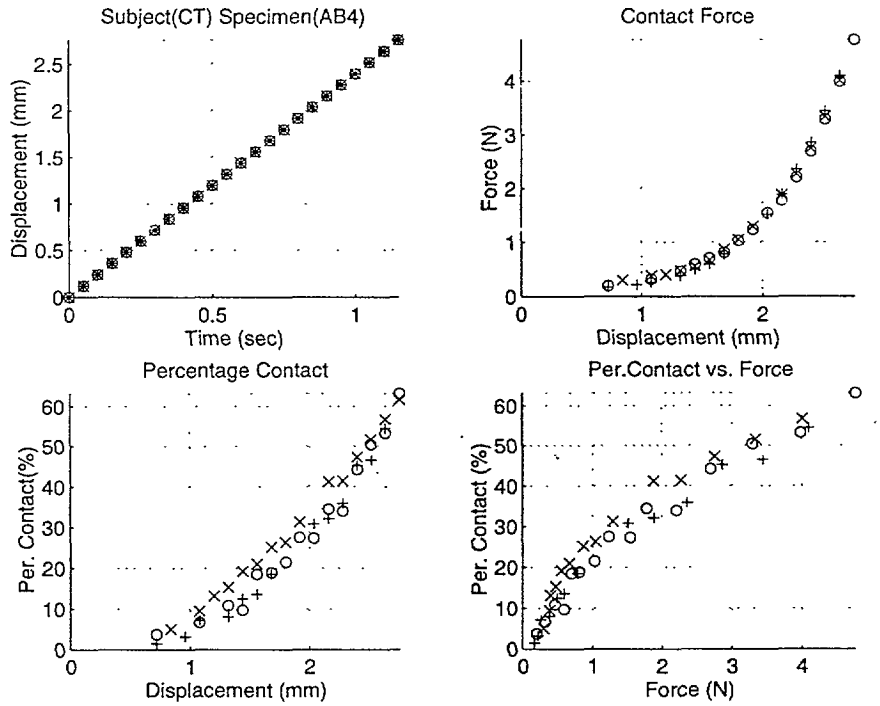

Figure G-24: Percentage contact area calculated from the image and force data obtained using high magnification (Subject:CT, Specimen:hard).

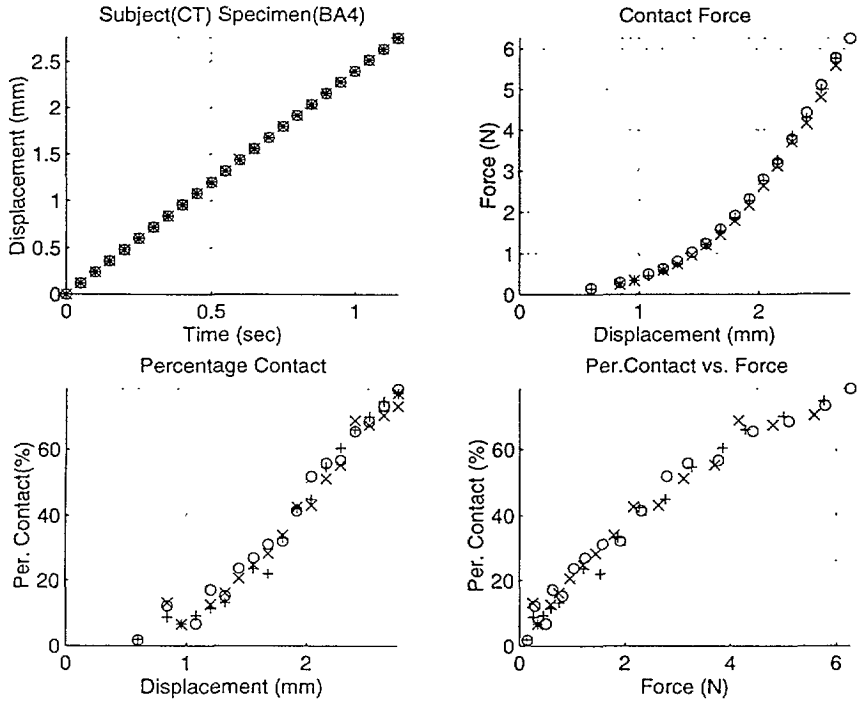

Figure G-25: Percentage contact area calculated from the image and force data obtained using high magnification (Subject:CT, Specimen:medium).

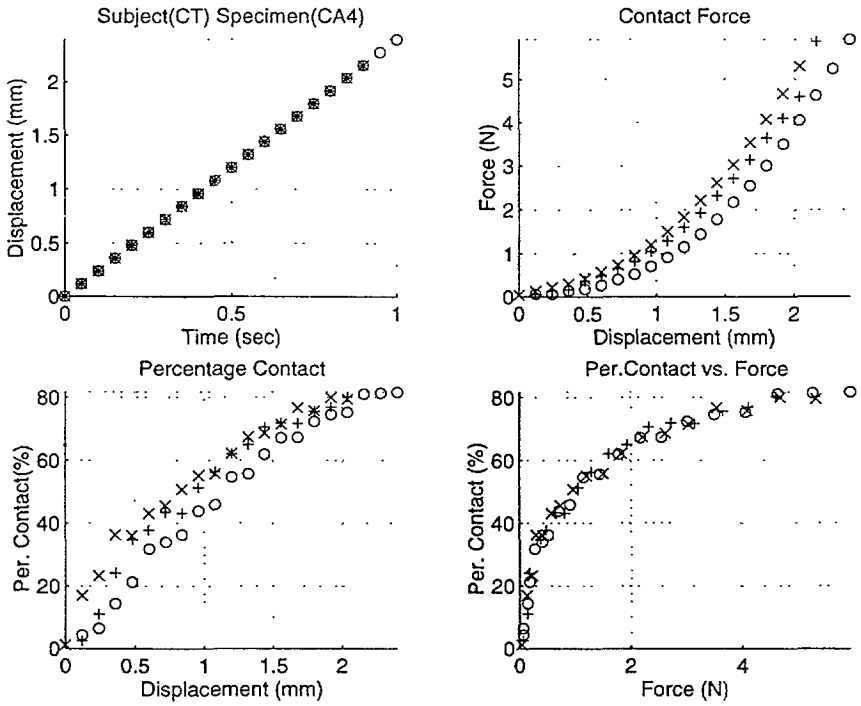

Figure G-26: Percentage contact area calculated from the image and force data obtained using high magnification (Subject:CT, Specimen:soft).

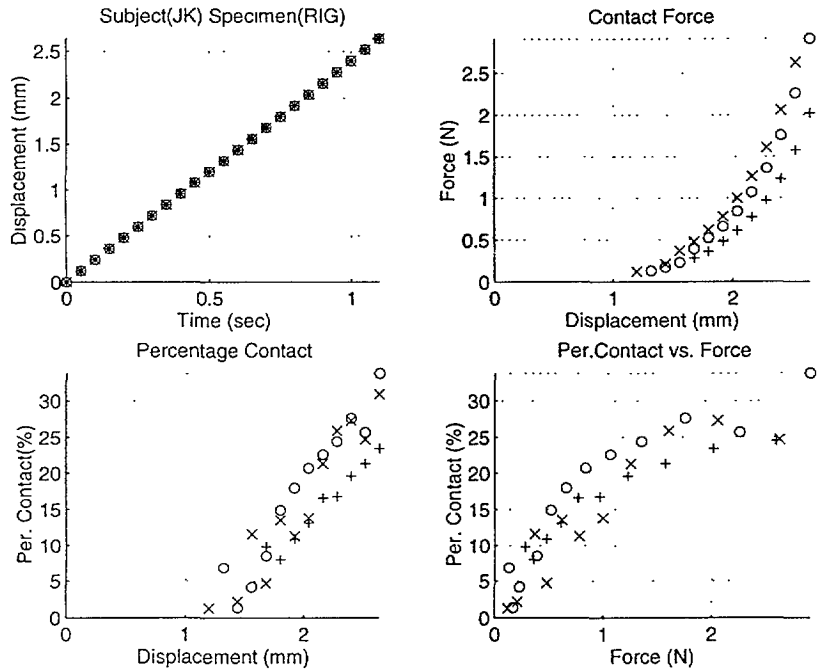

Figure G-27: Percentage contact area calculated from the image and force data obtained using high magnification (Subject:JK, Specimen: rigid).

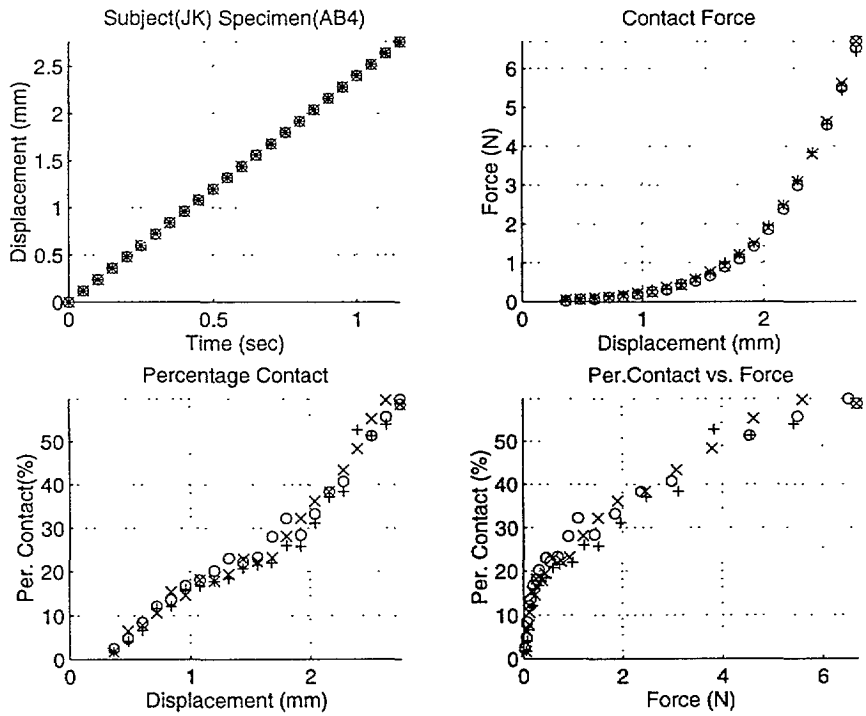

Figure G-28: Percentage contact area calculated from the image and force data obtained using high magnification (Subject:JK, Specimen:hard).

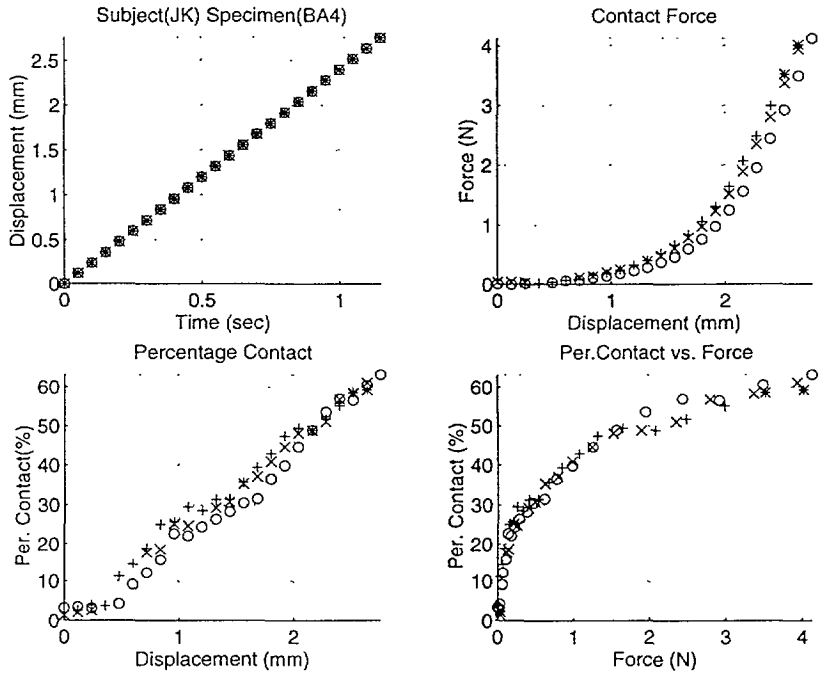

Figure G-29: Percentage contact area calculated from the image and force data obtained using high magnification (Subject:JK, Specimen:medium).

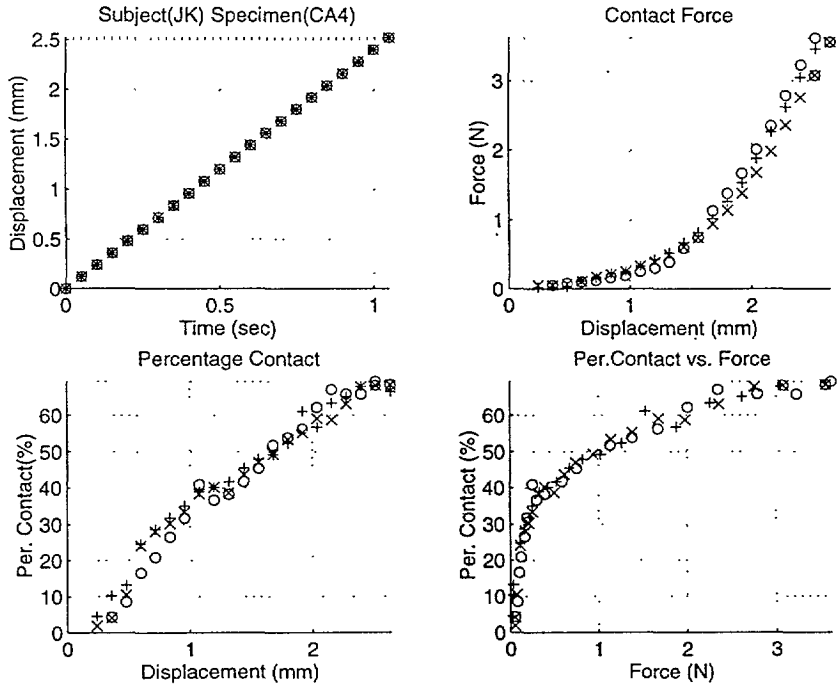

Figure G-30: Percentage contact area calculated from the image and force data obtained using high magnification (Subject:JK, Specimen:soft).

Bibliography

[1] G. A. Baxes. *Digital image processing.* John Wiley & Sons, Inc., New York, 1994.

[2] E. C. Botha and D. P. Casasent. Applications of optical morphological transformations. *Optical Engineering*, 28(5), 1989.

[3] Chris Brislawn. The FBI fingerprint image compression standard. *http://www.c3.lanl.gov/ brislawn/FBI/FBI.html*, 1995.

[4] Chris Brislawn. How wavelet/scalar quantization works. *http://www.c3.lanl.gov/ brislawn/FBI/OverCompress/HowItWorks/howitworks.html*, 1995.

[5] D. P. Casasent. Optical morphological processors. *SPIE: Image Algebra and Morphological Image Processing*, 1350:380–394, 1990.

[6] D. P. Casasent and Schaeffer R. Optical gray scale morphology for target detection. *SPIE: Image Algebra and Morphological Image Processing II*, 1568:313–326, 1991.

[7] Ho Chih-Hao. *Human Haptic Discrimination of Thickness.* Master's thesis, Massachusetts Institute of Technology, 1996.

[8] F J Clark and K W Horch. *Kinesthesia*, volume I of *Handbook of Perception and Human Performance - Sensory processes and perception, Eds. K. R. Boff, L. Kaufman and J. P. Thomas.* Wiley & Sons, New York, NY, 1986.

[9] Louis Coetzee and Elizabeth C. Botha. Fingerprint recognition in low quality images. *Pattern Recognition*, 26(10):1441–1460, 1993.

[10] Kiran Dandekar. *Role of Mechanics in Tactile Sensing of Shape.* Ph.D. thesis, Massachusetts Institute of Technology, 1995.

[11] I. Darian-Smith and P. Kenins. Innervation density of mechanoreceptive fibers supplying glabrous skin of the monkey's index finger. *Journal of Physiology*, 309:147–155, 1980.

[12] N. I. Durlach. A decision model for psychophysics. *Manuscript available at Communication Biophysics Group, Research Laboratory of Electronics, M.I.T.*, 1968.

[13] N. I. Durlach, L. A. Delhorne, A. Wong, W. Y. Ko, W. M. Rabinowitz, and J. Hollerbach. Manual discrimination and identification of length by the finger-span method. *Perception and Psychophysics*, 46(1):29–38, 1989.

[14] Frances. Having fun with science: How to be a fingerprint expert. *http://www.grfn.org/education/clonlara/index24.html*, Oct. 1994.

[15] D. Freides. Human information processing and sensory modality: Cross-modal functions,information complexity,memory and deficit. *Psychological Bulletin*, 81:284–310, 1974.

[16] Y. C. Fung. *Biomechanics: Mechanical Properties of Living Tissues.* Springer-Verlag, N.Y., second edition, 1993.

[17] R. C. Gonzalez and R. E. Woods. *Digital image processing.* Addison-Wesley Publishing Company, 1992.

[18] A. W. Goodwin, K. T. John, and A. H. Marceglia. Tactile discrimination of curvature by humans using only cutaneous information from the fingerpads. *Experimental Brain Research*, 86:663–672, 1991.

[19] Lee H. C. and R.E.Gaensslen. *Methods of Latent Fingerprint Development.* Advances in Fingerprint Technology, Eds. H. C., Lee and R.E.Gaensslen. Elsevier, New York, 1992.

[20] R. Harper and S.S. Stevens. Subjective hardness of compliant materials. *Quarterly Journal of Experimental Psychology*, 16:204–215, 1964.

[21] R. S. Johansson and A. B. Valbo. Tactile sensibility in the human hand: Relative and absolute densities of four types of mechanoreceptive units in glabrous skin. *Journal of Physiology*, 286:283–300, 1979.

[22] R S Johansson and G Westling. Roles of glabrous skin receptors and sensorimotor memory in automatic control of precision grip when lifting rougher or more slippery objects. *Experimental Brain Research*, 56:550–565, 1984.

[23] K. L. Johnson. *Contact Mechanics.* Cambridge University Press, Cambridge, 1985.

[24] R. Johnson and Bhattacharyya G. *Statistics: Princlples and Methods.* John Wiley & Sons, Inc., New York, 1985.

[25] L A Jones. Matching forces: constant errors and differential thresholds. *Perception*, 18:681–687, 1989.

[26] L. A. Jones and I. W. Hunter. A perceptual analysis of stiffness. *Experimental Brain Research*, 79:150–156, 1990.

[27] D. Katz. The judgements of test bakers. a psychological study. *Occupational Psychology*, 12:139–148, 1938.

[28] S. J. Lederman and R. A. Browse. *The Physiology and Psychophysics of Touch.* NATO ASI Series, Sensors and Sensory Systems for Advanced Robots, Ed. P. Dario. Springer-Verlag, Berlin, 1988.

[29] J. S. Lim. *Two-dimensional signal and image processing.* Prentice-Hall International Inc., Englewood Cliffs N.J., 1990.

[30] C. A. Lindley. *Practical Image Processing in C.* John Wiley & Sons, Inc., 1991.

[31] D. S. Moore and G. P. McCabe. *Introduction to the Practice of Statistics.* W.H. Freeman and Company, New York, 1989.

[32] Lawrence O'Gorman. An approach to fingerprint filter design. *Pattern Recognition*, 22(1):29–38, 1989.

[33] X D Pang, H Z Tan, and N I Durlach. Manual discrimination of force using active finger motion. *Perception and Psychophysics*, 49(6):531–540, 1991.

[34] X. D. Pang, H. Z. Tan, and N. I. Durlach. Manual discrimination of force using active finger motion. *Perception and Psychophysics*, 49(6):531–540, 1992.

[35] Roland P.E. and H. Ladegaard-Pedersen. A quantitative analysis of sensations of tension and of kinaesthesia in man. *Brain*, 100:671–692, 1977.

[36] W. H. Press, S. A. Teukolsky, W. T. Vetterling, and B. P. Flannery. *Numerical Recipes in C.* Cambridge University Press, Cambridge, 1992.

[37] C. E. Sherrick and R. W. Cholewiak. *Cutaneous Sensitivity.* Handbook of Perception and Human Performance - Sensory processes and perception, Eds. K. R. Boff, L. Kaufman and J. P. Thomas. Wiley & Sons, New York, NY, 1986.

[38] C. E. Sherrick and R. W. Cholewiak. *Tactual Perception.* Handbook of Perception and Human Performance - Sensory processes and perception, Eds. K. R. Boff, L. Kaufman and J. P. Thomas. Wiley & Sons, New York, NY, 1986.

[39] M. A. Srinivasan and J. Chen. Human performance in controlling normal forces of contact with rigid objects. *Advances in Robotics,Mechatronics,and Haptic Interfaces, ASME DSC-VOL:49*, pages 119–125, 1993.

[40] M. A. Srinivasan and R. H. LaMotte. Tactile discrimination of shape responses of slowly and rapidly adapting mechanoreceptive afferents to a step indented into the monkey fingerpad. *Journal of Neurophysiology*, 7:1682–1697, 1987.

[41] M. A. Srinivasan and R. H. LaMotte. *Encoding of shape in the responses of cutaneous mechanoreceptors.* Information Processing in the Somatosensory Systems Eds. O.Franzen and J. Westman. Macmillan, London, 1991.

[42] M. A. Srinivasan and R. H. LaMotte. Tactual discrimination of softness. *Journal of Neurophysiology*, 73(1):88–101, 1995.

[43] M. A. Srinivasan, J. M. Whitehouse, and R. H. LaMotte. Tactile discrimination of slip: surface microgeometry and peripheral neural codes. *Journal of Neurophysiology*, 63(6):1323–1332, 1990.

[44] J. A. Swets. *Signal Detection and Recognition by Human Observers.* Wiley, New York, 1964.

[45] H. Z. Tan, N. I. Durlach, G. L. Beauregard, and M. A. Srinivasan. Manual discrimination of compliance using active pinch grasp: the role of force and work cues. *Perception and Psychophysics*, 57(4):495–510, 1995.

[46] R. D. Walk and H. L. Pick. *Intersensory Perception and Sensory Integration.* Plenum, New York, 1981.

[47] G. H. Weinberg, J. A. Schumaker, and D. Oltman. *Statistics: an Intuitive Approach.* Brooks/Cole Publishing Company, Monterey, CA, 1981.

[48] R. B. Welch and D. H. Warren. Immediate perceptual response to intersensory discordance. *Psychological Bulletin*, 88:638–667, 1980.